



**IMPROVEMENT OF CONCRETE PERFORMANCE THROUGH
TREATMENT OF COARSE RECYCLED CONCRETE AGGREGATES WITH
ACID SOLUTIONS AND ADDITION OF ALUMINIUM SULPHATE**

JAVIER ANDRES FORERO VALENCIA

**TESE DE DOUTORADO EM ESTRUTURAS E CONSTRUÇÃO CIVIL
DEPARTAMENTO DE ENGENHARIA CIVIL E AMBIENTAL**

**FACULDADE DE TECNOLOGIA
UNIVERSIDADE DE BRASÍLIA**

**FACULDADE DE TECNOLOGIA
DEPARTAMENTO DE ENGENHARIA CIVIL E AMBIENTAL**

**IMPROVEMENT OF CONCRETE PERFORMANCE THROUGH
TREATMENT OF COARSE RECYCLED CONCRETE AGGREGATES WITH
ACID SOLUTIONS AND ADDITION OF ALUMINIUM SULPHATE**

JAVIER ANDRES FORERO VALENCIA

**ORIENTADOR: Cláudio Henrique de Almeida Feitosa Pereira
COORIENTADORES: Jorge Manuel Calião Lopes de Brito;
Luís Manuel Faria da Rocha Evangelista**

TESE DE DOUTORADO EM ESTRUTURAS E CIVIL

BRASÍLIA/DF: NOVEMBRO - 2023

UNIVERSIDADE DE BRASÍLIA
FACULDADE DE TECNOLOGIA
DEPARTAMENTO DE ENGENHARIA CIVIL E AMBIENTAL

**IMPROVEMENT OF CONCRETE PERFORMANCE THROUGH
TREATMENT OF COARSE RECYCLED CONCRETE AGGREGATES WITH
ACID SOLUTIONS AND ADDITION OF ALUMINIUM SULPHATE**

JAVIER ANDRES FORERO VALENCIA

APROVADA POR:

Prof. Cláudio Henrique de Almeida Feitosa Pereira, D.Sc. (UnB)
(Orientador)

Prof. Jorge Manuel Calição Lopes de Brito, D.Sc.(IST-ULisboa)
(Coorientador)

Prof. Luís Manuel Faria da Rocha Evangelista, D.Sc.(ISEL)
(Coorientador)

Prof. Michele Dal Toe Casagrande, D.Sc.(UnB)
(Examinador Interno)

Prof. Paulo Ricardo de Matos, D.Sc.(UDESC)
(Examinador Externo)

Prof. Afonso Rangel Garcez de Azevedo, D.Sc.(UENF)
(Examinador Externo)

BRASILIA/DF, 20 DE NOVEMBRO DE 2023

Agradecimentos

Antes de tudo, expresso minha gratidão a Deus por guiar-me nesta jornada e conceder-me força em todos os momentos. Sou imensamente grato aos meus pais Javier e Maria que foram fundamentais para me tornar na pessoa que sou hoje e também aos meus irmãos Angela e Dario, cujo carinho e apoio incondicional foram importantes nesta jornada onde estive longe da minha família.

Não posso deixar de mencionar minha companheira, Inês, que sempre esteve ao meu lado demonstrando seu apoio incondicional, alegria e conhecimento, e meu filho, Diego, cuja luz foi meu incentivo para concluir esta etapa importante em minha vida. A seus pais Francisco e Helena por acolher-me nesta família.

Gostaria de expressar minha profunda gratidão ao meu coorientador, Doutor Jorge de Brito, pelo seu conhecimento e amizade incondicional ao longo de quatro anos, ajudando-me no crescimento pessoal e profissional e nunca desistindo de mim nos momentos mais difíceis. Agradeço também por ter me apresentado ao Instituto Superior Técnico em Portugal, onde tive a oportunidade de trabalhar.

Não posso deixar de agradecer ao meu orientador, Doutor Claudio Henrique de Almeida Feitosa Pereira, pela sua orientação e apoio durante o desenvolvimento desta tese, bem como sua amizade. Ao meu coorientador, Doutor Luís Evangelista, agradeço pelo seu apoio científico e disposição em ajudar a concretizar esta tese, bem como a oportunidade de trabalhar em seu grupo de pesquisa.

Estou grato pela amizade e apoio incondicional da minha amiga Yoleimy Avila, cuja ajuda foi fundamental para o desenvolvimento desta tese. Seu carinho e disposição sempre foram uma constante. Gostaria de agradecer também ao meu amigo Carlos Seruti, por sua amizade e colaboração em todo momento, mesmo à distância.

Finalmente, agradeço aos meus amigos Tiago Liberalesso, Ferney Bohorquez, Erica Nóbrega, João Pacheco e Dani Kassim pela sua amizade e apoio em todos os momentos, bem como aos técnicos do laboratório de construção civil, Jorge Pontes e Francisco Almeida. Sem o apoio de todos eles, não teria sido possível concluir esta tese.

RESUMO

MELHORIA DO DESEMPENHO DO CONCRETO ATRAVÉS DO TRATAMENTO DE AGREGADOS GRAUDOS DE CONCRETO RECICLADO COM SOLUÇÕES ÁCIDAS E ADIÇÃO DE SULFATO DE ALUMÍNIO

Autor: Javier Andres Forero Valencia

Orientador: Cláudio Henrique de Almeida Feitosa Pereira

Coorientador: Jorge Manuel Calião Lopes de Brito e Luís Manuel Faria da Rocha Evangelista

Programa de Pós-graduação em Estruturas e Construção Civil

Brasília,

A heterogeneidade dos agregados reciclados de concreto (RCA) tem origem principalmente nas fontes das quais são gerados. Por este motivo, existem várias técnicas na literatura que ajudam a melhorar a performance dos agregados para adquirirem similaridade com os agregados naturais (AN). Embora em estudos prévios existam vários autores que relatam esta técnica para a remoção da argamassa aderida aos AN usando soluções ácidas, não existe ainda um consenso sobre qual o tempo de imersão e concentração ácida são adequados para uma melhoria do RCA. Uma campanha experimental de duas fases foi desenvolvida nesta investigação. A primeira fase teve como foco, a identificação da concentração ótima em termos de molaridade (M) e tempo de imersão usando ácido clorídrico (HCl) e ácido sulfúrico (H₂SO₄), e adicionalmente, a realização de uma análise das suas propriedades físicas. A segunda fase teve como foco, a produção de concretos com RCA tratados com soluções ácidas de HCl e H₂SO₄ e a produção de concretos com a incorporação de RCA e sulfato de alumínio (SA). Ambas as composições foram avaliadas nas suas propriedades mecânicas, fratura e durabilidade. Após a análise dos efeitos macro, ainda se procedeu a uma análise da microestrutura da zona de transição interfacial (ZTI) entre o RCA tratado e a matriz cimentícia, com o objetivo de observar e descrever a melhoria da ZTI. Na primeira fase, foi concluído que concentrações entre 1 M e 3 M de HCl e H₂SO₄ não apresentaram uma melhoria substancial na remoção da argamassa. Da mesma forma, o tempo de imersão não influenciou consideravelmente na remoção no RCA. Relativamente à segunda fase, os resultados do comportamento mecânico, durabilidade e fratura, demonstraram melhorias relativamente aos concretos que incorporam RCA tratados com soluções ácidas na sua concentração até 1M e adição de SA, em comparação aos concretos de referência com RCA não tratados. Não obstante, foi ainda concluído que a utilização de molaridades altas (3M) de H₂SO₄ nas propriedades mecânicas de durabilidade e fratura, tende a ser negativa, comparativamente aos concretos de referência com RCA não tratados. Como resultado, essas descobertas contribuíram para um entendimento mais aprofundado sobre a aplicação adequada dessas técnicas no contexto de concretos que empregam esse tipo de agregados.

Palavras-chave: Métodos de pré-tratamento (HCl, H₂SO₄), agregado de concreto reciclado (RCA), propriedades de fratura, propriedades mecânicas, durabilidade, concreto.

ABSTRACT

IMPROVEMENT OF CONCRETE PERFORMANCE THROUGH TREATMENT OF COARSE RECYCLED CONCRETE AGGREGATES WITH ACID SOLUTIONS AND ADDITION OF ALUMINIUM SULPHATE

Author: Javier Andres Forero Valencia

Supervisor: Cláudio Henrique de Almeida Feitosa Pereira

Co-supervisor: Jorge Manuel Calião Lopes de Brito and Luís Manuel Faria da Rocha Evangelista.

Post-Graduate Program on Structures and Civil Construction

Brasília,

The heterogeneity of Recycled Concrete Aggregate (RCA) originates mainly from the sources from which it is generated. For this reason, there are several techniques in the literature that help improve the performance of aggregates to achieve similarity with natural aggregate (NA). Although in previous studies there are several authors who report this technique for removing the adhered mortar from NA using acid solutions, there is still no consensus on the appropriate immersion time and acid concentration for improving RCA. A two-phase experimental campaign was conducted in this investigation. The first phase focused on identifying the optimal concentration in terms of molarity (M) and immersion time using hydrochloric acid (HCl) and sulphuric acid (H₂SO₄), as well as conducting an analysis of their physical properties. The second phase focused on producing concrete mixes with RCA treated with acid solutions of HCl and H₂SO₄, and mixes incorporating RCA and aluminium sulphate (AS). Both compositions were evaluated in terms of their mechanical properties, fracture, and durability. After analysing the macro effects, a microstructure analysis of the interfacial transition zone (ITZ) between the treated RCA and the cementitious matrix was carried out to observe and describe the improvement of the ITZ. In the first phase, it was concluded that concentrations between 1 M and 3 M of HCl and H₂SO₄ do not significantly improve mortar removal. Similarly, the immersion time does not have a considerable influence on mortar removal from RCA. Regarding the second phase, the results of mechanical behaviour, durability, and fracture demonstrated improvements in mixes incorporating RCA treated with acid solutions at concentrations up to 1 M and the addition of AS compared to untreated reference mixes with RCA. However, it was also concluded that the use of high molarities (3 M) of H₂SO₄ tends to be negative in terms of mechanical durability and fracture properties relative to reference mixes with non-treated RCA. As a result, all these findings have led to a more nuanced understanding of the appropriate use of these techniques in concretes employing such aggregates.

Key words: Pre-treatment methods (HCl, H₂SO₄), Recycled concrete aggregate (RCA), fracture properties, mechanical properties, durability, concrete.

INDEX

1	INTRODUCTION	1
1.1	Remarks from the literature review	5
1.2	Problem definition	6
1.3	Research question	6
1.4	Research hypothesis	6
1.5	Research contributions	7
2	LITERATURE REVIEW	11
2.1	Introduction	11
2.2	Chemistry of acid treatment in RCA	12
2.3	RCA properties	15
2.3.1	Water absorption.....	15
2.3.2	Determination of mortar loss.....	18
2.3.3	Bulk density.....	19
2.3.4	Microscopic analysis of the RCA.....	20
2.3.5	Statistical analysis of RCA properties.....	22
2.4	Properties of concrete with treated RCA.....	25
2.4.1	Fresh-state properties and density	25
2.4.2	Compressive strength	27
2.4.3	Tensile strength	30
2.4.4	Modulus of elasticity	31
2.4.5	Fracture energy	32
2.4.6	Shrinkage	32
2.4.7	Chloride ion penetrability and carbonation resistance	33
2.4.8	ITZ between cement paste and RCA.....	33
2.5	Concrete with addition of AS	35

2.6	Analysis of the literature review.....	38
3	EXPERIMENTAL PROGRAM	40
3.1	Test planning	40
3.2	Materials	42
3.2.1	Cement.....	42
3.2.2	Natural aggregates (NA) and water	42
3.2.3	Recycled concrete aggregates (RCA).....	42
3.2.4	Acids.....	43
3.2.5	Aluminium sulphate	44
3.3	Characterisation of Aggregates	44
3.3.1	Water absorption and saturated surface dried particle density of NA and RCA	44
3.3.2	Water absorption over time of NA and RCA	46
3.3.3	Size distribution analysis	46
3.3.4	Chemical treatments and adhered mortar content of RCA.....	47
3.3.5	X-Ray diffraction (XRD) and X-Ray fluorescence (XFR) analysis.....	48
3.4	Mix Design	49
3.5	Concrete production	50
3.6	Test procedures for fresh concrete properties.....	51
3.6.1	Workability.....	51
3.7	Properties in the hardened state	52
3.7.1	Compressive strength	53
3.7.2	Splitting tensile strength	54
3.7.3	Modulus of elasticity	55
3.7.4	Fracture energy	56
3.7.4.1	Test specimen preparation	57
3.7.4.2	Test specimen preparation and test procedure.....	57

3.7.5	Water absorption by immersion	58
3.7.6	Capillary water absorption test.....	60
3.7.7	Resistance to carbonation	61
3.7.8	Resistance to the penetration of chloride ions	62
3.7.9	Shrinkage	64
3.7.10	Microstructural analysis using Scanning Electron Microscopy (SEM).....	65
<i>FIRST STAGE RESULTS AND DISCUSSION: Optimal determination of acid molarity for removal of mortar adhered to RCA.</i>		67
4	Characterization of materials and mortar removal performance in RCA ..	68
4.1	X-Ray Diffraction Analysis (XRD).....	68
4.2	X-ray fluorescence spectroscopy	70
4.3	Characterization of aggregates	70
4.3.1	Determination of mortar loss	71
4.3.2	Aggregate size distribution.....	76
4.3.3	Bulk density and water absorption	82
4.4	Summary of Chapter 4 for the production of the second phase concrete.....	90
<i>SECOND STAGE RESULTS AND DISCUSSION: Evaluation of the mechanical, fracture and durability performance of concrete mixes incorporating rca treated with acid solutions and with addition of aluminium sulphate.</i>		91
5	Evaluation of the mechanical, fracture and durability performance of concrete mixes incorporating rca treated with acid solutions and with addition of aluminium sulphate	92
5.1	Mix design	92
5.2	Workability and bulk density	94
5.3	Microstructure of the ITZ of concrete mixes	97
5.3.1	Concrete incorporating NA	97
5.3.2	Concrete incorporating RCA	98
5.3.3	Concrete incorporating RCA treated with HCl	99

5.3.4	Concrete incorporating RCA treated with H ₂ SO ₄	101
5.3.5	Concrete incorporating aluminium sulphate (AS).....	106
5.4	Compressive strength	107
5.4.1	Compressive strength of concrete incorporating RCA treated with HCl 107	
5.4.2	Compressive strength of concrete incorporating RCA treated with H ₂ SO ₄ 109	
5.4.3	Concrete incorporating aluminium sulphate (AS).....	110
5.5	Splitting tensile strength	111
5.5.1	Tensile strength in concrete incorporating RCA treated with HCl	112
5.5.2	Tensile strength in concrete incorporating RCA treated with H ₂ SO ₄	113
5.5.3	Tensile strength in concrete incorporating aluminium sulphate (AS)	115
5.6	Modulus of elasticity	115
5.6.1	Modulus of elasticity in concrete incorporating RCA treated with HCl	115
5.6.2	Modulus of elasticity in concrete incorporating RCA treated with H ₂ SO ₄	117
5.6.3	Modulus of elasticity in concrete incorporating aluminium sulphate (AS) 119	
5.7	Fracture energy (G _F)	119
5.7.1	Fracture energy (G _F) in concrete incorporating RCA treated with HCl.....	122
5.7.2	Fracture energy (G _F) in concrete incorporating RCA treated with H ₂ SO ₄ 124	
5.7.3	Fracture energy (G _F) in concrete incorporating aluminium sulphate (AS) 125	
5.7.4	The effective double K _I fracture criterion	126
5.8	Combining mechanical properties and comparing standards	128
5.9	Water absorption by immersion	130
5.9.1	Water absorption by immersion in concrete incorporating RCA treated with HCl 130	

5.9.2	Water absorption by immersion in concrete incorporating RCA treated with H ₂ SO ₄	132
5.9.3	Water absorption by immersion in concrete incorporating aluminium sulphate (AS)	133
5.10	Water absorption by capillarity	134
5.10.1	Water absorption by capillarity in concrete incorporating RCA treated with HCl	135
5.10.2	Water absorption by capillarity in concrete incorporating RCA treated with H ₂ SO ₄	136
5.10.3	Water absorption by capillarity in concrete incorporating AS	138
5.11	Carbonation depth	140
5.11.1	Carbonation depth in concrete incorporating RCA treated with HCl.....	140
5.11.2	Carbonation depth in concrete incorporating RCA treated with H ₂ SO ₄	142
5.11.3	Carbonation depth in concrete incorporating AS	144
5.12	Resistance to the penetration of chloride ions	145
5.12.1	Resistance to the penetration of chloride ions in concrete incorporating RCA treated with HCl	145
5.12.2	Resistance to the penetration of chloride ions in concrete incorporating RCA treated with H ₂ SO ₄	147
5.12.3	Resistance to the penetration of chloride ions in concrete incorporating AS	148
5.13	Combination of durability and mechanical properties	148
5.14	Drying shrinkage of concrete	153
5.14.1	Drying shrinkage in concrete incorporating RCA treated with HCl	154
5.14.2	Drying shrinkage in concrete incorporating RCA treated with H ₂ SO ₄	157
5.14.3	Drying shrinkage in concrete in concrete incorporating AS	159
5.15	Summary of Chapter 5.....	161
6	Summary and final conclusions	163

6.1	Summary of phase 1- optimal determination of acid molarity for removal of mortar adhered to RCA.....	163
6.2	Summary of phase 2 - Evaluation of the mechanical, fracture and durability performance of mixes concrete incorporating RCA treated with acid solutions and with addition of aluminium sulphate	164
6.3	Final conclusions and future perspective.....	165
7	REFERENCES	167

LIST OF FIGURES

Figure 2-1 Calcium dissolved from RCA in acid solution.	14
Figure 2-2 Normal (untreated RCA) (a), treated RCA at 0.1 M (b), treated RCA at 0.5 M (c) and treated RCA at 0.8 M (d).....	21
Figure 2-3 CA particle size with different mortar contents; (a) relationship between concentration of HCl (M) and mortar loss of mass (% Wt) (b).....	23
Figure 2-4 Relationship between concentration of H ₂ SO ₄ and mortar loss of mass (% Wt).	24
Figure 2-5 Age of curing (days) versus compressive strength with HCl treatment.	30
Figure 2-6 Drying shrinkage of concrete mixes <i>versus</i> drying time.	33
Figure 2-7 ITZ for concrete with RCA without pre-soaking treatments(a); ITZ for RCA treatment with HCl (b); ITZ for RCA treatment with H ₂ SO ₄ (c); and ITZ for RCA treatment with H ₃ PO ₄ (d).....	34
Figure 3-1 Flowchart of the methodology of the experimental programme.	41
Figure 3-2 Jaw crusher used in the production of RCA (a); size fractions of RCA used in this study (b).	43
Figure 3-3 Water absorption measurement using hydrostatic weighing.	46
Figure 3-4 Procedure for pre-soaking RCA with HCl and H ₂ SO ₄	48
Figure 3-5 Slump test, Abrams cone.	52
Figure 3-6 Compressive strength test setup.....	53
Figure 3-7 Splitting tensile strength test procedure.....	55
Figure 3-8 Modulus of elasticity test procedure.....	56
Figure 3-9 Specimens' geometry: front view (a); top view (b).....	57
Figure 3-10 Manufacture of the fracture energy test specimens.	58
Figure 3-11 Application of the splitting load.	58
Figure 3-12- Water absorption by immersion test procedure.....	59
Figure 3-13 Water absorption by capillary test procedure.	61
Figure 3-14 Carbonation test procedure.	62
Figure 3-15 Resistance to the penetration of chloride ions test procedure.....	63
Figure 3-16 Concrete shrinkage test procedure.....	64
Figure 3-17 Sample for SEM analysis.....	66
Figure 3-18 microstructural analysis procedure using Scanning Electron Microscopy (SEM)	66

Figure 4-1 XRD pattern of the CEM I 42.5R Portland cement. 69

Figure 4-2 XRD pattern of the AS..... 70

Figure 4-3 Concentration of HCl *versus* mass loss (%) in diameters of 11.2 mm , 16 mm and 22.4 mm for 1, 3 and 6 days. 73

Figure 4-4 Concentration of H₂SO₄ *versus* mass loss (%) in diameters of 11.2 mm , 16 mm and 22.4 mm for 1, 3 and 6 days. 75

Figure 4-5 Particle size distribution for NA. 77

Figure 4-6 Particle size distribution for RCA treated with HCl pre-soaking one day (a); Particle size distribution for RCA treated with HCl pre-soaking 3 day (b); Particle size distribution for RCA treated with HCl pre-soaking one day 6 days (c)..... 78

Figure 4-7 Particle size distribution for RCA treated with H₂SO₄ pre-soaking one day (a); Particle size distribution for RCA treated with H₂SO₄ pre-soaking 3 day (b); Particle size distribution for RCA treated with H₂SO₄ pre-soaking one day 6 days (c)..... 80

Figure 4-8 HCl molaritty (M) *versus* oven-dry density of 11.2 mm diameter RCA (a); 16 mm diameter (b); and 22.4 mm in diameter (c)..... 83

Figure 4-9 H₂SO₄ molaritty (M) *versus* oven-dry density of 11.2 mm diameter RCA (a); 16 mm diameter (b); and 22.4 mm in diameter (c)..... 84

Figure 4-10 Relationship molarity and water absorption of RCA treated with HCl submerged for 1, 3 and 6 days for diameters 11.2mm (a); 16mm (b); 22.4mm (c). 85

Figure 4-11 Relationship between molarity and water absorption of RCA treated with H₂SO₄ submerged for 1, 3 and 6 days for diameters 11.2mm (a); 16mm (b); 22.4mm (c). 87

Figure 4-12 Relationship between oven-dry density and water absorption of RCA treated with HCl submerged for 1, 3 and 6 days for diameters 11.2mm (a); 16mm(b); 22.4mm(c). 88

Figure 4-13 Relationship between oven-dry density and water absorption of RCA treated with H₂SO₄ submerged for 1, 3 and 6 days for diameters 11.2mm (a); 16mm(b); 22.4mm(c). 89

Figure 4-14 Comparison between density and water absorption of recycled aggregates 90

Figure 5-1 Particle size distribution of the aggregates and Faury’s reference curve 93

Figure 5-2 Slump test of all concrete mixes containing treated RCA, untreated and with AS (a); slump test of concrete mixes *versus* acid concentration (M) of HCl and H₂SO₄. 95

Figure 5-3 Bulk density of all concrete mixes containing treated RCA (a); untreated and with AS (a); bulk density of concrete mixes *versus* acid concentration (M) of HCl and H₂SO₄ (b). 96

Figure 5-4 SEM/EDS observation of the concrete sample with AN at magnification 1500x showing the ITZ (a); general observation of the sample at magnification 500 (b); observation at magnification 5000x marking the EDS analysis points and the C-H formation (c); EDS spectrum of the evaluated line (ITZ) (d). 98

Figure 5-5 SEM/EDS observation of a concrete sample with RCA at 500x magnification showing the ITZ, pores and the analysis zone (a); general observation of the sample at 1500 magnification marking the EDS analysis points (b); observation at 5000x magnification showing the formed ITZ (c); EDS spectrum of the ITZ (d). 99

Figure 5-6 SEM/EDS observation of concrete sample with RCA treated with 0.3 HCl at 500x magnification showing the ITZ, pores and the analysis zone (a); general observation of the sample at 1500 magnification marking the EDS analysis points (b); observation at 5000x magnification showing the formed ITZ (c); EDS spectrum of the ITZ (d). 100

Figure 5-7 SEM/EDS observation of concrete sample with RCA treated with 1.0 HCl at 500x magnification showing the ITZ, pores and the analysis zone (a); general observation of the sample at 1500 magnification marking the EDS analysis points (b); observation at 5000x magnification showing the formed ITZ (c); EDS spectrum of the ITZ (d). 101

Figure 5-8 SEM/EDS observation of concrete sample with RCA treated with 3.0 HCl at 500x magnification showing the ITZ, pores and the analysis zone (a); general observation of the sample at 1500 magnification marking the EDS analysis points (b); observation at 5000x magnification showing the formed ITZ (c); EDS spectrum of the ITZ (d). 102

Figure 5-9 Relationship between concrete mixes with RCAs (RCA) treated with different concentrations of hydrochloric acid (HCl) and the ratio between the atomic masses of calcium and silicon (Ca/Si). 102

Figure 5-10 SEM/EDS observation of concrete sample with RCA treated with 0.3 H₂SO₄ at 500x magnification showing the ITZ, pores and the analysis zone (a); general observation of the sample at 1500 magnification marking the EDS analysis points (b);

observation at 5000x magnification showing the formed ITZ (c); EDS spectrum of the ITZ (d). 103

Figure 5-11 SEM/EDS observation of concrete sample with RCA treated with 1.0 HCl at 500x magnification showing the ITZ, pores and the analysis zone (a); general observation of the sample at 1500 magnification marking the EDS analysis points (b); observation at 5000x magnification showing the formed ITZ (c); EDS spectrum of the ITZ (d). 104

Figure 5-12 SEM/EDS observation of concrete sample with RCA treated with 3.0 H₂SO₄ at 500x magnification showing the ITZ, pores and the analysis zone (a); general observation of the sample at 1500 magnification marking the EDS analysis points (b); observation at 5000x magnification showing the formed ITZ (c); EDS spectrum of the ITZ (d). 105

Figure 5-13 Relationship between concrete mixes with RCA treated with different concentrations of hydrochloric acid (H₂SO₄) and the ratio between the atomic masses of calcium and silicon (Ca/Si). 105

Figure 5-14 SEM/EDS observation of concrete sample with RCA incorporating AS at 500x magnification showing the ITZ, pores and the analysis zone (a); general observation of the sample at 1500 magnification marking the EDS analysis points (b); observation at 5000x magnification showing the formed ITZ (c); EDS spectrum of the ITZ (d). 106

Figure 5-15 Compressive strength (f_{cm}) of RC, RC-RCA and RCA-HCl concrete mixes tested at 7 and 28 days (a); normalisation of compressive strength (f_{cm}) *versus* acid concentration of HCl (M) (b). 108

Figure 5-16 Compressive strength (f_{cm}) of RC, RC-RCA and RCA-H₂SO₄ concrete mixes tested at 7 and 28 days (a); normalisation of compressive strength (f_{cm}) *versus* acid concentration of H₂SO₄ (M) (b). 110

Figure 5-17 Comparison between experimental values from the literature *versus* molarity 112

Figure 5-18 Tensile strength ($f_{ctm,sp}$) of RC, RC-RCA and RCA-HCl concrete mixes tested at 7 and 28 days (a); normalisation of tensile strength ($f_{ctm,sp}$) *versus* acid concentration of HCl (M) (b). 113

Figure 5-19 Tensile strength ($f_{ctm,sp}$) of RC, RC-RCA and RCA-H₂SO₄ concrete mixes tested at 7 and 28 days (a); normalisation of tensile strength ($f_{ctm,sp}$) *versus* acid concentration of H₂SO (M) (b). 114

Figure 5-20 Modulus of elasticity of RC, RC-RCA and RCA-HCl concrete mixes tested at 28 days (a); normalisation of modulus of elasticity (E_{cm}) <i>versus</i> acid concentration of HCl (M) (b).....	116
Figure 5-21 Modulus of elasticity of RC, RC-RCA and RCA-H ₂ SO ₄ concrete mixes tested at 28 days (a); normalisation of modulus of elasticity (E_{cm}) <i>versus</i> acid concentration of H ₂ SO ₄ (M) (b).	118
Figure 5-22 Tensile behaviour of concrete.....	120
Figure 5-23 Splitting force <i>versus</i> CMOD curves for mixes RC.	121
Figure 5-24 Splitting force <i>versus</i> CMOD curves for mixes RCA.	122
Figure 5-25 Splitting force <i>versus</i> CMOD curves for mixes: RCA-0.3HCl(a), RCA-1.0HCl (b), RCA-3.0HCl (c).	123
Figure 5-26 Splitting force <i>versus</i> CMOD curves for mixes: RCA-0.3 H ₂ SO ₄ (a), RCA-1.0 H ₂ SO ₄ (b), RCA-3.0 H ₂ SO ₄ (c).	125
Figure 5-27 Splitting force <i>versus</i> CMOD curves for mixes incorporating AS.	126
Figure 5-28 Normalized relations between compressive strength (f_{cm}), tensile strength (f_{ctm}) and modulus of elasticity (E_{cm}) of concrete mixes with RCA treated with HCl (a); H ₂ SO ₄ (b); and comparison of concrete mixes with RCA treated with HCl, H ₂ SO ₄ and AS with ACI, NBR and Eurocode 2 (c).	129
Figure 5-29 Normalised relationships between compressive strength (f_{cm}), fracture energy (f_{ctm}) and intensity factor (K_I) of concrete mixes with RCA treated with HCl (a); H ₂ SO ₄ (b).	130
Figure 5-30 Water absorption by immersion (%) <i>versus</i> mixes of concrete with RCA treated with HCl (a); normalization of water absorption (%) <i>versus</i> HCl concentration (M) (b).	131
Figure 5-31 Water absorption <i>versus</i> oven-dry density (kg/m ³).....	132
Figure 5-32 Water absorption by immersion (%) <i>versus</i> concrete mixes with RCA treated with H ₂ SO ₄ (a); normalization of water absorption (%) <i>versus</i> H ₂ SO ₄ concentration (M) (b).	133
Figure 5-33 Water absorption <i>versus</i> oven-dry density (kg/m ³).	134
Figure 5-34 Water absorption by capillarity of concrete mixes with RCA treated with RCA (a); correlation between HCl concentration (M) <i>versus</i> water absorption by capillarity (g/mm ²).....	136

Figure 5-35 Evolution of water absorption by capillarity over time in concrete mixes with RCA treated with HCl.	137
Figure 5-36 Water absorption by capillarity of concrete mixes with RCA treated with RCA (a); correlation between H ₂ SO ₄ concentration (M) <i>versus</i> water absorption by capillarity (g/mm ²).....	138
Figure 5-37 Evolution of water absorption by capillarity over time in concrete mixes with RCA treated with H ₂ SO ₄	139
Figure 5-38 Evolution of water absorption by capillarity over time in concrete mixes with RCA incorporating AS.	139
Figure 5-39 Depth of carbonation (mm) of concrete mixes with RCA treated with HCl (a); HCl concentration <i>versus</i> carbonation depth normalisation (b).	141
Figure 5-40 Evolution of carbonation depth with time in RCA treated with HCl.	142
Figure 5-41 Depth of carbonation (mm) of concrete mixes with RCA treated with H ₂ SO ₄ (a); H ₂ SO ₄ concentration <i>versus</i> carbonation depth normalisation (b).	143
Figure 5-42 Evolution of carbonation depth with time in RCA treated with H ₂ SO ₄ . ..	144
Figure 5-43 Depth of carbonation (mm) of concrete mixes with RCA and addition of AS (a); evolution of carbonation depth with time in RCA and addition of AS (b).....	145
Figure 5-44 Resistance to penetration of chloride ions in concrete mixes with RCA treated with HCl (a); relationship between HCl concentration and resistance to penetration of chloride ions at 28 days (b).....	146
Figure 5-45 Resistance to penetration of chloride ions in concrete mixes with RCA treated with H ₂ SO ₄ (a); relationship between H ₂ SO ₄ concentration and resistance to penetration of chloride ions at 28 days (b).	147
Figure 5-46 Relationship between water absorption by immersion and compressive strength (f _{cm}) (a); relationship between water absorption by capillarity and water absorption by immersion (b)	149
Figure 5-47 Capillary water absorption of the RCA concrete treated with HCl (a); H ₂ SO ₄ (b); and AS (c).....	150
Figure 5-48 Relationship between carbonation resistance and water absorption by immersion (a); relationship between carbonation resistance and compressive strength (f _{cm}) (b).	152
Figure 5-49 Relationship between Chloride diffusion coefficient (x10 ⁻¹² m ²) and Water absorption by capillarity (g/mm ²) (a); and f _{cm} (MPa) (b).....	153

Figure 5-50 Drying shrinkage of HCl-treated RCA concrete mixes *versus* drying time.
..... 154

Figure 5-51 Shrinkage calculated according to the EC2 prediction model (a); ACI 209.2
R prediction model (b)..... 157

Figure 5-52 Drying shrinkage of H₂SO₄-treated RCA concrete mixes *versus* drying time.
..... 158

Figure 5-53 Shrinkage calculated according to the EC2 prediction model (a); ACI 209.2
R prediction model (b)..... 159

Figure 5-54 Drying shrinkage of concrete mixes with RCA and addition of AS *versus*
drying time..... 160

Figure 5-55 Shrinkage calculated according to the EC2 prediction model (a); ACI 209.2
R prediction model (b)..... 161

Figure 5-56 Relationship between shrinkage ($\mu\text{m/m}$) and modulus of elasticity (E_{cm}) 161

LIST OF TABLES

Table 1-1 Comparison of international standards for RCA.....	4
Table 2-1 Summary of the physical and mechanical properties measured in concrete and mortar mixes, and techniques reported for RCA.....	22
Table 2-2 Pearson correlation for RCA treated HCl.	23
Table 2-3 Pearson correlation for RCA treated with H ₂ SO ₄	24
Table 2-4 Physical property requirements for the proposed classes.	25
Table 2-5 Summary of measurements of fresh-state properties, mechanical properties and durability.....	35
Table 3-1 Independent and dependent variables of this study.	41
Table 3-2 Reference concrete composition.	50
Table 3-3 Experimental campaign summary second stage.	51
Table 4-1 Chemical composition of cement (% by mass).....	70
Table 4-2 Mass loss of RCA in % with HCl.	72
Table 4-3 Mass loss of RCA in % with H ₂ SO ₄	74
Table 4-4 Particle size distribution for NA.	76
Table 4-5 Particle size distribution for RCA treated with HCl pre-soaking one day.....	79
Table 4-6 Particle size distribution for RCA treated with HCl pre-soaking 3 days.	79
Table 4-7 Particle size distribution for RCA treated with HCl pre-soaking 6 days.	79
Table 4-8 Particle size distribution for RCA treated with H ₂ SO ₄ pre-soaking one day.	81
Table 4-9 Particle size distribution for RCA treated with H ₂ SO ₄ pre-soaking 3 days. ...	81
Table 4-10 Particle size distribution for RCA treated with H ₂ SO ₄ pre-soaking 6 days.	81
Table 4-11 Characteristics of NA.	82
Table 5-1 Concrete mix proportions.....	94
Table 5-2. Slump test of concrete mixes.	95
Table 5-3. Bulk density of concrete mixes.	96
Table 5-4 Compressive strength of cylindrical specimens in concrete mixes with RCA treated with HCl.	108
Table 5-5 Compressive strength of cylindrical specimens in concrete mixes with RCA treated with H ₂ SO ₄	109
Table 5-6 Compressive strength of cylindrical specimens in concrete mixes with RCA treated with the addition of AS.....	111
Table 5-7 Tensile strength in concrete mixes with RCA treated with HCl.....	113

Table 5-8 Tensile strength in concrete mixes with RCA treated with H₂SO₄..... 114

Table 5-9 Tensile strength in concrete mixes with RCA treated with the addition of AS.
..... 115

Table 5-10 Modulus of elasticity (E_{cm}) at 28 days of concrete mixes with RCA treated
with HCl. 117

Table 5-11 Modulus of elasticity (E_{cm}) at 28 days of concrete mixes with RCA treated
with H₂SO₄. 118

Table 5-12 Modulus of elasticity (E_{cm}) at 28 days of concrete mixes with RCA and
incorporation of aluminium sulphate (AS)..... 119

Table 5-13 Fracture energy (G_F) for RC and RC-RCA reference mixes. 122

Table 5-14 Fracture energy (G_F) for the mixes with HCl treated RCA..... 124

Table 5-15 Fracture energy (G_F) for the mixes with H₂SO₄ treated RCA..... 125

Table 5-16 Fracture energy (G_F) for the mixes incorporating AS..... 126

Table 5-17 Stress intensity factor (K_I) results. 127

Table 5-18 Water absorption at 28 days in concrete mixes with RCA treated with HCl.
..... 131

Table 5-19 Water absorption at 28 days in concrete mixes with RCA treated with H₂SO₄.
..... 133

Table 5-20 Water absorption at 28 days in concrete mixes with RCA treated with AS
..... 134

Table 5-21 Results of water absorption by capillarity for the mixes with RCA treated with
HCl 136

Table 5-22 Results of water absorption by capillarity for the mixes with RCA treated with
H₂SO₄. 138

Table 5-23 Water absorption by capillarity for the mixes with RCA incorporating AS 139

Table 5-24 Carbonation depth (mm) for mixes with RCA treated with HCl..... 141

Table 5-25 Carbonation depth (mm) for mixes with RCA treated with H₂SO₄. 143

Table 5-26 Carbonation depth (mm) for mixes with RCA and addition of AS. 144

Table 5-27 Resistance to penetration of chloride ions in concrete mixes with RCA treated
with HCl. 146

Table 5-28 Resistance to penetration of chloride ions in concrete mixes with RCA treated
with H₂SO₄. 148

Table 5-29 Resistance to penetration of chloride ions for mixes with RCA and addition of AS..... 148

Table 5-30 Capillary water absorption, sorptivity, and adjustment parameters of the Hall's capillarity model for each concrete mix. 151

Table 5-31 Drying shrinkage of concrete mixes with RCA treated with HCl. 155

Table 5-32 Drying shrinkage of concrete mixes with RCA treated with H₂SO₄. 158

Table 5-33 Drying shrinkage of concrete mixes with RCA and addition of AS..... 160

List of acronyms

3PBT	Three point bending test
AS	Aluminium sulphate
CH	Calcium hydroxide
CH ₃ COOH	Acetic acid
CMOD	Crack mouth opening displacement
C-S-H	Calcium silicate hydrate
CTT	Compact tension test
E _{cm}	Secant modulus of elasticity of concrete
f _{cm}	Mean value of concrete cylinder compressive strength
f _{ctm}	Mean value of axial tensile strength of concrete
G _F	Fracture energy
H ₂ SO ₄	Sulphuric acid
H ₃ PO ₄	Phosphoric acid
HCl	Hydrochloric acid
HNO ₃	Nitric acid
ITZ	Interfacial transition zone
K _I	Stress intensity factor
M	Molar concentration
NA	Natural aggregate
Na ₂ SO ₄	Sodium sulphate
p.a	Purity analytics
RCA	Recycled concrete aggregate
WST	Wedge splitting test method
XRD	X-ray diffraction
XRF	X-ray fluorescence

1 INTRODUCTION

The world is undergoing a series of political and economic changes aimed at improving the health and sustainability of the environment in response to environmental problems caused by pollution and climate change. In recent years, CO₂ levels have increased significantly by 40% over the last 200 years, with a further 6% increase from 2020 to 2021 (AKTAR; ALAM; AL-AMIN, 2021). This increase in CO₂ emissions is directly related to the 2 °C increase in global temperature (2022b), representing a major threat to the planet's ecosystem and to human life.

The construction industry plays a crucial role in promoting sustainability, but it is also one of the most polluting sectors of human activity, being responsible for 40% of CO₂ emissions, according to IEA, Buildings (2022a). In addition, waste generated by construction and demolition has devastating effects on natural resources and is expected to reach 2.2 billion tonnes per year by 2025, according to market reports.

Several researchers are currently studying civil engineering practices and production methods to address the concrete performance problem. One of the most important challenges is the lack of reuse of aggregates in new construction projects and factories dealing with recycled materials (SALESA; PÉREZ-BENEDICTO; COLORADO-ARANGUREN; LÓPEZ-JULIÁN *et al.*, 2017; YU; YAZAN; BHOCHHIBHOYA; VOLKER, 2021). The study of recycled aggregates offers a promising solution to the problem of materials currently being sent to landfill.

Recycled Concrete Aggregate (RCA) is a material obtained through the transformation of demolition waste, resulting in a product with suitable chemical and physical characteristics for the construction industry. In Brazil, it is estimated that approximately 84 million cubic meters of construction and demolition waste are generated annually, according to PESQUISA SETORIAL-ABRECON (2022) data. According to the ABRELPE PANORAMA (2022) (2019, based on 2018 data), municipalities collected about 45 million tons of construction and demolition waste in 2018, with the Southeast region accounting for over 50% of this total. The generation of construction waste is usually predicted using socio-economic indicators. Surveys

conducted in different Brazilian municipalities indicate that *per capita* construction waste generation ranges from 168 to 760 kg/hab.year (ANGULO,2005; ANGULO *et al.* 2022; JOHN, 2000), resulting in a median value close to 500 kg/hab.year for the country's municipalities in 2022. Due to the predominant construction patterns in Brazil, the highest proportion of material found in construction waste is mortar (63%), especially concrete mortar used in structural compositions, making recycled crushed stone or aggregate the most commonly generated recyclable material in construction waste recycling units. Concrete and blocks follow at 29%, organic waste at 1%, and others at 7% (ANGULO, 2022). Brazil has put forward a strategic Action Plan as part of the 2030 Agenda, comprising four key components, with one of them aligning with the Sustainable Development Goals (SDGs). This plan encompasses 17 distinct objectives along with 169 specific targets to be accomplished by the year 2030. The 12th goal, identified as Responsible Consumption and Production, is geared towards curtailing waste generation through a spectrum of measures, including prevention, reduction, recycling, and reuse. This latter aspect holds significant value in the realm of sustainability, as it delivers advantages such as diminished energy consumption, reduced emissions of pollutants (gases), and decreased water usage, surpassing the benefits offered by recycling alone (Instituto Brasileiro de Geografia e Estatística, 2022). Therefore, RCA is a promising solution for sustainability in the construction industry, as its use can significantly reduce the amount of waste sent to landfills, thereby helping to mitigate the environmental impact of construction activities.

Recycled concrete aggregate (RCA) is often used as a substitute for natural aggregate (NA) in the construction industry. While these new materials have potential environmental benefits, they face limitations in achieving conventional performance. Several codes and regulations have been established around the world to address the use of recycled aggregate, more specifically recycled concrete, in concrete applications.

Countries such as Germany, Italy, Spain, Portugal, Brazil, Japan, the United Kingdom, Hong Kong and the United States have specific guidelines for the use of recycled concrete aggregate (RCA) in non-structural and structural applications, including maximum stresses to ensure proper use of this aggregate by limiting the percentage of replacement in the volume of concrete. Table 1-1 presents an overview of the use and regulations that some countries specify for the use of RCA. It is important to

note that these guidelines aim to ensure that the use of RCA does not compromise the safety or quality of the concrete produced.

The limitation of using RCA is due to the fact that it has high porosity, high water absorption, low density, and weak adhesion between the interfacial transition zone (ITZ) and the contained mortar, resulting in low mechanical strength of the concrete (EVANGELISTA; DE BRITO, 2014; POON; SHUI; LAM, 2004; SIDOROVA; VAZQUEZ-RAMONICH; BARRA-BIZINOTTO; ROA-ROVIRA et al., 2014; SILVA; NEVES; DE BRITO; DHIR, 2015). Therefore, the modification of the ITZ microstructure has been a major concern for improving the properties of recycled aggregate concrete (RAC). Generally, the content of mortar adhered to the recycled aggregate varies between 20-70% by weight (RODRÍGUEZ; ALEGRE; MARTÍNEZ, 2007) being influenced by the grinding process. Due to the negative impact of adhered mortar on recycled aggregate properties, several researchers have explored different approaches and techniques to improve them (AKBARNEZHAD; ONG; ZHANG; TAM *et al.*, 2011; ISMAIL, S.; RAMLI, M., 2013; LEE; DU; SHEN, 2012; MAKUL, 2021; SUI; MUELLER, 2012; TAM, V. W.; TAM, C. M.; LE, K. N., 2007). There are two main techniques to improve the adhesion between recycled aggregate and cement paste. The first technique involves the removal of the mortar adhered to the recycled aggregate, which can be performed by chemical treatments (ABBAS; FATHIFAZL; ISGOR; RAZAQPUR *et al.*, 2007; AKBARNEZHAD; ONG; ZHANG; TAM, 2013; AKBARNEZHAD; ONG; ZHANG; TAM *et al.*, 2011; AL-BAYATI; DAS; TIGHE; BAAJ, 2016; ISMAIL, S.; RAMLI, M., 2013; ISMAIL; RAMLI, 2014; KIM, Y.; HANIF, A.; KAZMI, S. M. S.; MUNIR, M. J. *et al.*, 2018; PANDURANGAN; DAYANITHY; PRAKASH, 2016; PURUSHOTHAMAN; AMIRTHAVALLI; KARAN, 2014; SARAVANAKUMAR; ABHIRAM; MANOJ, 2016; TAM, V. W. Y.; TAM, C. M.; LE, K. N., 2007), heat treatments (such as traditional heating and microwave heating) (AKBARNEZHAD; ONG; ZHANG; TAM *et al.*, 2011; SHIMA; TATEYASHIKI; MATSUHASHI; YOSHIDA, 2005), mechanical treatments (OGAWA; NAWA, 2012; YONEZAWA; KAMIYAMA; YANAGIBASHI; KOJIMA et al., 2001), combination of heating and mechanical treatments (SUI; MUELLER, 2012), or even, the combination of chemical and mechanical treatments (WANG; WANG; QIAN; CHEN et al., 2017). The second technique consists of improving the adhesion between the recycled aggregate and the cement paste through the use of polymers (KOU; POON, 2010), silicones, biodeposition

of calcium carbonate, incorporation of pozzolanic materials such as fly ash, silica fume, carbonation and sodium silicate solution.

The improvement of the recycled aggregate of RCA concrete can increase the possibilities of using this aggregate in more demanding applications, contributing to the reduction of the environmental impact of concrete produced with conventional materials, as well as to the safe and sustainable disposal of construction and demolition waste generated worldwide. In the present thesis, the elimination of the mortar adhered to the concrete aggregate was evaluated, using acid solutions (HCl and H₂SO₄) to improve the matrix-aggregate interface, in addition to the use of aluminium sulphate (AS). The use of these techniques allowed the use of mining waste (acid solutions), and aluminium sulphate can be obtained from wastewater treatment sludge. This work was carried out in response to the effectiveness of acid and aluminium sulphate treatments in improving the mechanical properties and durability of mixes with 100% incorporation of RCA.

Table 1-1 Comparison of international standards for RCA.

Standard	Classification	Coarse	Applications	Maximum strength	References
Germany, DIN 4226-100	RCA	20-35%	Structural concrete, prestressed concrete not allowed	C30/37 (20% replacement), C25/30 (35% replacement)	(DIN 4226-100, Aggregates for concrete and mortar - Part 100: Recycled aggregates, 2002)
USA, ACI 555R-01	RCA	50%	Non-structural concrete	—	(ACI, 2022)
UK, BS 8500-2	RCA	20%	Structural concrete	C40/50	(BRITISH STANDARD, 2016)
ABNT NBR 15116	RCA	20%	Structural concrete	20 MPa	(ABNT, 2004)
HK, WBTC No.12/2002	RCA	100%	Less demanding applications	20 MPa	(WBTC, 2002)
		20%	Structural concrete	35 MPa	
Japan, JIS A5021	RCA		Structural concrete	—	(JIS, 2006)
Portugal, LNEC-E471	RCA 1	25%		C35/45	(LNEC, 2009)
	RCA 2	20%		C40/50	
Italy, NTC-2008, UNI EM 12620:2013	RCA	30%	Structural concrete	30 MPa	(NTC, 2008)
		60%	Structural concrete	25 MPa	
RILEM, TC-121 DRC, 37 DRC Butler et al., de Brito <i>et al.</i> (1994)	Type 2	20%	Structural concrete	50 MPa	(RILEM, 1994) (DE BRITO; AGRELA; SILVA, 2019; HANSEN, 1986)
		100%	Non-structural concrete	—	

1.1 Remarks from the literature review

According to the analysis of literature review (part of chapter 2), it can be concluded that treatments with acids HCl and H₂SO₄ are effective in removing the mortar adhered to NA, improving its physical and morphological characteristics. However, there are some gaps to have in consideration to create new concrete with RCA. These are identified below:

- It is known that pre-soaking in HCl and H₂SO₄ acids are effective in removing the adhered mortar from the RCA, but it is still unclear to what extent the acid molarity is effective in removing it without damaging the RCA;
- The pre-soaking time is a determining factor for the effectiveness of the method, but it is still not clear which immersion time in an acid solution optimizes this removal without losing performance;
- Although the benefits of using treated RCA on the mechanical properties of concrete with this type of aggregates are known, there are not enough analyses to correlate these properties with the acid molarities or the type of acid used. This type of correlations will allow a better understanding of the interaction of the RCA treated with the cement matrix;
- The study of the literature showed that, in terms of fracture properties, there are some gaps that can be studied. They refer to the use of only one type of acid (HCl) and obtaining parameters such as the intensity factor;
- Some properties in terms of durability were studied in the literature review on concrete treated with RCA, but there are still gaps in these properties with HCl and H₂SO₄ acids;
- Regarding AS, there are gaps that can be filled, since it is known that concrete with addition of aluminium sulphate in percentages of 1.1% improve the mechanical characteristics, it is not fully clarified what the influence on the durability and fracture mechanics properties is.

1.2 Problem definition

Despite the treatments with HCl and H₂SO₄ acids have shown improvements in the physical and morphological properties of RCA, its acid concentration and pre-immersion time is not yet clearly determined which represents a gap in the research of removing the mortar adhered to NA. Moreover, it is also necessary to study the influence of the addition of aluminium sulphate in concrete mixes with RCA on the durability and fracture properties.

1.3 Research question

According to the conclusions from literature review and the gaps that were previously described, the research work presented in this thesis relies on the following research question:

What are the effects of treatments made with acids of hydrochloric acid (HCl) and sulphuric acid (H₂SO₄) and the addition of aluminium sulphate (AS) on the performance of recycled concrete aggregates and its derived concrete?

1.4 Research hypothesis

The presented research question leads to the hypothesis of this thesis described here. If the use of HCl, H₂SO₄, and AS improves the performance of concrete, any excess of these components will be harmful to its properties due to the interaction between the aggregate and the cementitious matrix, besides reducing the quality of the RCA by having residual content of sulphate ions.

The study of this hypothesis in the present research work aims to evaluate the improvement of RCA treated with the acids of HCl and H₂SO₄. Furthermore, the study also addresses the incorporation of the RCA treated with these acids and the addition of AS to answer the framed hypothesis.

To this end, several research goals were defined as followed in both first and second stage of the study that compounds this thesis:

During the first stage, the goals were the following:

- Production and crushing of the RCA to isolate and monitor the effects produced

by this type of aggregates in concrete mixes.

- Characterization of the RCA by means of its physical properties (water absorption, density, and grading tests);
- Mortar removal analysis of RCAs with HCl and H₂SO₄ solutions;
- Analysis of the mortar removal in the RCA defining the acid ratio and pre-immersion time for the concrete production phase.

During the second stage, the goals derived directly on the first stage analysis of the results that framed the development of concrete mixes, which were the following:

- Development of mixes with RCA alone and RCA treated with HCl and H₂SO₄ for the analysis in the fresh and hardened state;
- Characterization in the fresh state of concrete mixes with NA, RCA alone, RCA treated and with the addition of AS;
- Characterization of concrete in the hardened state in terms of its mechanical properties, durability, and fracture mechanics;
- Microstructure analysis through observations on the scanning electron microscope (SEM) of the concrete with NA, RCA alone, RCA treated, and with added AS.

1.5 Research contributions

This section consists of a description over the thesis structure and the way this research was organized according to its contributions to literature. The procedures and outcomes of the research work are organized into five main chapters. After introducing the research problem, the research question and the hypothesis over the topic of this thesis on the present chapter of the introduction, chapter 2 presents a literature review, followed by the procedures and methods undertaken on the experimental program, in chapter 3. Both chapters 4 and 5 present findings and the results of the research study and the conclusion can be found on the last chapter of the document including future work directions (chapter 6). A brief summary of each chapter is presented, respectively:

Chapter 1 - Introduction

The first chapter presents the motivation and considerations that derived from literature review, presenting the main conclusions of related work from other authors who address treatments with acids HCl and H₂SO₄ as a way to remove the mortar adhered to NA. Gaps to create new concrete with RCA are listed accordingly. Problem definition, research question and hypothesis are framed, followed by the research contributions.

Chapter 2 - Literature review

The second chapter consists on the literature review of the removal of mortar adhered to NA using the acid solution removal technique. In the initial part of the chapter, the physical and chemical properties of RCA treated with acid solutions are explained. Subsequently, the mechanical, fracture and durability properties of concrete with the incorporation of this type of RCA are addressed. After describing the properties of the treated RCA, a statistical analysis of the physical properties (water absorption) and the mortar removal rate is presented as a function of the acid concentration of the two most common types of acid found in the literature (HCl and H₂SO₄) in order to determine the best combination of acid concentration (M) and pre-soaking time for mortar removal. At the end, the properties of concrete with the use of aluminium sulphate in the properties in the hardened state are described.

A review about the improvement of the quality of RCA subjected to chemical treatments was published alongside this thesis, highlighting the main factor that alters the quality of RCA as being the paste adhered to NA (DE JUAN; GUTIÉRREZ, 2009). The paper presents a review of treatments for the removal of adhered paste using acid solutions on the RCA, and their influence on the mechanical properties and durability of concrete produced with RCA.

Chapter 3 - Experimental program

The third chapter describes the materials and methodologies that were used in the production of the several mixes. Firstly, the characterization on how the materials (cement, NA and RCA) were made, are explained, as well as the techniques that were carried out and used for this purpose. Subsequently, the formulation of the reference concrete composition can be found, in addition to the tests carried out on the fresh and hardened mixes, followed by the process for a microstructural analysis of the mixes with

regard to the improvement of the ITZ.

First phase: Optimal determination of acid molarity for removal of mortar adhered to recycled concrete aggregate.

Chapter 4 - Characterization of materials and mortar removal performance in RCA

In this chapter, the results of the characterizations of the aggregates and the materials used in the experimental campaign that comprises this thesis are detailed. Initially, the results obtained in the crystallographic and chemical analysis of cement and aluminium sulphate are explained. Afterwards, a rigorous analysis of the natural and recycled aggregates was carried out, namely in the 24-hour water absorption, water absorption over time and volumetric mass tests, is described. By the end, the results in percentage of mortar removal in the RCA can be found and the limitations of this procedure are clearly explained.

Second phase: Mechanical properties of fracture and durability of produced concrete mixes with RCA.

Chapter 5 - Mechanical properties of fracture and durability of produced concrete mixes with RCA

Chapter 5 derives from the results obtained in the previous chapter in what concerns the rigorous analysis of the reduction of the mortar adhered to RCA. At this point, an analysis of the rheological behaviour in the fresh state (Abrams's cone) of the concrete that incorporate recycled aggregates concrete treated with acid solutions (HCl and H₂SO₄) and the addition of sulphate to its behaviour in the hardened state, more specifically in the mechanical, fracture and durability properties, is provided. Finally, observations were made in the scanning electron microscope of the different compositions and a comparative analysis between its properties.

Chapter 6 - Conclusion and future work

Chapter 6 presents the conclusions obtained in the experimental campaign that was conducted during the development of this thesis and the analysis of the results of this research. The goal of the research work is discussed in order to identify the advantages and disadvantages of using the technique of removing mortar by acid solutions and improvements in mechanical properties, durability and fracture in the incorporation of this

type of aggregates and addition of aluminium sulphate, focusing on filling the gaps that were initially found in the literature review. Likewise, future directions were provided, according to the presented results, which may inspire other authors in related work.

2 LITERATURE REVIEW

2.1 Introduction

This chapter presents a comprehensive literature review on the physical properties of acid-treated recycled concrete aggregate (RCA) and the understanding on the mechanical properties in the making in the production of concrete. As it is known, acid treatment of RCA tends to improve its physical properties and therefore the properties in the hardened state of concrete made with it.

In addition to acid treatments in RCA, a literature review was also performed on the use of AS as an additive that improves the mechanical properties in concrete containing RCA as aggregate.

A systematic review was carried out to identify the main topics of the improvement of treated RCA on the different properties to list all relevant information concerning the acid treatment (molarity and suitable acid type). The review covers all kinds of acids used for mortar removal in RCA, and how they affect the other properties. For this review, a statistical analysis was performed on the physical properties of RCA treated with different acids using Pearson's correlation, which relates continuous variables by measuring the degree of correlation between variables. This correlation is of great importance to determine the content of the acid solution and the pre-soaking time of the RCA.

Therefore, there are some lacunas in the knowledge about this type of treatment and additions that can be studied, mainly regarding the immersion time and acid molarity, besides the properties in terms of durability and fracture in concrete containing treated RCA. There are several acids used for this improvement, but the analysis was focused on the acids HCl and H₂SO₄ because they result from residues of primary industries. Concerning AS, this polymer was chosen because it is one of the main components used in the flocculation of wastewater treatment.

Finally, the analysis in this chapter has already been published in Materials Journal referenced as Forero *et al.* (2022).

2.2 Chemistry of acid treatment in RCA

The chemical treatment technique of pre-soaking RCA in acid solutions has been an effective method for the elimination of adhered mortar in RCA and the improvement of its properties. It consists of an acid attack associated with the reaction of an acid (HX) and the calcium hydroxide (CH) portion of the cement paste. This produces a highly soluble calcium salt (CX, where X is the negative ion of the acid) by-product that is easily removed from the cement paste, thus weakening the paste's structure as a whole Equation 2-1 (BEDDOE; DORNER, 2005; SCRIVENER; YOUNG, 2014).

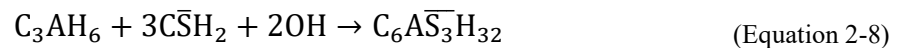
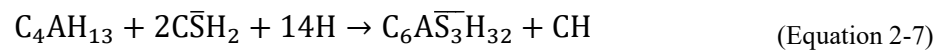
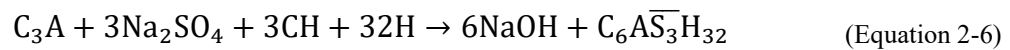
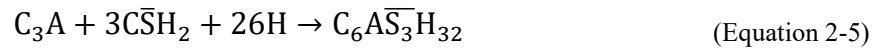
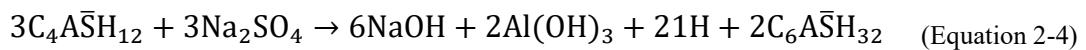
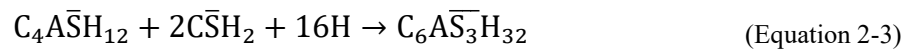
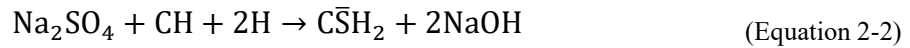


Once the acid interacts with concrete, three major reactions are triggered. Firstly, the hydration products react with acid, forming dissolved ions, thus losing the mortar adhered to the NA; this reaction is called acidolysis. Secondly, depending on the type of acid, insoluble salts form and precipitate, causing expansion and cracking. Other reactions create complexes with calcium, aluminium, iron, and silicate ions, which produce much higher concentrations of these ions in the solution that would otherwise lead to dissolution. This can potentially occur under pH conditions in which cement would normally be relatively stable (complexolysis). Depending on the acid used, more than one of these detrimental mechanisms can be effective (HEWLETT; LISKA, 2019; KURDOWSKI, 2014).

The first mechanism increases the content of sulphate ions (SO_4^{2-}) in the adhered mortar of the RCA through the addition of HCl, H_2SO_4 , and H_3PO_4 . The chemical reactions responsible for cement corrosion depend on the type of acid solution. Cement is an alkaline material with C_3S , C_2S , C_3A and C_4AF as its main components, whose reaction with water form hydration products—calcium silicate hydrate (C-S-H), calcium hydroxide or portlandite (CH), ettringite ($\text{C}_6\text{AS}_3\text{H}_{32}$), calcium monosulphoaluminate ($\text{C}_4\text{AS}_3\text{H}_{12}$), and hydrogarnet (C_3AH_6), among others. Thus, they constitute a cementitious structure that can easily be attacked by strong acids (MEHTA; MONTEIRO, 2017; MINDESS, SIDNEY; YOUNG, FJ; DARWIN, DAVID, 2003).

A sulphate attack generates a series of reactions in the cementitious matrix of the concrete, due to the penetration of SO_4^{2-} in the cement structure from the exposure of the RCA to acids and the environment. When external sources of sulphate ions penetrate the

cementitious matrix, initiating chemical reactions with the hydrated products such as portlandite (Equation 2-2), they form gypsum and calcium aluminate phases, which form ettringite. This is followed by reactions of monosulphate (Equation 2-3 and Equation 2-4), tricalcium aluminate (Equation 2-5 and Equation 2-6), tetracalcium aluminate hydrate (Equation 2-7) and hydrogarnet (Equation 2-8) (CLIFTON; POMMERSHEIM, 1994; SARKAR; MAHADEVAN; MEEUSSEN; VAN DER SLOOT *et al.*, 2010). The calcium ions are initially supplied by portlandite and, when the ions are no longer available, the calcium silicate hydrate dissociates in the silica gel, providing the ions for the formation of ettringite (BROWN; TAYLOR, 1999; CLIFTON; POMMERSHEIM, 1994).



The acidolysis mechanism takes place when the cement hydration products react with acids in the form of dissolved ions (HEWLETT; LISKA, 2019). In particular, when the acid solution penetrates the pores of concrete, it dissolves the constituents; calcium cation is the first to be dissolved (Figure 2-1), given that portlandite becomes soluble at high pH values. Exposure to the acid solution also causes loss of calcium—descaling—from the C-S-H gel, leaving behind a relatively weak silica gel. These poorly soluble salts can act as a partial inhibitor of the general process, blocking the tiny passage of cement paste through which water flows (BEDDOE; DORNER, 2005; HEWLETT; LISKA, 2019;

LEE; DU; SHEN, 2012).

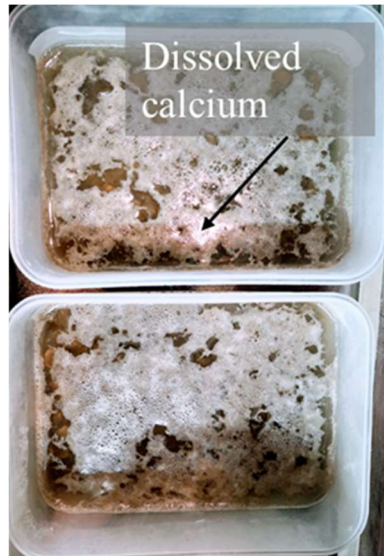


Figure 2-1 Calcium dissolved from RCA in acid solution.

Consumption of cement hydration products, particularly $\text{Ca}(\text{OH})_2$ due to the action of HCl and nitric acid (HNO_3), results in the formation of CaCl_2 and $\text{Ca}(\text{NO}_3)_2$ salts, respectively. These soluble salts can be easily transported to the external parts of mortar using water. In this situation, the continuous reactions increase the porosity of the cement paste, and the increase in pore volume accelerates the reaction rate. In the case of an attack of H_2SO_4 , the assessment of deleterious reactions can be divided into two parts. In the first stage, the deterioration of $\text{Ca}(\text{OH})_2$ results in expansive plaster formation. Then, the plaster reacts with C-S-H in an aqueous environment and forms a more expansive product called ettringite (ALLAHVERDI; SKVARA, 2000; WANG; WANG; QIAN; CHEN *et al.*, 2017).

Another chemical reaction present in the removal of adhered mortar in RCA is the one between the mineralogical nature of the RCA and acids. According to Dyer (2014), when limestone aggregate is in contact with an acid, the following reaction occurs (Equation 2-9):



Limestone aggregates neutralize acids as they dissolve, making it difficult to remove mortar from the RCA, whereas siliceous aggregates are inert to acid attack

(ALEXANDER; FOURIE, 2011; RAMASWAMY; SANTHANAM, 2019).

2.3 RCA properties

The mechanical and durability properties of concrete produced with RCA are directly influenced by the characteristics of the source material, e.g. w/c ratio, type of cement, and strength, in addition to other factors such as production and storage (DE BRITO; SAIKIA, 2012; DE BRITO; SILVA, 2016; SILVA; DE BRITO; DHIR, 2015; VERIAN; ASHRAF; CAO, 2018). This high variability in the RCA can affect the removal of adhered mortar using acids. RCA made with cement with a high C_3S content shows higher compressive strength at 28 days, demands a higher w/c ratio, and hydrates faster. The abovementioned results in a higher content of $Ca(OH)_2$ and a larger porous structure that is more vulnerable to an acid attack, increasing the removal of adhered mortar (ALLAHVERDI; ŠKVÁRA, 2000). The effectiveness of removing mortar in RCA from concrete with a partial replacement of cement with pozzolanic admixtures or chemical admixtures varies due to differences in their chemical composition, i.e. the type of cement or chemical admixtures used. Pavlík and Unčik (1997) investigated the influence of the w/c ratio on the mortar corrosion process by acetic acids (CH_3COOH) and HNO_3 , showing that the corrosion rate decreases with an increase in the cement content per unit volume of the hardened paste. The author stated that there are two main causes related to this fact: the increased neutralization capacity of the matrix and the increase in diffusion resistance of the corroded layer. The following are the main properties of RCA after being treated with acid solutions.

2.3.1 Water absorption

Owing to its porous structure, the paste adhered to RCA is more susceptible to water absorption than NA and needs extra water during mixing. A failure to compensate this water will negatively affect the concrete's performance (AMORIM; DE BRITO; EVANGELISTA, 2012; FERREIRA; DE BRITO; BARRA, 2011). There is a high dispersion of water absorption values in RCA, ranging from 1% to 20% (BARBUDO; DE BRITO; EVANGELISTA; BRAVO *et al.*, 2013; BELIN; HABERT; THIERY; ROUSSEL, 2014; CUI; SHI; MEMON; XING *et al.*, 2014; DE BRITO; SAIKIA, 2012; SILVA; DE BRITO; DHIR, 2014), depending on particle size and density. There are

several techniques to improve or modify these characteristics. One of the main techniques for the removal of mortar in RCA is pre-soaking in acid solutions.

The technique initially proposed by Tam *et al.* (2007), consists of the immersion of RCA in acid solutions at different concentrations and immersion times, in order to eliminate the mortar adhered to NA. Afterwards, the RCA is washed with water and oven-dried for 24 h at 100 °C, which allows it to be used. This technique is easy to implement and does not require specific equipment. Tam *et al.* (2007), superficially treated RCA in acid solutions at low concentrations of 0.1 mol with HCl, H₂SO₄, and H₃PO₄. In addition, RCAs with particle sizes of 20 and 11 mm were soaked for 24 h at 20 °C and the decrease in water absorption was obtained: 12.16% for HCl-treated RCA, 11.0% for H₂SO₄-treated RCA, and 8.36% for H₃PO₄-treated RCA for size 11 mm. The results were similar for a particle size of 20 mm, with a reduction in water absorption of 12.12% for HCl-treated RCA, 10.3% for H₂SO₄-treated RCA, and 7.27% for H₃PO₄-treated RCA. The different acids increase the content of SO₄²⁻ in the adhered paste of RCA; when reacting with the main mortar compounds of RCA, as described in Section 2, this allows the removal of the adhered mortar, reducing the water absorption capacity of RCA.

Akbarnezhad *et al.* (2011) showed that acid treatment at low concentrations reduces the RCA's water absorption. Nevertheless, none of these values approaches those of NA. Akbarnezhad *et al.* (2011), used H₂SO₄ to remove the bonded mortar in NA at concentrations of 0.1 M, 0.5 M, and 1 M, with a pre-soaking time of 1 and 5 days. The water absorption reductions of RCA were 2.3% for a 0.1 M molar concentration soaked for 24 h and 120 h, and 16.6% and 61.9% for 1 M molarity submerged for 24 h and 120 h, respectively. Additionally, greater effectiveness occurred when using higher acid concentrations.

Ismail and Ramli (2013) studied the immersion of RCA in low HCl molarities of 0.1 M, 0.5 M, and 0.8 M, with pre-soaking times of 1, 3, and 7 days to improve RCA's characteristics. The study showed that water absorption was reduced in the range of 1% to 28%. Greater reduction was observed at 0.5 M and 0.8 M concentrations and in smaller RCA particle sizes. In addition, it was observed that the pre-soaking time of RCA in the acid solution was not a determining factor in reducing water absorption. Ismail and Ramli (2014), who analysed the effect of using HCl in a 0.5 M concentration solution for a period of 24 h, reported a reduction in the water absorption of RCA of between 19.3% and 16.6%, relative to untreated RCA.

Purushothaman *et al.* (2014), observed that RCA treated with HCl and H₂SO₄ in five particle sizes (20.0, 16.0, 12.5, 10.0 and 4.75 mm), at a concentration of 0.1 M and pre-soaked for 24 h, had a reduction in water absorption of 41% and 58%, respectively, for HCl and H₂SO₄, compared to untreated RCA.

Acid treatments of RCA have been explored by Pandurangan *et al.* (2016), who studied the effects of the bond between acid-treated RCA concrete and reinforcement. Nitric acid (HNO₃) was used to pre-soak RCA at a 1 M molarity for 24 h, a procedure described by Movassaghi (MOVASSAGHI, 2006). The author obtained a 36.7% reduction relative to untreated RCA.

Saravankumar *et al.* (2016) improved the water absorption of RCA using HCl, H₂SO₄, and HNO₃, at a concentration of 0.1 M and after pre-soaking for 24 h. They showed that there was an improvement in water absorption of 10%, 11% and 13% for HCl, HNO₃ and H₂SO₄, respectively.

Al-Bayati *et al.* (2016) analysed the effect of acid solutions of HCl and acetic acid (C₂H₄O₂) on RCA, treated at a concentration of 0.1 M and with a 24 h soaking time. There was a decrease in water absorption of 4.22% for HCl, and of 4.33% for C₂H₄O₂.

Kim *et al.* (2018) studied the effect of acid treatment on RCA, by treating RCA with HCl and sodium sulphate (Na₂SO₄) in an acid solution at a 1:4.5 aggregate: acid ratio (1.2 M), submerged for 48 h, and replacing the solution with a new one after 12 hours of pre-soaking. The results showed a reduction of 38.6% for HCl and of 34.9% for Na₂SO₄.

Tang *et al.* (2019) treated RCA using a 0.5 M solution of H₂SO₄ by pre-soaking it for 24 h and shaking the RCA occasionally inside the acid solution. Then, to ensure that the treated RCA has no residue from the acid solution, the RCA was washed and submerged in water for 24 h. The results after treatment showed a 10% reduction in water absorption compared to untreated RCA.

Wang *et al.* (2017) pre-soaked RCA in an acetic acid (CH₃COOH) solution at an ambient temperature at three different acid concentrations (1%, 3%, 5%), and three different immersion durations (1, 3, and 5 days). The water absorption of all RCA samples was reduced by 9%–19%. The lowest water absorption performance was achieved for RCA treated with 1% acetic acid. The authors mentioned that greater incorporation of

acetic acid increases water absorption of the treated RCA. The authors also explained that this occurs mainly because more pores were produced in the treated RCA samples due to the dissolution of more hydration products, and possibly some NA in the acetic acid.

2.3.2 Determination of mortar loss

The percentage of mass adhered to RCA is determined by the difference between the initial weight and the final weight, as shown in Equation 2-10. Ismail and Ramli (2013) studied the effect of HCl acid on RCA at different concentrations (0.1 M, 0.5 M, and 0.8 M) and immersion times (1, 3, and 7 days). The results showed that at high concentrations the loss of mass is higher, with a linear correlation between these two factors; moreover, the soaking time did not have a great influence on removed mortar mass. Ismail and Ramli (2013; 2014) showed that the removal is greater at smaller RCA sizes. This can be explained by Juan and Gutierrez (2009), who removed the mortar adhered to RCA using HCl acid, showing that smaller aggregates have a range of mortar adhered around 33% to 55% while larger fractions range from 23% to 44%. Other authors also report that the content of adhered mortar is higher in smaller RCA sizes (ABBAS; FATHIFAZL; FOURNIER; ISGOR *et al.*, 2009; ABBAS; FATHIFAZL; ISGOR; RAZAQPUR *et al.*, 2007). The removal of the paste adhered to the RCA is more efficient in aggregates with a higher mortar content, considering that the removal of the mortar depends on the type of cementitious material used in the RCA (SHI; STEGEMANN, 2000). Pavlik (1996) showed the rate of corrosion decreases with an increase in cement content per unit volume of hydrated cement paste (increases with w/c).

$$\% \text{Adhered mortar loss} = \frac{\text{Mass of RCA} - \text{Mass of RCA after treatment}}{\text{Mass of RCA}} \quad (\text{Equation 2-10})$$

A more aggressive and destructive case of acid attack occurs when concrete is exposed to sulphuric acid. The calcium salt produced by the reaction of the H₂SO₄ and calcium hydroxide is calcium sulphate which, in turn, causes increased degradation due to a sulphate attack.

Akbarnezhad *et al.* (2013), used the H₂SO₄ treatment technique to determine the amount of paste adhered to RCA, and proposed four techniques for total removal of the mortar: submerge the RCA in H₂SO₄ at concentrations of 1 M to 6 M; submerge the RCA

in H_2SO_4 at concentrations of 1 M to 6 M, renewing it after every 8 h of immersion, after which the RCA was washed before submerging it again in the solution submerge the RCA at the same concentrations but with continuous agitation of the particles; consider all the procedures previously described in the second and third cases. The results showed that the removal of mortar varied between 12% and 100%, showing that the main factors for this removal were acid concentration and the removal technique (best results: techniques II and IV). In addition, it was observed that the acid concentration lost H^+ ions over time, reducing the degree of attack of the mortar. Washing the RCA before each replacement removed a layer of silica and aluminosilicate gels released by C-S-H from the RCA surface (SHI; STEGEMANN, 2000), increasing the removal efficiency.

Akbarnezhad *et al.* (2011), used H_2SO_4 to remove the mortar at concentrations of 0.1, 0.5 and 1M, reporting mass losses of 2%, 14%, 34% after one day of exposure and mass losses of 2%, 13% and 34% after 5 days of exposure, respectively. Authors such as Al-Bayati *et al.* (2016) and Saravankumar *et al.* (2016), reported mass losses of 3.92% and 5% for RCA for one day of soaking at a concentration of 0.1 M and 2.7 M respectively.

Pre-soaking in acid to determine the mortar loss was also investigated by Kim *et al.* (2018), who studied the effect of using HCl and Na_2SO_4 . The author obtained mass losses between 2.66% and 9.09% for RCA sizes from 2.36 mm to 19 mm for Na_2SO_4 . The values for HCl were 5.34% to 19.91% for the same aggregate sizes. The biggest removal was for HCl as it is a more aggressive acid.

2.3.3 Bulk density

Akbarnezhad *et al.* (2013), produced two types of concrete with 30 MPa and 60 MPa of compressive strength for the production of RCA, using only particles between 8 and 12 mm. There was a linear correlation between the content of mortar in RCA and the decrease in bulk density for the two types of aggregate. There was an increase in mortar content from 0% to 52% (by mass) for RCA produced from 30 MPa concrete resulting in an almost linear decrease in the apparent density of RCA from 2590 to 2295 kg/m^3 . Similarly, an increase in mortar content from 0% to 58% (by mass) for RCA produced from 60 MPa concrete led to a linear decrease in the bulk density of RCA from 2590 to 2340 kg/m^3 . As the density of mortar in 60 MPa concrete is higher than that of 30 MPa concrete, a similar mortar content in RCA produced from 60 MPa concrete has a higher bulk density

than RCA produced from 30 MPa concrete.

Ismail and Ramli (2013) showed that untreated RCA has lower physical properties than NA, and that the particle densities (dry oven condition) of 20 mm and 10 mm RCA were 2330 kg/m³ and 2230 kg/m³, respectively. These figures were lower than those of 20 mm and 10 mm NA (2600 kg/m³ and 2580 kg/m³, respectively). However, the physical properties of RCA improved after immersion in acid, with a higher increase for 10 mm aggregates (4.7%) than for 20 mm aggregates (2.2%) owing to the content of adhered mortar tending to be greater in smaller aggregates than in coarser aggregates (DE JUAN; GUTIÉRREZ, 2009). Due to the relationship between aggregates' density and absorption (DE BRITO; SAIKIA, 2012; SILVA; DE BRITO; DHIR, 2014; TAM; TAM, 2009), the increase in RCA density results in the significant decrease in RCA water absorption. The density of RCA increases in varying concentrations of acid treatment.

Al-Bayati *et al.* (2016), saw improvements of 7.37%, 5.40% in bulk density for C₂H₄O₂ and HCl, relative to untreated RCA. Saravanakumar *et al.* (2016), observed that, after RCA treatment using three acids (H₂SO₄, HNO₃ and HCl), the bulk density had variations of less than 10%, 13% and 13% for each acid relative to untreated RCA, which showed a variation of 15% in relation to NA.

2.3.4 Microscopic analysis of the RCA

According to Ismail and Ramli (2013; 2014), acid treatment at low molarities (0.1 M and 0.5 M) with HCl in RCA reduces the number of loosely adhered particles, leaving a cleaner, smoother surface with less-sharp angles (SILVA; DE BRITO; DHIR, 2014). The authors observed that, with the increase in molar concentration, the brittle particles of the mortar are released due to the increased attack on the mortar caused by the greater addition of H⁺. Figure 2-2 shows a change in the morphology of RCA before (Figure 2-2a) and after treatment with HCl at molar concentrations of 0.1 M (Figure 2-2b), 0.5 M (Figure 2-2c), and 0.8 M (Figure 2-2d). A scanning electron microscope (SEM) clearly shows cleaner and more uniform surfaces.

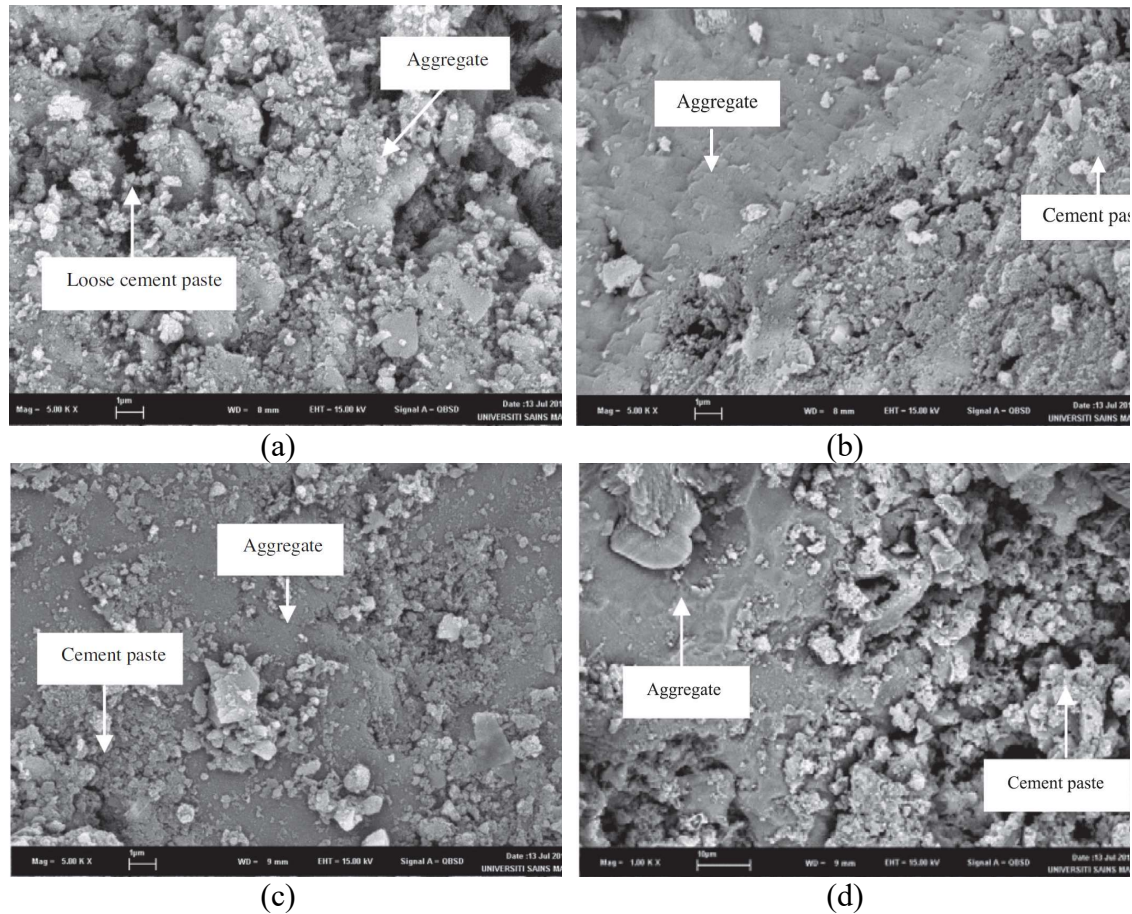


Figure 2-2 Normal (untreated RCA) (a), treated RCA at 0.1 M (b), treated RCA at 0.5 M (c) and treated RCA at 0.8 M (d) (Ismail and Ramli (2013)).

Saravanakuar *et al.* (2016) analysed the microstructural morphology of the effects of treatments with HCl, HNO₃ and sulphuric acid on the surface of RCA, showing the same degradation of the paste observed by Ismail and Ramli (2014). Al-Bayati *et al.* (2016) showed that there are differences on the surface when RCA is treated with strong acids than with weak ones, reaching the same conclusion as the previous authors. A summary of the techniques discussed in this section is presented in Table 2-1.

From the analysis of the collected data, it was observed that there are parameters that seem to be more influential in removing the mortar adhered to RCA. The main parameters observed from the literature review were molar concentration, pre-soaking time, type of acid solution, and aggregate size. For this statistical analysis, two types of acid were chosen (HCl and H₂SO₄), because they are the ones most used by researchers. The analysis established the correlations that exist between the input parameters and the improvement after processing.

Table 2-1 Summary of the physical and mechanical properties measured in concrete and mortar mixes, and techniques reported for RCA.

Measured parameters	Technique	References
Water absorption	Immersion of RCA in acid HCl, H ₂ SO ₄ , and H ₃ PO ₄	Tam <i>et al.</i> (2007)
Water absorption, mortar content, and bulk density	Immersion of RCA in acid H ₂ SO ₄ .	Akbarnezhad <i>et al.</i> (2013); Akbarnezhad <i>et al.</i> (2011)
Water absorption, mortar content, bulk density, and microscopic analysis of the RCA	Immersion of RCA in acid HCl	Ismail and Ramli (2013); Ismail and Ramli (2014);
Water absorption	Immersion of RCA in acid HCl and H ₂ SO ₄	Purushothaman <i>et al.</i> (2014)
Water absorption	Immersion of RCA in acid HNO ₃	Pandurangan <i>et al.</i> (2013); Purushothaman <i>et al.</i> (2016)
Water absorption, mortar content, and bulk density	Immersion of RCA in acid HCl, H ₂ SO ₄ and HNO ₃	Saravankumar <i>et al.</i> (2016)
Water absorption, mortar content, and microscopic analysis of the RCA	Immersion of RCA in acid HCl and C ₂ H ₄ O ₂	Al-Bayati <i>et al.</i> (2016)
Water absorption and mortar content	Immersion of RCA in acid HCl and Na ₂ SO ₄	Kim <i>et al.</i> (2018)
Mortar content	Immersion of RCA in acid HCl	Juan and Gutierrez (2009)
Mortar content	Immersion of RCA in sodium sulphate (Na ₂ SO ₄), magnesium sulphate (MgSO ₄), and magnesium chloride (MgCl ₂)	Abbas <i>et al.</i> (2007); Abbas <i>et al.</i> (2009)
Water absorption, bulk density, and specific gravity	Immersion of RCA in acid H ₂ SO ₄	Tang <i>et al.</i> (2019)
Water absorption and apparent density	Immersion of RCA in acid CH ₃ COOH	Want <i>et al.</i> (2017)

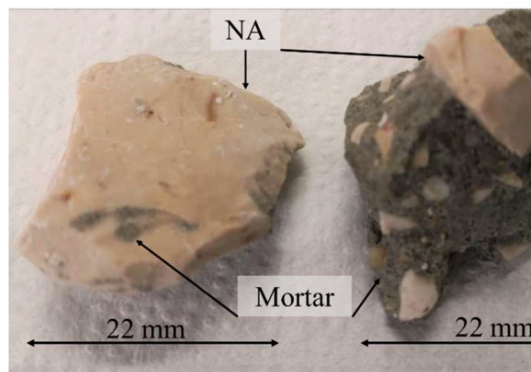
2.3.5 Statistical analysis of RCA properties

Using Pearson's correlation to determine the intensity and direction of the linear relationship between variables (BROWN, 2018; MEYER; KRUEGER, 2001; WALPOLE; MYERS; MYERS; YE, 1993), an analysis was made regarding molar concentration, soaking time, RCA size and water absorption. The analysis shows that there is a small number of relevant correlations. As shown in Figure 2-3a, only some correlations are significant, and they have a reduced degree of significance (p -value equal to or less than 0.05) (BARBUDO; AGRELA; AYUSO; JIMÉNEZ *et al.*, 2012; WALPOLE; MYERS; MYERS; YE, 1993). The results for the HCl treatment of RCA show that Pearson's correlation between molar concentration and mortar loss is $r = 0.40$, indicating a weak correlation between these two variables. This can be explained by the high variability in the mortar content of the RCA, which means that the same aggregate sizes can have different percentages of adhered mortar (ÇAKIR, 2014; DE JUAN; GUTIÉRREZ, 2009; MAKUL, 2020; SHABAN; YANG; SU; MO *et al.*, 2019; SHI; LI; ZHANG; LI *et al.*, 2016; TAM; SOOMRO; EVANGELISTA, 2018), as seen in Figure 2-

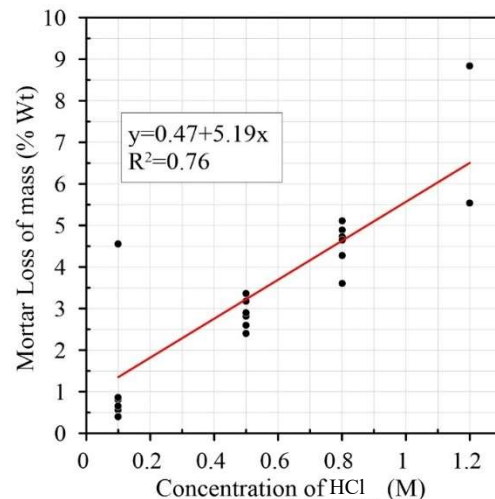
3a. Another important parameter is the degree of significance between the two variables, p -Value = 0.05, with a 95% chance of loss of mass with an increase in acid molarity. The results show that there is a linear correlation between molarity and mass-loss, as seen in Figure 2-3b, with a correlation coefficient $R^2 = 0.76$; this indicates that the variation in removal is explained by the molarity in 76.3% of cases.

Table 2-2 Pearson correlation for RCA treated HCl.

	Molarity (M)	Time (days)	Size of aggregate (mm)	Water absorption (%)
Molarity (M)	1	-	-	-
p -Value	1	-	-	-
Time	-0.094	1	-	-
p -Value	0.633	1	-	-
Size of aggregate (mm)	0.077	-0.007	1	-
p -Value	0.708	0.975	1	-
Water absorption (%)	-0.140	0.235	-0.211	1
p -Value	0.478	0.230	0.300	1
Mortar loss (%)	0.400	-0.170	-0.368	-0.632
p -Value	0.050	0.415	0.077	0.000



(a)



(b)

Figure 2-3 CA particle size with different mortar contents; (a) relationship between concentration of HCl (M) and mortar loss of mass (% Wt) (AKBARNEZHAD; ONG; ZHANG; TAM, 2013; AL-BAYATI; DAS; TIGHE; BAAJ, 2016; ISMAIL, S.; RAMLI, M., 2013; ISMAIL; RAMLI, 2014; KIM, Y.; HANIF, A.; KAZMI, S. M. S.; MUNIR, M. J. *et al.*, 2018; PURUSHOTHAMAN; AMIRTHAVALLI; KARAN, 2014; SARAVANAKUMAR; ABHIRAM; MANOJ, 2016; TAM, V. W. Y.; TAM, C. M.; LE, K. N., 2007) (b).

Another important correlation for the HCl surface treatment is the one between loss of mass and water absorption, with a value of $r = -0.683$. This indicates that there is a moderate correlation between loss of mass and water absorption, the relationship is negative because, if the loss of mass increases, the water absorption decreases, with no linear correlation between the two variables (p -value = 0.05). The analysis concludes that factors such as particle size/soaking time ($r = -0.007$, p -value = 0.0975) are not significant correlations in the removal of mortar from the RCA.

On the other hand, Pearson’s correlations for H₂SO₄ treatment between molarity and water absorption ($r = 0.055$, not linearly associated between them— p -value = 0.00), time and molarity ($r = 0.022$, p -value = 0.022 linearly related), and time and mass-loss ($r = -0.170$, p -value = 0.015 linearly related) have a very low degrees of correlation (Table 2-3). The two factors that have a reasonable level of correlation are the loss of mass and molarity ($r = 0.563$), and the negative correlation between loss of mass and water absorption ($r = -0.992$). Neither of these is linearly related. This means that just like in HCl treatment, the variable that is most relevant for mass-loss is molarity, with a degree of variation of 56%. Moreover, in this case, the water absorption is 99% correlated with the loss of mass. Figure 2-4 shows a weak linear correlation between molar concentration and mass-loss where the coefficient is $R^2 = 0.31$.

Table 2-3 Pearson correlation for RCA treated with H₂SO₄.

	Molarity (M)	Time (days)	Water absorption (%)
Molarity (M)	1	-	-
p -Value	1	-	-
Time	-0.300	1	-
p -Value	0.022	1	-
Water absorption (%)	0.055	0.135	1
p -Value	0.889	0.730	1
Mortar loss (%)	0.563	-0.170	-0.992
p -Value	0.000	0.015	0.000

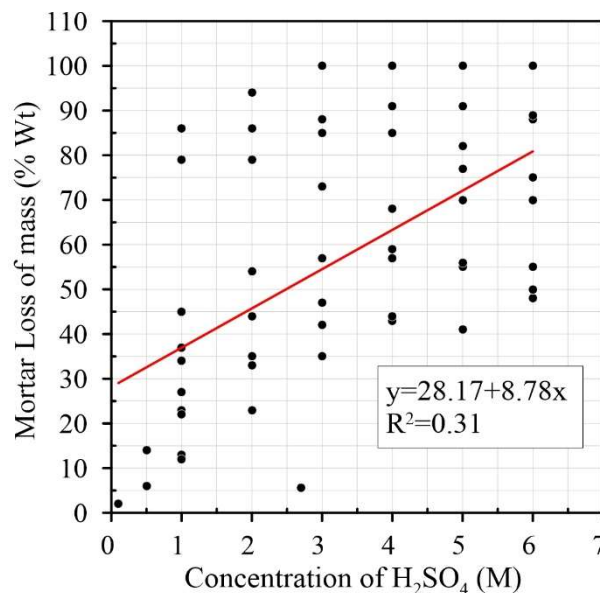


Figure 2-4 Relationship between concentration of H₂SO₄ and mortar loss of mass (% Wt) (AKBARNEZHAD; ONG; ZHANG; TAM, 2013; AKBARNEZHAD; ONG; ZHANG; TAM *et al.*, 2011; PURUSHOTHAMAN; AMIRTHAVALLI; KARAN, 2014; SARAVANAKUMAR; ABHIRAM; MANOJ, 2016; TAM, V. W. Y.; TAM, C. M.; LE, K. N., 2007).

In order to check whether the acid treatments for the removal of mortar in RCA have a considerable impact on the quality of the aggregates, the proposal of Silva *et al.*

(2014), which classifies the aggregates according to the minimum value of oven-dried density and maximum water absorption (Table 2-4), was considered. An analysis was made comparing the water absorption before and after the treatments of RCA with HCl using data collected in the literature. This type of acid was chosen because it had a significant amount of data from the authors, while other types of acid were evaluated because there are not enough data for analysis. From the authors' water absorption values before RCA was treated with HCl, it is observed that the untreated RCAs are classified in the following way: 41.3% as BII, 34.4% as BI, 3.44% as AIII, 20.0% as AII, and 0.0% as AI. After the aggregates are treated, the percentages change to 13.3% as BII, 50.0% as BI, 6.66% as AIII, 10.0% as AII and 20.0% as AI, evidencing that there is a significant change in the properties of RCA when treated with HCl.

Table 2-4 Physical property requirements for the proposed classes (SILVA; DE BRITO; DHIR, 2014).

Aggregate class	A			B			C			D
	I	II	III	I	II	III	I	II	III	
Maximum water absorption (%)	1.5	2.5	3.5	5	6.5	8.5	10.5	13	15	No limit

2.4 Properties of concrete with treated RCA

The main characteristic of the RCA is the amount of mortar adhered to the AN, creating a lighter system, modifying the physical properties and its influence on the hardened state. Many studies were conducted evaluating the main properties of RCA in concrete (AMORIM; DE BRITO; EVANGELISTA, 2012; DE BRITO; SAIKIA, 2012; FERREIRA; DE BRITO; BARRA, 2011; KWAN; RAMLI; KAM; SULIEMAN, 2012; SILVA; DE BRITO; DHIR, 2014; SRI RAVINDRARAJAH; TAM, 1985; VERIAN; ASHRAF; CAO, 2018) showing that the RCA is a good option for the replacement of AN. A systematic literature review on the mechanical, durability, and fracture properties of concrete with the replacement of treated RCA is presented below.

2.4.1 Fresh-state properties and density

The properties of the fresh state of RCA-containing concrete are directly affected by its presence, as it has sharper geometries that reduce the slip between particles and increase water absorption, decreasing the workability of concrete. Controlling workability is important to achieve adequate compaction (MEHTA; MONTEIRO, 2017). The main

results of the influence of chemical treatments on the production of concrete with RCA are shown below.

Ismail and Ramli (2013; 2014) produced concrete with various ratios of RCA incorporation (15%, 30%, 45%, 60%) treated with HCl at molar concentrations of 0.1 M, 0.3 M, and 0.8 M with pre-soaking times of 1, 3, and 7 days. They noted that workability did not show significant differences: 17% higher in concrete produced with treated RCA than in concrete with untreated RCA. This result may be attributed to the high absorptivity of coarse RCA caused by the porous mortar attached to it, which absorbs more water during concrete mixing, thus lowering the workability of concrete. Ismail and Ramli (2013) also observed that workability decreases linearly with the increase in the incorporation ratio of acid-treated RCA. The author also reported that the density of concrete made with treated and untreated RCA has no significant difference. In fact, the density of concrete with treated RCA is slightly higher due to the reduction in the adhered mortar to the original NA. This behaviour was also observed by Al-Bayati *et al.* (2016), who treated RCA with HCl and $C_2H_4O_2$ at 0.1 M and a 24-h pre-soaking time. The authors also noted that there is a tendency for density to decrease when the incorporation ratio of treated RCA increases. This trend is also the same as other reported by other authors when using untreated RCA in the manufacture of concrete (PEDRO; DE BRITO; EVANGELISTA, 2014; SILVA; DE BRITO; DHIR, 2018).

Purushothaman *et al.* (2014) saturated RCA after treatment with HCl and H_2SO_4 before the production of concrete, and showed that concrete with treated RCA had an improvement in workability of around 23.5% for both acids relative to concrete with untreated RCA. Similar results were recorded by Pandurangan *et al.* (2016) and Butler *et al.* (2011) in concrete made with RCA treated with HNO_3 .

Similar results were obtained by Kim *et al.* (2018), as they observed an improvement in the workability of acid-treated RCA concrete. The authors noted that workability improves when RCA is treated with strong acids (HCl), as they have a greater degree of removal than weak acids, leaving a less angular surface that promotes fluidity due to a ball bearing effect (EVANGELISTA; DE BRITO, 2014; RAMASWAMY; SANTHANAM, 2019).

In summary, it was observed that all authors reported insignificant increases in the

workability of concrete mixes containing RCA treated with acid solutions of low molarities. The differences are because mortar adhered to NA still remains.

2.4.2 Compressive strength

As mentioned before, concrete with RCA presents a weaker ITZ behaviour. Tam *et al.* (2007), tested several mixes with coarse RCA treated in acidic solutions of HCl, H₂SO₄, and H₃PO₄, and substitution ratios of 5%, 10%, 15%, 20%, 25%, and 30%. The authors showed that the compressive strength after treatment had significant improvement i.e. specifically, the incorporation of 20% of RCA resulted in a 10.1% increase for HCl, a 0.07% increase for H₂SO₄, and a 12.8% increase for H₃PO₄. When the incorporation ratio was raised to 25% of RCA, the improvements were even more pronounced, with an 11% increase for HCl, a 6.67% increase for H₂SO₄, and a 14% increase for H₃PO₄.

Ismael and Ramli (2013) studied several mixes incorporating coarse RCA at 15%, 30%, 45%, and 60% replacement ratios, treated with HCl at molarities of 0.1 M, 0.5 M and 0.8 M, a water/cement ratio (w/c) of 0.4, a cement content of 537 kg/cm³, and a 28-day compressive strength of 50 MPa. The results presented by the authors showed that the maximum replacement level to maintain strength at 28 days is up to 45% for RCA treated with HCl at molarities of 0.1 M and 0.5 M and not 0.8M. This is because high concentrations are detrimental to the surface of RCA, leaving it more brittle and fragile and interfering with the good connection between cement and the particles. It was also observed that ratios of 15% incorporation of RCA in the mixes result in improvements in compressive strength, relative to mixes that incorporate untreated RCA. On the other hand, the authors showed that the effect of different RCA soaking ages on the compressive strength is insignificant.

A study by Ismail and Ramli (2014) determined the influence of RCA treated with HCl at 0.5 M, submerged for 1 day, on its mechanical and drying properties. The characteristics of the mixes were: a w/c ratio of 0.40, a cement content of 510 kg/m³, a 28-day compressive strength of 50 MPa, and a 60% replacement ratio of NA with treated RCA. The authors determined the compressive strength of concrete at 7, 28, 90, and 180 days. Concrete prepared with treated RCA had better performance than that prepared with untreated RCA. At 7 days, treated RCA concrete had a compressive strength 3% higher than that of control concrete. At 28, 90 and 180 days, the compressive strength of concrete

with treated RCA was 96%, 99%, and 98% that of the control concrete, respectively, i.e. almost the same.

Ismail and Ramli (2014) determined the ultrasonic pulse velocity (UPV) in mixes containing treated RCA and untreated RCA. They found that the UPV values are slightly higher in mixes with treated RCA. This is due to the improvement of RCA properties, thus improving the ITZ microstructure and increasing the bond strength between the new cement paste and RCA.

Purushothaman *et al.* (2014) studied various concrete mixes, including 100% coarse RCA treated with two types of acid—HCl and H₂SO₄—at a concentration of 0.1 M, soaked for 24 h, with a w/c ratio of 0.45, containing 380 kg/m³ of cement, and a 28-day compressive strength of under 30 MPa. It was observed that the mixes with untreated RCA reached 80% of the reference mix's 28-day compressive strength, while the mixes with treated RCA reached 90% and 95% of the same value for HCl and H₂SO₄, respectively.

Saravanakumar *et al.* (2016) studied the effect on concrete of RCA treated with H₂SO₄, HNO₃, and HCl designed according to the ACI method (2002), and mixing ratios of 1:1.4:2.3 (cement: sand: gravel) were used with a w/c ratio of 0.45. Ordinary Portland cement ASTM type 1, with a specific surface area of 3960 cm²/g and specific gravity of 3.15, was used. The authors replaced NA with RCA at 100%. The 28-day compressive strength of concrete made with recycled aggregates was 25% lower than that of concrete made with NA aggregates. In the treated aggregates, the loose mortar was removed as much as possible, and the characteristics of the aggregate's surface were improved. The contact in the ITZ between the treated RA and the new cement paste improved and; thus, the 28-day compressive strength of concrete improved the treated RCA by 8% to 18% relative to concrete made with untreated RCA. The compressive strength development in concrete of RCA treated at later ages, between 28 and 91 days, was considered good. The relative strength development of concrete with recycled aggregate treated with HCl, HNO₃ and H₂SO₄ was 18%, 18.5%, and 20%, respectively, at the age of 91 days. Among all the treated aggregate mixes, the development of strength was lower for the one treated with HCl.

Pandurangan *et al.* (2016) produced mixes of concrete with RCA to assess the pull-out force between steel and concrete. The mixing ratio by weight was designed according to the ACI method (COMMITTEE, 2002) as 1:2.18:2.82 (cement: sand: gravel), with a

cement content of 380 kg/m³, and a w/c ratio of 0.45 for concrete class M35. The replacement ratio was 91.5% according to the design method established by Fathifazl *et al.* (2009). The authors showed that the compressive strength improves by treating the recycled aggregates and represents more than 95% that of concrete with NA only.

Kim *et al.* (2018), obtained results that are in accordance with the existing literature on mechanical properties of concrete with RCA. The compressive strength decreased when NA was replaced with RA. Concrete that incorporated treated RCA exhibited better strength attributes than that with untreated RCA. Compressive strength increased by about 4.5%. This showed that pre-treatment of RCA with HCl is beneficial to the mechanical performance of concrete with RCA.

Wang *et al.* (2017), showed that all concrete mixes containing RCA treated with 1% and 3% acetic acid have higher compressive strength compared to the reference concrete. The strength increased more than 25% at 28 days in mixes with treated RCA. The authors showed that during the process, in higher acid solutions, the residual effect of the acid negatively influences the compressive strength with a greater influence at the ages of 3 and 7 days. Another possible reason for this reduction was indicated by the potential damage induced to the RCA.

The removal of mortar adhered to RCA is not limited only to the coarse aggregates. Kim *et al.* (2017) studied the effect on the compressive strength of mortars manufactured with fine aggregates of RCA treated with H₂SO₄ and HCl. Unlike the trends of previous authors, they obtained lower results for compressive strength in mortars treated with acidic solutions. This behaviour was explained by the production of gypsum in the removal, which, if not correctly eliminated, would come into contact with the calcium alumina of the cement, generating a greater number of voids.

Figure 2-5 Figure 2-5 Age of curing (days) versus compressive strength with HCl treatment (ISMAIL.; RAMLI, 2013; ISMAIL; RAMLI, 2014; KIM, Y.; HANIF, A.; KAZMI, S. M. S.; MUNIR, M. J. *et al.*, 2018; PURUSHOTHAMAN; AMIRTHAVALLI; KARAN, 2014; SARAVANAKUMAR; ABHIRAM; MANOJ, 2016).shows the compressive strength results of several authors (ISMAIL, S.; RAMLI, M., 2013; ISMAIL; RAMLI, 2014; KIM, Y.; HANIF, A.; KAZMI, S. M. S.; MUNIR, M. J. *et al.*, 2018; PURUSHOTHAMAN; AMIRTHAVALLI; KARAN, 2014; SARAVANAKUMAR;

ABHIRAM; MANOJ, 2016) on concrete mixes with aggregates treated with HCl solutions at different ages of curing. A correlation of $R^2 = 0.70$ between the different results can be observed. This variability is because the removal is directly linked to the type of cement and the aggregate size. The results also show that there is a positive evolution in the compressive strength when the acid concentration is increased. This evolution in the compressive strength can be affected by the ionization of the acid increasing the content of ions in RCA (BROWN; LEMAY; BURSTEN, 2007; KIM; KIM; KIM; KIM, 2017; MEHTA, 1983; NEVILLE, 1995). It also presents a confidence interval of 95% (p -Value = 0.0001) for the response in compression with this type of treatment.

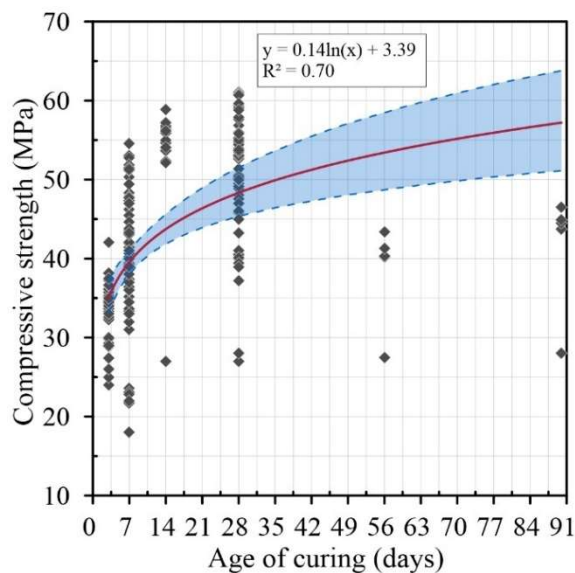


Figure 2-5 Age of curing (days) versus compressive strength with HCl treatment (ISMAIL.; RAMLI, 2013; ISMAIL; RAMLI, 2014; KIM, Y.; HANIF, A.; KAZMI, S. M. S.; MUNIR, M. J. *et al.*, 2018; PURUSHOTHAMAN; AMIRTHAVALLI; KARAN, 2014; SARAVANAKUMAR; ABHIRAM; MANOJ, 2016).

2.4.3 Tensile strength

Tam *et al.* (2007) reported increases in tensile strength in concrete containing acid-treated RCA. They stated that the best performance improvements in 28-day flexural strength were 4.44% for 25% incorporation of RCA treated with HCl, 5.10% for a 10% RCA treated with H_2SO_4 and 18.58% for 10% RCA treated with H_3PO_4 .

Ismail and Ramli (2014) also reported improvements in the flexural strength of concrete containing treated RCA *versus* untreated RCA. For treated RCA concrete, the reduction was 4%, 9%, 3%, and 5% relative to the reference concrete at 7, 28, 90, and 180 days, respectively. This indicates that the treatment of the RCA with acid improved the

flexural strength, because the reduction without treatment was 3%, 12%, 10%, and 13% at the same ages. Another important result is the good linear correlation that exists between flexural strength and compressive strength, which had a Pearson's coefficient of $R^2 = 0.88$.

2.4.4 Modulus of elasticity

The modulus of elasticity (E) of concrete is directly related to the characteristics of the materials that compose it. RCA can be treated as a composite material of NA and mortar; therefore, the E of RCA is related to the E of the mortar (low) and to that of NA (high), in addition to other factors such as the resistance of the ITZ, stiffness, porosity and volumetric fraction of the paste in the RCA (BESHR; ALMUSALLAM; MASLEHUDDIN, 2003; KHEDER; AL-WINDAWI, 2005; ZHOU; LYDON; BARR, 1995), resulting in concrete with lower E values than those of mixes produced with NA only (PEDRO; DE BRITO; EVANGELISTA, 2014).

Tam *et al.* (2007) showed that E had significant improvements when using treated RCA. These improvements reached up to 20.4% (30% RCA treated with HCl), 15.37% (10% RCA treated with H₂SO₄) and 10.82% (30% RCA treated with H₃PO₄) in relation to the reference concrete at 7 days. The improvement was related to the amount of adhered mortar removed using the different acid solutions, which led to a less porous aggregate with less-fragile particles.

Ismail and Ramli (2014) also found improvements in E values for mixes produced with treated RCA. The mixes with treated RCA had reductions of 4%, while the ones with untreated RCA showed reductions of 12%, in both cases, when compared to the corresponding reference mixes. These improvements were due to the treatment effects mentioned in the previous paragraph.

Purushothaman *et al.* (2014) observed that, in mixes with untreated RCA, the reduction in E was almost 35% relative to the reference concrete, while in mixes treated with HCl and H₂SO₄, the reductions in E relative to the mixes with NA were less than 8% and 22%, respectively. This better behaviour was because the RCA had an increase in density, a removal of adhered mortar, and an improvement in the ITZ between the RCA and the cementitious paste.

2.4.5 Fracture energy

Authors such as Ishiguro and Stanzl-Tschegg (1995), who replaced 100% of NA with RCA, obtained a 60% reduction in fracture energy compared to a reference concrete. Other authors such as Casuccio *et al.* (2008), Gesoglu *et al.* (2015) and Garcia-Gonzales *et al.* (2017) claim that the fracture energy can be reduced by between 20-75% relative to a conventional concrete, depending on the incorporation ratio of RCA.

On the other hand, Kazemian *et al.* (2019) showed a noticeable reduction of the fracture energy when RCA is incorporated, which produces negative effects on crack growth that is more intense when adding RCA. When RCA was treated with 0.1M HCl and calcium metasilicate was added, the fracture energy of concrete made with RCA was greater than that of mixes with untreated RCA. These results can be attributed to the treatment process and the availability of pozzolanic particles that coated RCA, which consequently reacted with cement during the hydration process and improved the ITZ.

To predict the fracture's properties in concrete with incorporation of RCA, Ghorbel *et al.* (2019) proposed a prediction model for fracture's properties based on the model of Ghorbel and Wardeh (2017), where the fit was improved with an inverse analysis of data collected in the literature, giving a good approximation of the G_F .

2.4.6 Shrinkage

Studies carried out on the shrinkage of RCA reported a significant increase in the shrinkage of mixes with RCA, compared to conventional concrete.

From the results of shrinkage, Ismail and Ramli (2014) observed that the shrinkage of mixes with treated and untreated RCA, which was measured for up to 180 days in total, fell below a micro strain of 500. From the results at the early ages (up to 28 days), the drying shrinkage behaviour of all concrete mixes with untreated RCA was observed to be extremely steep (Figure 2-6). After 28 days, however, the drying shrinkage measured after 180 days for concrete with untreated RCA was 26% greater than that of the control concrete. The high shrinkage of concrete with untreated RCA was related to the low quality and low stiffness of the untreated, coarse RCA. The volume and stiffness of the aggregates are considered important factors that prevent the shrinkage of concrete

(ADAM; SAKATA; AYANO, 2001).

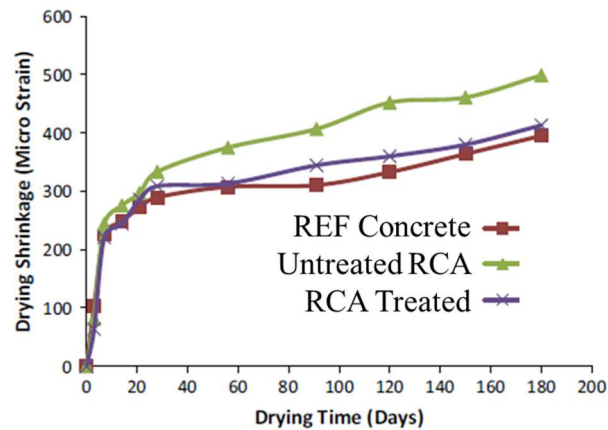


Figure 2-6 Drying shrinkage of concrete mixes *versus* drying time (ISMAIL; RAMLI, 2014).

2.4.7 Chloride ion penetrability and carbonation resistance

The results presented by Kim *et al.* (2018) showed the permeability to chloride ions of untreated RCA mixes to be 27% higher than that of the mixes with NA only. Concerning the permeability to chloride ions of mixes containing RCA treated with HCl and Na₂SO₄, the penetration was 11% and 14% higher, and those with NA observed an improvement. The carbonation depth of the mixes followed similar trends to those in the chloride penetration tests. The carbonation depth of cast concrete increased by 9% compared to the concrete made with NA. This clearly shows the reduced durability characteristics of this mix when subjected to severe exposure conditions. According Kim *et al.* (2018), the greater depth of carbonation is attributed to the limited formation of C-S-H gel during hydration, resulting in greater porosity and a less dense matrix.

2.4.8 ITZ between cement paste and RCA

As previously described, the quality of the ITZ depends on the characteristics of the RCA surface. This topic presents ITZ improvement differences between the treated and untreated RCA. Tam *et al.* (2007) performed SEM on concrete mixes with treated and untreated RCA. In Figure 2-7(a), a less dense ITZ between the paste and RCA is clearly observed. This behaviour of the ITZ was also observed by Poon *et al.* (2004), Sidorova *et al.* (2014) and Xiao *et al.* (2013). When the RCA were treated with HCl, H₂SO₄ and H₃PO₄, the ITZ was reduced as seen in Figure 2-7(b) to Figure 2-7(d), resulting in stronger bond between the aggregate and the cementitious paste, reflected on improved

mechanical properties of concrete, as explained above.

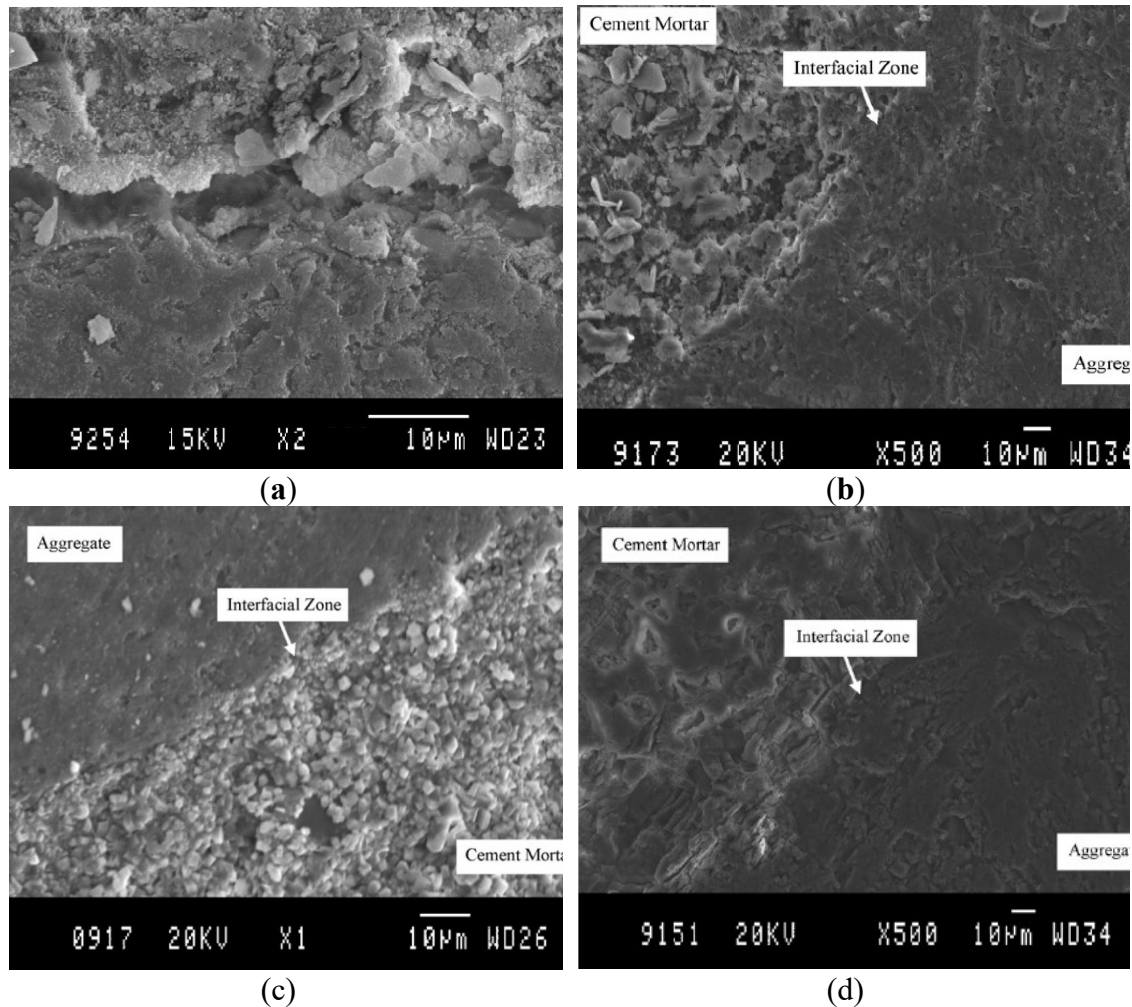


Figure 2-7 ITZ for concrete with RCA without pre-soaking treatments(a); ITZ for RCA treatment with HCl (b); ITZ for RCA treatment with H₂SO₄ (c); and ITZ for RCA treatment with H₃PO₄ (d)(TAM, V. W. Y.; TAM, C. M.; LE, K. N., 2007).

Similar research has been conducted reporting the effectiveness of incorporating RCA treated with different acid solutions in concrete and mortar mixes. A summary of the different mechanical parameters that have been determined so far for concrete made with RCA treatment, and the type of acidic solution, is provided in Table 2-5.

The results indicated that the properties of the treated RCAs depend mainly on the molar concentration of the acid solution used for treatment, the amount of cement paste adhered to NA, and the aggregates and water/cement ratio used.

Table 2-5 Summary of measurements of fresh-state properties, mechanical properties and durability.

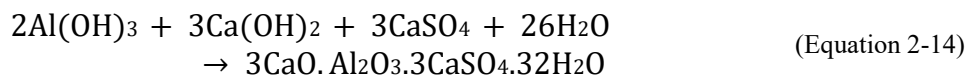
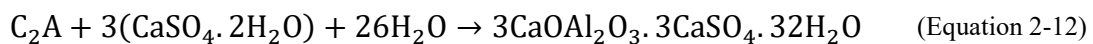
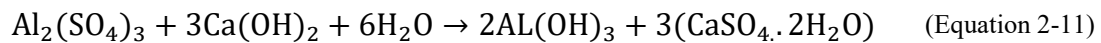
Parameter	Concrete mix	References
Density	Concrete with RCA treated with HCl and Na ₂ SO ₄	Al-Bayati <i>et al.</i> (2016)
Workability of concrete, density compressive strength, tensile strength, UPV, modulus of elasticity (E), and shrinkage	Concrete with RCA treated with HCl	Ismail and Ramli (2013); Ismail and Ramli (2014)
Workability of concrete and compressive strength	Concrete with RCA treated with HNO ₃	Pandurangan <i>et al.</i> (2016)
Compressive strength and modulus of elasticity (E)	Concrete with RCA treated with HCl, H ₂ SO ₄ , and H ₃ PO ₄	Purushothaman <i>et al.</i> (2014)
Compressive strength	Concrete with RCA treated with HCl, H ₂ SO ₄ , and HNO ₃	Saravanakumar <i>et al.</i> (2016)
Compressive strength, tensile strength, and modulus of elasticity (E)	Concrete with RCA treated with HCl, H ₂ SO ₄ , and H ₃ PO ₄	Tam <i>et al.</i> (2007)
Compressive strength, tensile strength, and modulus of elasticity (E)	Concrete with RCA treated with HCl and H ₂ SO ₄	Wang <i>et al.</i> (2017)
Compressive strength	Concrete with RCA treated with HNO ₃	Pandurangan <i>et al.</i> (2016)
Compressive strength, chloride ion penetrability, and carbonation resistance	Concrete with RCA treated with HCl and Na ₂ SO ₄	Kim <i>et al.</i> (2018)
Compressive strength, flexural strength and modulus of elasticity (E)	Mortar with RCA treated with HCl and H ₂ SO ₄	Kim <i>et al.</i> (2017)
Workability of concrete	Concrete with RCA treated with HCl and HNO ₃	Butler <i>et al.</i> (2011)
Fracture energy	Concrete with RCA untreated	Stanzl-Tschegg (1995)
Fracture energy	Concrete with RCA treated with HCl	Kazemian <i>et al.</i> (2019)
Fracture energy	Concrete with RCA untreated	Ghorbel <i>et al.</i> (2019)
Fracture energy	Concrete with RCA untreated	Stanzl-Tschegg (1995)
Fracture energy	Concrete with RCA untreated	Casuccio <i>et al.</i> (2008)
Fracture energy	Concrete with RCA untreated	Gesoglu <i>et al.</i> (2015)
Fracture energy	Concrete with RCA untreated	Garcia-Gonzalez <i>et al.</i> (2017)

2.5 Concrete with addition of AS

The specific use of aluminium recycling waste as a pozzolan or additive in the hydration of normal Portland cement shows a reduction in the setting time of the cement paste. This is due to the rapid formation of ettringite from the reaction between Ca(OH)₂ and gypsum (BRYKOV; ANISIMOVA, 2013) The early formation of ettringite in the initial phase is extremely important as it regulates the hydration process (BARGER, BAYLES, BLAIR, BROWN, CHEN, CONWAY, HAWKINS, 2001). The presence of aluminium hydroxides and oxides as the main components of accelerating admixtures can contribute to the formation of ettringite. Aluminium sulphate (AS) is recognised as an accelerator component in the hydration of concrete, as well as acting as a waterproofing and spreading agent. The mechanism of action of AS in cement is based on its reaction

with calcium ions, resulting in the formation of primitive gypsum, which is more active than derived gypsum. AS acts as a tricalcium aluminate, facilitating the formation of ettringite, as shown in Equations 2-11 and 2-12. In addition, aluminium is able to react with calcium hydroxide to form ettringite directly in the absence of tricalcium aluminate (Equation 2-13).

When an amount of AS is added to cement, ettringite is mainly formed in small-size agglomerates. When the aluminium sulphate content is high, calcium is consumed in small concentrations and the alkalinity of the solution decreases. Therefore, ettringite grows to a large size and is widely spread. In short, on the one hand, the addition of aluminium sulphate consumes the calcium ion in solution and on the other hand provides aluminium ion and sulphate ion that formed the ettringite. Forming an environment for ettringite formation. Equation 2-14 is the intermediate product - aluminium hydration - generally cannot exist constantly, so it soon turns to ettringite in the presence of calcium hydroxide and gypsum. At the same time, these reactions consume calcium hydroxide. Reduction of calcium hydroxide accelerates hydration of calcium silicate. Consequently, the ettringite crystals grow and intersect in a large network, generating a cement paste skeleton, and the C-S-H gel helps to fill it, forming a denser structure. Then, the rapid and massive formation of ettringite and C-S-H gel accelerates the cement setting (CHATTERJI; JEFFERY, 1963; KAN; LAN; KONG; YANG, 2013; WANG; HE; SU; MA et al., 2018).



The study by Briendl et al. (2022) explored the initial hydration mechanisms of shotcrete binders. In this research, mixes containing low sulphate content were compared with those that included the addition of aluminium sulphate, an accelerator. The process in which Al^{3+} ions from the accelerator rapidly transformed into $\text{Al}(\text{OH})_4^-$ ions in the alkaline

conditions of the cement paste was detailed. These aluminium ions interacted with SO_4^{2-} ions (from the accelerator or the pore solution) and Ca^{2+} ions (from the pore solution) to form ettringite, which plays a crucial role in rapid hardening. The rapid formation of ettringite, together with the acid nature of the accelerator, reduced Ca^{2+} levels and the pH in the pore solution, promoting the dissolution of alite and C_3A . This resulted in greater supersaturation in relation to calcium (aluminium) silicate hydrates (C-(A)-S-H) and the subsequent precipitation of nuclei of these phases. When analysing the compressive strength under different wet and dry curing conditions, it was observed that, compared to the dry mix, the samples subjected to wet curing had higher compressive strength values and lower total porosity calculated after 24 hours and in later hydration phases. It is important to note that although the accelerator contained approximately 65% water by weight, it had a minimal effect on the water available for cement hydration. The addition of 7% accelerator corresponded to 2.45 g of $\text{Al}_2(\text{SO}_4)_3$ and 4.55 g of H_2O per 100g of cement. This amount of accelerator was able to produce approximately 9 g/100 g of ettringite cement, containing around 4.13 g of H_2O . This indicates that most of the water present in the accelerator was consumed by the ettringite, formed as a result of the reaction between $\text{Al}_2(\text{SO}_4)_3$ and Ca^{2+} from the pore solution. After 6 hours of hydration, the compressive strength was equivalent in both types of samples, while the calculated total porosity was lower in the sample with wet curing. Therefore, it is suggested that in the early stages of hydration, the morphology and mechanical properties of the phases formed are also crucial to the compressive strength of the cement matrix. After 6 hours of hydration, the compressive strength was equivalent in both types of samples, while the calculated total porosity was also lower in the sample with wet curing. It can therefore be assumed that, in the initial stages of hydration, the morphology and mechanical properties of the phases formed are also relevant to the compressive strength of the cementitious matrix.

Braz *et al.* (2019) collected samples of metal waste from aluminium recycling in a tertiary aluminium industry. This waste is obtained from the black/salt dross from the secondary aluminium industry. In the tertiary industry, the raw material (black salt) is received in solid blocks from various locations in Brazil, broken up manually and leached with water in rotating drums to recover the metallic aluminium. In the study carried out by Braz *et al.* (2019), the incorporation of this aluminium waste into mortars containing 100% of this material was investigated, resulting in significantly lower strengths compared to reference mortars containing cement. The values obtained were 42.25%,

indicating the absence of calcium silicate hydrate (C-S-H) formation, the component responsible for concrete strength. This absence is due to the lack of reactive silica in the composition containing the aluminium residue.

Kan *et al.* (2013) showed that aluminium sulphate increases the curing time of concrete when 6% of AS is used and decreases as the amount of AS is reduced (2.5%). This effect is reflected in the fluidity of concrete, maintaining a constant fluidity in ranges from 1% to 2% of AS, whereas higher ranges of AS (2% to 10%) fluidity is reduced because of the accelerating effect of AS.

Kan *et al.* (2013) also observed that the compressive strength increases with respect to the concrete mixes without AS when up to 5% of AS was added. Additions greater than 8% the resistance at 28 days tends to be lower compared to the reference concrete. On the other hand, the tensile strength tends to be lower when any amount of AS is added to the 28-day strength.

Song *et al.* (2015) studied concrete mixes with RCA and AS addition in amounts of 0.65% and 1.10% of the cement weight. The results showed that the mixes with 1.10% AS addition increased the strength by around 14.7% with respect to the reference concrete. Song *et al.* (2015) attributes this improvement to the fact of increasing the production of ettringite capable of reducing the porosity of the RCA and increasing the solidity of the mortar. At the same time, too much calcium hydroxide, can reduce the preferential orientations of portlandite in ITZ and accelerate the process of consumption of tricalcium silicate/dicalcium silicate. These chemical reactions help to improve the ITZ and, therefore, improve the strength of the cement paste and of RCA.

2.6 Analysis of the literature review

Based on the review and analysis of the literature, the main conclusions of the chapter are as follows.

RCA has seen improvements in its physical and mechanical characteristics when treated with solutions at low concentrations, e.g. improving water absorption, density, and RCA surface. From the literature data, it can be concluded that treatments with acids can change the quality classification of RCA for the better.

The immersion time in the acid solution does not linearly relate to the adhered mortar removal volume. This is because, during the removal of mortar, the sulphate ions (SO_4^{2-}) are consumed in the reaction in the first steps. The total removal of the paste present in the RCA occurs when the acid concentrations are increased to values greater than 3 M (AKBARNEZHAD; ONG; ZHANG; TAM, 2013).

Concrete mixes that contain treated RCA showed better mechanical behaviour than those incorporating RCA without treatment. Thanks to the removal of the paste and improvement of the ITZ between RCA and the new cement paste, higher compressive strength, modulus of elasticity, and tensile strength are achieved. In terms of durability, treated RCA mixes had better values than untreated RCA ones.

There is no strong linear relationship between the variables that control mortar removal and the final physical properties of RCA. This can be explained by the high variability of RCAs both in their physical and mechanical properties.

From the literature review carried out, it can be concluded that the use of acids as a treatment for improving the physical and mechanical properties of RCAs can be an optimal solution, depending on the environment to which concrete will be exposed. An option for this type of treatment would be acid drainage generated by the mining industry, where there is potential for using this type of waste.

AS is a meaningful alternative to improve the mechanical properties of concrete mixes with RCA as replacement for NA if AS is limited to 5% of the mass value of cement.

3 EXPERIMENTAL PROGRAM

This chapter discusses the organisation and experimental program concerning the test procedures and materials of each phase that constitute this thesis for the determination of the physical properties of aggregates and concrete properties in the fresh and hardened states.

It starts by characterizing and analysing the materials used in the production of all concrete mixes, including cement, acids, aluminium sulphate, and aggregates (natural and RCA). This characterisation allowed relating the influence of each component on the mechanical, fracture, and durability properties of each concrete mix. Regarding RCA, the production processes, sorting, and separation by sizes for use in the different concrete mixes are described.

Subsequently, the results of the aggregates characterization are used to formulate the most relevant mixes that were used in the production of concrete. These mixes were subjected to compressive strength, splitting tensile strength, modulus of elasticity, and fracture energy tests for mechanical characterisation. To evaluate the performance in terms of durability, these mixes were submitted to tests of water absorption by immersion, water absorption by capillarity, shrinkage by drying, resistance to carbonation, and resistance to chlorides penetration. Finally, for a more comprehensive understanding, microstructural characterisation tests were performed on the evaluated concrete mixes. Additionally, it's worth noting that the results obtained can be used as a foundation for a life cycle analysis of aggregates with acid removal, contributing to a holistic assessment of sustainability in the construction industry.

3.1 Test planning

To meet the objectives of this research, the experimental program was divided into two stages: (1) material characterisation; (2) production of the concrete mixes with NA, RCA, treated RCA, and AS and evaluation of their mechanical behaviour, durability and microstructure. Figure 3-1 presents an organization chart detailing the stages of this research with the materials to be used and the tests to be performed.

In this study, the variables were catalogued as dependent and independent. Independent variables are those that affect other variables, but are not necessarily correlated

among themselves, and dependent variables are those directly affected by the independent variables. Table 3-1 details the dependent and independent variables of this study.

Table 3-1 Independent and dependent variables of this study.

Independent variables	Dependent variables		
	Recycled aggregate	Concrete	
		Fresh state	Hardened state
Coarse aggregate	Water absorption for recycled aggregates	Workability	Compressive strength
	Water absorption over time for recycled aggregates		Splitting tensile strength
Recycled aggregate	Saturated and surface-dried particle density		Modulus of elasticity
Concentration HCl (M)	Size distribution analysis		Fracture properties
Concentration H ₂ SO ₄ (M)	Recycled aggregate mass loss		Water absorption by immersion
Aluminium sulphate (AS)			Capillary water absorption
			Carbonation
			Resistance to the penetration of chloride ions
			Shrinkage

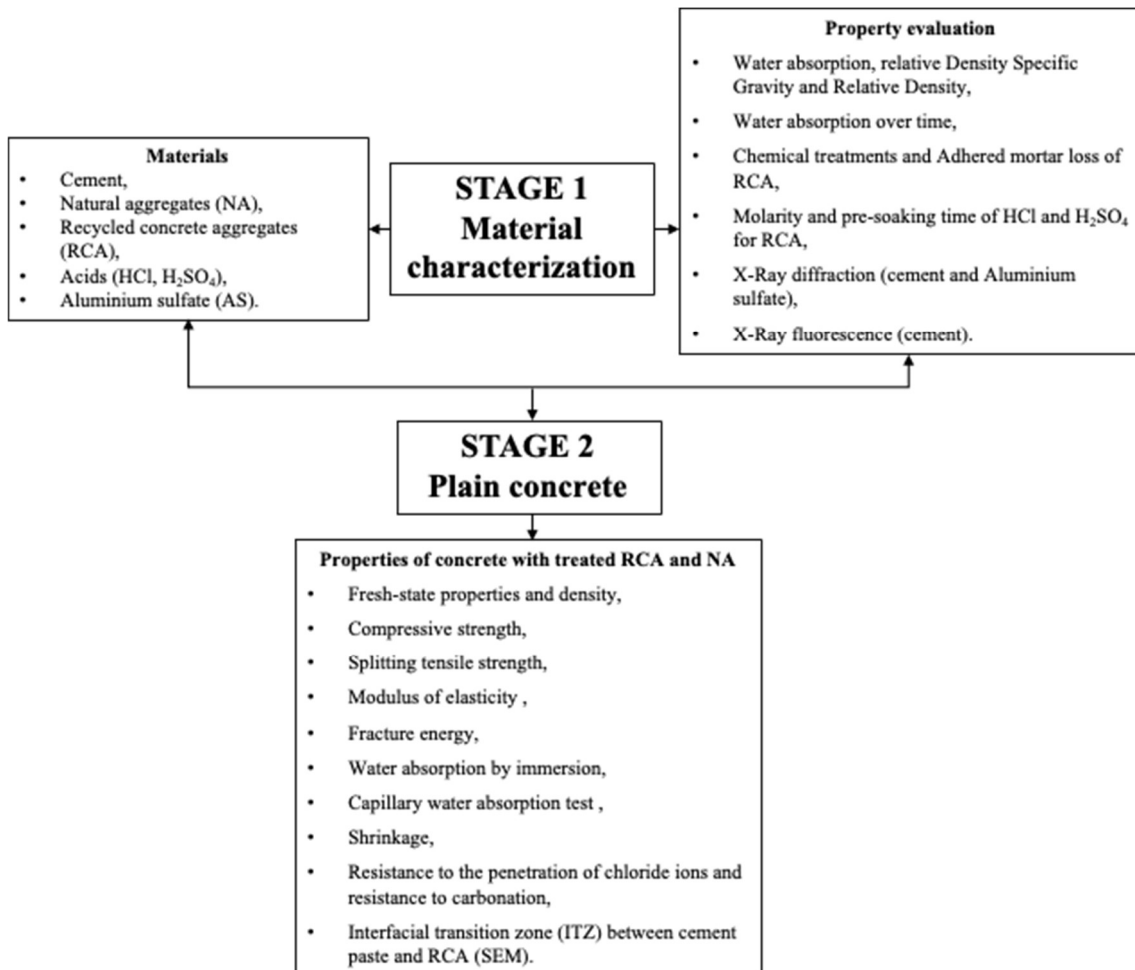


Figure 3-1 Flowchart of the methodology of the experimental programme.

3.2 Materials

The materials used in this research for both stage 1 and stage 2 are described in the following sub-items. All materials were provided by Instituto Superior Técnico in Lisbon, Portugal. In this experimental campaign, all materials and procedures were kept rigidly identical in the two stages of this research so that the results can be compared.

3.2.1 Cement

The cement used in the present research was Portland cement type I 42.5R, produced by the company CIMPOR in Portugal. The cement is made up of a minimum of 95% clinker, with the remaining 5% being additions in accordance with NP EM 197-1 (2001). This binder was used for all concrete mixes and in the production of the RCA.

3.2.2 Natural aggregates (NA) and water

For the manufacture of the reference concrete mixes and mixes with RCA and for the production of RCA, three types of coarse NA were used: CA1 (particle size), CA2 (particle size), CA3 (particle size) and two siliceous sands, FA1 (grain 0-2 mm) and FA2 (0-4 mm), all of them complying with the requirements of EN 12620 (2002). The choice of this combination of sizes of NA was made in order to facilitate obtaining the necessary quantities of each size fraction.

Because they are of calcareous origin, the coarse NA used to produce RCA can be affected by HCl (DE JUAN; GUTIÉRREZ, 2009; SÁNCHEZ DE JUAN, 2004). Consequently, different acid molarities were chosen to establish the impact of HCl on the limestone NA and the removal performance. Finally, tap water was used for both mixing and the acid solutions in accordance with Directive 98/83/EC (EU, 1998).

3.2.3 Recycled concrete aggregates (RCA)

A correct crushing procedure provides a good production flow and particle distribution of the recycled aggregates. To obtain the RCA used in the mixes of this research, concrete blocks of strength class C30/37 were produced, cured at ambient temperature, and crushed in a jaw crusher at 28 days of curing. According to Hansen *et al.* (1983), the use of jaw crushers provides a better particle size distribution of the

recycled aggregate than other types of crushers.

The production process of RCA is shown in Figure 3-2, where firstly the produced concrete blocks are presented (Figure 3-2a). The jaw crusher is shown next, where the concrete blocks were crushed (Figure 3-2b). Once the concrete blocks were crushed, the material was screened to obtain fractions of 4-5.6 mm, 5.6-8 mm, 8-11.2 mm, 11.2-16 mm, 16-22.4 mm and above 22.4 mm (Figure 3-2c-d). Finally, the RCA aggregates were stored to be used in the mixes production and their physical characterisation.

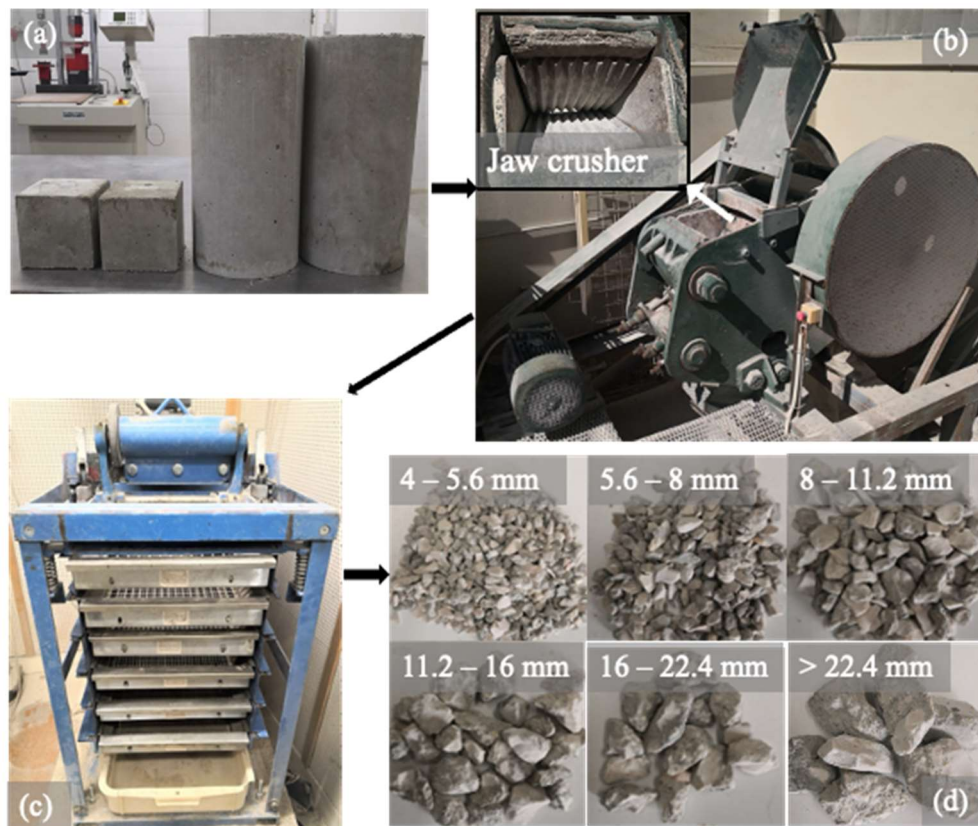


Figure 3-2 Jaw crusher used in the production of RCA (a); size fractions of RCA used in this study (b).

3.2.4 Acids

Two types of acids were used as a solvent for the removal the adhered old paste in RCA: hydrochloric acid (HCl) at 37% purity analytics (p.a.) with a molecular weight of 36.46 g/mol, a specific gravity of 1.19 g/ml, pH < 1; and sulphuric acid (H₂SO₄) at 95-97% p.a. with a molecular weight of 98.08 g/mol, a specific gravity of 1.84 g/ml, and pH < 1. These acids were prepared in different acid solutions for the two stages of this research.

3.2.5 Aluminium sulphate

Aluminium sulphate (AS) was used in this investigation as an accelerator of cement hydration, allowing improving the ITZ of cement with RCA. The value of AS in mass in the mixes is important because an excessive amount of this component will be reflected in a reduction of the mechanical properties of concrete. The amount used in the mixes was 1.10% of the cement mass following the procedure described by Song *et al.* (2015).

The AS used came from the Chem-Lab company, and it is a solid crystal in powder with a molecular weight of 666.42 g/mol, density of 1.72 g/cm³, pH 3-4 and solubility in water of 30 g/100ml.

3.3 Characterisation of Aggregates

Aggregates significantly influence the properties of concrete. For this reason, a detailed analysis of the physical properties of aggregates was carried out for both NA and RCA.

The physical and geometric properties of each aggregate type were determined. With respect to the geometric properties, the aggregates were characterised through a size distribution analysis. With respect to the physical properties, tests to determine the density mass and water absorption were performed, fundamental properties for the formulation of the concrete compositions. Finally, the mortar loss in percentage of RCA was determined for each acid molarity.

The procedures used for the characterisation of the aggregates (NA and RCA) following the corresponding standards are presented in detail below.

3.3.1 Water absorption and saturated surface dried particle density of NA and RCA

The test procedure used for NA and RCA followed the principles described in standard NP EN 1097-6 (2013) "Testing of mechanical and physical properties of aggregates. Part 6: Determination of density and water absorption". The pycnometer method was always used with a division of particles between 4-31.5 mm and 0.063-4 mm.

The determination of the density of aggregates is fundamental to calculate the

composition of concrete in terms of mass. The transformation from volume to mass is performed using the saturated surface dry density mass of the aggregates, preventing them from absorbing water from the mix. For this effect and because usually the aggregates in the mixes are used in the non-saturated condition, it is important to know the moisture content of the aggregate and its water absorption until reaching the saturated surface dry state. The amount of water absorbed by the aggregates depends mainly on the amount and size of the pores present in them, while the absorption rate depends mainly on the continuity that exists between the pores, allowing obtaining the necessary changes in the water/cement ratio of the concrete compositions.

In addition to the above mentioned, the determination of water absorption and particle density is important in this investigation because these parameters describe the performance of the treatments with HCl, H₂SO₄ in the RCA aggregates. The aggregates' density masses and water absorption (as a percentage of dry mass), after immersion for 24 hours, were calculated using the following equations:

$$\rho_a = \frac{M_4}{[M_4 - (M_2 - M_3)]/\rho_w} \quad (\text{Equation 3-1})$$

$$\rho_{rd} = \frac{M_4}{[M_1 - (M_2 - M_3)]/\rho_w} \quad (\text{Equation 3-2})$$

$$\rho_{ssd} = \frac{M_1}{[M_1 - (M_2 - M_3)]/\rho_w} \quad (\text{Equation 3-3})$$

The water absorption, as a percentage of dry mass, after immersion for 24 hours, is given by Equation 3-4:

$$WA_{24} = \frac{100 \times (M_1 - M_4)}{M_4} \quad (\text{Equation 3-4})$$

Where,

- ρ_a - apparent particle density in (kg/dm³);
- ρ_{rd} - oven dry particle density in (kg/dm³);
- ρ_{ssd} - saturated surface dry particle density in (kg/dm³);

- ρ_w - density of water at test temperature (kg/dm^3);
- WA_{24} - water absorption after immersion for 24 h (%);
- M_1 - mass of the saturated surface dry aggregate in the air (g);
- M_2 - mass of the pycnometer containing the sample of saturated aggregate and water (g);
- M_3 - mass of the pycnometer filled with water only (g);
- M_4 - mass of the oven-dried test portion in air (g).

3.3.2 Water absorption over time of NA and RCA

In order to quantify the evolution rate of water absorption of RCA, with the purpose of predicting the necessary pre-saturation time and the level of water that should be added to the mix, the sample was weighed on a hydrostatic balance, keeping the aggregates immersed for 24 hours. Regular readings were taken during the first 10 minutes, becoming more spaced after this time until one hour of testing. After the first hour of testing, the readings continued every hour until completing 24 hours, thus obtaining a graph of the evolution of water absorption. This procedure was done following the study made by Leite (2001) and shown in Figure 3-3, where the procedure described above can be observed.

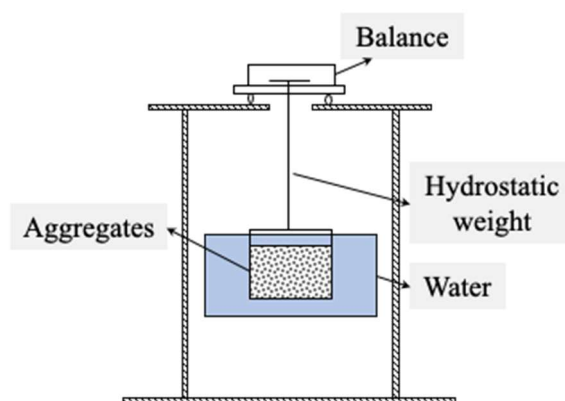


Figure 3-3 Water absorption measurement using hydrostatic weighing.

3.3.3 Size distribution analysis

The NA and RCA used in the present experimental campaign were sieved and

separated in different size fractions in order to perform a size distribution analysis following the methodology and principles adopted in the NP EN 933-1 standard.

The purpose of this test is to determine the size distribution of the aggregates, using the test sieves described in the standard NP EN 933-2 “Test for the determination of the geometric characteristics of the aggregates”.

The test consists of separating, by means of a set of sieves, a material into different size distribution classes of decreasing size, each containing particles with dimensions between the limits corresponding to the opening of the respective sieves. With the result of this test, it is possible to establish a size distribution curve referring to a given type of aggregate. These curves are a fundamental calculation element for designing the composition of concrete, allowing the definition of the contents of its various components. They may also have the function of assessing the size distribution of the aggregate and the deficiencies that it may have at the level of some size fractions (for example, the lack of particles of a given size) in addition to having consequences on the workability, segregation and mechanical performance of concrete.

3.3.4 Chemical treatments and adhered mortar content of RCA

The mortar present in RCA is constituted of weakly adhered mortar particles due to the crushing of concrete and other factors such as: non-hydrated cement, different types of cement from the origin of concrete, rheological constitution, and water-cement ratio. The amount of mortar present in RCA varies according to the size of the aggregates. According to De Juan and Gutiérrez (2009) and Silva *et al.* (2014), the size of the aggregate influences the content of adhered mortar, where the larger fractions have a lower content of adhered mortar to the NA than the smaller fractions.

The method that was followed for pre-soaking RCA is the one adopted by Ismail and Ramli (2013), Tam *et al.* (2007), Akbarnezhad *et al.* (2013) and Purushothaman *et al.* (2014). In this research, the procedure to determine the loss of mortar adhered in the RCA was divided into two phases, the first one focused on the loss of mortar and the physical properties of the RCA with diameters of 22.4, 16 mm and 11.2 mm, treated with HCl and H₂SO₄ in molarities of 0.1 M, 0.2 M, 0.3 M, 0.4 M, 0.5 M, 0.6 M, 1 M and 3 M prepared at 22 °C submerged for 1, 3 and 6 days, in order to observe which molarity

relationship and immersion time has the best performance. After analysing the results of the first phase described above, four acid molarities (HCl and H₂SO₄) of 0.3 M, 1.0 M and 3.0 M with immersion time of 1 day were chosen for the RCA fractions from 4 mm to 22.4 mm. This choice will be further discussed in Chapter 4.

Figure 3-4 presents the procedure for removing the mortar adhered in the RCA, where the fraction that will be treated is first chosen, recording the initial weight as M1. Then the RCA is pre-soaked in the acid solutions for the specified time. After the pre-soaking time, the RCA is washed and dried in an oven at 110 °C for 24 hours and the final weight is recorded as M2. The percentage of mass loss is calculated by the mass difference given by Equation 3-5:

$$\%Adhered\ mortar\ loss = \frac{M1 - M2}{M1} \times 100 \quad (\text{Equation 3-5})$$

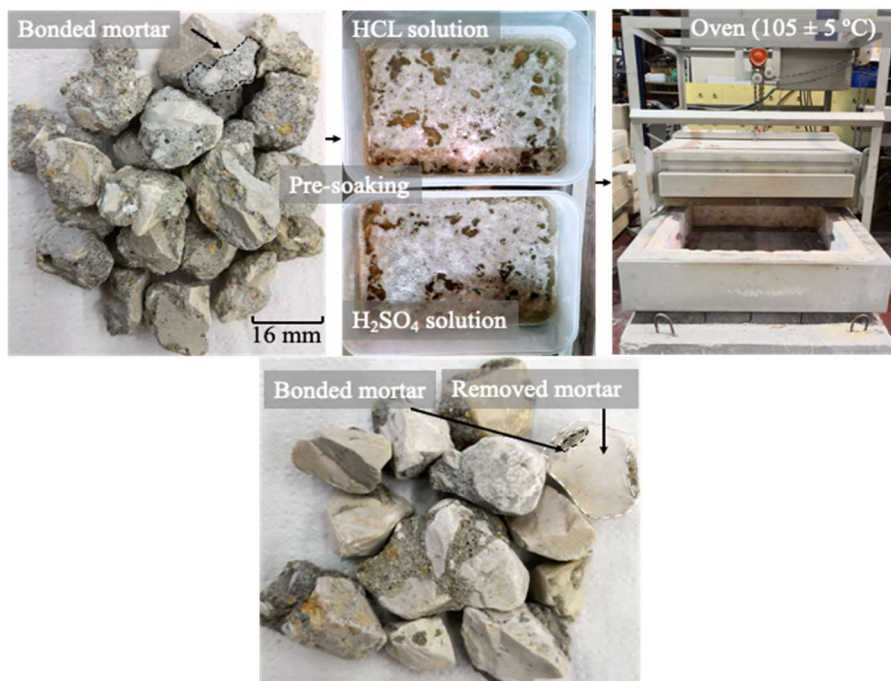


Figure 3-4 Procedure for pre-soaking RCA with HCl and H₂SO₄.

3.3.5 X-Ray diffraction (XRD) and X-Ray fluorescence (XFR) analysis

The X-ray diffraction test was carried out in the Mining and Energy Resources Engineering laboratory at Instituto Superior Técnico. X-ray diffraction was employed to qualitatively characterise the crystalline compounds of AS and cement. Although this technique is qualitative, it is possible to observe that the lower the incidence of well-defined

peaks in the resulting graph of the element the higher the degree of vitrification of the product.

Chemical analysis by X-ray fluorescence was carried out to characterise chemically the cement through quantitative analysis of the concentration of elements in the samples.

3.4 Mix Design

The composition of the mixes was based on the Faury reference curve method. This method makes it possible to determine the best proportion of each of the solid components of concrete so that the resulting size distribution curve (real curve) approximates the reference curve. Based on the NP EM 206-1 (2005) standard, the following data were defined for the calculation of concrete:

- Strength class: C30/37;
- Consistency class: S3 (125 ± 15 mm);
- Environmental exposure class: XC3;
- Binder: CEM I 42.5R;
- Type of aggregates: coarse crushed aggregates and rolled sand of limestone origin;
- Type of water: tap water.

To determine the composition of the concrete mixes, a maximum aggregate size of 22.4 mm was considered. This parameter influences the size of the concrete voids, i.e. the greater the maximum size the lower the void index of concrete and the weaker the wall effect and difficulty of vibration of concrete.

For a class C30/37 concrete, a cement class CEM I 42.5R with 350 kg/m^3 was used, taking into account the aspects mentioned in the LNEC E-464 specification (2007) and a water-cement ratio of 0.50, which corresponds to 175 l/m^3 . Since concrete is a porous material, the volume of voids was calculated using the estimate proposed by the American Concrete Institute (194) as a function of the maximum size of the aggregate used in the mix, and it is possible to calculate the volume that the aggregates take.

Faury's reference curve allows the weighted amount of each of the aggregates in the final concrete composition to be as compact as possible, allowing determining the reference concrete composition shown in Table 3-2. Annex D presents the compositions of the concrete mixes made in this experimental campaign.

Table 3-2 Reference concrete composition.

Size of the aggregates	Volume (m³/m³)
22.4-16	0.0038
16-11.2	0.0882
11.2-8	0.1535
8-5.6	0.0725
5.6-4	0.0582
4-2.0	0.0572
2-1.0	0.0329
1-0.5	0.0543
0.5-0.25	0.0677
0.25-0.125	0.0667
0.125-0.063	0.0259
Volume of aggregates per m³	0.6810
Cement [m³/m³]	0.1284
Water	0.18
Voids	0.02
Total	1.00

3.5 Concrete production

The production of all mixes took into account the replacement of NA with RCA. The mixes with RCA had a replacement content of 100% of coarse aggregates (particles larger than 4 mm) of the NA. The mixing process was carried out following a procedure that takes into account the initial saturation of RCA during the 10 minutes that the concrete production lasts, described below:

- The concrete mixer is humidified to ensure that the w/c ratio is maintained;
- Afterwards, the concreting process begins;
- The NA reference concrete production process was divided into three phases. First, the three fractions of limestone gravel CA1, CA2 and CA3 were mixed for 4 minutes with 2/3 of the total mixing water. Then, sand FA1 and FA2 were added and mixed for two minutes (second phase) and, finally, the cement and 1/3 of the mixing water were added into the mixer, resulting in a total of 10 minutes of mixing,

This production process with pre-saturation during the production of concrete makes it possible to improve the interface between the paste and the aggregate. This improvement was observed in a similar production process in the investigation of Ferreira *et al.* (2011).

Once the concrete was mixed and the moulds prepared (moulds lubricated with release agent), it was poured into the moulds and vibrated using a needle vibrator that ensures an adequate surface finish. After casting the moulds, the specimens were demoulded after 24 hours and placed in the corresponding curing environment for each test. Table 3-3 shows the quantity and dimensions of the specimens used for each test. These tests were carried out for each concrete composition.

Table 3-3 Experimental campaign summary second stage.

Test	Age of the test (days)	Number of specimens	Sizes (mm)
Workability	0	-	-
Compressive strength in cylinders	7	3	d150x300
	28	3	d150x300
Tensile strength in cylinders	28	3	d150x300
Elasticity modulus	28	3	d150x300
Fracture energy	28	3	150x150x150
Water absorption by immersion	28	4	100x100x100
Capillary water absorption test	28	4	d150x100
	7	3	d100x40
	28	3	d100x40
Resistance to carbonation	91	3	d100x40
	28	3	d100x50
Resistance to the penetration of chloride ions	28	3	d100x50
Shrinkage	91	2	100x100x450

3.6 Test procedures for fresh concrete properties

The determination of the characteristics of concrete in the fresh state allows having an idea about the viscosity of concrete that will be reflected in its workability. This characterisation is important because it allows a comparison of the fluidity of the reference mixes in relation to the mixes that incorporate RCA with different treatments and additions. For this characterisation, a single-point test was carried out with the Abrams cone for all mixing.

3.6.1 Workability

Workability is defined as “the amount of mechanical work, or energy, required to produce full compaction of concrete without segregation” (MINDESS, SIDNEY; YOUNG, F; DARWIN, DAVID, 2003). In this experimental campaign, the workability

of concrete was indirectly evaluated following the methodology described in standard NP EN 12350-2 “Tests of fresh concrete. Part 2: Slump test”. The test intends to determine the consistency of concrete in the fresh state measured through slump using the Abrams cone with the parameters of a class S3 concrete (100 mm to 150 mm).

The procedure for this test consists of filling with concrete a frustoconical mould open at both ends with 200 mm at the bottom, 100 mm at the top and a height of 300 mm. Then the concrete is compacted with 25 strokes in three layers, after which the cone is removed to record the slump, which consists of the difference between the height of the concrete cone and the top of the sample (Figure 3-5). The incorporation of RCA in concrete negatively influences the workability of concrete. In this work, it was chosen to change the effective w/c ratio to compensate for this effect by adjusting the water used in the mixing.



Figure 3-5 Slump test, Abrams cone.

3.7 Properties in the hardened state

This section describes the tests carried out on hardened concrete in order to analyse the effect of incorporating treated RCA treated with AS, and to understand how it will influence the mechanical and durability performance in relation to a reference concrete with NA and untreated RCA. The study of these properties makes it possible to determine which acid concentration will be the most suitable for improving them and reducing the environmental impacts.

3.7.1 Compressive strength

To determine the value of the compressive strength of concrete under uniform stress, cylindrical specimens of 15 cm in diameter and 30 cm in height were used in conformity with NP EN 12390-2 (2012) "Tests on hardened concrete. Part 1: Shape, size and other requirements for testing specimens and moulds". Compressive resistance is a primary function of concrete in a structure subjected to forces. The determination of this property, in hardened concrete specimens, is the main objective of this test. In short, the specimens are tested, applying a uniform compressive stress until failure, and the ultimate load to which they resist is recorded. The test methodology is described in standard NP EN 12390-3 (2021) "Test hardened concrete. Part 3: Compressive strength of test specimens".



Figure 3-6 Compressive strength test setup.

To evaluate the evolution of the compressive strength, three specimens were tested at 7 and 28 days. Figure 3-6 shows the procedure performed on the specimens submitted to the compression test. Finally, the compressive strength of each specimen is given by Equation 3-6:

$$f_c = \frac{F}{A_c} \quad \text{(Equation 3-6)}$$

Where;

- f_c - test piece compressive strength (MPa or N/mm²);

- F - maximum breaking load (N);
- A_c - cross-sectional area of the specimen to which the compressive strength is applied (mm^2).

3.7.2 Splitting tensile strength

The splitting tensile strength test is an indirect method of obtaining the tensile strength of concrete, important for certain problems such as cracking, deformation, shear stress, adherence and the sliding of reinforcement, among others (MEHTA; MONTEIRO, 2014). In addition to this test, there are two other types to determine the tensile strength of concrete: direct tensile and flexural tensile. The splitting tensile strength test was used to evaluate the concrete mixes in this experimental campaign because it is the simplest test to be performed and uses cylindrical specimens equal to those of the modulus of elasticity.

The splitting tensile strength test is performed by applying a compressive load to a cylindrical specimen that is located between two rectangular pieces, with dimensions depending on the diameter of the specimen, located diametrically opposite Figure 3-7. The test mechanism develops as follows: for an elastic material, the conditions imposed by the load, in addition to causing compression, also produce a practically uniform tensile stress along a significant area of the diametric plane containing the applied load, generating tensile stresses. uniform tension perpendicular to this diameter (THOMPSON, 1966).

Concrete mixes incorporating RCA generally tend to have a greater loss in splitting tensile strength with increasing aggregate content. This reduction in behaviour is due to the fact that the aggregates have a weaker matrix than NA's, which is reflected in the mechanical performance of the aggregate and the chemical interactions in concrete (ITZ interface transition zone) (DE BRITO; SAIKIA, 2012). The splitting tensile strength of each specimen is given by the following Equation 3-7:

$$f_{ct} = \frac{2 \times F}{\pi \times L \times d} \quad (\text{Equation 3-7})$$

Where,

- f_{ct} - splitting tensile strength (MPa or N/mm^2);

- F - maximum strength (F);
- L - length of specimen contact line (mm);
- d - diameter of the cross section (mm).



Figure 3-7 Splitting tensile strength test procedure.

3.7.3 Modulus of elasticity

The modulus of elasticity of concrete was measured following the methodology described in “Eurocode 2: Design of concrete structures. Part 1-1: General rules and rules for buildings” (2004). The test consists of the analysis of the deformations between two load levels of 1 MPa and a 1/3 of the failure load, with the objective that the slope of this straight line that passes through the two points coincides with the secant modulus of elasticity of concrete that is the objective of this experimental campaign. The value corresponding to the modulus of elasticity for a given load cycle results from Equation 3-8:

$$E_c = \frac{\Delta\sigma}{\Delta\varepsilon} = \frac{\sigma_f - \sigma_i}{\varepsilon_f - \varepsilon_i} \times 10^{-3} \quad (\text{Equation 3-8})$$

Where:

- E_c - modulus of elasticity in compressive strength (GPa);
- σ_i - initial compressive stress applied (MPa);

- σ_f - maximum compressive stress applied (MPa);
- ε_i - recorded strain corresponding to the stress σ_i ;
- ε_f - recorded strain corresponding to the stress σ_f .

The test was performed on cylindrical specimens of 15 cm in diameter and 30 cm in height. Figure 3-8 shows the test assembly procedure, where, to begin with, the cylindrical specimens were subjected to the process of grinding their top and bottom, which ensures that there is no eccentricity when applying the load. Next, the apparatus is placed in order to apply the vertical force, which positions the vertical displacement transducers that will measure the deformation in the elastic regime (70% of the failure load). The modulus of elasticity of each specimen is given by the simple average of the various load cycles performed. For each concrete family, this property results from the simple average of the results of the respective test pieces.

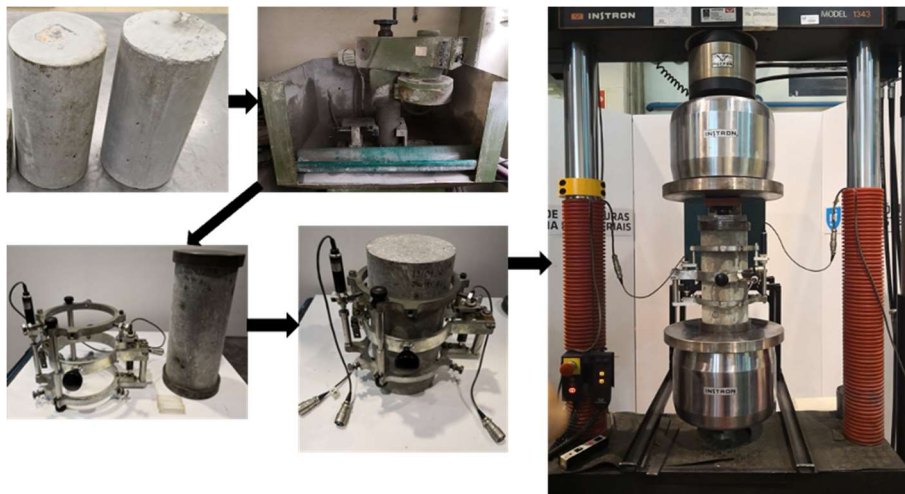


Figure 3-8 Modulus of elasticity test procedure.

3.7.4 Fracture energy

This phase of the experimental program was carried out to meet the objective of investigating the effect of using RCA treated with acid solutions of HCl and S₂SO₄ in concrete mixes with the addition of AS on the fracture energy. For this purpose, six concrete mixes with NA and RCA were produced with different acid treatments and additions of AS described in detail in 4.3.2, all specimens being tested at 28 days of curing. A. The preparation of specimens, description and procedure of the fracture energy test are presented below.

3.7.4.1 Test specimen preparation

Three cubic specimens of 150 mm x 150 mm x 150 mm were produced for each concrete mix, totalling 18 cubes in this experimental campaign. The geometry of the specimens for this test complied with the NT BUILD 511 standard (2005), as shown in Figure 1a,b. There, the specimens are provided with a central groove of 30 mm x 22 mm x 150 mm and sides 4 mm deep. The central notch allows applying the load that will divide the specimen and the sides guarantee the opening of the crack and minimize the wall effects. The lateral and upper notches of the specimen were made using prismatic plastic elements that were adhered to the moulds before each casting (Figure3-9).

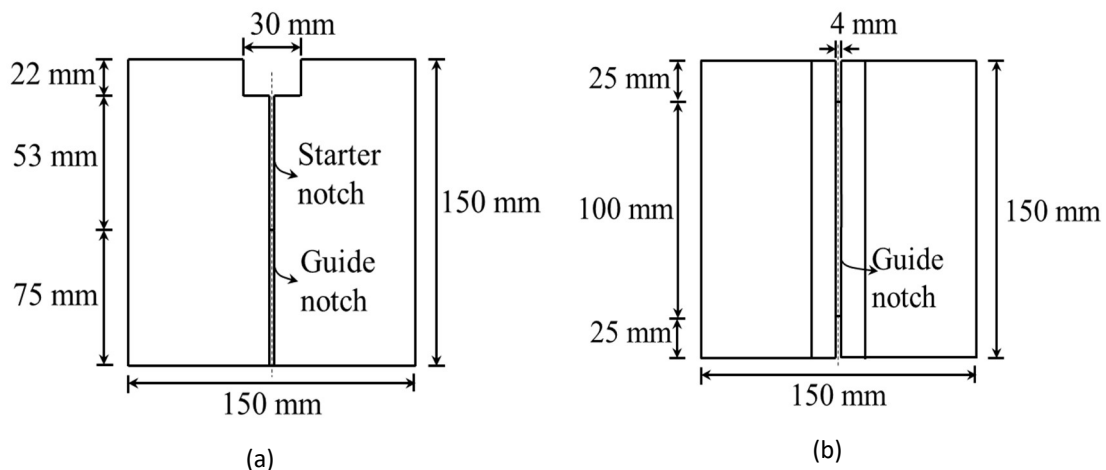


Figure 3-9 Specimens' geometry: front view (a); top view (b) as per NT BUILD 511 (N.BUILD, 2005).

3.7.4.2 Test specimen preparation and test procedure

To perform the fracture energy test, the specimens were first cured for 28 days in a wet chamber at a temperature of 20 ± 2 °C and relative humidity of $95 \pm 5\%$. After 15 days of curing, the specimens were cut to make the upper groove Figure 3-10. After curing for 28 days, the specimens are removed from the humid chamber and dried in the open air for 60 minutes before starting the test. The test system consists of a hydraulic clamp with displacement control, data accuracy, and clip gauge as shown in Figure 3-11.

The test begins by positioning the specimen on the hydraulic press and placing a wedge-shaped device with bearings to transfer the load vertically (F_v) to receive a steel wedge that divides the specimen into two parts (Figure 3-11). The load must be measured to an accuracy of $\pm 1\%$ of the maximum load value by applying a preload of 50 to 100 N.

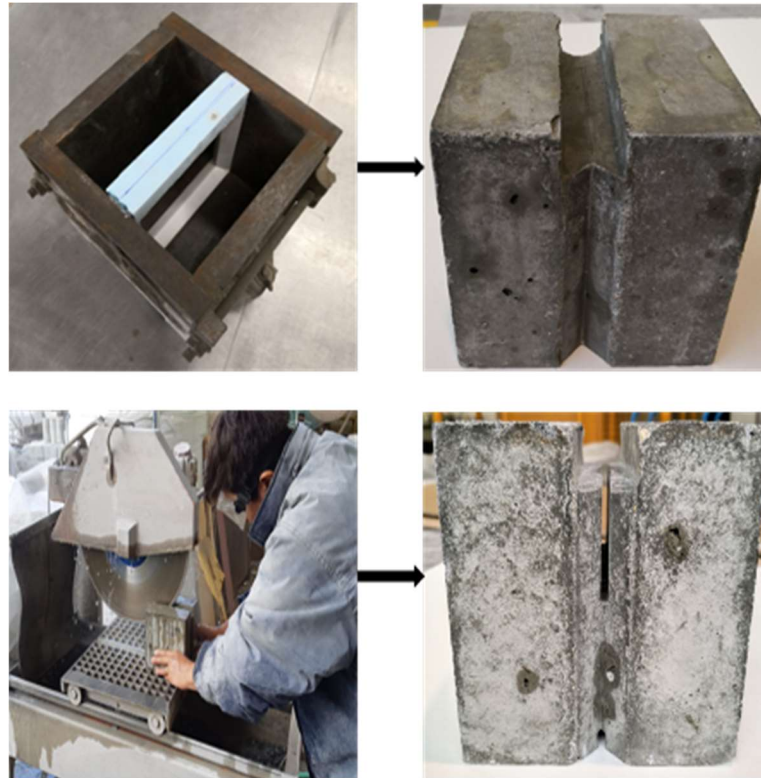


Figure 3-10 Manufacture of the fracture energy test specimens.

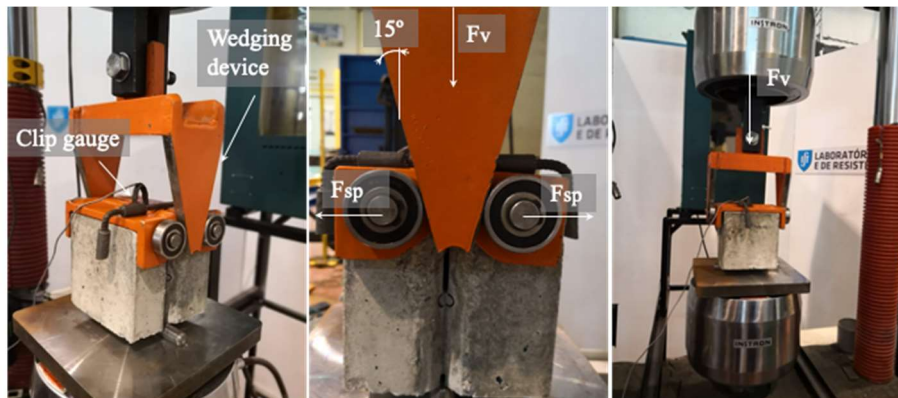


Figure 3-11 Application of the splitting load.

3.7.5 Water absorption by immersion

The test consists of measuring the mass of the specimens before and after immersion in water, in order to determine the water absorption capacity. In this process, water tends to occupy the permeable pores of concrete, indirectly measuring its open porosity, which is more than pores or capillary channels that communicate with each other. This property is directly influenced by recycled aggregates as it has a high-water absorption compared to NA, which reduces the durability of concrete. Mixes with recycled aggregates tend to have greater water absorption as the recycled aggregate content increases. The matrix of the aggregates is what influences the water absorption capacity. In RCA, the increase in water

absorption is due to the old mortar adhered while in mixed aggregates it depends on the type of constituent material.

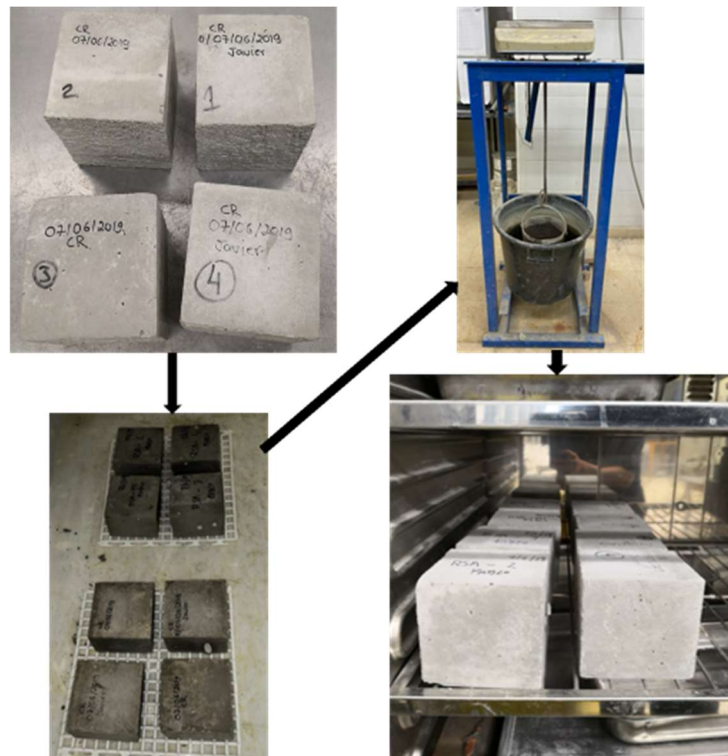


Figure 3-12- Water absorption by immersion test procedure.

Figure 3-12 shows the test procedure for immersion water absorption. The water absorption by immersion is calculated, for each specimen, through Equation 3-9:

$$A_i = \frac{m_1 - m_3}{m_1 - m_2} \times 100 \quad (\text{Equation 3-9})$$

Where,

- A_i - water absorption by immersion (%);
- m_1 - mass of the sample saturated in air (g);
- m_2 - hydrostatic mass of the saturated specimen (g);
- m_3 - dry specimen mass (g).

3.7.6 Capillary water absorption test

The objective of this procedure is to monitor the increase in the mass of the samples due to the absorption of water through the transport of liquids due to the surface tension acting on the capillary pores of concrete. The surface tension of the liquid that penetrates the pores causing the emergence of capillary forces that causes the liquid to rise through the pores. The intensity of capillary forces depends on the characteristics of the liquid (viscosity, density and surface tension), on the characteristics of the porous solid (radius, tortuosity and pore continuity), on the surface energy and on the moisture content (COUTINHO; GONÇALVES, 1997; HELENE, 1993).

The test methodology is described in LNEC E-393 (1993) specification “Determination of water absorption by capillarity”. The specimens must have a minimum volume of 0.001 m³ and a square or circular section. The test was carried out on cylindrical specimens, 150 mm in diameter and 100 mm in length. To obtain these dimensions, it was necessary to saw cylindrical specimens of equal diameter and length of 300 mm. For each concrete composition, four specimens were tested.

Before carrying out the test itself, the specimens were stored in a wet chamber for 28 days, at a temperature of 20 ± 2 °C and relative humidity of 95 ± 5%, and then dried for 14 days in a ventilated oven at room temperature of 60 ± 5 °C. The capillary absorption at time t_i is calculated, for each specimen, by Equation 3-10:

$$A_c = \frac{M_i - M_0}{A_s} \quad (\text{Equation 3-10})$$

Where;

- A_c - water absorption by capillarity, at the instant t_i (g/mm²);
- M_0 - mass of the oven-dry test specimen (g);
- M_i - mass of the specimen, at the moment t_i (g);
- A_s - area of the specimen face that was in contact with water (mm²).

Figure 3-13 presents the description of the capillary water absorption test, where the procedure that was carried out in this experimental campaign can be observed in detail.

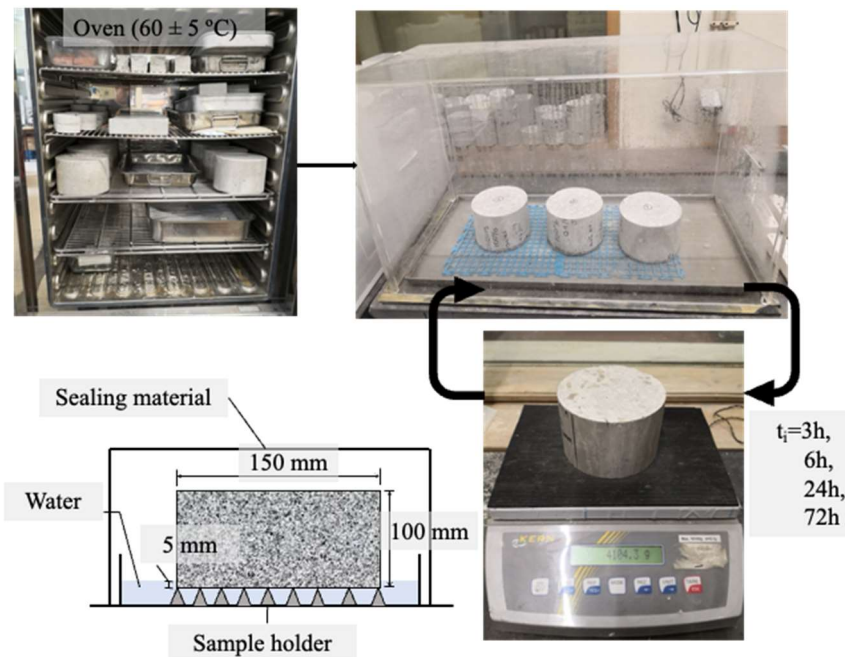


Figure 3-13 Water absorption by capillary test procedure.

3.7.7 Resistance to carbonation

The resistance to carbonation of the different compositions is given by the simple average of the depths of the carbonated products deposited in the concrete pores (CaCO_3). It is very important to control this property because, in reinforced concrete, when the carbonation front reaches the reinforcement, it generates CO_2 diffusion phenomena when it is dissolved in concrete. When CO_2 is dissolved in concrete, calcium hydroxide is transformed into calcium carbonate, which reduces the pH, leaving an alkaline environment that enhances the corrosion of the reinforcement (MEHTA; MONTEIRO, 2014; NEVILLE; BROOKS, 1987).

This test was carried out in accordance with LNEC E-391 (1993) specification “Determination of resistance to carbonation”. The test consists of evaluating the depth of penetration of CO_2 in the concrete specimens (Figure 3-14). The test begins after the specimens undergo a 14-day wet-chamber cure and a 14-day dry-chamber cure. After curing, the specimens are subjected to conditions of concentration of CO_2 in a 5% CO_2 chamber and a temperature of 20 ± 2 °C, accelerating the exposure of concrete to this environment (Figure 3-14). After the exposure time (7, 28 and 91 days), the penetration of CO_2 in mm is measured with a minimum of eight readings per part of the specimen. The result of this reading is called d_k and can be a homogeneous front of carbonated concrete or zones with different depths ($d_{k\text{max}}$). In both cases, the maximum penetration

depths were measured (Figure 3-14).

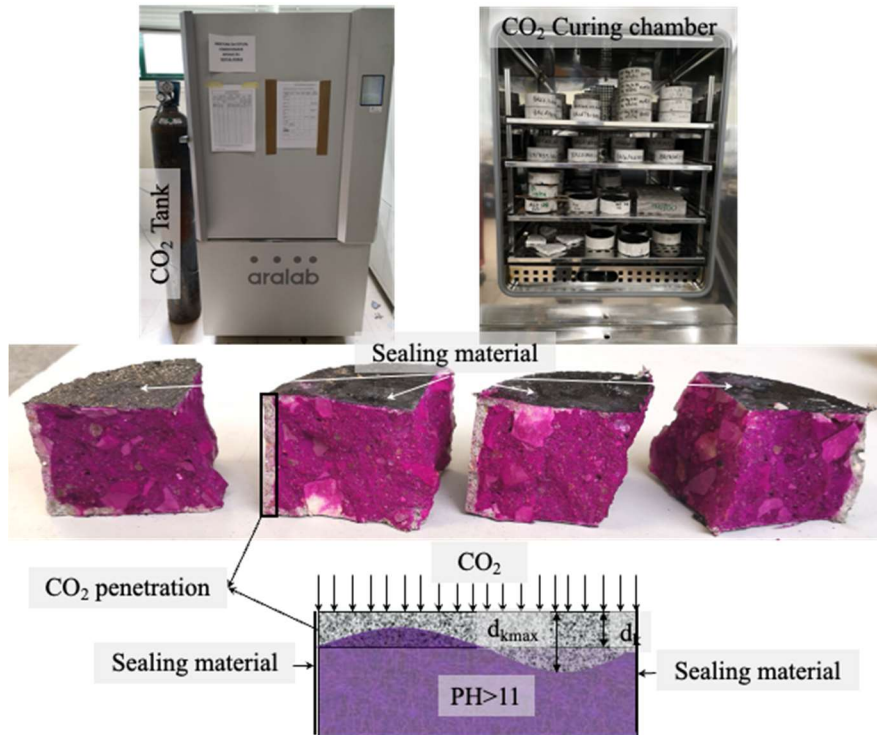


Figure 3-14 Carbonation test procedure.

3.7.8 Resistance to the penetration of chloride ions

The penetration of chloride ions into concrete is usually done with diffusion tests, as chlorides are responsible for the corrosion of reinforcement and the fact that the chloride ions size is 181×10^{-12} m guarantees the diffusion process. The methodology and principles adopted for this test are described in the LNEC specification E-463(2004) “Determination of the chloride diffusion coefficient by migration test in a non-stationary regime”. The diffusion of chlorides consists of the transport of these ions by concentration difference in different regions resulting from the flow of these ions from the region of high concentration to the region of low concentration, not depending on the movement of water, but rather on the existence of an electrolyte and a gradient. of concentration (LI, 2022).

In this work, cylindrical specimens with 100 mm in diameter and 50 mm in height were cured in two phases: 14 days in a wet chamber (temperature of 20 ± 2 °C and relative humidity of $95 \pm 5\%$), followed by 14 days in a dry chamber (temperature of 20 ± 2 °C and relative humidity of $60 \pm 5\%$). The test starts by saturating the specimens with a solution of calcium hydroxide with the help of a vacuum pump. The specimen is sealed on the side and a solution of NaCl (negative terminal) and NaOH (positive terminal) is added. Then a current

is added at the terminals for 24 hours and finally, using AgNO_3 , the penetration of chloride ions is observed. Figure 3-15 shows the test procedure performed for all mixes.

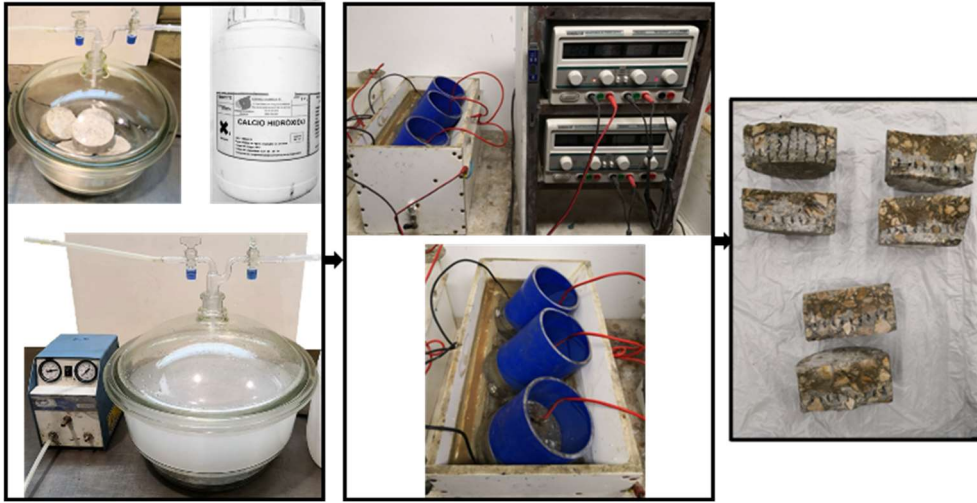


Figure 3-15 Resistance to the penetration of chloride ions test procedure.

The value of the chloride migration coefficient is calculated by Equation 3-11:

$$D_{nssm} = \frac{R \times T}{z \times F \times E} \times \frac{x_d - \alpha \sqrt{x_d}}{t} \quad (\text{Equation 3-11})$$

Where,

$$E = \frac{U - 2}{L} \quad (\text{Equation 3-12})$$

$$\alpha = 2 \times \sqrt{\frac{R \times T}{z \times F \times E}} \times \text{erf}^{-1} \left(1 - \frac{2c_d}{c_0} \right) \quad (\text{Equation 3-13})$$

Where,

- D_{nssm} - migration coefficient in non-stationary regime (m^2/s);
- R - perfect gas constant ($8.314 \text{ J}/(\text{K} \cdot \text{mol})$);
- T - average temperature between the beginning and end of the test in the anodic solution (K);
- z - absolute valence value of chloride ion ($z = 1$);
- F - Faraday's constant ($9.648 \times 10^4 \text{ J}/(\text{V} \cdot \text{mol})$);

- x_d - average penetration depth value (m);
- t - test duration time (s);
- U - voltage applied to the circuit (V);
- L - test piece thickness (mm);
- erf^{-1} - inverse of the error function;
- c_d - concentration of chlorides at which the silver solution reacts ($c_d = 0.07 N$);
- c_0 - chloride concentration at the cathode ($c_0 = 2 N$).

3.7.9 Shrinkage

The phenomenon of dimensional change that concrete by shrinkage can be of several types such as: thermal shrinkage, plastic shrinkage, autogenous shrinkage, chemical shrinkage and drying shrinkage. In this study, drying shrinkage was studied, which is the mechanism of excess water that has not reacted with the cement migrating from the interior of the concrete mass to the surface. The evaporation of moisture decreases the volume of concrete (2022).

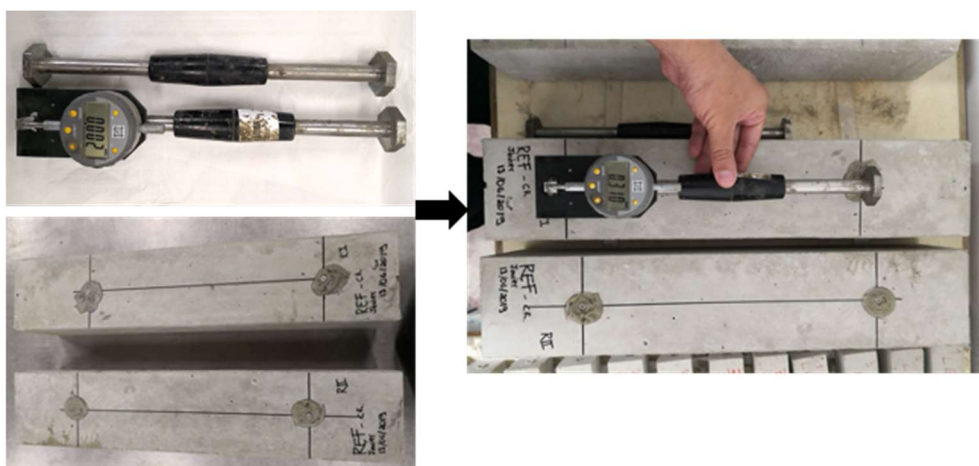


Figure 3-16 Concrete shrinkage test procedure.

The test procedure was carried out following the LNEC E-398 (1993) specification “Determination of shrinkage and expansion”, in prismatic specimens with dimensions of 450 mm in length and edges of 100 mm. Two specimens were tested for

each mix. The test methodology establishes the bonding of two metallic chemical nails 300 mm apart measured using a standardized bar. The test duration is 90 ± 1 days stored in a dry chamber at a temperature of 20 ± 2 °C and a relative humidity of $50 \pm 5\%$. The measurement is taken every day after demoulding for the first 7 days, then the reading is taken every two days for two weeks and then every five days until the test is completed. Figure 3-16 presents the methodology of the shrinkage test, where the strain gauge and specimens can be observed during the test.

The result of the shrinkage test of each composition is made by the average of the test specimens Equation 3-14:

$$\varepsilon = \frac{d_f - d_i}{d_i} \quad (\text{Equation 3-14})$$

Where;

- ε - shrinkage (mm/mm);
- d_i - distance between reference points after placement of the metal inserts (mm);
- d_f - distance, after a certain time from the start of the test, between the metal inserts (mm).

3.7.10 Microstructural analysis using Scanning Electron Microscopy (SEM)

Microstructural analysis using Scanning Electron Microscopy (SEM) is a widely used technique to study the microstructure of concrete. The application of this technique in this specific case has as main objective to understand the existing interaction between RCA and the cementitious matrix, after treatments with acids (HCl and H₂SO₄) and addition of aluminium sulphate (AS). The study intends to observe the behaviour of the transient interface zone (ITZ) between the aggregates and the cementitious matrix, because this zone determines the macroscopic behaviour of the concrete and its properties in the hardened state.

The concrete samples are obtained from square specimens with 10 mm edge, which are cured in a humid chamber (20°C and 100% humidity) for 28 days. Then, the samples are dried in an oven at 40 °C and impregnated with a gold and palladium solution

before being introduced in the SEM to perform the test (Figure 3-17)

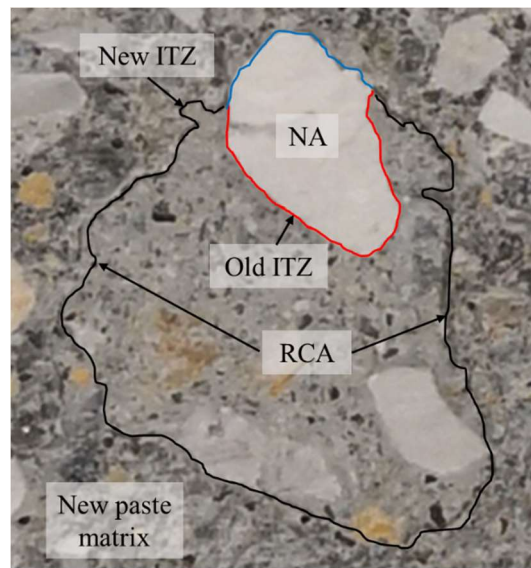


Figure 3-17 Sample for SEM analysis.

SEM works by directing a beam of electrons onto the surface of the material and observing how these electrons are dispersed. From this information, it is possible to generate a magnified image of the material's surface, allowing microscopic details such as cement grains, aggregates, voids, and cracks to be seen. This technique is useful to evaluate the quality of concrete, identify weak points and analyse the hardening and degradation process. Figure 3-18 presents the analysis procedure performed on all concrete mixes of this experimental campaign.

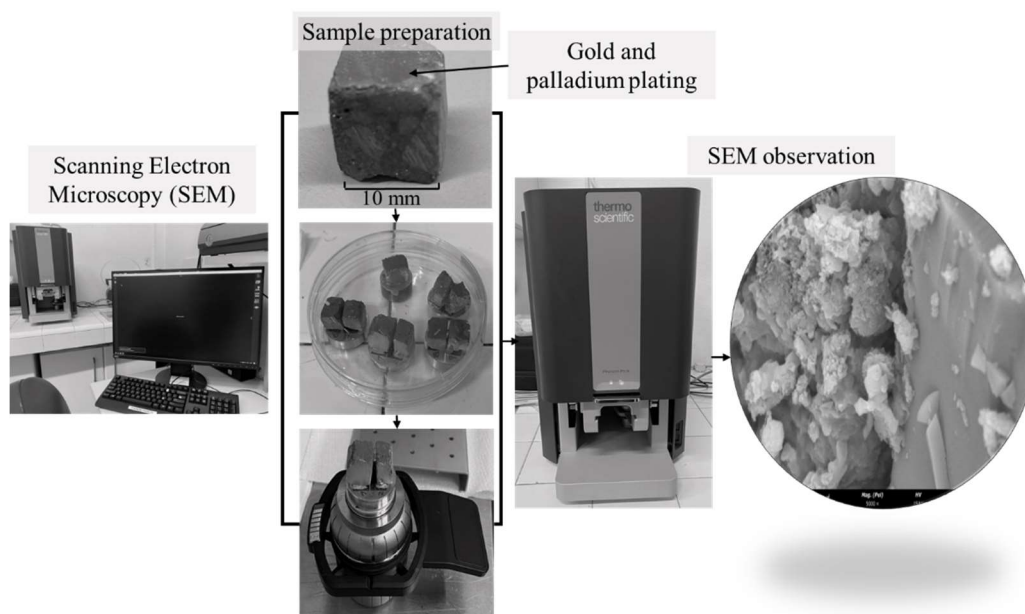


Figure 3-18 microstructural analysis procedure using Scanning Electron Microscopy (SEM)

*FIRST STAGE RESULTS AND DISCUSSION:
OPTIMAL DETERMINATION OF ACID
MOLARITY FOR REMOVAL OF MORTAR
ADHERED TO RCA.*

“Let the future tell the truth and evaluate each one according to his work and accomplishments. The present is theirs; the future, for which I have really worked, is mine.”
Nikola Tesla

4 CHARACTERIZATION OF MATERIALS AND MORTAR REMOVAL PERFORMANCE IN RCA

In this chapter, the results and analysis of the characterization tests are presented, as well as the performance of the removal of the mortar adhered to RCA performed on the materials used in this thesis. The characterization of the materials will help in understanding the performance of the mixes in the fresh and hardened state, because the effects of each component of the mixes and its influence on each property can be isolated.

This chapter first shows the characterization of the crystalline compounds and their chemical composition of both cement and aluminium sulphate (AS) using the techniques of x-ray diffraction and chemical characterization by x-ray fluorescence spectroscopy. After that, density, water absorption, size distribution of NA and RCA tests were performed. Subsequently, mortar removal was performed on the RCA using different acid concentrations of hydrochloric acid (HCl) and sulphuric acid (H₂SO₄) as well as pre-soaking times in order to determine the best removal performance index.

Finally, the correlations between the physical properties and the acid concentrations used for removal are presented, and the results are compared with existing literature.

4.1 X-Ray Diffraction Analysis (XRD)

X-ray diffraction (XRD) analysis is a technique used to identify the crystalline phases present in a sample of cement. X-rays are directed at the sample, and the diffraction pattern created by the interaction of the X-rays with the sample's atoms can be used to identify the crystals present in the sample. This technique is commonly used in the cement industry to study the composition of cement samples and to identify impurities or other phases that may affect the properties of the cement. XRD can also be used to determine the crystal size and to study the microstructure of the cement. Figure 4-1 presents the XRD plot of Portland cement type I 42.5R with its main mineralogical compounds. The X-ray diffractogram of Portland cement type I 42.5R showed peaks calcium silicate (Ca₂SiO₄), calcium aluminium and gypsum. These elements found are in accordance with EN 197-1 (2001) and with authors who used the same type of cement (SZELAĞ, 2018).

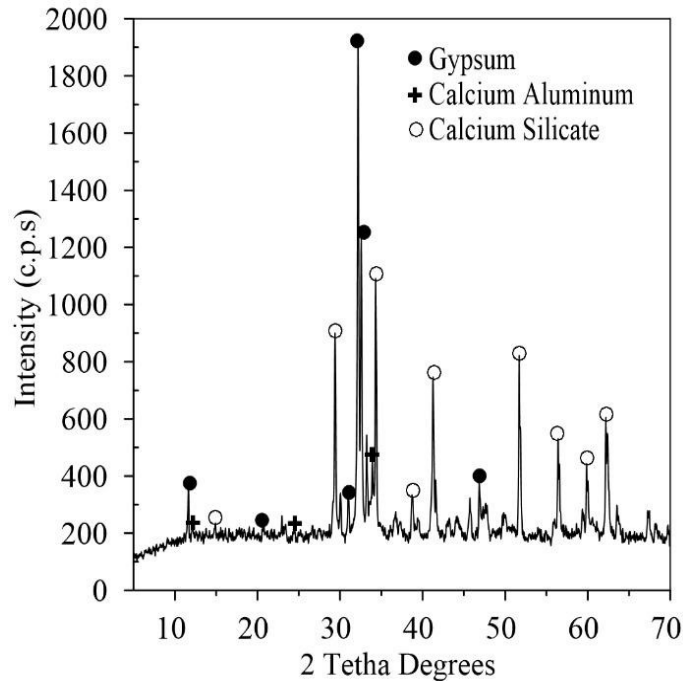


Figure 4-1 XRD pattern of the CEM I 42.5R Portland cement.

Crystallographic analysis of aluminium sulphate revealed an anortic (orthorhombic) structure, characterised by the absence of rotational symmetry or reflection about a specific axis. This compound is associated with the P-1 space group, indicating a non-centred translational symmetry. In the context of cement hydration, aluminium sulphate plays a significant role. Its crystalline structure and properties can influence the development of phases during the cement hydration process, affecting the characteristics of the resulting concrete. The presence of aluminium sulphate can influence the formation of different crystalline phases during hydration, directly impacting on the mechanical and chemical properties of the final material. Understanding the P-1 space group and the crystalline structure of aluminium sulphate is fundamental to elucidating how this component interacts during cement hydration, allowing for a more in-depth analysis of crystalline transformations and their impact on the performance of the resulting concrete. The results indicated that the crystal structure was aluminium sulphate hydrate or aluminium octadecahydrate. The diffractogram presented in Figure 4-2 illustrates the crystal structure of aluminium sulphate ($\text{Al}_2(\text{SO}_4)_3 \cdot 18\text{H}_2\text{O}$), allowing the identification of the crystal structure of aluminium sulphate, concluding of a high degree of purity of the compound.

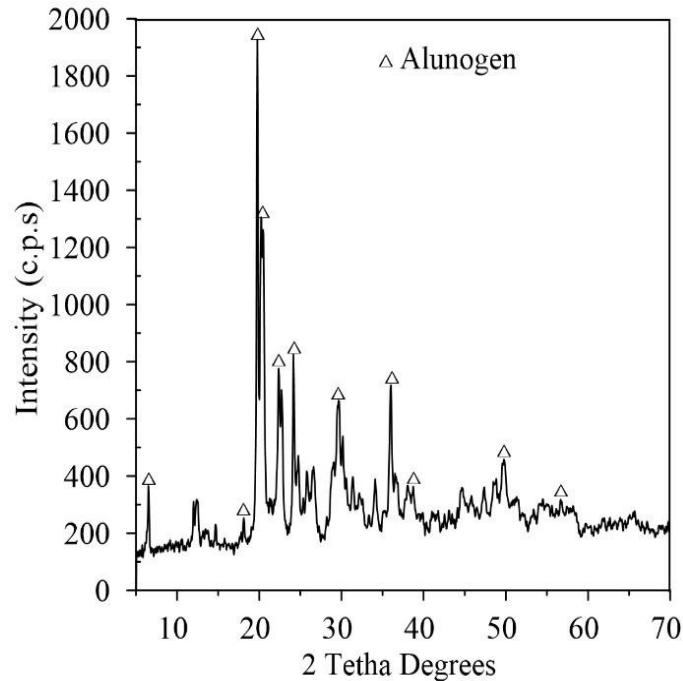


Figure 4-2 XRD pattern of the AS.

4.2 X-ray fluorescence spectroscopy

X-ray fluorescence spectroscopy (XRF) was used to determine the chemical composition of the cement. This technique analysed the main elements found in the cement, and this information is used to control the chemical composition of the CEM I 42.R cement and ensure that it meets the required chemical and physical specifications. According to Table 4-1, the main compound is CaO (Calcium oxide) with 62.71%, followed by SiO₂ (Silicon dioxide) with 19.59%. Other elements found in smaller quantities are: Al₂O₃ (Aluminium oxide) with 5.245%, Fe₂O₃ (Iron oxide) with 3.17%, MgO (Magnesium oxide) with 2.23% and SO₃ (Sulphur trioxide) with 3.13%.

All the elements found in the CEM I 42.5 R cement are in accordance with the chemical composition classification presented in the EN197-1 (2001).

Table 4-1 Chemical composition of cement (% by mass).

Component	SiO ₂	Al ₂ O ₃	Fe ₂ O ₃	CaO	MgO	SO ₃	Cl ⁻	LOI	Insoluble residue
CEM I 42.5 R	19.59	5.24	3.17	62.71	2.23	3.13	0.01	2.94	1.37

4.3 Characterization of aggregates

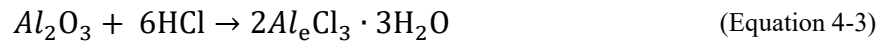
The following intends to describe and analyse the results of the tests carried out on NA and RCA. This analysis is crucial for accurately designing the mixes and

evaluating the efficiency of removing the mortar adhered on the RCA, which will be used in the aggregates present in the production of mixes with RCA incorporation.

In the following, the results obtained from the physical tests performed are described and analysed, including volume mass and water absorption, water absorption in time, removal of mortar adhered to the RCA and size distribution.

4.3.1 Determination of mortar loss

The description of adhered mass loss in RCA is presented in section 2.3.2, where diameters of 11.2 mm, 16 mm and 22.4 mm were evaluated. Table 4-2 shows the mass loss of adhered mortar in relation to different HCl concentrations and immersion durations. The results indicate that mass loss increases with acid concentration. For example, removal with 1 day immersion varies from 0.63% to 14.3% for an aggregate diameter of 11.2 mm with concentrations of 0.1 M and 3 M, respectively. Mortar removal with 3- and 6-day immersion did not show a significant increase compared to 1 day immersion. This trend was also observed at 16 mm and 22.4 mm diameters. This is because the acid loses OH⁻ ions during the reaction with the mortar, as described in section 2.2 simplified with HCl (RYU; KIM; SHIN; LIM *et al.*, 2018; SHI; STEGEMANN, 2000). The reactions of the removal mechanism with HCl are described in Equations 4-1, 4-2 3 4-3 described below:



According to a research conducted, the trends of the results obtained were similar to those observed by Ismail and Ramli (2013) These authors studied the removal of mortar at acid concentrations of 0.1M, 0.5M and 0.8M, with pre-soaking times of 1, 3 and 7 days. They found a linear correlation between mass loss and molarity, with a removal of approximately 4-5% for 0.8M and between 1-3% for the 0.1M and 0.5M molarities, Ismail and Ramli (2013) concluded that the increase in immersion times of 3 and 7 days did not show a significant increase in the percentage removal.

According to Table 4-2, the mass loss of RCA is greater for the diameter 11.2mm, confirming the same trend found by Juan and Gutierrez (2009) These authors found a larger range of mortar adhered to aggregates with small diameters (33% to 55% mortar), which was eliminated with HCl, increasing the efficiency of the acid removal.

The relationship between the acid concentration of HCl and the lost mass of the RCA is presented in Figures 4-3a,b,c. In them, it is possible to observe the trends for each RCA diameter and immersion period. Figure 4-3a shows the relationship between molar concentration of HCl and lost mass of RCA with diameter of 11.2 mm, with $R^2 = 0.87$, 0.80 and 0.86 for 1, 3 and 6 days of immersion, respectively. Similarly, the relationship was analysed for the RCA with 16 mm diameter (Figure 4-3b), revealing a strong correlation between the variables, with $R^2 = 0.84$, 0.83 and 0.80 for 1, 3 and 6 days of immersion, respectively. Finally, the same trend is observed for the RCA with a diameter of 22.4 mm, with $R^2 = 0.77$, 0.76 and 0.76 for 1, 3 and 6 days of immersion, respectively.

Table 4-2 Mass loss of RCA in % with HCl.

Pre-soaking time	Molarity (M)	11.2 mm			16 mm			22.4 mm		
		Mortar loss of mass (%Wt)	σ	CoV	Mortar loss of mass (%Wt)	σ	CoV	Mortar loss of mass (%Wt)	σ	CoV
1 Day	RCA	0.0	0.0	0.0	0.0	0.0	0.0	0.0	0.0	0.0
	0.1	0.63%▲	0.11	17.56%	0.79%▲	0.01	1.64%	0.83%▲	0.125	15.02%
	0.2	0.84%▲	0.12	14.29%	0.82%▲	0.18	21.95%	0.93%▲	0.15	16.13%
	0.3	3.92%▲	1.77	45.09%	3.02%▲	0.25	8.27%	2.30%▲	0.88	38.26%
	0.4	3.78%▲	1.30	34.39%	3.50%▲	0.23	6.57%	3.20%▲	0.78	24.38%
	0.5	3.84%▲	0.51	13.31%	4.20%▲	0.56	13.34%	4.85%▲	1.2	24.74%
	0.6	8.03%▲	1.16	14.50%	3.65%▲	0.45	12.34%	9.61%▲	0.25	2.60%
	1.0	9.35%▲	1.39	14.90%	8.64%▲	1.30	15.05%	11.33%▲	0.56	4.94%
	3.0	14.30%▲	1.60	11.19%	10.50%▲	0.80	7.62%	12.60%▲	0.14	1.11%
3 Days	RCA	0.0	0.0	0.0	0.0	0.0	0.0	0.0	0.0	0.0
	0.1	1.13%▲	0.33	29.00%	1.33%▲	0.33	24.54%	0.92%▲	0.56	60.87%
	0.2	1.23%▲	0.15	12.20%	0.95%▲	0.12	12.63%	1.02%▲	0.78	76.47%
	0.3	4.24%▲	1.30	30.66%	3.15%▲	1.77	56.10%	2.45%▲	0.12	4.90%
	0.4	4.55%▲	1.40	30.77%	3.65%▲	1.60	43.84%	3.56%▲	0.14	3.93%
	0.5	4.63%▲	1.40	30.24%	4.44%▲	0.51	11.52%	5.02%▲	0.25	4.98%
	0.6	8.43%▲	1.10	13.05%	4.56%▲	1.16	25.53%	11.00%▲	0.23	2.09%
	1.0	9.60%▲	1.70	17.71%	9.43%▲	1.39	14.77%	12.10%▲	0.36	2.98%
	3.0	14.78%▲	1.90	12.86%	11.20%▲	1.60	14.29%	13.60%▲	1.2	8.82%
6 Days	RCA	0.0	0.0	0.0	0.0	0.0	0.0	0.0	0.0	0.0
	0.1	1.82%▲	0.17	9.17%	1.62%▲	0.25	15.43%	1.41%▲	0.56	39.78%
	0.2	2.74%▲	0.06	2.09%	2.67%▲	0.36	13.47%	2.81%▲	0.23	8.18%
	0.3	4.06%▲	0.32	7.97%	4.16%▲	0.15	3.61%	4.79%▲	0.54	11.27%
	0.4	4.66%▲	0.19	4.12%	4.37%▲	0.25	5.72%	4.84%▲	0.12	2.48%
	0.5	6.37%▲	1.14	17.89%	5.71%▲	0.23	4.03%	8.39%▲	0.18	2.14%
	0.6	7.82%▲	0.86	10.95%	5.84%▲	0.58	9.93%	7.42%▲	0.23	3.10%
	1.0	12.13%▲	0.29	2.39%	11.44%▲	0.63	5.51%	11.91%▲	0.17	1.43%
	3.0	14.00%▲	0.89	6.36%	12.90%▲	0.56	4.34%	14.60%▲	0.14	0.96%

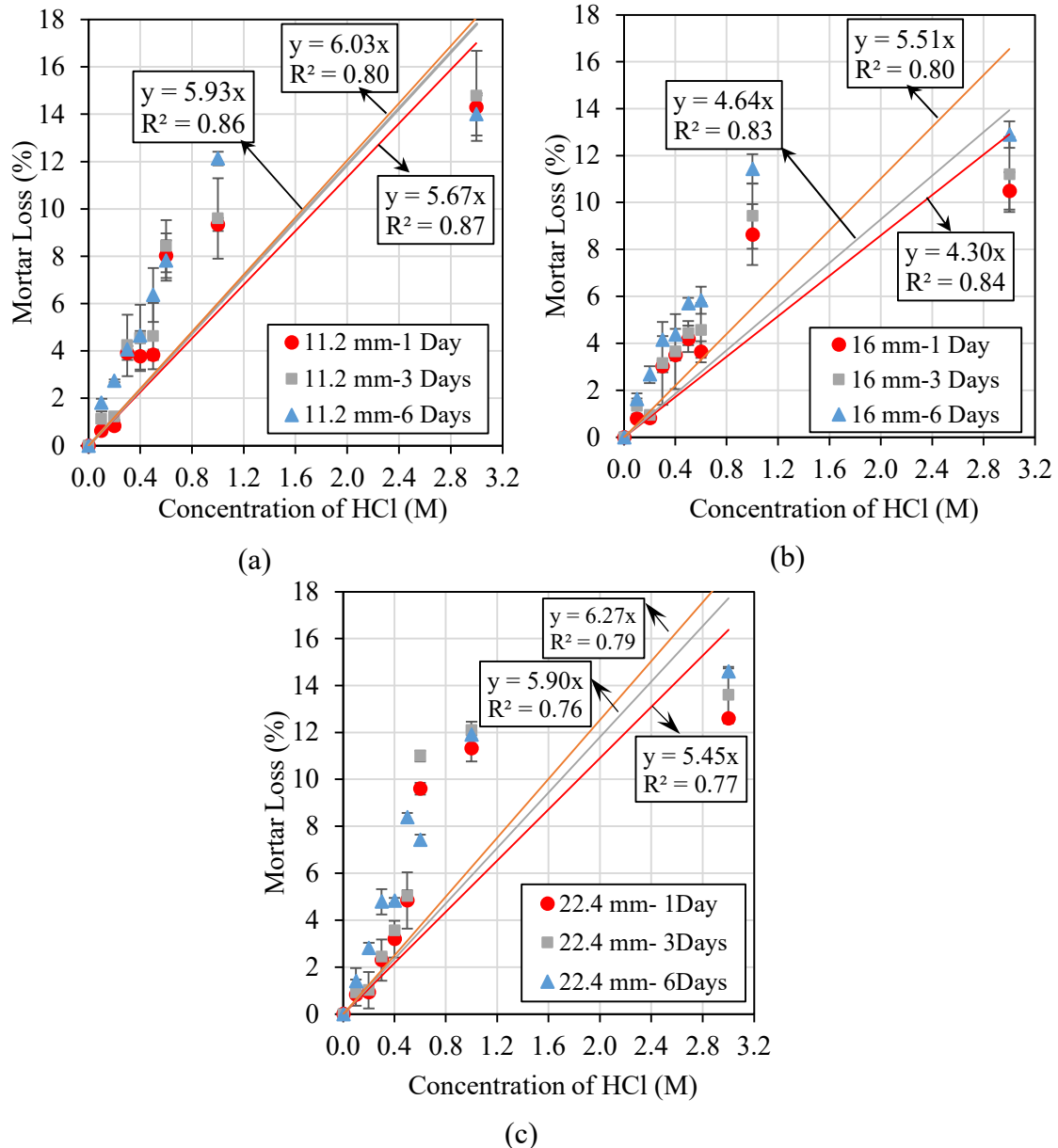
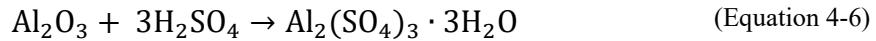
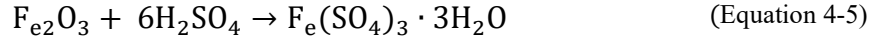
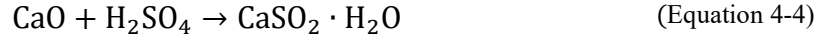


Figure 4-3 Concentration of HCl versus mass loss (%) in diameters of 11.2 mm , 16 mm and 22.4 mm for 1, 3 and 6 days.

A second acid was selected to evaluate the mortar removal efficiency in the RCA. The chosen acid was H_2SO_4 , used at the same acid molarities (0.1 M, 0.2 M, 0.3 M, 0.4 M, 0.5 M, 0.6 M, 1.0 M and 3.0 M) and immersion periods for comparison with the first acid (HCl). The results of mortar removal with H_2SO_4 are shown in Table 4-3, where it can be seen that the mass loss ranges from 1.38% to 4.66% for RCA treated with molarities from 0.1 M to 3.0 M and 1 day of pre-soaking. The mass loss increases to ranges from 1.52% to 5.10% after 3 days of immersion and from 2.11% to 5.89% after 6 days.

Sulphuric acid corrosion of concrete is caused by the reactions with the strong acid. H_2SO_4 reacts with the $Ca(OH)_2$ present in the concrete, dissolving the calcium salts

and reducing the alkalinity of the material (MIN; SONG, 2018). The reactions that occur in the corrosion layer formed by sulphuric acid can be represented as:



According to Akbarnezhad *et al.* (2013) , H₂SO₄ was used to remove mortar at concentrations of 0.1, 0.5 and 1 M, resulting in mass losses of 2%, 14% and 34% after one day of exposure and mass losses of 2%, 13% and 34% after 5 days of exposure. Al-Bayati *et al.* (2016) and Saravankumar *et al.* (2016) reported mass losses of 3.92% and 5% for RCA after one day of immersion at 0.1 M and 2.7 M concentration, respectively. These results agree with the trend of the results found in this research.

Table 4-3 Mass loss of RCA in % with H₂SO₄.

Pre-soaking time	Molarity (M)	11.2 mm			16 mm			22.4 mm		
		Mortar loss of mass (%Wt)	σ	CoV	Mortar loss of mass (%Wt)	σ	CoV	Mortar loss of mas (%Wt)	σ	CoV
1 day	RCA	0,0	0,0	0,0	0,0	0,0	0,0	0,0	0,0	0,0
	0.1	1.38%▲	0.11	7.63%	1.59%▲	0.15	9.44%	1.68%▲	0.25	14.88%
	0.2	1.14%▲	0.63	55.11%	1.68%▲	0.24	14.26%	1.56%▲	0.35	22.44%
	0.3	2.42%▲	0.66	27.44%	2.28%▲	0.75	32.84%	2.45%▲	1.23	50.20%
	0.4	2.04%▲	0.46	22.42%	2.84%▲	0.84	29.57%	2.68%▲	1.12	41.79%
	0.5	3.14%▲	0.40	12.71%	3.10%▲	0.58	18.71%	3.25%▲	0.98	30.15%
	0.6	3.43%▲	0.35	10.32%	2.93%▲	0.95	32.47%	2.87%▲	0.57	19.86%
	1.0	4.08%▲	0.53	12.96%	4.19%▲	0.75	17.88%	4.23%▲	1.21	28.61%
3 days	RCA	0.00%▲	0.0	0.0	0.00%▲	0.0	0.0	0.00%▲	0.0	0.0
	0.1	1.52%▲	0.14	9.21%	1.65%▲	0.21	12.73%	1.75%▲	1.2	68.57%
	0.2	1.56%▲	0.78	50.00%	1.89%▲	0.14	7.41%	1.89%▲	1.02	53.97%
	0.3	2.89%▲	0.89	30.80%	2.56%▲	0.23	8.98%	3.15%▲	1.23	39.05%
	0.4	2.15%▲	0.56	26.05%	3.25%▲	0.15	4.62%	3.56%▲	1.23	34.55%
	0.5	3.21%▲	0.42	13.08%	3.45%▲	0.87	25.22%	4.01%▲	0.98	24.44%
	0.6	3.56%▲	0.69	19.38%	3.89%▲	0.98	25.19%	4.15%▲	0.78	18.80%
	1.0	4.25%▲	0.78	18.35%	4.56%▲	0.78	17.11%	4.25%▲	0.89	20.94%
6 days	RCA	0.00%▲	0.0	0.0	0.00%▲	0.0	0.0	0.00%▲	0.0	0.0
	0.1	2.11%▲	1.15	54.50%	2.15%▲	0.15	6.98%	2.87%▲	0.55	19.16%
	0.2	2.15%▲	1.24	57.67%	2.25%▲	0.24	10.67%	2.44%▲	0.25	10.25%
	0.3	3.25%▲	1.56	48.00%	2.69%▲	0.75	27.88%	2.75%▲	0.98	35.64%
	0.4	3.55%▲	1.21	34.08%	3.65%▲	0.84	23.01%	3.55%▲	1.23	34.65%
	0.5	3.89%▲	0.45	11.57%	3.78%▲	0.58	15.34%	3.89%▲	0.45	11.57%
	0.6	4.12%▲	0.55	13.35%	4.15%▲	0.95	22.89%	4.15%▲	0.25	6.02%
	1.0	4.25%▲	0.65	15.29%	4.78%▲	0.75	15.69%	4.88%▲	1.23	25.20%
	3.0	5.89%▲	0.78	13.24%	4.89%▲	0.45	9.20%	4.59%▲	1.11	24.18%

Figure 4-3a,b,c presents the relationship between H₂SO₄ concentration and mass loss for diameters of 11.2mm, 16mm and 22.4mm and pre-soaking times of 1 day, 3 days and 6 days. It was observed that the coefficient of determination (R²) was 0.76, 0.79 and 0.89 for 11.2mm diameter and 0.77, 0.78, 0.83 for 16mm diameter and 0.76, 0.80, 0.87 for 22.4mm diameter, respectively. The trend of mass loss was logarithmic with respect to H₂SO₄ concentration. The analysis indicates that there is a non-linear correlation between these two parameters.

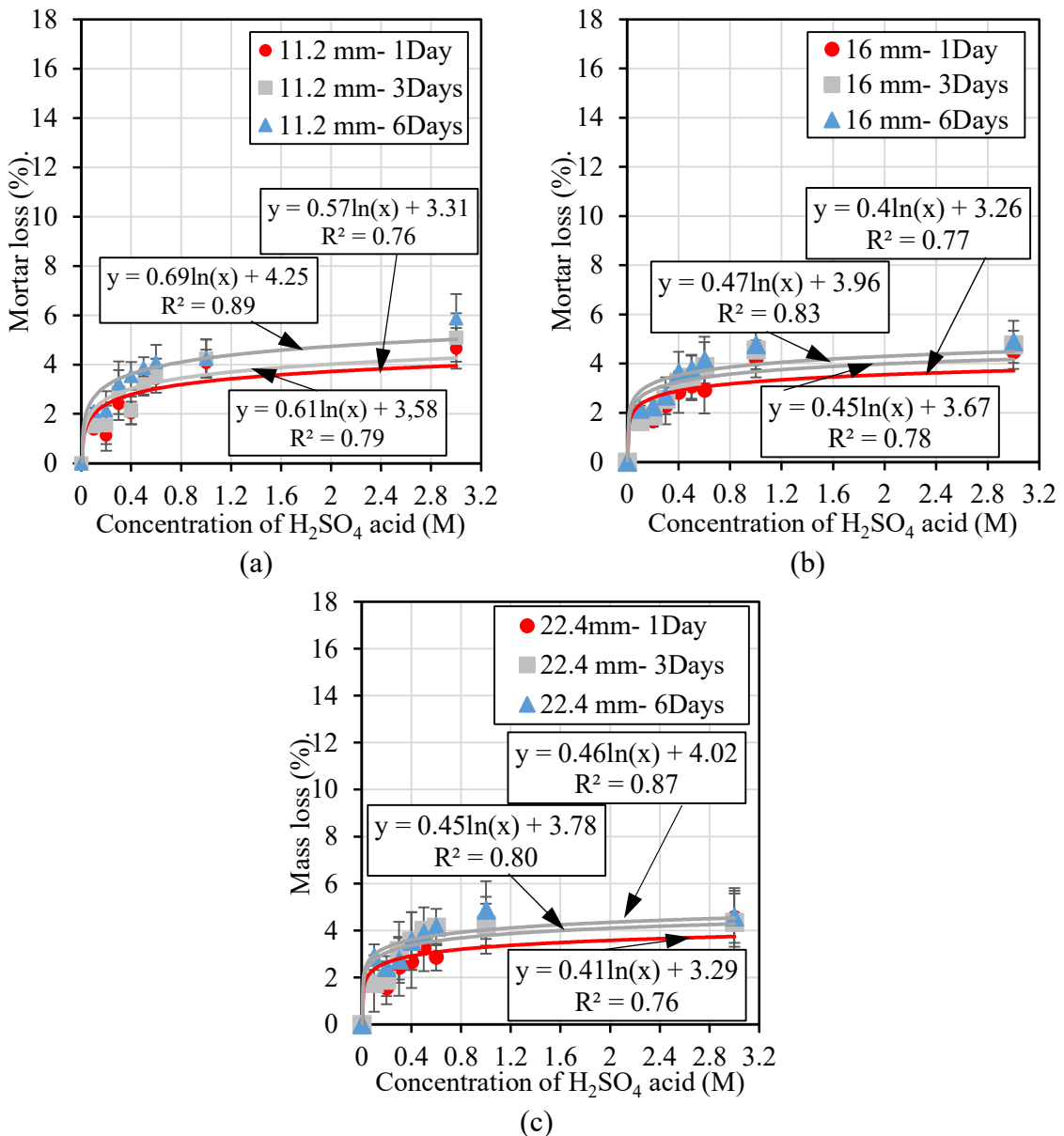


Figure 4-4 Concentration of H₂SO₄ versus mass loss (%) in diameters of 11.2 mm , 16 mm and 22.4 mm for 1, 3 and 6 days.

4.3.2 Aggregate size distribution

Particle size is an important aspect to be considered in the evaluation of natural (NA) and RCA. The size distribution of aggregates influences the mechanical properties and durability of concrete and is therefore a critical aspect in its production. Particle size is defined as the size distribution of aggregate particles and is determined through sieving. NA and RCA can present different particle size distributions, which affects their ability to fill the voids in fresh concrete and their mechanical and durability properties. Therefore, it is important to control and ensure the quality of the particle size distribution of aggregates to ensure the quality and durability of concrete.

Particle size analysis of NA and RCA was performed according to the standard NP EN 933-1 (2014) to characterize the particles used in concrete production. The aim of this analysis was to determine the adjustment of the size distribution of the RCA after mass loss. The results of the particle size analysis of the NA in sands and coarse aggregates were presented in Table 4-4, including the maximum and minimum dimension of the aggregates besides fineness modulus of these.

Table 4-4 Particle size distribution for NA.

Diameter (mm)	NA sand (0/2)	NA sand (0/4)	NA gravel (2/6)	NA gravel (6/12)	NA gravel (12/20)
22.4	100.00%	100.00%	100.00%	100.00%	98.40%
16	100.00%	100.00%	100.00%	100.00%	61.60%
11.2	100.00%	100.00%	100.00%	79.10%	9.50%
8	100.00%	100.00%	100.00%	40.20%	1.50%
5.6	100.00%	99.10%	87.30%	6.60%	0.70%
4	100.00%	97.20%	17.60%	2.40%	0.50%
2	100.00%	84.90%	3.30%	0.90%	0.50%
1	98.70%	55.10%	1.10%	0.40%	0.40%
0.5	76.60%	24.60%	0.60%	0.40%	0.40%
0.25	23.80%	7.20%	0.30%	0.20%	0.30%
0.125	1.70%	1.20%	0.20%	0.10%	0.20%
0.0065	0.00%	0.00%	0.00%	0.00%	0.00%
Fineness modulus	2.00	3.30	5.80	6.60	7.30
Maximum diameter (mm)	1	5.2	5.6	11.2	22.4
Minimum diameter (mm)	0.125	0.125	0.5	4	8

From the results presented in Table 4-4, Figure 4-5 was obtained graphically presenting the particle distribution for NA (sands and gravels).

The particle distribution of the RCA and HCl-treated RCA was determined based on the analysis of the data present in Table 4-2 and Table 4-3. Four types of molarities were chosen for the HCl and H₂SO₄ treatments, including low concentrations of 0.1M and 0.3M and high concentrations of 1.0M and 3.0M. With this, it was possible to obtain the particle size distribution of the RCA treated with these molarities after 1 day, 3 days and 6 days of pre-soaking. Figure 4-6a indicates that the particle size distribution changes from a granular distribution to a finer distribution compared to the untreated RCA, which is consistent with the mass loss and improvement in the surface area of the RCA.

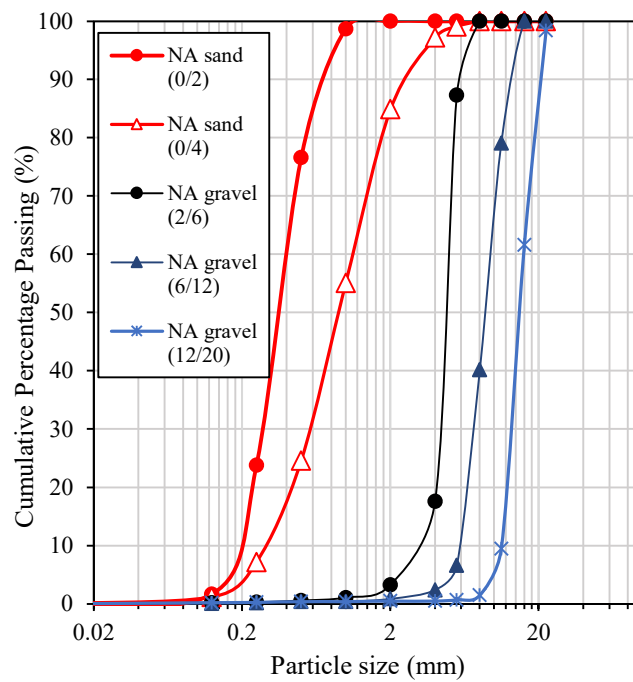


Figure 4-5 Particle size distribution for NA.

Figure 4-6b shows a similar trend without a significant reduction at 3 days of acid immersion. Finally, Figure 4-6c shows the particle size distribution of the RCA after 6 days of acid immersion.

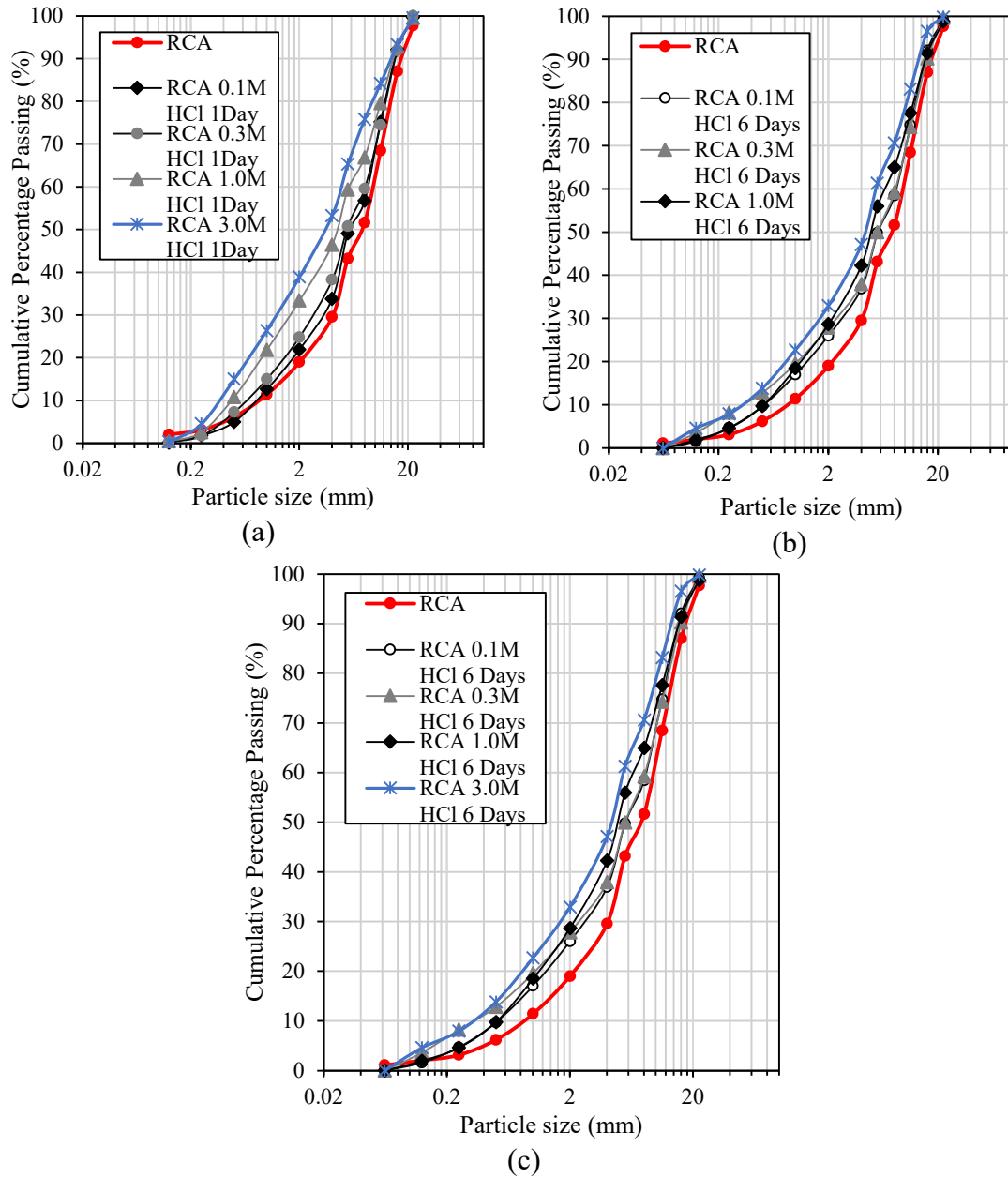


Figure 4-6 Particle size distribution for RCA treated with HCl pre-soaking one day (a); Particle size distribution for RCA treated with HCl pre-soaking 3 day (b); Particle size distribution for RCA treated with HCl pre-soaking one day 6 days (c).

The particle size distribution and fineness modulus values of untreated RCA and RCA treated with 0.1M, 0.3M, 1.0M and 3.0M for the pre-soaking days of 1, 3 and 6 days are presented in Tables 4-5, 4-6 and 4-7, respectively. The fineness of aggregate is considered important for concrete performance in relation to its strength, density, permeability and workability. Therefore, the fineness modulus is an important measure in evaluating the quality of aggregates for concrete production.

Table 4-5 Particle size distribution for RCA treated with HCl pre-soaking one day.

Diameter (mm)	RCA	RCA 0.1M HCl 1 day (%)	RCA 0.3M HCl 1 day (%)	RCA 1.0M HCl 1 day (%)	RCA 3.0M HCl 1 day (%)
22.4	97.70	99.665	100.000	100.000	99.572
16	87.02	92.096	91.857	91.857	93.187
11.2	68.47	75.171	74.470	74.470	84.146
8	51.63	56.731	59.592	59.592	75.818
5.6	43.20	49.125	50.819	50.819	65.311
4	29.56	33.806	38.256	38.256	53.249
2	19.02	21.949	24.809	24.809	38.893
1	11.42	12.616	15.023	15.023	26.369
0.5	6.19	5.010	7.274	7.274	15.021
0.25	3.14	1.796	1.749	1.749	4.533
0.125	2.06	0.155	0.264	0.264	0.329
0.0065	1.08	0	0	0.00	0.00
Fineness modulus	5.79	5.68	5.53	5.53	4.86

Table 4-6 Particle size distribution for RCA treated with HCl pre-soaking 3 days.

Diameter (mm)	RCA	RCA 0.1M HCl 6 days (%)	RCA 0.3M HCl 6 days (%)	RCA 1.0M HCl 6 days (%)	RCA 3.0M HCl 6 days (%)
22.4	97.70	99.64	100.00	99.80	99.77
16	87.02	92.88	92.86	94.29	95.23
11.2	68.47	76.30	75.34	82.88	86.16
8	51.63	58.98	60.97	70.30	76.40
5.6	43.20	48.49	52.16	58.10	63.24
4	29.56	36.31	39.65	43.94	48.93
2	19.02	24.46	25.75	30.36	32.59
1	11.42	14.32	15.79	18.95	22.37
0.5	6.19	7.56	7.90	11.08	12.60
0.25	3.14	4.23	3.26	4.00	6.24
0.125	2.06	2.03	0.70	0.46	0.74
0.0065	1.08	0.00	0.00	0.00	0.00
Fineness modulus	5.79	5.52	5.46	5.21	5.00

Table 4-7 Particle size distribution for RCA treated with HCl pre-soaking 6 days.

Diameter (mm)	RCA	RCA 0.1M HCl 6 days (%)	RCA 0.3M HCl 6 days (%)	RCA 1.0M HCl 6 days (%)	RCA 3.0M HCl 6 days (%)
22.4	97.70	99.23	99.60	98.79	99.79
16	87.02	92.07	90.21	91.42	96.51
11.2	68.47	74.78	74.28	77.58	83.15
8	51.63	58.46	59.24	64.99	70.59
5.6	43.20	49.80	49.98	55.98	61.28
4	29.56	36.93	37.92	42.28	47.13
2	19.02	26.02	27.86	28.70	32.92
1	11.42	17.05	19.59	18.50	22.72
0.5	6.19	9.70	12.82	9.74	13.82
0.25	3.14	4.70	8.21	4.61	7.91
0.125	2.06	1.60	3.60	1.93	4.59
0.0065	1.08	0.00	0.00	0.00	0.00
Fineness modulus	5.79	5.46	5.31	5.30	5.01

RCA were treated with H_2SO_4 at the same molarities and immersion times as the aggregates with HCl. Figure 4-7a shows the particle size distribution of the RCA treated with H_2SO_4 after one day of pre-soaking. It can be seen that the acid concentration of H_2SO_4 did not have a significant impact on the particle size distribution, maintaining a similar trend at all concentrations. This trend was also maintained for all immersion times, as can be seen in Figures 4-7b and 4-7c.

The values of particle size distribution corresponding to figures 4-7a, b and c with their respective fineness modulus are presented in Tables 4-8, 4-9 and 4-10.

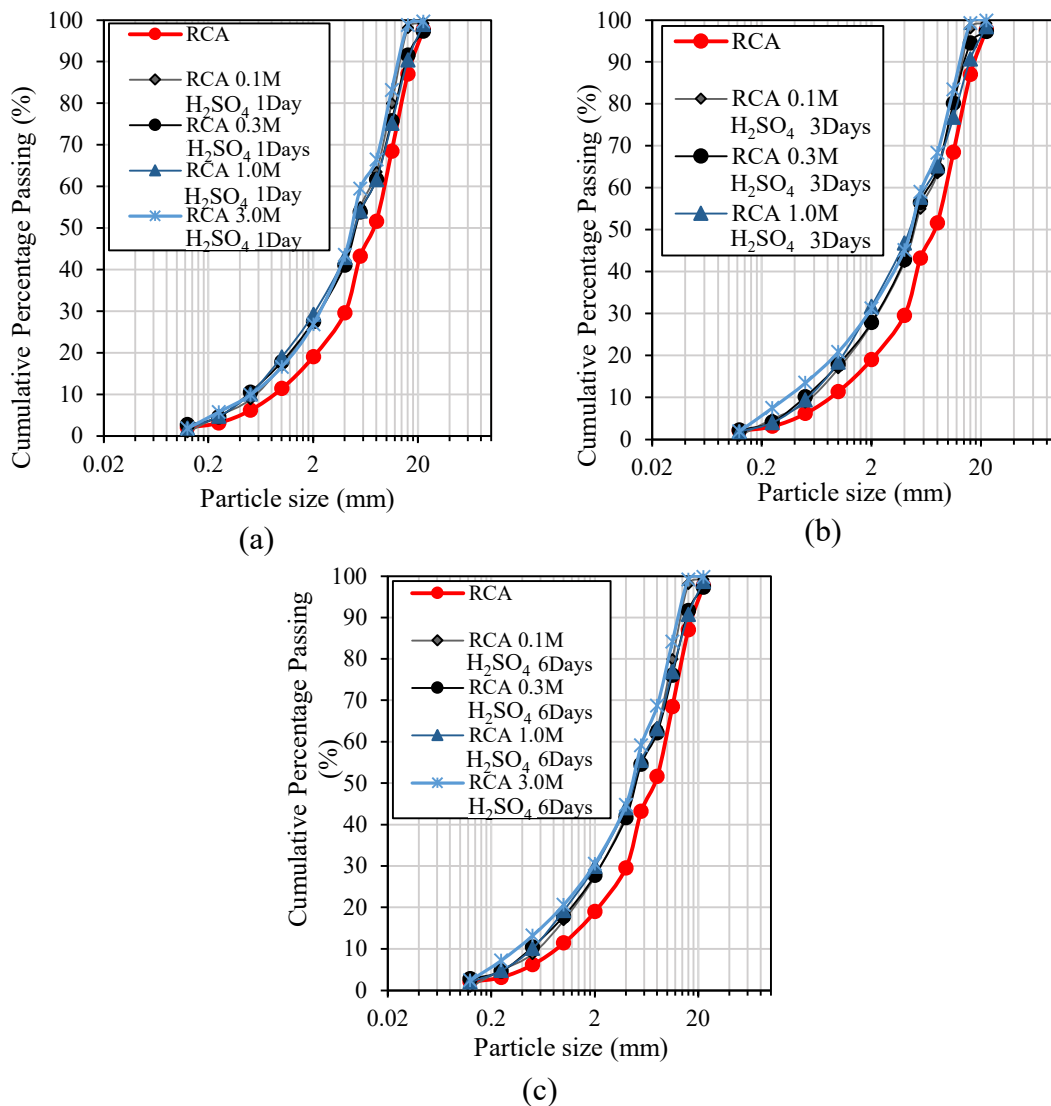


Figure 4-7 Particle size distribution for RCA treated with H_2SO_4 pre-soaking one day (a); Particle size distribution for RCA treated with H_2SO_4 pre-soaking 3 day (b); Particle size distribution for RCA treated with H_2SO_4 pre-soaking one day 6 days (c).

Table 4-8 Particle size distribution for RCA treated with H₂SO₄ pre-soaking one day.

Diameter (mm)	RCA	RCA 0.1M H ₂ SO ₄ 1 day (%)	RCA 0.3M H ₂ SO ₄ 1 day (%)	RCA 1.0M H ₂ SO ₄ 1 day (%)	RCA 3.0M H ₂ SO ₄ 1 days (%)
22.4	97.70	99.14	97.35	98.92	99.65
16	87.02	98.06	91.52	90.36	98.78
11.2	68.47	79.96	75.76	75.13	83.17
8	51.63	63.45	61.70	61.63	66.49
5.6	43.20	54.97	53.80	54.04	59.42
4	29.56	42.28	41.09	42.93	43.53
2	19.02	27.51	27.53	29.24	26.86
1	11.42	16.93	17.84	19.01	16.61
0.5	6.19	8.78	10.52	10.12	9.87
0.25	3.14	4.86	4.57	4.72	5.76
0.125	2.06	0.86	2.71	1.91	1.81
0.0065	1.08	0.00	0.00	0.00	0.00
Fineness modulus	5.79	5.36	5.37	5.32	5.29

Table 4-9 Particle size distribution for RCA treated with H₂SO₄ pre-soaking 3 days.

Diameter (mm)	RCA	RCA 0.1M H ₂ SO ₄ 3 days (%)	RCA 0.3M H ₂ SO ₄ 3 days (%)	RCA 1.0M H ₂ SO ₄ 3 days (%)	RCA 3.0M H ₂ SO ₄ 3 days (%)
22.4	97.70	99.64	97.25	98.39	99.89
16	87.02	96.73	94.50	90.69	99.28
11.2	68.47	77.95	80.16	76.80	83.45
8	51.63	62.19	64.26	65.18	68.35
5.6	43.20	54.32	56.47	57.73	59.02
4	29.56	41.94	42.86	46.83	45.14
2	19.02	28.02	27.86	31.69	31.21
1	11.42	17.27	17.88	18.44	20.89
0.5	6.19	9.52	10.17	9.40	13.51
0.25	3.14	5.29	4.12	4.02	7.49
0.125	2.06	1.33	2.21	1.87	1.93
0.0065	1.08	0	0	100	0
Fineness modulus	5.79	5.35	5.33	5.24	5.12

Table 4-10 Particle size distribution for RCA treated with H₂SO₄ pre-soaking 6 days.

Diameter (mm)	RCA	RCA 0.1M H ₂ SO ₄ 6 days (%)	RCA 0.3M H ₂ SO ₄ 6 days (%)	RCA 1.0M H ₂ SO ₄ 6 days (%)	RCA 3.0M H ₂ SO ₄ 6 days (%)
22.4	97.70	99.14	97.29	98.74	99.76
16	87.02	98.06	91.64	90.73	99.15
11.2	68.47	79.96	76.08	76.92	84.14
8	51.63	63.45	62.17	63.16	68.73
5.6	43.20	54.97	54.60	55.48	59.17
4	29.56	42.28	41.63	44.08	44.75
2	19.02	27.51	27.77	29.91	30.57
1	11.42	16.93	17.89	19.27	20.67
0.5	6.19	8.78	10.48	10.13	13.22
0.25	3.14	4.86	4.64	4.77	7.21
0.125	2.06	0.86	2.77	2.02	2.40
0.0065	1.08	0.00	0.00	0.00	0.00
Fineness modulus	5.79	5.36	5.35	5.28	5.13

4.3.3 Bulk density and water absorption

The determination of particle density of aggregates is a crucial factor that directly influences the density of concrete and, consequently, its mechanical strength. The importance of this property is evident in the concrete production process since it is easier to measure the components by mass than by volume. To ensure the accuracy of the dosage of the components and ensure that the concrete meets the established standards, it is necessary to convert the volume values resulting from the calculation of the optimal concrete composition to the corresponding values in mass.

The density test is performed to determine the physical properties of the aggregates, which are the components of the concrete, in addition to the cement. The results of this test allow the determination of the saturated and surface-dried particle density (ρ_{ssd}), the apparent particle density (ρ_a) and the oven-dried particle density (ρ_{rd}). These values are used to optimize the mix of components in the production of concrete.

The test methodology used to determine the volumetric mass followed the standards of NP EN 1097-6 (2013), In this process, the pycnometer was used and the samples were separated into two categories, with sizes ranging from 0.063 to 4mm and from 4mm to 22.4 mm. Before performing each test, the samples were separated and prepared. Firstly, the NA was tested, and the results were recorded in Table 4-11. The analysis of the results of the NA indicates that RCA presents a lower oven-dried density and higher water absorption, which suggests a porous nature compared to NA.

Table 4-11 Characteristics of NA.

Material	NA sand (0/2)	NA sand (0/4)	NA gravel (2/6)	NA gravel (6/12)	NA gravel (12/20)
ρ_a (kg/m ³)	2690.00	2656.12	2710.10	2708.12	2701.23
ρ_{rd} (kg/m ³)	2670.12	2672.13	2660.00	2660.20	2661.20
ρ_{ssd} (kg/m ³)	2592.30	2595.32	2642.20	2641.36	2639.30
Water absorption (%)	0.20%	0.30%	1.0%	1.5%	1.3%

Figure 4-8a presents the trend of RCA with a diameter of 11.2 mm that were treated with HCl solutions at molarities of 0.1M, 0.2M, 0.3M, 0.4M, 0.5M, 0.6M, 1.0M and 3.0M for 1, 2 and 3 days of pre-soaking. The trend is positive, with R² values of 0.66, 0.97 and 0.56, indicating that oven-dried particle density increases proportionally to the increase in HCl molarity. Figure 4-8b shows the same trend of increasing oven-dried particle density for RCA with 16 mm diameter treated under the same conditions

($R^2=0.90, 0.84$ and 0.77 for 1, 3 and 6 days respectively). However, when compared with the previous diameters, the oven-dried particle density for the RCA with a diameter of 22.4 mm proved to be almost constant for all molarities and pre-soaking days, with R^2 values of 0.031 for one day of pre-soaking, 0.047 for 3 days of pre-soaking, and 0.12 for six days of pre-soaking (Figure 4-8c).

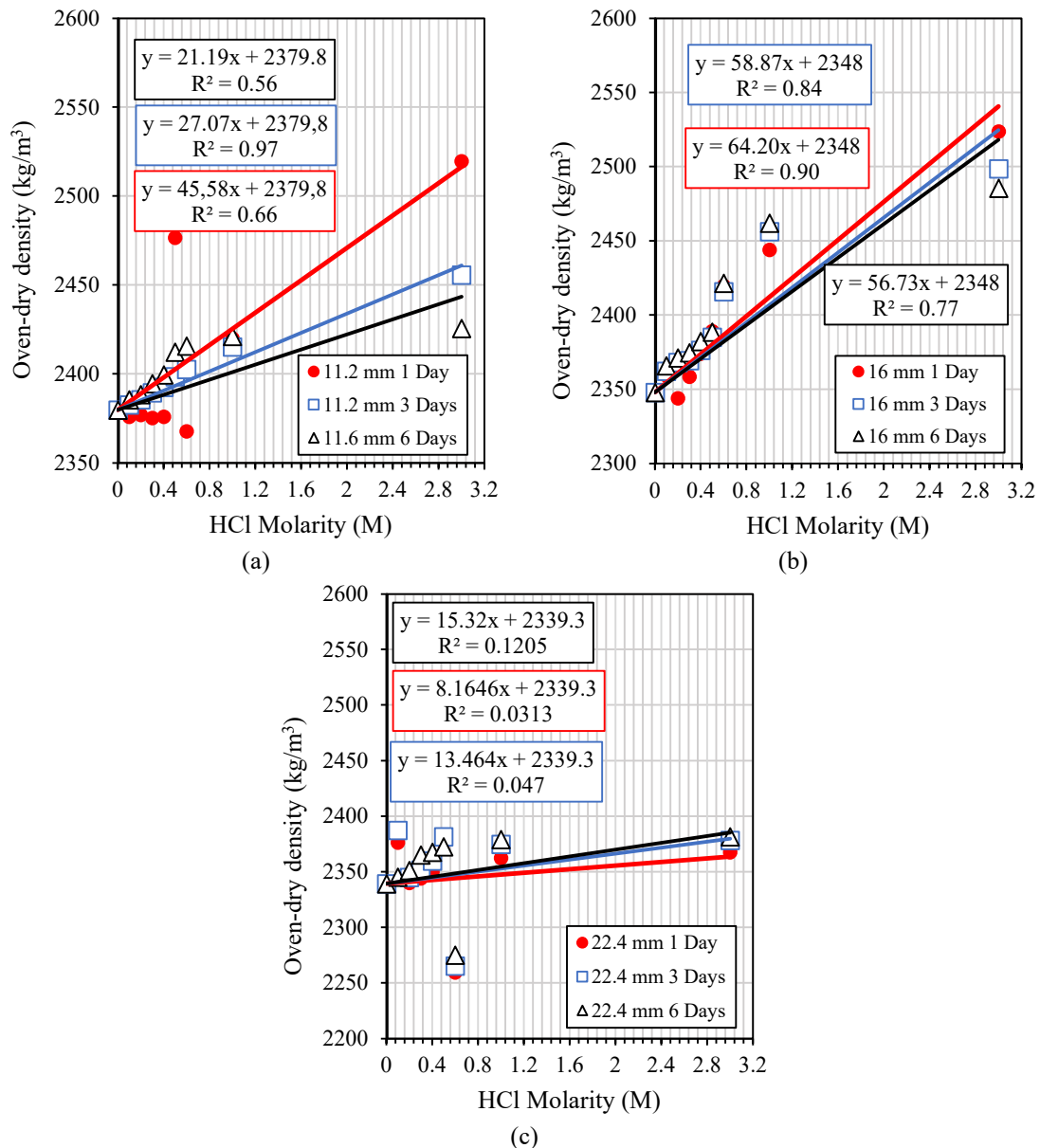


Figure 4-8 HCl molarity (M) versus oven-dry density of 11.2 mm diameter RCA (a); 16 mm diameter (b); and 22.4 mm in diameter (c).

Unlike the RCA treated with HCl, the bulk density of the RCA treated with H_2SO_4 also tended to increase, but in a power manner, and this was the best trend that fitted the results obtained. In the case of RCA with a diameter of 11.2 mm treated with H_2SO_4 , the R^2 values were 0.52, 0.60 and 0.64 for immersion days 1, 3 and 6, respectively, as can be

seen in Figure 4-9a. For the 16 mm diameter, the R^2 values were 0.48, 0.65 and 0.58 for the same immersion days (Figure 4-9b). Finally, for the RCA with 22.4 mm diameter, the R^2 values were calculated to be 0.14, 0.44 and 0.44 for days 1, 3 and 6, respectively. This lack of correlation can be explained by the lower amount of mortar adhered to NA compared to the smaller diameters.

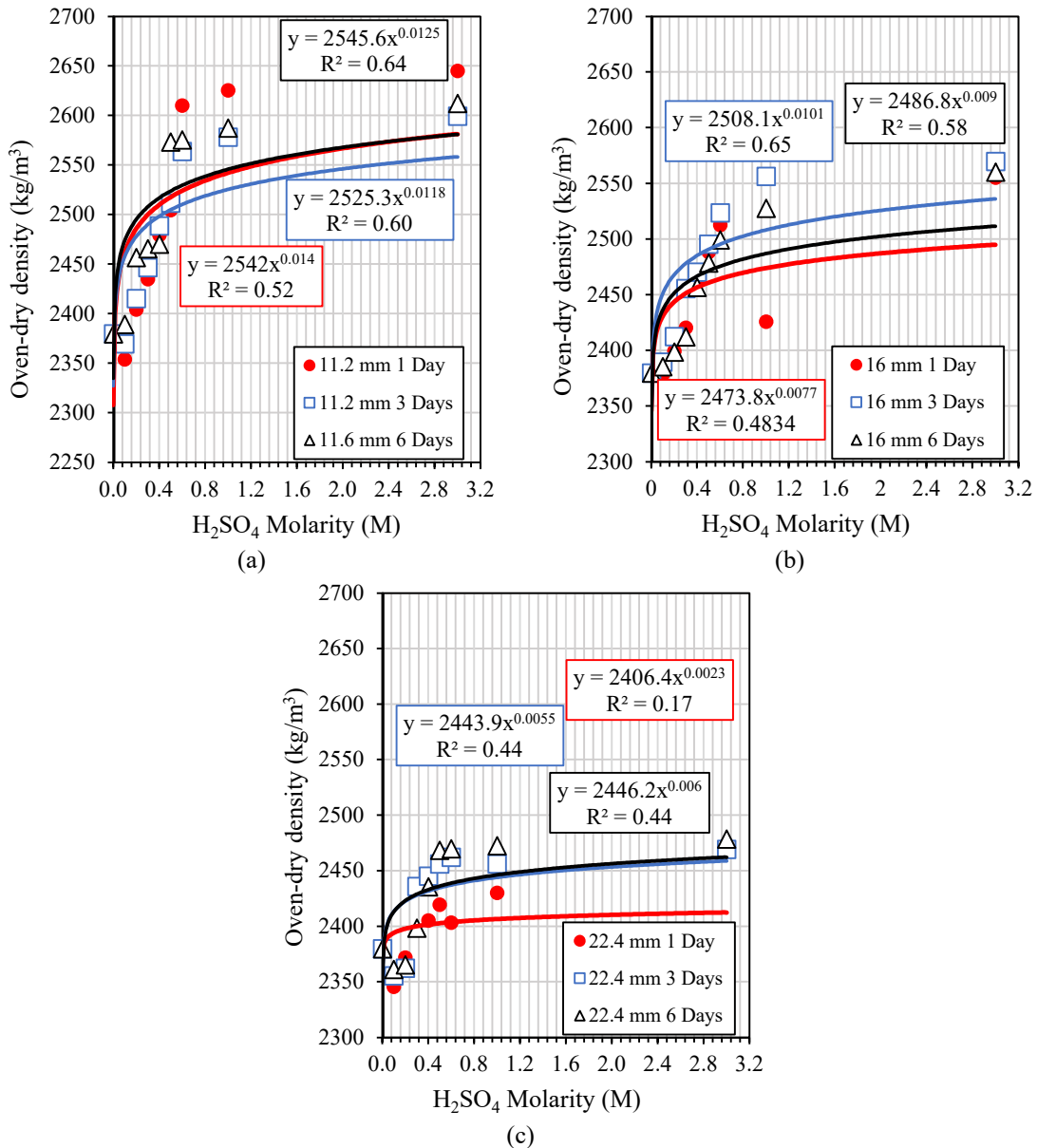


Figure 4-9 H₂SO₄ molarity (M) versus oven-dry density of 11.2 mm diameter RCA (a); 16 mm diameter (b); and 22.4 mm in diameter (c).

The studies conducted by Ismail and Ramli (2013) proved that untreated concrete waste (RCA) has lower relative densities compared to those that were treated with HCl. According to the results, the particle densities of 20 mm and 10 mm RCA were 2330 kg/m³ and 2230 kg/m³, respectively, lower values than those recorded for 20 mm and 10 mm NA,

which were 2600 kg/m³ and 2580 kg/m³. However, acid immersion resulted in improvements in the physical properties of RCA, and the improvements were greater for 10 mm NAs (4.7%) than for 20 mm NAs (2.2%). According to Al-Bayati *et al.* (2016), the bulk density of HCl-treated RCA showed a 5.40% improvement over untreated RCA. Saravanakumar *et al.* (2016) observed that treatment with H₂SO₄ and HCl resulted in minor variations of 10% and 13% in bulk density, respectively, compared to untreated RCA.

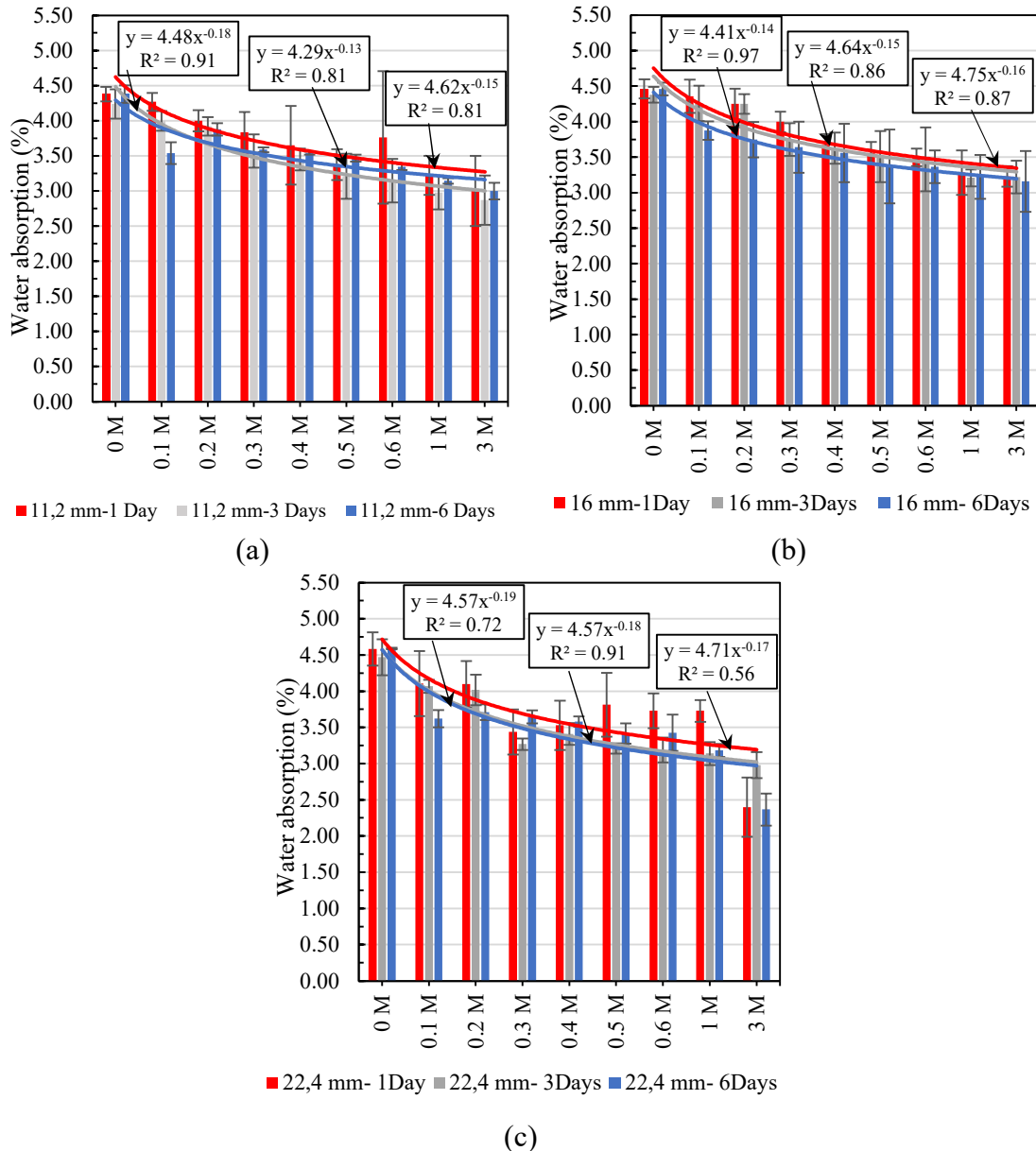


Figure 4-10 Relationship molarity and water absorption of RCA treated with HCl submerged for 1, 3 and 6 days for diameters 11.2mm (a); 16mm (b); 22.4mm (c).

Due to the link between aggregates density and water absorption, absorption was also evaluated and comprises the increase in aggregates weight due to water penetration into their open pores. The water absorption of aggregates can have a significant impact

on the water/cement (w/c) ratio of manufactured concrete, affecting its consistency. In addition, water absorption also affects the performance of hardened concrete, since an increase in water absorption is associated with an increase in porosity, which impairs both the mechanical strength and durability of concrete.

In Figure 4-10a, the water absorption of the 11.2mm diameter RCA treated with HCl is presented after 1, 3 and 6 days of immersion. It is possible to observe a loss in water absorption with increasing molarity, which is due to the loss of mortar adhered to the RCA, making it less porous. In addition, the power trend of reduction in water absorption with R^2 of 0.81, 0.81 and 0.91 for days 1, 3 and 6, respectively, can also be noted. For the 16mm diameters (Figure 4-10b), the trend was maintained with R^2 of 0.87, 0.86 and 0.97 for the immersion days. However, for the 22.4mm diameters, this trend was reduced, obtaining lower R^2 , with values of 0.52, 0.72 and 0.91, due to the lower amount of mortar adhered to the RCA, which results in a greater variability (Figure 4-10c) (DE JUAN; GUTIÉRREZ, 2009; KAPOOR; BOHROO, 2019).

The water absorption of the aggregates treated with H_2SO_4 is presented in Figures 4-11a, b and c. It can be concluded that there is a tendency to linear decrease in water absorption for all diameters tested with increasing molarity of H_2SO_4 . The coefficients of determination (r^2) for the 11.2 mm diameter are 0.84, 0.92 and 0.87 for 1, 3 and 6 days of immersion (Figure 4-11a), respectively. Similarly, the correlation coefficients (R^2) for the 16 mm diameter were 0.58, 0.9 and 0.91, and for the 22.4 mm diameter, an R^2 of 0.94, 0.91 and 0.95 for the same immersion days (Figures 4-10 b and c).

In some studies, the reduction of water absorption in aggregate concrete waste (RCA) has been investigated by acid treatments. Akbarnezhad *et al.* (2011) found that treatment with H_2SO_4 at low concentrations (0.1 M, 0.5 M, 1 M) resulted in reductions in water absorption of RCA, with a higher efficiency observed at higher concentrations. Ismail and Ramli (2013), on the other hand, found that immersion of RCA in HCl solutions with concentrations from 0.1 M to 0.8 M resulted in a reduction in water absorption from 1% to 28%. Purushothaman *et al.* (2014) found that treatment with HCl and H_2SO_4 at a concentration of 0.1 M resulted in a reduction in water absorption of 41% and 58%, respectively. In summary, the studies indicate that acid treatment can be effective in reducing water absorption of RCA, and that the concentration and type of acid used influence the treatment efficiency.

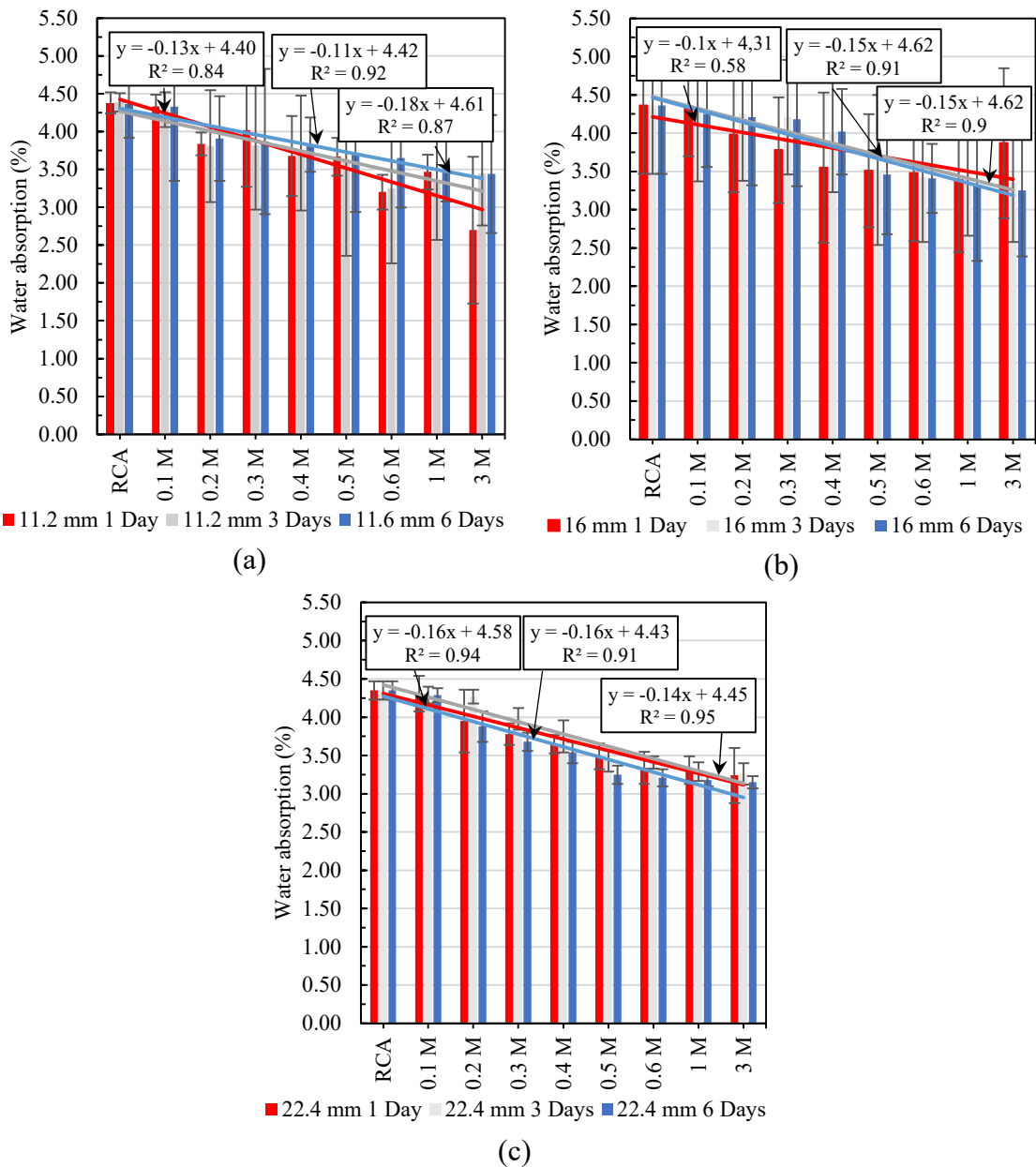


Figure 4-11 Relationship between molarity and water absorption of RCA treated with H₂SO₄ submerged for 1, 3 and 6 days for diameters 11.2mm (a); 16mm (b); 22.4mm (c).

An important analysis of the RCA treated with HCl and H₂SO₄ is the relationship between oven-dry density and water absorption, in order to understand the influence of oven-dry density on water absorption. Figure 4-12a shows the power regressions for all diameters (11.2 mm, 16 mm and 22.4 mm) at all ages (1, 3 and 6 days) treated with HCl, with determination coefficients (R^2) between 0.61 and 0.77. Similarly, the determination coefficients for the 16 mm diameter were between 0.72, 0.90 and 0.93, as presented in Figure 4-12b. For the 22.4 mm diameter, these determination coefficients no longer present a viable correlation due to their extremely low values, between 0 and 0.09 (Figure 4-12c).

RCA treated with H₂SO₄ showed similar trends to those of RCA treated with HCl. Figure 4-13a,b,c shows the relationship between oven-dry density and water absorption, with their respective coefficients of determination, indicating a strong power correlation between these two properties for RCA with a diameter of 11.2 mm. Similarly, these relationships are presented for the RCA diameters of 16mm and 22.4 mm, in Figures 4-13b and 4-13c, respectively, with the respective correlation coefficients.

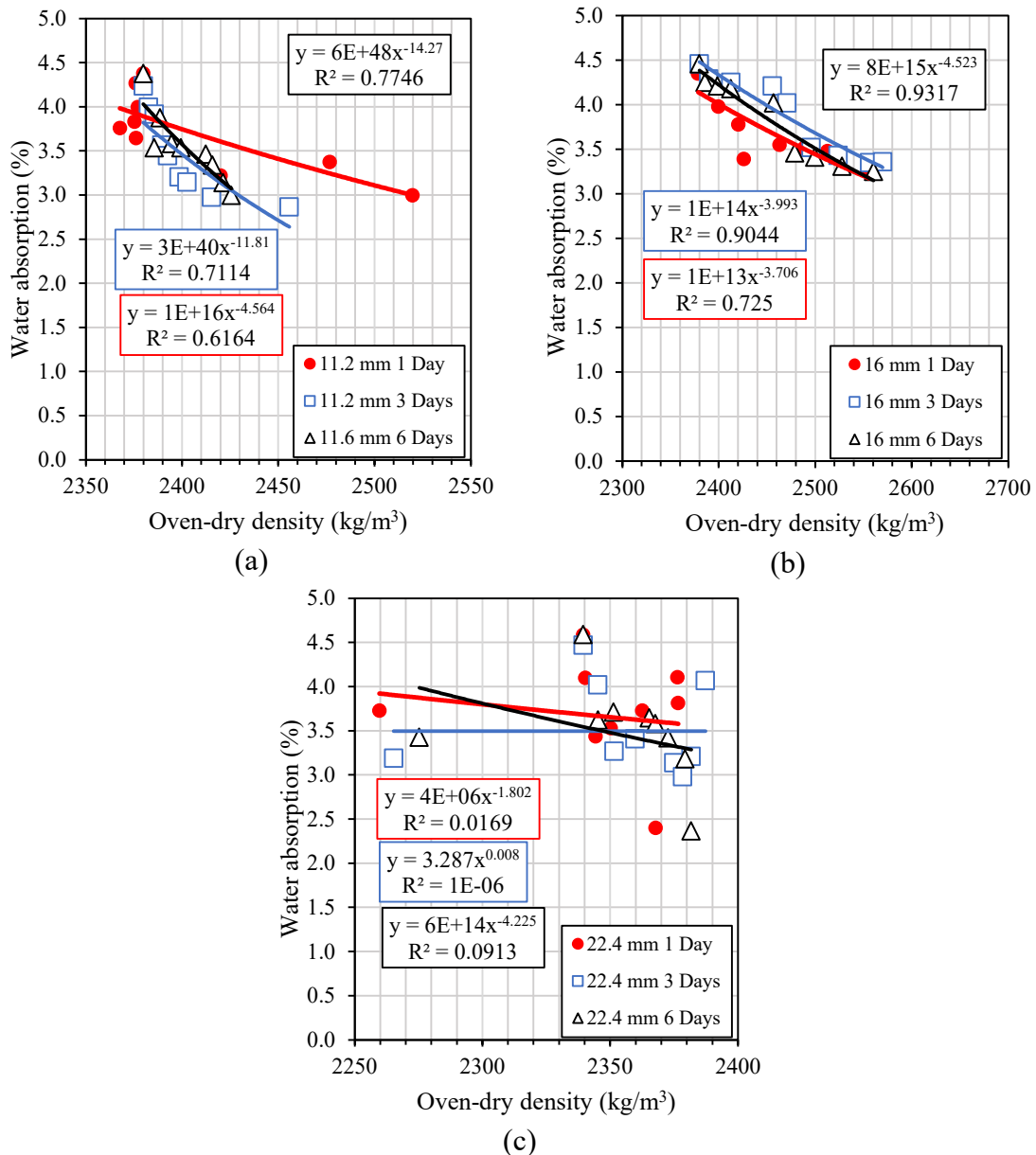


Figure 4-12 Relationship between oven-dry density and water absorption of RCA treated with HCl submerged for 1, 3 and 6 days for diameters 11.2mm (a); 16mm(b); 22.4mm(c).

From the results of the relationship between oven-dry density and water absorption, it can be concluded that for both HCl and H₂SO₄ acids, the correlation is better in the smaller sizes of 16mm than in the size of 22.4mm, due to the greater variability in the content of

mortar adhered in the RCA in the latter, as mentioned earlier.

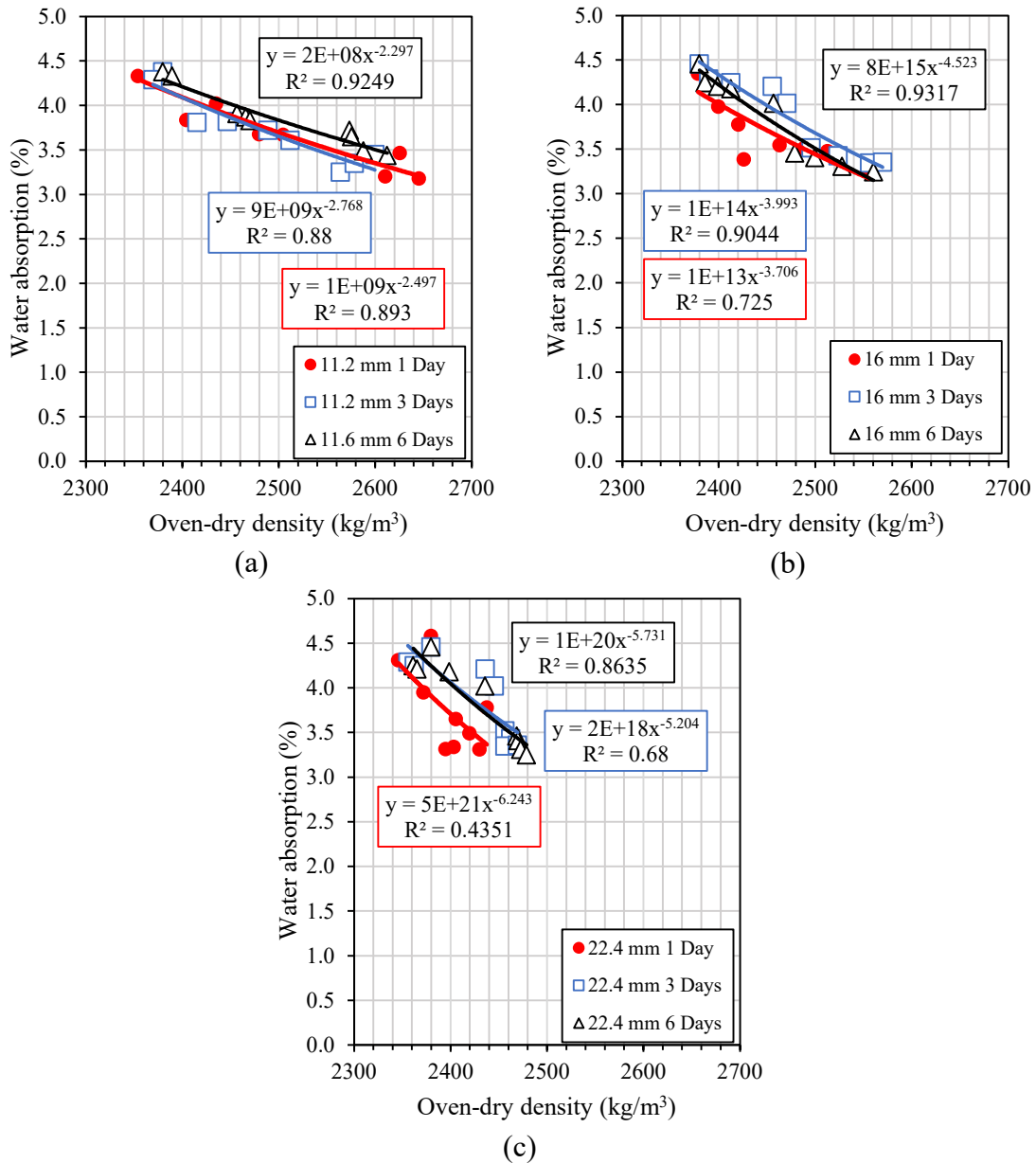


Figure 4-13 Relationship between oven-dry density and water absorption of RCA treated with H₂SO₄ submerged for 1, 3 and 6 days for diameters 11.2mm (a); 16mm(b); 22.4mm(c).

To conclude the analysis of the RCA treated with HCl and H₂SO₄, the oven-dry density and water absorption results were compared with those from Silva *et al.* (2014), where several properties of aggregates coming from construction waste were analysed, based on 236 publications from 1977 to 2014. These aggregates were classified into four categories, A, B, C and D, where A, B and C are divided into three subgroups, with A being the best quality aggregate. In Figure 4-15, it can be seen that the results obtained in this experimental campaign are within the A-III and B-I classification. Therefore, it can be concluded that the treatments performed on the RCA were effective in improving their quality.

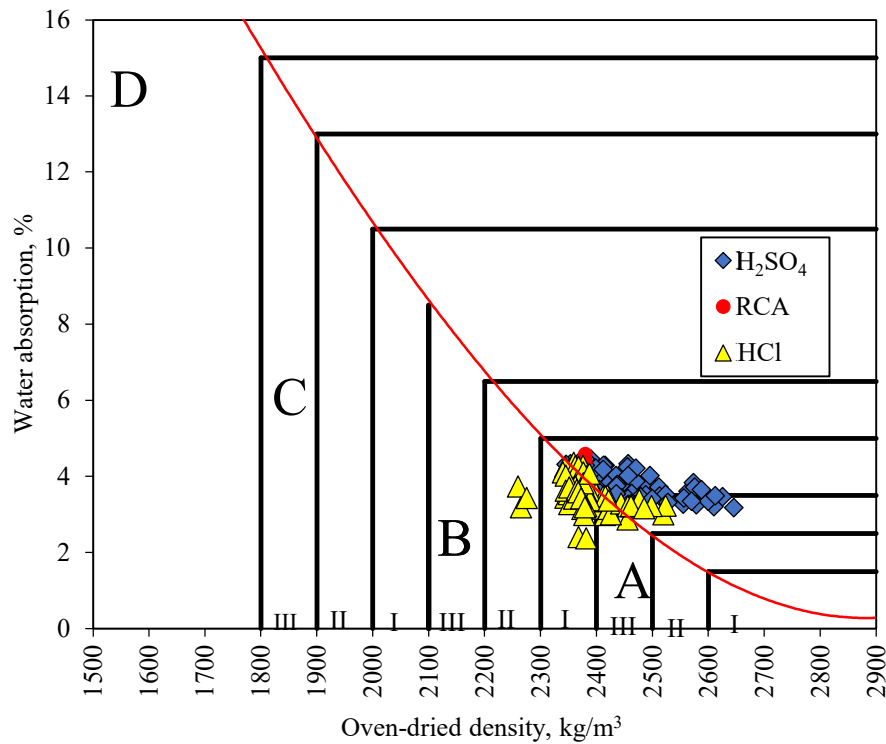


Figure 4-14 Comparison between density and water absorption of recycled aggregates (adapted from Silva *et al.* (2014))

4.4 Summary of Chapter 4 for the production of the second phase concrete

The results of 1-day immersion in HCl and H₂SO₄ acids were evaluated with respect to mortar removal, oven-dry density, and water absorption. Previously, the molarities of the acids were set as one low molarity of 0.3M and two high molarities (1.0M and 3.0M). However, the results obtained after days 1, 3 and 6 of immersion did not exceed 10%, which suggests that the immersion time is not a determinant in the removal of the RCA mortar. Thus, it is possible to conclude that the molarity of the acid is a more important factor than the immersion time for mortar removal.

The results of tests involving the removal of mortar with HCl and H₂SO₄ acids are of paramount importance for the Life Cycle Assessment (LCA) of concrete production using recycled aggregates. These tests provide a detailed insight into the pros and cons of this specific technique, enabling all stakeholders to make well-informed decisions regarding the balance between quality improvement and associated environmental and economic implications. This, in turn, contributes significantly to the adoption of sustainable practices in the construction industry.

*SECOND STAGE RESULTS AND DISCUSSION:
EVALUATION OF THE MECHANICAL,
FRACTURE AND DURABILITY PERFORMANCE
OF CONCRETE MIXES INCORPORATING RCA
TREATED WITH ACID SOLUTIONS AND WITH
ADDITION OF ALUMINIUM SULPHATE.*

*“Science is but a perversion of itself unless it has as its ultimate goal the betterment of
humanity.”
Nikola Tesla.*

5 EVALUATION OF THE MECHANICAL, FRACTURE AND DURABILITY PERFORMANCE OF CONCRETE MIXES INCORPORATING RCA TREATED WITH ACID SOLUTIONS AND WITH ADDITION OF ALUMINIUM SULPHATE

The objective of this chapter is to describe and analyse the results of tests conducted on concrete with RCA treated with acid solutions (HCl and H₂SO₄) and with the addition of aluminium sulphate (AS), in comparison to concrete with untreated RCA and NA in the fresh and hardened states. The characterization of the results in the fresh state is important to evaluate the performance of concrete mixes in the hardened state, and tests were carried out on slump using the Abrams cone and density in the fresh state to evaluate the consistency and compaction of the concrete mixes.

Next, a microstructural analysis of concrete was performed to study the improvement of the ITZ between the treated RCA and cementitious matrix, in addition to that when AS is added. This analysis is important to explain the improvements in mechanical and durability properties at the microstructural level.

According to the results of the mechanical tests in the hardened state, a detailed description and analysis of the results are presented. The experimental part included four types of tests: compressive strength in cylinders, tensile strength, modulus of elasticity, and fracture energy. An analysis of the trend curves of the obtained results was performed, rather than focusing solely on individual values, in order to understand the influence of aggregates on these properties.

The durability of concrete with NA, untreated RCA, treated RCA, and addition of AS was also evaluated. Tests of water absorption by immersion and by capillarity, resistance to carbonation, chloride ion penetration, and drying shrinkage were performed.

5.1 Mix design

The mixes' composition was based on the Faury's reference curve method (FAURY, 1985), taking into account the following parameters: C30/37 strength class, XC3 exposure

class and S3 slump in accordance with the EN 206-1 standard (2007). Using the Faury curve for the reference concrete (RC), 100% coarse NA were replaced (particles size over 4 mm) with RCA through volumetric substitution performed by size fraction, ensuring the same equivalent volumetric fraction of the RC aggregates (Figure 5-1).

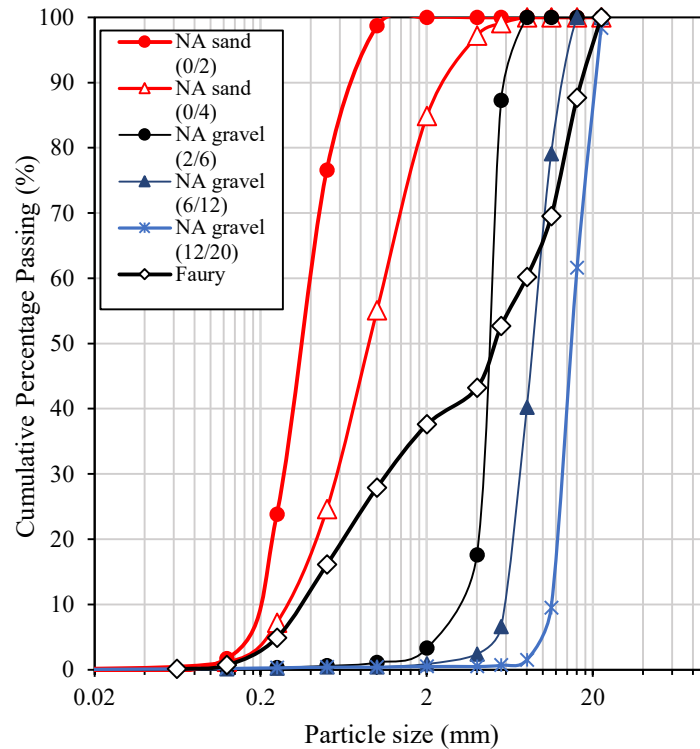


Figure 5-1 Particle size distribution of the aggregates and Faury's reference curve

Because the water absorption of RCA is greater than the one of NA (ANGULO; CARRIJO; FIGUEIREDO; CHAVES et al., 2010; CUI; SHI; MEMON; XING et al., 2014; DE BRITO; SAIKIA, 2012; PURUSHOTHAMAN; AMIRTHAVALLI; KARAN, 2014), it was necessary to compensate the loss of free water in the mixes with RCA. The amount of water that was expectedly absorbed by RCA was 92% of the total water absorption of each type of RCA used, corresponding to the 10-minute absorption (time that the concrete production lasts): the water absorption for untreated RCA is 3.72%; 3.35% for RCA pre-soaked in 0.3 M HCl; 3.0% for RCA pre-soaked in 1.0 M HCl; 2.98% for RCA pre-soaked in 3.0 M HCl; 3.52% for RCA pre-soaked in 0.3 M H₂SO₄; 3.47% for RCA pre-soaked in 0.3 M H₂SO₄; 3.60% for RCA pre-soaked in 1.0 M H₂SO₄ and 3.60% for RCA pre-soaked in 3.0 M H₂SO₄.

The mix proportions are shown in Table 5-1. RC is the reference concrete (with NA), RC-RCA is the mix with 100% replacement of NA coarse (> 4 mm) with RCA, RCA-0.3

HCl is the mix with 100% of RCA treated with 0.3 M HCl, RCA-1.0 HCl is the mix with 100% of RCA treated with 1.0 M HCl, RCA-3.0 HCl is the mix with 100% of RCA treated with 3.0 M HCl, RCA-0.3 H₂SO₄ is the mix with 100% of RCA treated with 0.3 M H₂SO₄, RCA-1.0 H₂SO₄ is the mix with 100% of RCA treated with 1.0 M H₂SO₄, RCA-3.0 H₂SO₄ is the mix with 100% of RCA treated with 3.0 M H₂SO₄, and RCA-AS is the mix with 100% of RCA with addition of 1.10% AS of the mass of cement.

Table 5-1 Concrete mix proportions.

Material (kg)/properties	Mix proportions (kg/m ³)								
	RC	RC-RCA	RCA-0.3 HCl	RCA-1.0 HCl	RCA-3.0 HCl	RCA-0.3 H ₂ SO ₄	RCA-1.0 H ₂ SO ₄	RCA-3.0 H ₂ SO ₄	RCA-AS
RCA incorporation ratio	0%	100%	100%	100%	100%	100%	100%	100%	100%
Cement (CEM I 42.5R)	350	350	350	350	350	350	350	350	350
Aluminium sulphate (AS)	-	-	-	-	-	-	-	-	0.035
Water	175	175	175	175	175	175	175	175	175
Additional water	-	20.9	18.4	17.6	17.6	18.7	19.0	19.1	-
W/C	0.5	0.55	0.55	0.55	0.55	0.55	0.55	0.55	0.5
NA sand (0/2)	179.4	179.4	179.4	179.4	179.4	179.4	179.4	179.4	179.4
NA sand (0/4)	446.8	446.8	446.8	446.8	446.8	446.8	446.8	446.8	446.8
NA gravel (2/6)	365.7	-	-	-	-	-	-	-	-
NA gravel (6/12)	640.0	-	-	-	-	-	-	-	-
NA gravel (12/20)	182.8	-	-	-	-	-	-	-	-
RCA > 22.4 mm	-	10.0	10.0	10.0	10.0	10.0	10.0	10.0	10.0
RCA 16-22.4 mm	-	232.0	232.0	232.0	232.0	232.0	232.0	232.0	232.0
RCA 11.2-16 mm	-	403.7	403.7	403.7	403.7	403.7	403.7	403.7	403.7
RCA 8-11.2 mm	-	193.4	193.4	193.4	193.4	193.4	193.4	193.4	193.4
RCA 5.6-11.2 mm	-	155.3	155.3	155.3	155.3	155.3	155.3	155.3	155.3
RCA 4-5.6 mm	-	152.8	152.8	152.8	152.8	152.8	152.8	152.8	152.8

5.2 Workability and bulk density

As explained in Chapter 3, this research intended that all concrete mixes had a slump within the range 125 ± 15 mm, belonging to consistency class S3 (100 to 150 mm).

Figure 5-2 presents the slump test values of all concrete mixes and shows that there is improvement for concrete mixes containing RCA treated with HCl and H₂SO₄. This improvement is more evident in the HCl treated aggregates where it amounts to 2.61%, 4.35% and 6.09% at molarities 0.3 M, 1.0 M and 3.0 M respectively (Table 5-2). The mixes treated with H₂SO₄ also showed improvements with respect to RC-RCA: 0.87%, 2.61% and 4.35% for molarities 0.3 M, 1.0 M and 3.0 M (Table 5-2). Figure 5-2b, shows the evolution of the slump test as a function of the acid molarity, where an area of improvement can be observed when the acid concentration is increased. This can be explained by the removal of the mortar adhered to NA, reducing the water absorption of these aggregates besides improving the aggregate shape, a little more rounded, thus improving the mobility between particles

(PURUSHOTHAMAN; AMIRTHAVALLI; KARAN, 2015).

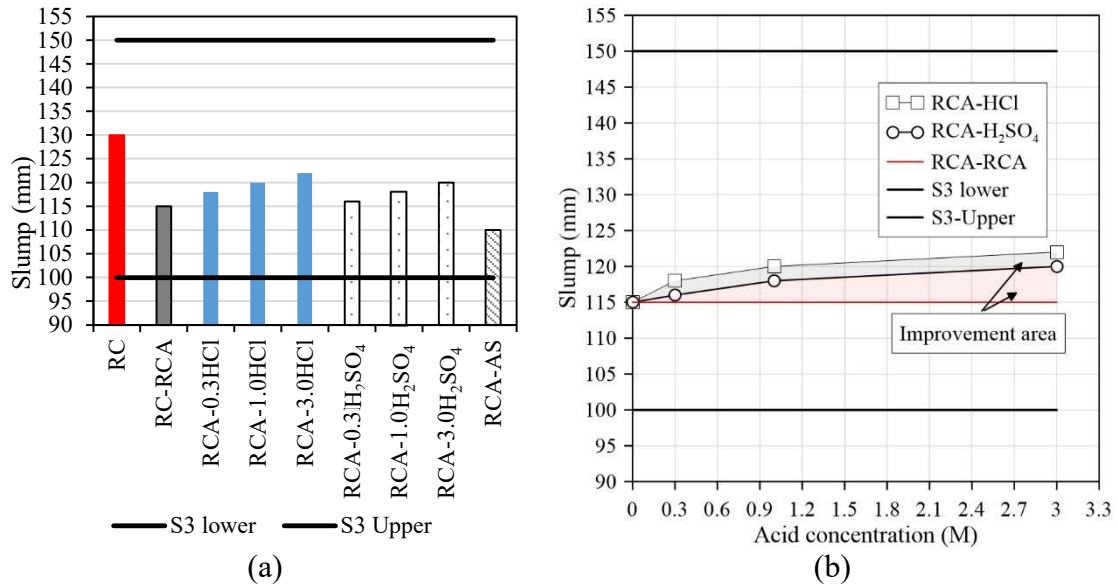


Figure 5-2 Slump test of all concrete mixes containing treated RCA, untreated and with AS (a); slump test of concrete mixes versus acid concentration (M) of HCl and H₂SO₄.

Regarding the RCA-AS mixes, it can be observed that there is a workability reduction of 4.35% relative to the RCA-RCA mix (Table 5-2). This reduction is attributed to the accelerating property of AS sulphate in cement hydration. AS acts on C₃A as it is the fastest forming mineral (LIU; MA; TAN; GU et al., 2020). Han *et al.* (2016) studied the hydration rate of AS with cement and observed that when AS is added in cement hydration the release of heat of hydration is due to the increased amount and formation rate of sulfoaluminate hydrate, promoting the hydration of C₃A. The promoted hydration process of C₃A can accelerate the rate of hardening of the paste and thus accelerate the setting time.

As mentioned above, Table 5-2 shows the slump values of all concrete mixes as well as their percent variation relative to the RC and RC-RCA reference concrete mixes.

Table 5-2. Slump test of concrete mixes.

Mix	Slump test (mm)	w/c	% improvement relative to RC	% improvement relative to RC-RCA
RC	130	0.50	—	—
RC-RCA	115	0.55	11.54% ▼	—
RCA-0.3HCl	118	0.55	9.23% ▼	2.61% ▲
RCA-1.0HCl	120	0.55	7.69% ▼	4.35% ▲
RCA-3.0HCl	122	0.54	6.15% ▼	6.09% ▲
RCA-0.3H ₂ SO ₄	116	0.55	10.77% ▼	0.87% ▲
RCA-1.0H ₂ SO ₄	118	0.55	9.23% ▼	2.61% ▲
RCA-3.0H ₂ SO ₄	120	0.55	7.69% ▼	4.35% ▲
RCA-AS	110	0.50	15.38% ▼	4.35% ▼

The bulk density of fresh concrete reflects the density of each of its components and its degree of compaction. The determination of the bulk density of concrete mixes is described in NP EN 12350-6 (NP EN 12350-6. Ensaio do betão fresco. Parte 6, 2002) and the results are presented in Table 5-2, as well as the respective variation with the RC and RC-RCA reference mixes. Figure 5-3a presents the results of the bulk density of all mixes and their difference to the reference mixes.

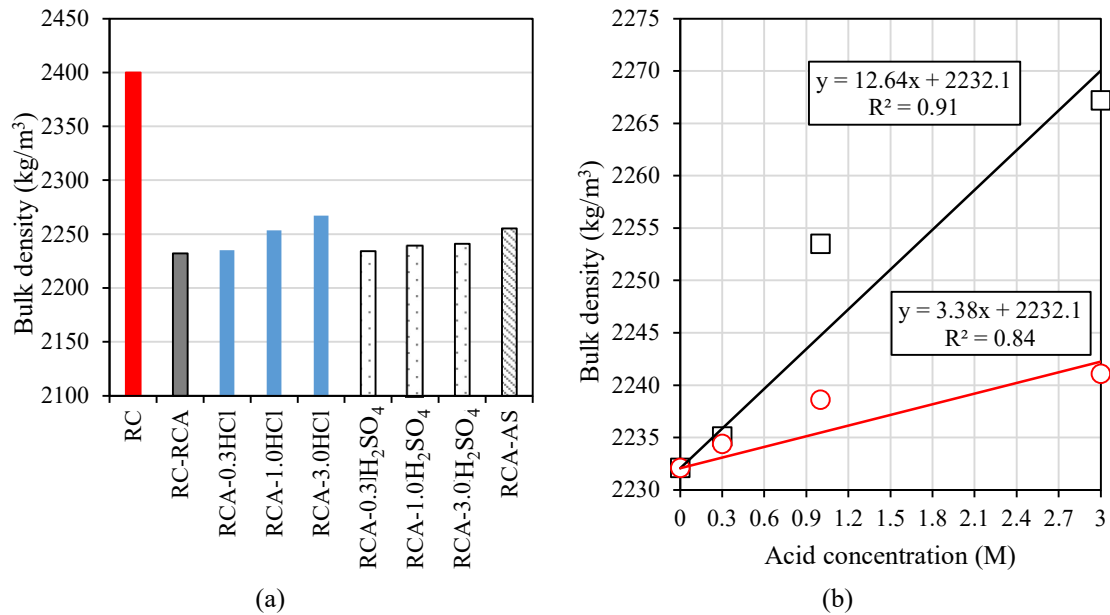


Figure 5-3 Bulk density of all concrete mixes containing treated RCA (a); untreated and with AS (a); bulk density of concrete mixes versus acid concentration (M) of HCl and H₂SO₄ (b).

Through the results, one can observe that the higher the molarity (M) of HCl and H₂SO₄, the greater the difference in bulk density (Figure 5-3b). One can conclude that there is a linear increase in the apparent density as a function of the acid concentration, which is more visible in RCA-HCl mixes ($R^2 = 0.91$) than in those with H₂SO₄ ($R^2 = 0.84$). Regarding the mix of AS, this increase is also observed in relation to the RC-RCA concrete.

Table 5-3. Bulk density of concrete mixes.

Mix	Bulk density (kg/m ³)	% improvement relative to RC	% improvement relative to RC-RCA
RC	2400.1	—	—
RC-RCA	2232.1	7.00% ▼	—
RCA-0.3HCl	2235.1	6.87% ▼	0.13% ▲
RCA-1.0HCl	2253.5	6.11% ▼	0.96% ▲
RCA-3.0HCl	2267.2	5.54% ▼	1.57% ▲
RCA-0.3 H ₂ SO ₄	2234.4	6.90% ▼	0.10% ▲
RCA-1.0 H ₂ SO ₄	2238.6	6.73% ▼	0.29% ▲
RCA-3.0 H ₂ SO ₄	2241.1	6.62% ▼	0.40% ▲
RCA-AS	2255.3	6.03% ▼	1.04% ▲

5.3 Microstructure of the ITZ of concrete mixes

The ITZ is the microstructure of the cement paste close to the aggregate in the cementitious matrix and is crucial to determine the mechanical behaviour and durability of concrete. Observations were made using scanning electron microscopy (SEM) and chemical analyses with energy dispersive X-ray spectroscopy (EDS) in the second phase of the experimental campaign of this thesis, which evaluated mixes produced with natural (NA) and RCA treated with acids (HCl and H₂SO₄) and addition of aluminium sulphate (AS). All mixes were cured for 180 days in a humid chamber (20 °C and 100% humidity) to ensure complete hydration (CHU; KLEIB; AMAR; BENZERZOUR *et al.*, 2021; MEHTA; MONTEIRO, 2014). The results and analysis of the concrete mixes are presented below, and a comparative analysis of the microstructure of the mixes is performed.

5.3.1 Concrete incorporating NA

To analyse the microscopy of the mixes, the compounds Ca, Si, Al and Fe were identified as the main components formed during the hydration of concrete. The modifications in the thickness of the ITZ between the aggregate and the cement matrix were investigated using semi-quantitative analysis by EDS associated with SEM at four points perpendicular to the matrix-aggregate interphase. According to Taylor *et al.* (1984), the numerical values between the atomic masses of the oxides present in the cement matrix (SiO₂[Si], CaO [Ca], Fe₂O₃ [Fe] Al₂O₃[Al] and SO₃[S]) were associated with the cement hydration products. These relationships are presented below:

$$\text{C-S-H} \quad 0.8 \leq \text{Ca/Si} \leq 2.5 \quad (\text{Al+Fe})/\text{Ca} \leq 0.2 \quad (\text{Equation 5-1})$$

$$\text{CH} \quad \text{Ca/Si} \geq 10 \quad (\text{Al} + \text{Fe})/\text{Ca} \leq 0.04 \quad \text{S/Ca} \leq 0.04 \quad (\text{Equation 5-2})$$

$$\text{AFm} \quad \text{Ca/Si} \geq 4 \quad (\text{Al} + \text{Fe})/\text{Ca} > 0.4 \quad \text{S/Ca} > 0.15 \quad (\text{Equation 5-3})$$

The analysis of the hydrated products reveals a correlation between the total atomic masses of calcium and silicon oxides (Ca/Si). When the ratio is below 2.5, the presence of high C-S-H content is admitted. However, Ca/Si ratios higher than 10 indicate a reduced amount of C-S-H and the presence of phases like CH and AFm (ettringite). Kunther *et al.* (2017) and Pelisser *et al.* (2012) have shown that these ratios can be correlated with the mechanical properties of the mixes, with lower Ca/Si ratios showing better results in macro properties.

Figure 5-4a presents the observation of the reference concrete mix (RC) sample by scanning electron microscopy (SEM). A representative section was selected for analysis by X-ray photoelectron spectroscopy (EDS), as seen in Figures 5-4b-d. The analysis revealed an average Ca/Si ratio = 2.71, indicating a possible formation of C-S-H due to the hydration of cement CEM 42.5 R. No ettringite formations were observed at the analysed points.

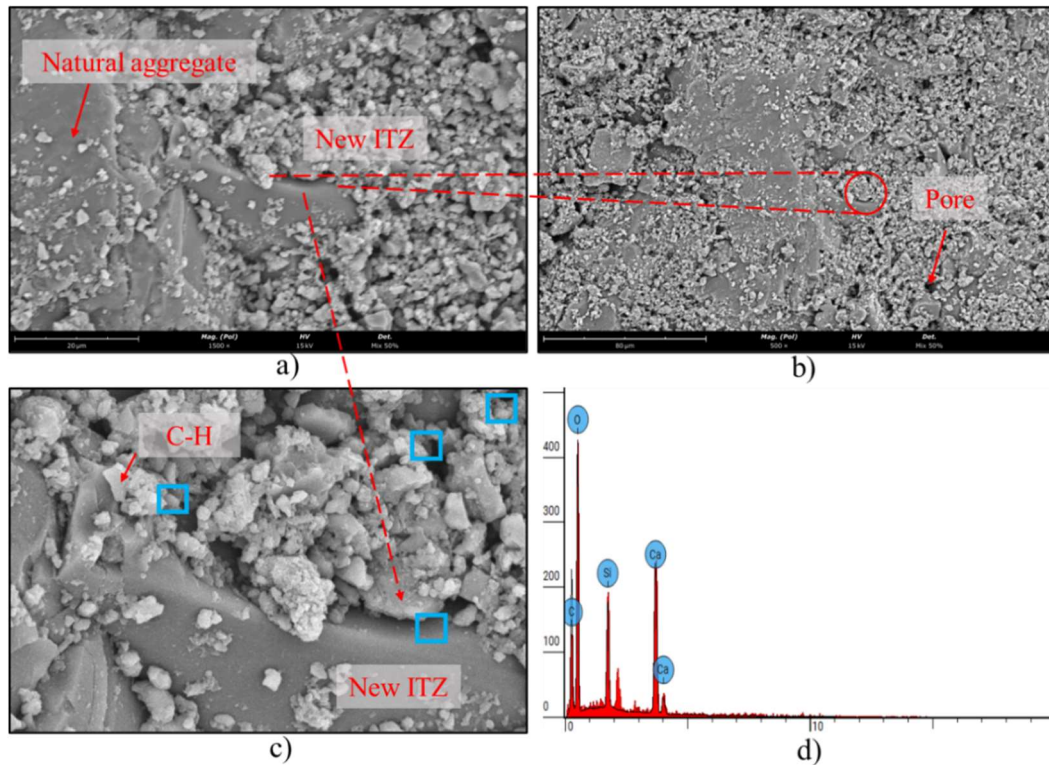


Figure 5-4 SEM/EDS observation of the concrete sample with AN at magnification 1500x showing the ITZ (a); general observation of the sample at magnification 500 (b); observation at magnification 5000x marking the EDS analysis points and the C-H formation (c); EDS spectrum of the evaluated line (ITZ) (d).

5.3.2 Concrete incorporating RCA

RCA is comprised of a multitude of ITZ, involving NA (new aggregate) with its original ITZ, adhered mortar, and new ITZ. The new ITZ is situated between the adhered mortar and the fresh matrix. Figure 5-5a showcases the region of the cement matrix containing the RCA and the novel cementitious matrix. This SEM analysis reveals an increased presence of pores, originating from both the new cement matrix and the former cement matrix. For the EDS analysis (Figures 5-5c,d), a section of the sample where the ITZ between the RCA and the new cement matrix was identified (Figure 5-5b) was selected. The EDS results from the points within this area demonstrated a relationship between the Ca/Si = 3.45 products.

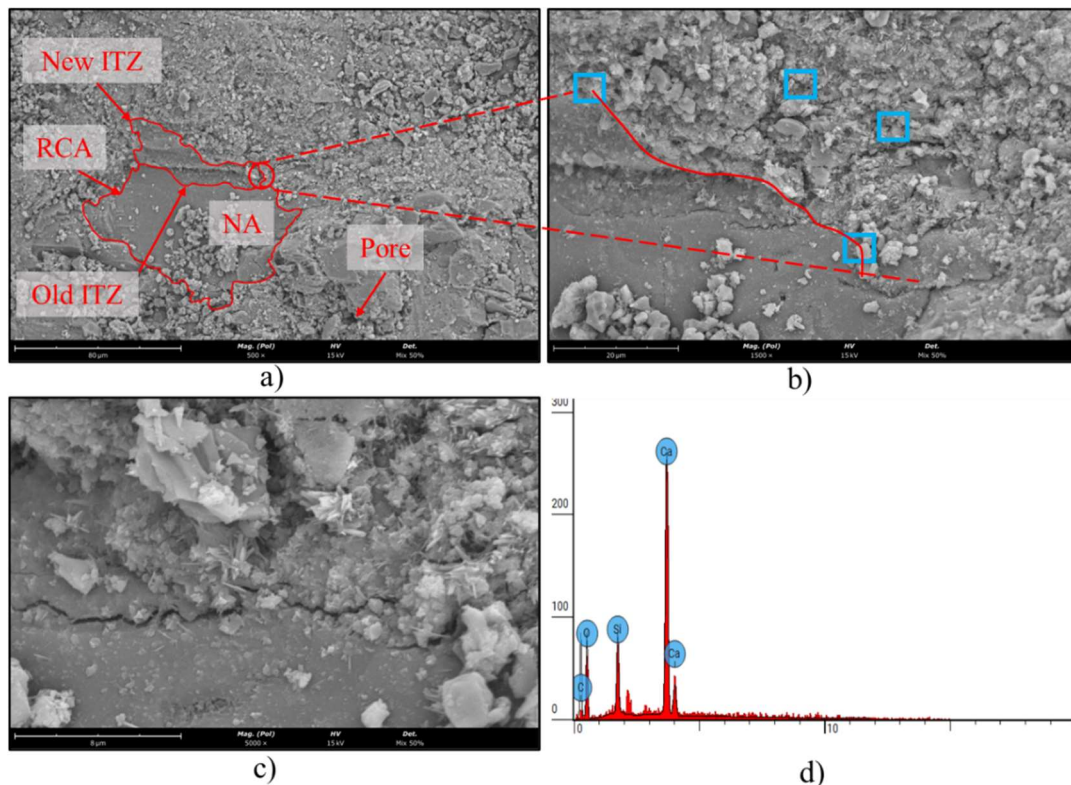


Figure 5-5 SEM/EDS observation of a concrete sample with RCA at 500x magnification showing the ITZ, pores and the analysis zone (a); general observation of the sample at 1500 magnification marking the EDS analysis points (b); observation at 5000x magnification showing the formed ITZ (c); EDS spectrum of the ITZ (d).

5.3.3 Concrete incorporating RCA treated with HCl

Observations made through SEM revealed that concrete mixes with RCA treated with 0.3 M of HCl (Figure 5-6a, b, c) showed RCA in the cement matrix, where a representative boundary between the two was chosen to analyse the ITZ. Figure 5-6b provides a more detailed view of the ITZ between the RCA and the cement matrix, as well as the formed products (Figure 5-6c) during hydration. Analysis by EDS (Figure 5-6d) presented a Ca/Si ratio of 2.91, indicating an improvement condition in the formation of C-S-H compared to concrete with untreated RCA incorporation. This improvement is attributed to the elimination of weakly adhered elements in the RCA, since the mixes have the same ratio $w/c=0.55$ and cement content.

Tam *et al.* (2007) conducted a study which observed that the ITZ increased in density after RCA was treated with hydrochloric acid (HCl) at an acid concentration of 0.1 M. This increase in density was reflected in the improvement of the mechanical properties of these mixes. On the other hand, Radevic *et al.* (2018) found that the mixes that used RCA treated with HCl presented a higher quantity of pores compared to the reference

concrete with untreated RCA.

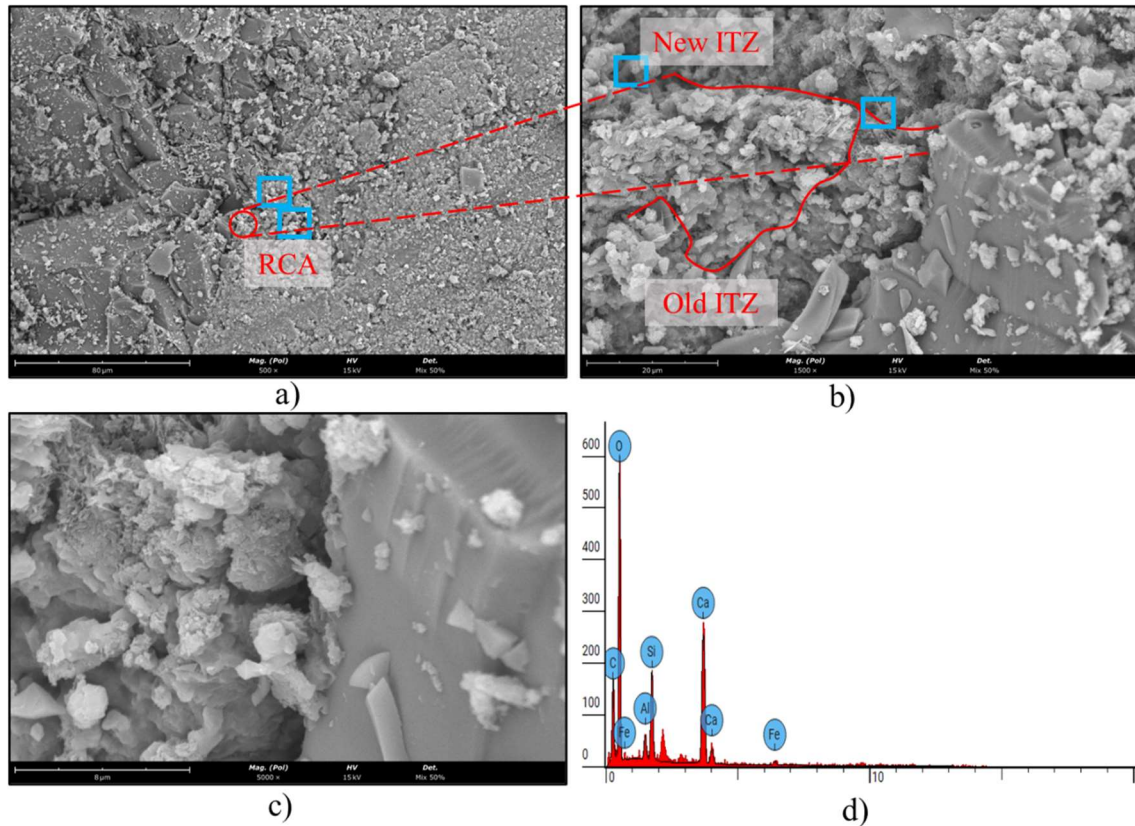


Figure 5-6 SEM/EDS observation of concrete sample with RCA treated with 0.3 HCl at 500x magnification showing the ITZ, pores and the analysis zone (a); general observation of the sample at 1500 magnification marking the EDS analysis points (b); observation at 5000x magnification showing the formed ITZ (c); EDS spectrum of the ITZ (d).

A SEM analysis showed that the quantity of pores in concrete with RCA (Figure 5-6a) treated with 0.3 M of HCl is slightly reduced when compared to the reference RC-RCA mix (Figure 5-6a). This can be explained by the fact that the mixes have the same water-to-cement ratio (w/c) (ISMAIL, SALLEHAN; RAMLI, MAHYUDDIN, 2013).

The observations of the mixes RCA-1.0HCl and RCA-3.0HCl (Figures 5-7a,b,c,d and 5-8a,b,c,d respectively) also indicated an improvement in the values of the Ca/Si ratios, reaching 2.85 and 2.81, respectively. These results confirm a densification of the ITZ. As mentioned earlier, this improvement is attributed to the removal of the mortar adhered to the recycled aggregate (RCA), which resulted in a more uniform RCA surface. It is important to note that the water/cement (w/c) ratios were 0.55 in all concrete mixes analysed, and that a similar pore distribution was observed among them.

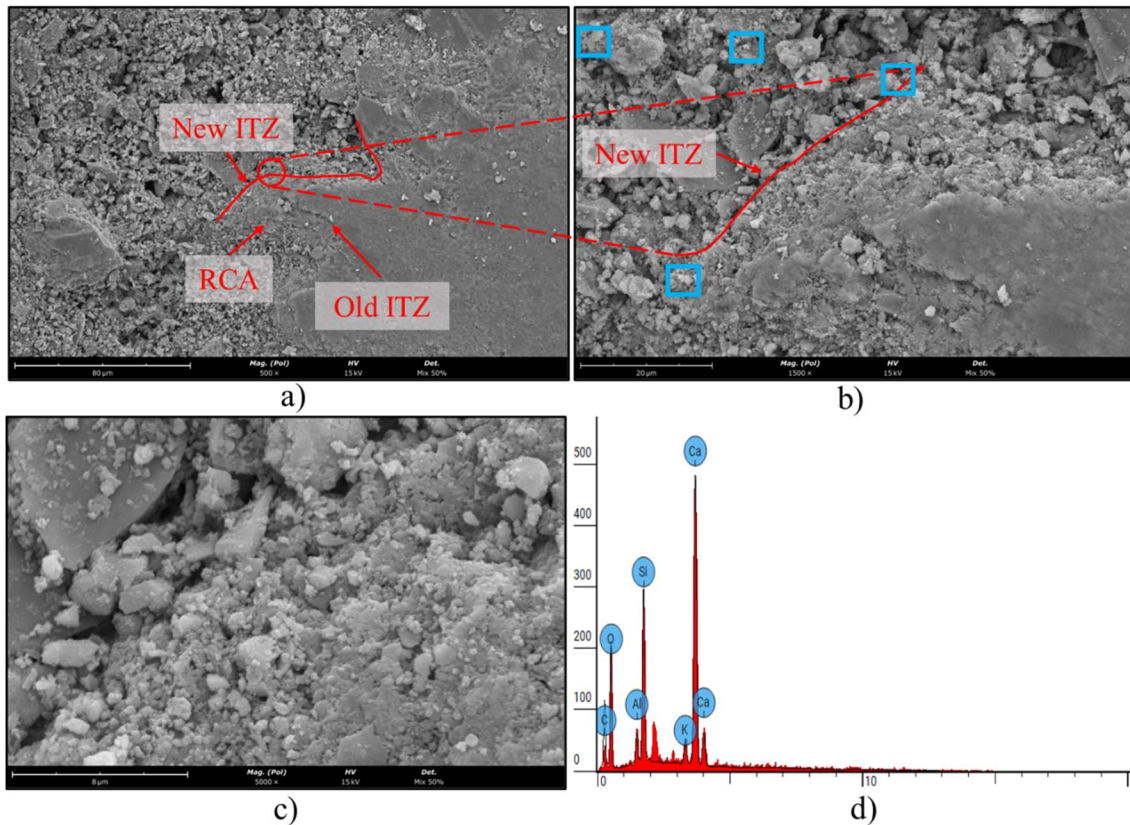


Figure 5-7 SEM/EDS observation of concrete sample with RCA treated with 1.0 HCl at 500x magnification showing the ITZ, pores and the analysis zone (a); general observation of the sample at 1500 magnification marking the EDS analysis points (b); observation at 5000x magnification showing the formed ITZ (c); EDS spectrum of the ITZ (d).

A quantitative comparison of the normalised ratio of the Ca/Si products and the molarity used to treat the recycled aggregates (RCA) was finally carried out (Figure 5-9). A negative linear trend was observed, with a coefficient of determination R^2 of 0.69. From this analysis, it is highlighted that, for concentrations above 3.0 M, the Ca/Si ratio does not show significantly different values, which suggests that RCA has a more uniform morphology.

5.3.4 Concrete incorporating RCA treated with H_2SO_4

The density of the ITZ is a crucial factor that is closely related to its porosity, directly affecting the mechanical performance and durability of concrete (MEHTA; MONTEIRO, 2014; NEVILLE; BROOKS, 1987; ZHAO; WU; LIU; ZHANG, 2022). The morphology and texture of aggregates, which can be rounded or irregular and smooth or rough, respectively, also exert an important influence on ITZ properties. Aggregates with irregular surfaces and rough textures have a better response (SIMEONOV; AHMAD, 1995; ZIMBELMANN, 1985).

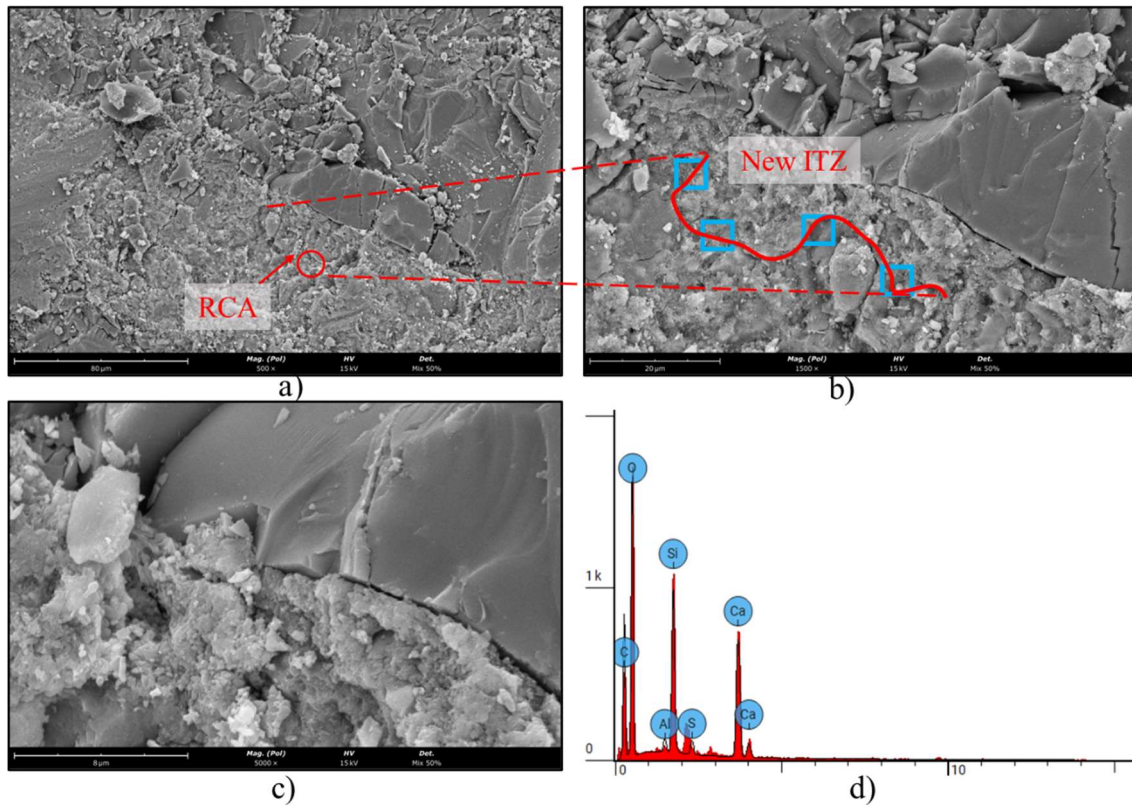


Figure 5-8 SEM/EDS observation of concrete sample with RCA treated with 3.0 HCl at 500x magnification showing the ITZ, pores and the analysis zone (a); general observation of the sample at 1500 magnification marking the EDS analysis points (b); observation at 5000x magnification showing the formed ITZ (c); EDS spectrum of the ITZ (d).

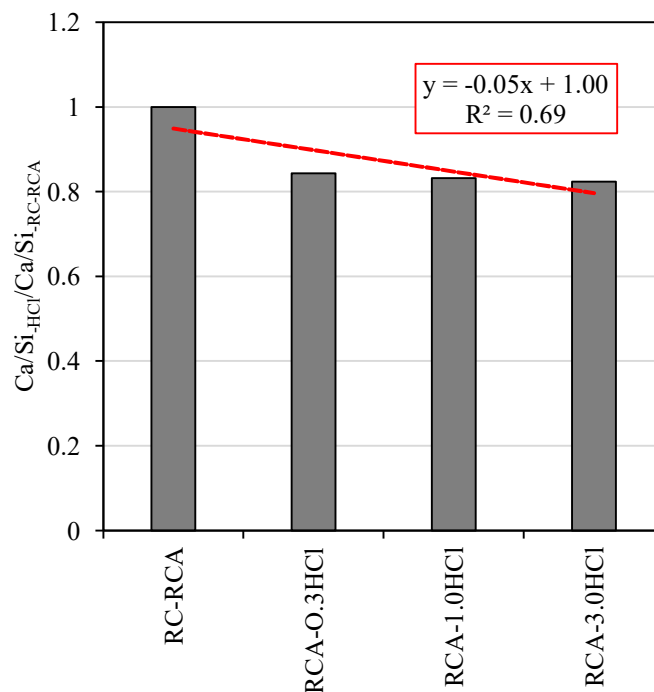


Figure 5-9 Relationship between concrete mixes with RCAs (RCA) treated with different concentrations of hydrochloric acid (HCl) and the ratio between the atomic masses of calcium and silicon (Ca/Si).

Figure 5-10 a,b,c,d presents scanning electron microscopy (SEM) observations of the ITZ between recycled RCA aggregate treated with 0.3 M H₂SO₄. Figure 5-10a shows

the zone chosen to observe the ITZ between RCA and the new cementitious matrix (magnification 500x). Then, Figure 5-10b shows the energy dispersive spectroscopy (EDS) analysis points, which were chosen in a zone close to the ITZ. The ITZ is shown in Figure 5-10c, with a magnification of 5000x, and, finally, the standard result of the chosen EDS points can be observed in Figure 5-10d.

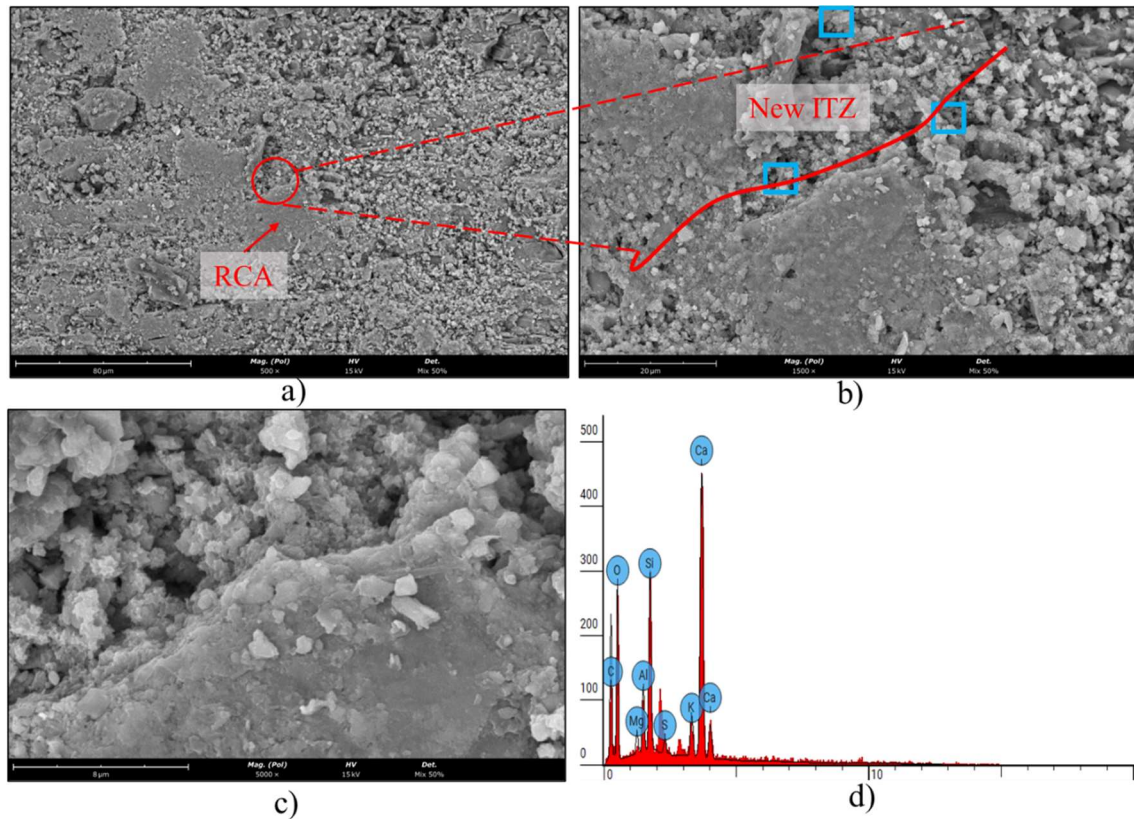


Figure 5-10 SEM/EDS observation of concrete sample with RCA treated with 0.3 H₂SO₄ at 500x magnification showing the ITZ, pores and the analysis zone (a); general observation of the sample at 1500 magnification marking the EDS analysis points (b); observation at 5000x magnification showing the formed ITZ (c); EDS spectrum of the ITZ (d).

Figures 5-11a,b,c,d and 5-12a,b,c,d show the SEM analysis of the mixes with RCA treated with H₂SO₄ in 1.0 M and 3.0 M solutions, where it is possible to observe the selected region between the aggregate and the cementitious matrix (Figure 5-11a and Figure 5-12a, with 500x magnification) and the points analysed by EDS (Figure 5-11b and Figure 5-12b). It is noted that this region is not densifying due to ionization, which may cause a second degradation (BROWN; LEMAY JR; BURSTEN; BURDGE, 2004; SCRIVENER; YOUNG, 1997). However, contrary to what was observed in this study, Tam *et al.* (2007) noticed a densification of ITZ in concrete mixes containing RCA treated with H₂SO₄ at a concentration of 0.1 M, compared to mixes with the same RCA without treatment, resulting in an increase of the mechanical properties of these mixes. It is

concluded that low concentrations of H_2SO_4 can improve the physical and chemical characteristics of RCA.

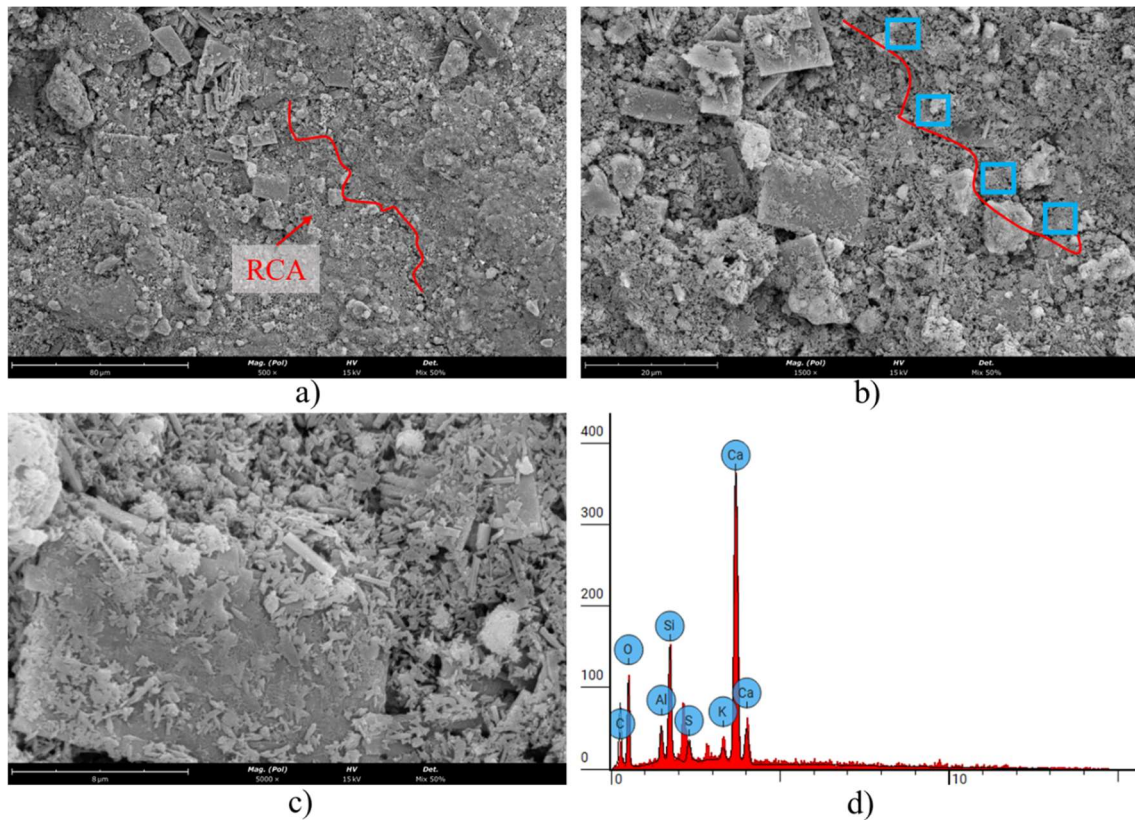


Figure 5-11 SEM/EDS observation of concrete sample with RCA treated with 1.0 HCl at 500x magnification showing the ITZ, pores and the analysis zone (a); general observation of the sample at 1500 magnification marking the EDS analysis points (b); observation at 5000x magnification showing the formed ITZ (c); EDS spectrum of the ITZ (d).

To obtain a quantitative analysis on the possible improvement of the ITZ, a comparison was performed between the ratio of the atomic weights of the Ca/Si components obtained from the EDS analysis of each composition and the molarity of the H_2SO_4 that was used to treat the RCA, as presented in Figure 5-13. It is observed that there is no significant trend as the molarity is increased ($R^2 = 0.17$), due to the reasons mentioned above.

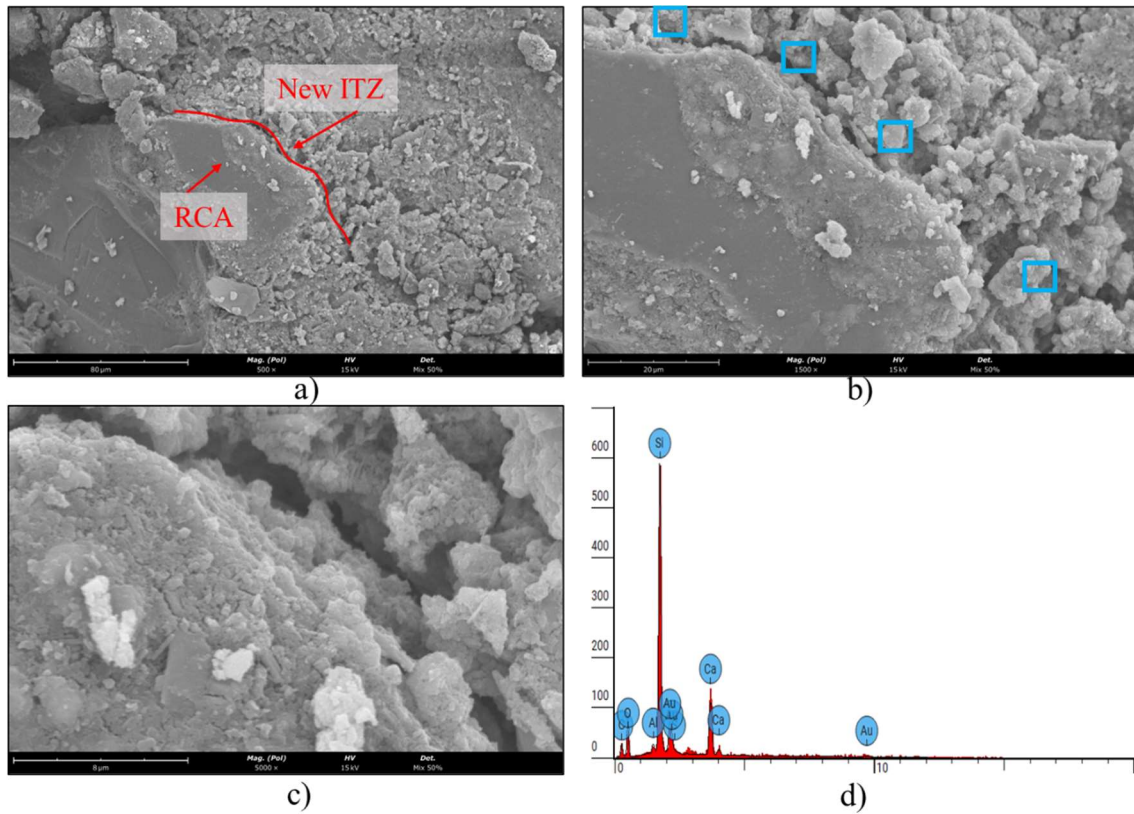


Figure 5-12 SEM/EDS observation of concrete sample with RCA treated with 3.0 H₂SO₄ at 500x magnification showing the ITZ, pores and the analysis zone (a); general observation of the sample at 1500 magnification marking the EDS analysis points (b); observation at 5000x magnification showing the formed ITZ (c); EDS spectrum of the ITZ (d).

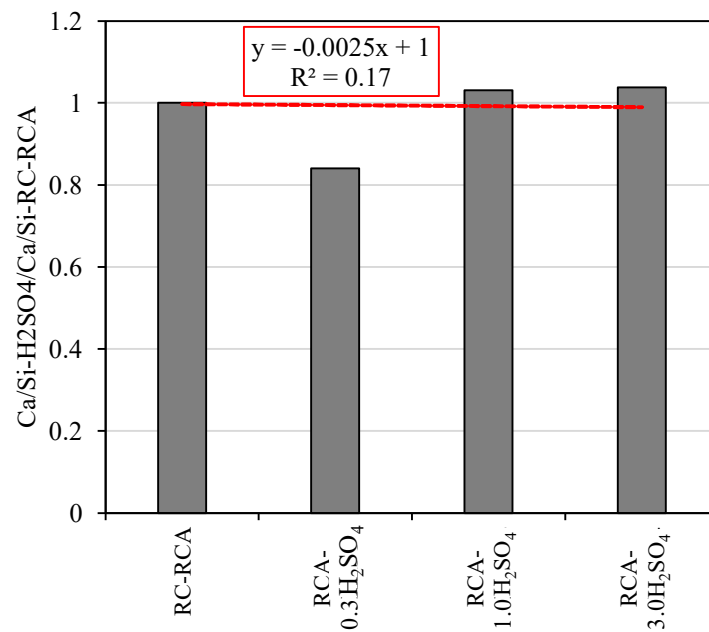


Figure 5-13 Relationship between concrete mixes with RCA treated with different concentrations of hydrochloric acid (H₂SO₄) and the ratio between the atomic masses of calcium and silicon (Ca/Si).

5.3.5 Concrete incorporating aluminium sulphate (AS)

Figure 5-14a,b,c,d presents the image of the zone between RCA and the cementitious matrix, where the presence of some ettringite formations can be observed, which is a normal formation when an accelerant is introduced into the cementitious matrix (CHEN; SUN, 2018; WANG; HE; SU; MA et al., 2018). In Figure 5-14c, it can be seen that the ettringite is compacted due to the morphology of RCA and of the cementitious matrix. This ettringite tends to have a circular shape, since the analysis was performed at 28 days and the formation of ettringite in slender shapes that appear in the first days of hydration disappears, giving rise to a short and circular ettringite.

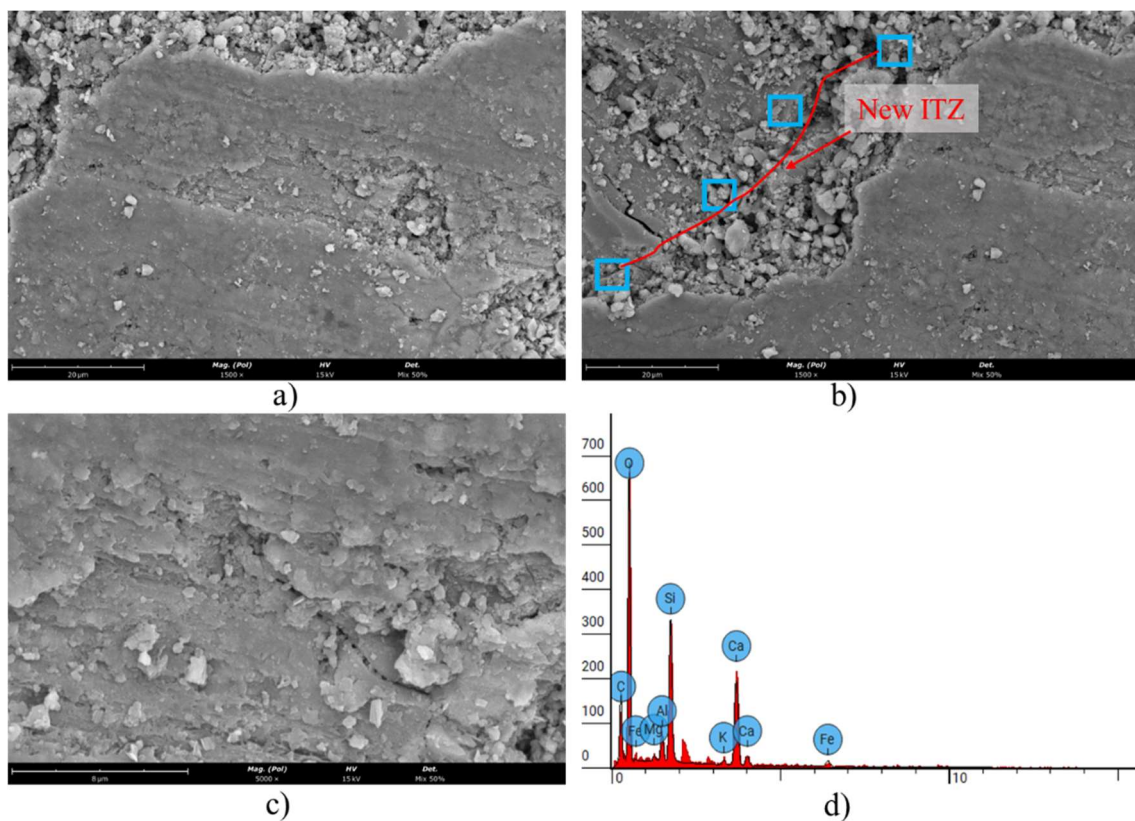


Figure 5-14 SEM/EDS observation of concrete sample with RCA incorporating AS at 500x magnification showing the ITZ, pores and the analysis zone (a); general observation of the sample at 1500 magnification marking the EDS analysis points (b); observation at 5000x magnification showing the formed ITZ (c); EDS spectrum of the ITZ (d)

The EDS analysis of the ratio of atomic weights between Ca/Si showed a value of 0.9, which indicates a densification of the zone between the aggregate and the cementitious matrix. The analysis points are shown in Figure 5-14d. Song *et al.* (2015) analysed the ITZ of mixes with RCA and stated that the incorporation of different contents of AS helps in the densification of the ITZ because AS helps to reduce the

preferential orientations of portlandite in the ITZ. Song *et al.* (2015) mention that the maximum value that can be added is 1.10%, due to the fact that higher values can generate a late ettringite formation (CODY; LEE; CODY; SPRY, 2004; DERMATAS, 1995).

5.4 Compressive strength

The compressive strength is the most common property used to evaluate the performance and general mechanical characteristics of concrete, since it allows evaluating the behaviour by describing the ability of concrete to resist the stresses requested without cracking. There are several factors that directly affect concrete strength such as: cement composition, concrete porosity, water-cement ratio (w/c) and the factor that is the focus of this study, the reliability of RCA and its interaction between it and the cementitious matrix (interface transition zone -ITZ). The compressive behaviour of the mixes was investigated by the analysis of 54 cylindrical specimens tested at 7 and 28 days of age.

5.4.1 Compressive strength of concrete incorporating RCA treated with HCl

Table 5-4 shows the compressive strength results for different ages ($f_{cm,7}$ and $f_{cm,28}$) of the mixes with incorporation of RCA treated with HCl in molarity of 0.1 M, 0.3 M, and 3.0 M, as well as the variations in strength relative to the reference concrete with NA (RC) and with RCA (RC-RCA).

Initially, it is observed that the results of the compressive strength at 7 days of the mixes, RCA-0.3 HCl and RCA-1.0 HCl had a reduction of 15.50% and 2.29% relative to the reference concrete RC. However, the mix RCA-3.0 RCA showed a slight improvement compared to RC: 2.10%. The compressive strength in relation to RC-RCA concrete presents a reduction of 1.72% for the RCA-0.3 HCl mix, a negligible value because it is within the range of variation of the test. On the other hand, mixes RCA-1.0 HCl and RCA3.0 HCl had improvements of 13.24% and 18.34% relative to the RC-RCA mix.

The results of the compressive strength at 28 days show higher values in the mixes containing RCA treated with HCl compared to RC-RCA, with improvements of 7.76%, 10.96% and 12.17% for the mixes RCA-0.3 HCl, RCA-1.0 HCl, and RCA-3.0 HCl, respectively. Likewise, the mixes containing RCA treated with HCl had smaller

reductions (around 13%) relative to RC than to RC-RCA (19.79%).

Table 5-4 Compressive strength of cylindrical specimens in concrete mixes with RCA treated with HCl.

Mix	7 days				28 days			
	$f_{cm,7}$ (MPa)	σ	% improvement relative to $f_{cm,7}$ of:		$f_{cm,28}$ (MPa)	σ	% improvement relative to $f_{cm,28}$ of:	
			RC	RC-RCA			RC	RC-RCA
RC	34.42	0.47	—	—	47.54	0.68	—	—
RC-RCA	29.70	0.36	13.72%▼	—	38.13	1.29	19.79%▼	—
RCA-0.3HCl	29.19	1.22	15.20%▼	1.72%▼	41.09	0.54	13.56%▼	7.76%▲
RCA-1.0HCl	33.63	1.43	2.29%▼	13.24%▲	42.31	0.81	10.99%▼	10.96%▲
RCA-3.0HCl	35.15	0.77	2.10%▲	18.34%▲	42.77	0.16	10.03%▼	12.17%▲

To better understand the results, the compressive strength values at 28 and 7 days were graphically represented (Figure 5-15a).

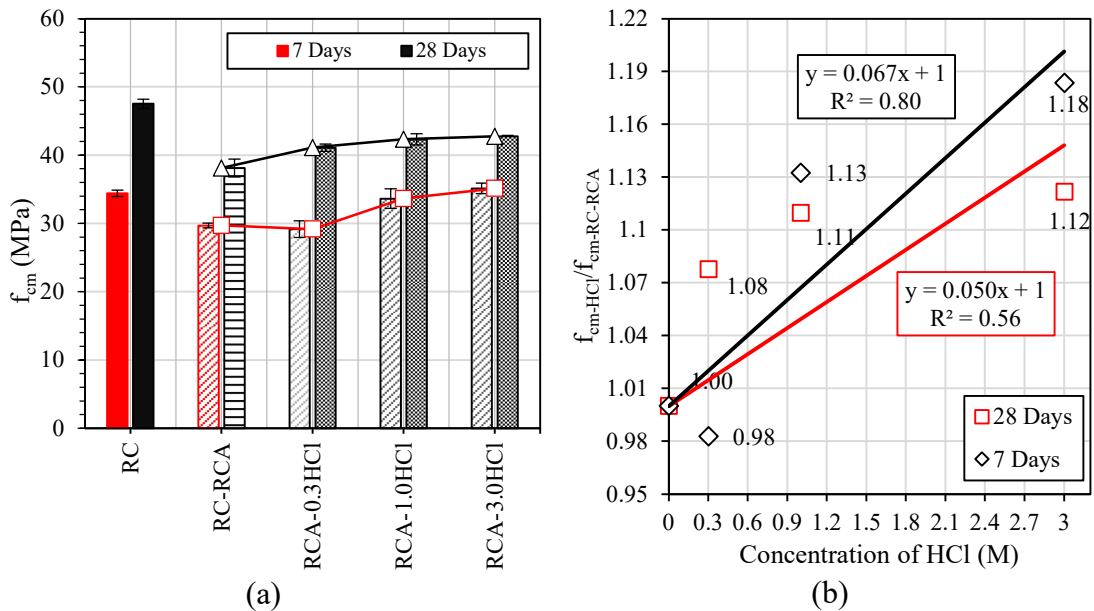


Figure 5-15 Compressive strength (f_{cm}) of RC, RC-RCA and RCA-HCl concrete mixes tested at 7 and 28 days (a); normalisation of compressive strength (f_{cm}) versus acid concentration of HCl (M) (b).

It can be observed that there is a trend towards improvement in the values of compressive strength when the acid concentration of HCl at 28 days is increased. However, in the compressive strength evaluated at 7 days, this tendency is more visible for concentrations higher than 0.3 M of HCl. Studies by Ismail and Ramli (2013), Juan and Gutierrez (2009), Kim *et al.* (2018), Abbas *et al.* (2007), Al-Bayati *et al.* (2016) and Saravankumar *et al.* (2016) have shown that, by increasing the acid concentration (M), the removal of the paste adhered to the RCA is greater because the dissolution of calcium hydroxide caused by acid attack proceeds in two phases. The first one is the reaction of the acid with the calcium hydroxide (base) in the cement paste. The second phase is the chemical reaction with the calcium silicate hydrate. As expected, the second phase does not begin

until all calcium hydroxide is consumed (ALLAHVERDI; ŠKVÁRA, 2000; BEDDOE; DORNER, 2005; CLIFTON; POMMERSHEIM, 1994). When the acid molarity is increased, the pH lowers, and the dissolution of calcium hydroxide occurs more quickly, reducing the amount of mortar in RCA, improving its quality. For this reason, it is reasonable to assume that there is a relationship between molarity and compressive strength. Figure 5-15b shows the positive correlation between HCl concentration and compressive strength at 7 and 28 days with a linear fit with good correlation ($R^2 = 0.80$) at 7 days and a reasonable one ($R^2 = 0.56$) at 28 days.

5.4.2 Compressive strength of concrete incorporating RCA treated with H₂SO₄

The results of compressive strength at 7 and 28 days of mixes with RCA treated with H₂SO₄ are shown in Table 5-5 as well as their standard deviations and their variation in relation to RC and RC-RCA. From the results obtained, it can be observed that there is a reduction of the compressive strength of all mixes, of 13.72%, 13.36%, 18.89%, and 22.12% respectively for the compositions RC-RCA, RCA-0.3 H₂SO₄, RCA-1.0 H₂SO₄ and RCA-3.0 H₂SO₄ relative to RC evaluated at 7 days. Regarding RC-RCA, these reductions are more evident in the RCA-RCA-1.0 H₂SO₄ (5.99%) and RCA-3.0 H₂SO₄ (9.74%) mixes at 7 days. Nevertheless, the RCA-0.3 H₂SO₄ mix showed a slight improvement of 1.58% that is not representative as it was within the experimental error. The results of the compressive strength at 28 days were negative for all mixes, with reductions of up to 30% in relation to RC. However, at acid concentration of 0.3 M (RCA-0.3H₂SO₄), an improvement in compressive strength of 7.71% was observed relative to RC-RCA, showing that there is a negative influence for higher acid concentrations (RCA-1.0 H₂SO₄ and RCA-3.0 H₂SO₄) compared to RC-RCA.

Table 5-5 Compressive strength of cylindrical specimens in concrete mixes with RCA treated with H₂SO₄.

Mix	7 days				28 days			
	f _{cm} (MPa)	σ	% improvement relative to f _{cm} of:		f _{cm} (MPa)	σ	% improvement relative to f _{cm} of:	
			RC	RC-RCA			RC	RC-RCA
RC	34.42	0.47	—	—	47.54	0.68	—	—
RC-RCA	29.70	0.36	13.72% ▼	—	38.13	1.29	19.79% ▼	—
RCA-0.3H ₂ SO ₄	30.17	2.23	12.36% ▼	1.58% ▲	41.07	0.99	13.60% ▼	7.71% ▲
RCA-1.0H ₂ SO ₄	27.92	0.28	18.89% ▼	5.99% ▼	34.14	0.30	28.19% ▼	10.47% ▼
RCA-3.0H ₂ SO ₄	26.81	0.55	22.12% ▼	9.74% ▼	32.97	0.34	30.64% ▼	13.53% ▼

Figure 5-16a show the evolution of the compressive strength for the mixes with RCA treated with H₂SO₄. It can be observed that there is a decrease in compressive strength at 7 and 28 days. This negative correlation of the mixes with RCA treated with H₂SO₄ increases when molarity rises (Figure 5-16b), with a linear fit ($R^2 = 0.83$ and 0.62 , at 7 and 28 days, respectively). This can be explained because of the ionization of H₂SO₄ (Equation 5-4) (BROWN; LEMAY JR; BURSTEN; BURDGE, 2004), meaning that it is possible that there is a new degradation reaction in the RCA when it comes in contact with the water in the mix. When the pH of the treated RCA was measured, the result was 5.2, indicating the presence of the hydronium ion.

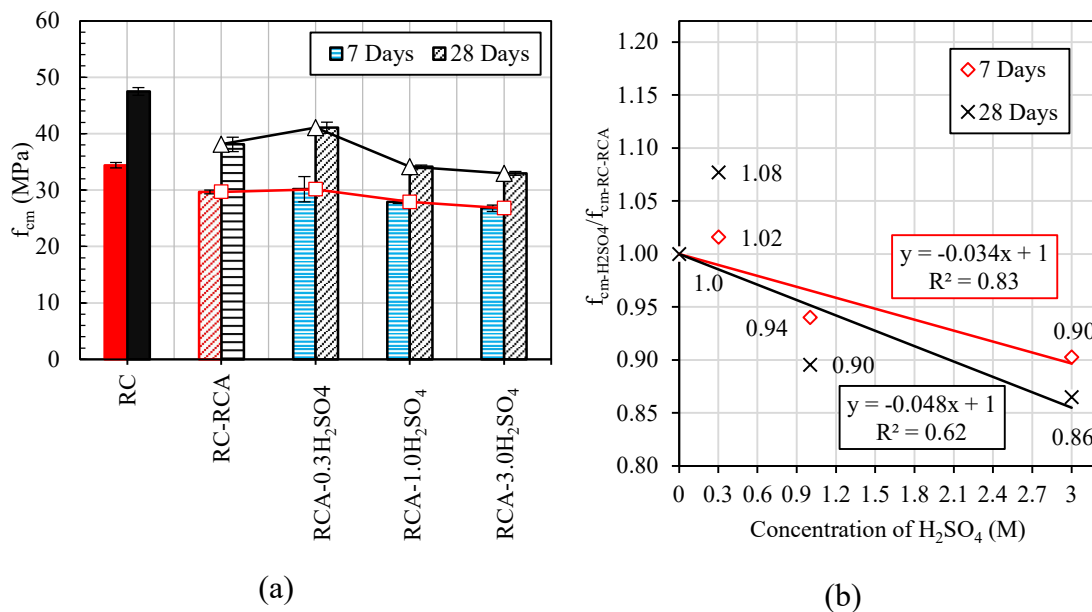
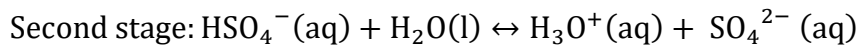
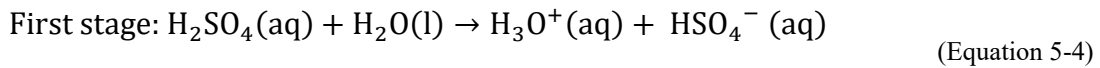


Figure 5-16 Compressive strength (f_{cm}) of RC, RC-RCA and RCA-H₂SO₄ concrete mixes tested at 7 and 28 days (a); normalisation of compressive strength (f_{cm}) versus acid concentration of H₂SO₄ (M) (b).

5.4.3 Concrete incorporating aluminium sulphate (AS)

In the mixes with addition of AS, RCA-AS, the compressive strength increased by 16.60% with respect to RC-RCA concrete, and 0.61% to RC concrete (Table 5-6). This high initial strength is explained by the fact that AS increases the acceleration of cement hydration by increasing the formation of calcium hydroxide, visible in the strength at 7 days (KAN; LAN; KONG; YANG, 2013). This reaction generates an amount of ettringite capable of reducing the porosity of the cementitious matrix between the RCA, increasing

the solidity of the ITZ due to the formation of calcium hydroxide, which reduces the ITZ due to the increase in silicate/dicalcium tricalcium. This behaviour continues until 28 days, where the difference to the strength at 7 days is not significant, since most of the calcium hydroxides are already formed (SONG; QIAO; WEN, 2015).

Song *et al.* (2015) observed similar results in concrete mixes with RCA as aggregate, and fly ash (FA). Noting improvements of 42% and 34.1% of compressive strength for 7 and 28 days, respectively. Other authors like Kan *et al.* (2013), studied the addition of aluminium sulphate in concrete mixes, showing an improvement in compressive strength when the ratio of AS is between 6% and 8% at 28 days. The author explains this improvement with the formation of hydration products and the degree of hydration.

Table 5-6 Compressive strength of cylindrical specimens in concrete mixes with RCA treated with the addition of AS.

Mix	7 days			28 days				
	f _{cm} (MPa)	σ	% improvement relative to f _{cm} of:		f _{cm} (MPa)	σ	% improvement relative to f _{cm} of:	
			RC	RC-RCA			RC	RC-RCA
RC	34.42	0.47	—	—	47.54	0.68	—	—
RC-RCA	29.70	0.36	13.72%▼	—	38.13	1.29	19.79%▼	—
RCA-AS	34.63	1.44	0.61%▲	16.61%▲	40.34	0.80	15.15%▼	5.78%▲

Figure 5-17 show the values and their variations of the different investigations that used acid treated RCA with 100% substitution and the values obtained in the present investigation. It can be concluded that the results obtained for compressive strength in this investigation are within the limits proposed by Silva *et al.* (2015) who collected the results from 65 publications on the compressive behaviour of concrete mixes with recycled aggregate and RCA, as well as by Purusthaman *et al.* (2014), Pandurangan *et al.* (2016). Kim *et al.* (2017) and Saravanakumar and Abhiram (2016). Furthermore, this investigation enables the analysis of predictions for different levels of coarse RCA replacement, using the upper and lower limits set for 100% substitution of untreated RCA.

5.5 Splitting tensile strength

This topic presents the results of splitting tensile strength testing on various mixes. The results are divided into three categories: tensile strength in mixes with incorporated RCA treated with HCl, mixes with RCA treated with H₂SO₄, and mixes with the addition of AS. Analysing this property in concrete is fundamental to determine the response to serviceability limit state.

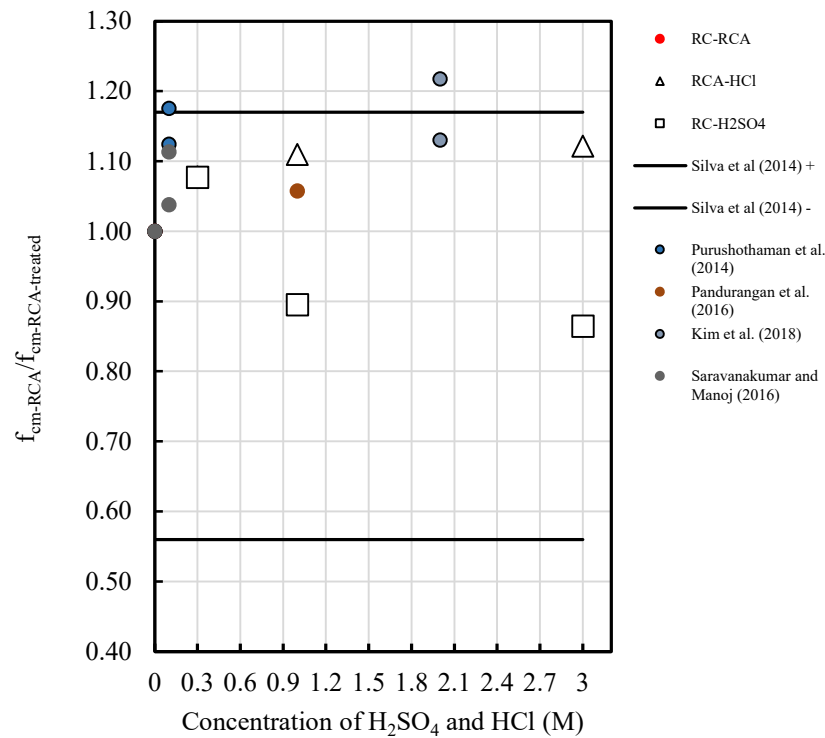


Figure 5-17 Comparison between experimental values from the literature *versus* molarity (PURUSHOTHAMAN; AMIRTHAVALLI; KARAN, 2014), (PANDURANGAN; DAYANITHY; PRAKASH, 2016), (KIM; KIM; KIM; KIM, 2017), (SARAVANAKUMAR; ABHIRAM; MANOJ, 2016)

5.5.1 Tensile strength in concrete incorporating RCA treated with HCl

Figure 5-18a presents the results of the splitting tensile strength ($f_{ctm,sp}$) of the HCl treated concrete mixes tested at 28 days of curing in a humid chamber compared to the RC and RC-RCA reference concrete mixes. It can be observed that there is an improvement in the tensile strength for all concentrations at which RCA was treated (0.3 M, 1.0 M and 3.0 M) surpassing even the RC mix that incorporates NA. This behaviour clearly presents a tendency as the acid HCl solution increases. Figure 5-18b presents the normalized values of each concrete mix with RCA treated with HCl as a function of concentration, and an power trend can be observed with an $R^2 = 0.98$. The increase in tensile strength is attributed to there being a removal of weakly adhered particles in the loose RCA on the surface, improving the physical and mechanical quality of RCA. Besides that, the improvement of the aggregate surface produces a better contact with the cementitious matrix (ITZ) improving the mechanical properties. This reduction of the ITZ between the aggregates and the cementitious matrix will be further developed in the item corresponding to the microstructural part of the concrete mixes of this chapter.

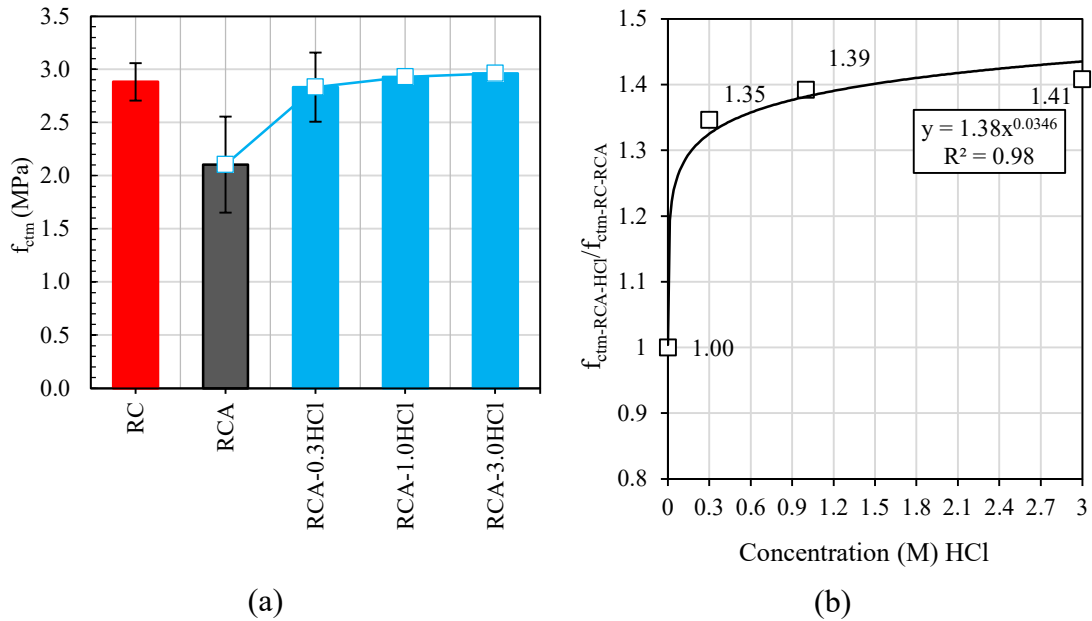


Figure 5-18 Tensile strength ($f_{ctm,sp}$) of RC, RC-RCA and RCA-HCl concrete mixes tested at 7 and 28 days (a); normalisation of tensile strength ($f_{ctm,sp}$) versus acid concentration of HCl (M) (b).

For a better understanding, the values of the tensile strength, as well as their variation with respect to the RC and RC-RCA reference mixes, are presented in Table 5-7. As previously mentioned, there is an improvement of 34.64%, 39.21% and 40.82%, respectively, relative to the RC-RCA mix. Regarding the two mixes RCA-1.0 HCl and RCA-3.0 HCl, it was observed that it had a similar performance to that of the reference mix (RC) with NA.

Table 5-7 Tensile strength in concrete mixes with RCA treated with HCl.

Mix	f_{ctm} (MPa)	σ	% improvement relative to RC	% improvement relative to RC-RCA
RC	2.88	0.18	—	—
RC-RCA	2.10	0.45	27.03% ▼	—
RCA-0.3 HCl	2.83	0.33	1.75% ▼	34.64% ▲
RCA-1.0 HCl	2.93	0.06	1.58% ▲	39.21% ▲
RCA-3.0 HCl	2.96	0.04	2.75% ▲	40.82% ▲

5.5.2 Tensile strength in concrete incorporating RCA treated with H₂SO₄

The results corresponding to the concrete mixes with RCA treated with H₂SO₄ are presented in the histogram of Figure 5-19a. There is a clear improvement in the RCA-0.3 H₂SO₄ mixes that goes down as the concentration of H₂SO₄ increases. As observed in the histogram, the best concentration to improve the tensile strength is 0.3 M. This is because ionization still continues after washing the RCA after H₂SO₄ exposure, which generates a new degradation of the cementitious paste, as explained in the previous section for the 1.0 M and 3.0 M concentrations. Due to the phenomena happening with the continuous

degradation, there is a non-representative correlation as a function of molarity with $R^2 = 0.22$, as shown in Figure 5-19b. Figure 5-8b shows the normalized values with the RC-RCA mix of tensile strength *versus* acid molarity.

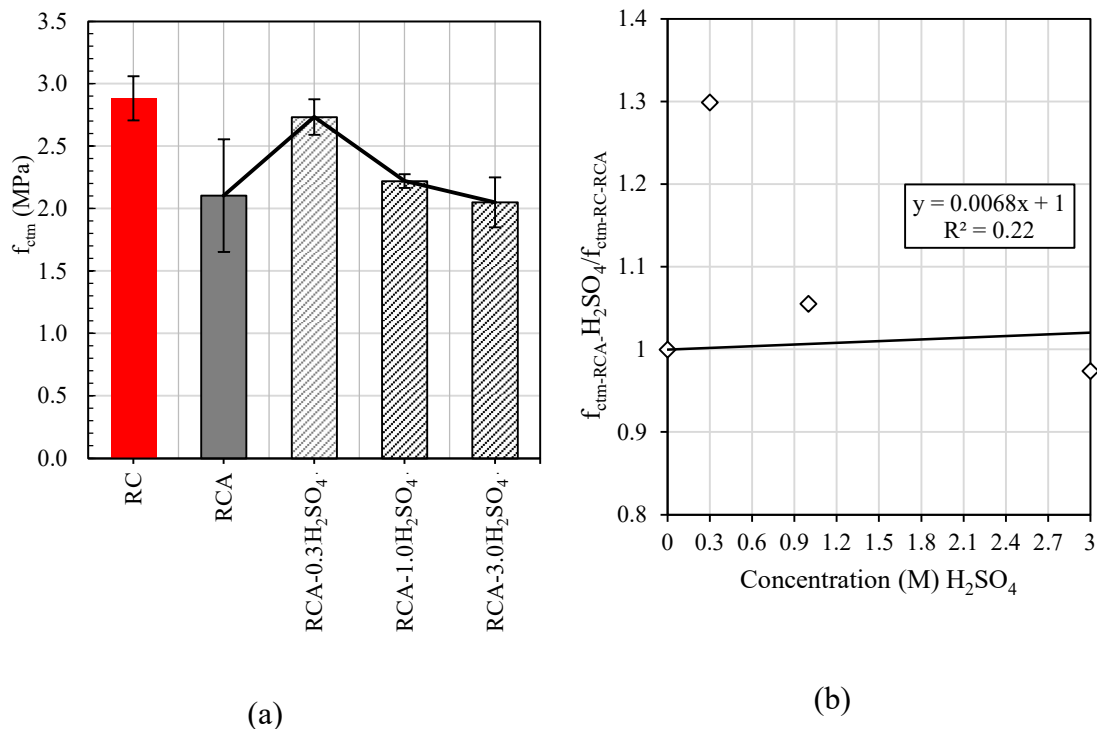


Figure 5-19 Tensile strength ($f_{ctm,sp}$) of RC, RC-RCA and RCA-H₂SO₄ concrete mixes tested at 7 and 28 days (a); normalisation of tensile strength ($f_{ctm,sp}$) *versus* acid concentration of H₂SO₄ (M) (b).

The tensile strength results, their coefficients of variation and standard deviation for the concrete mixes with RCA treated with H₂SO₄ are presented in Table 5-8.

Table 5-8 shows the values of variation of the mixes with H₂SO₄ with respect to RC and RC-RCA mixes, i.e. reductions of 27.03%, 5.205, 22.97% and 28.9% for the RC-RCA, RCA-0.3 H₂SO₄, RCA-1.0 H₂SO₄, and RCA-3.0 H₂SO₄ mixes, respectively, compared to the RC concrete mix. Finally, one can observe the variation of the mixes with respect to RC-RCA concrete mixes, where the variations had a relevant increment in molarity 0.3M (29.92%) and a negligible increment for 1.0 M (5.57%), and with respect to molarity 3.0 M, it had a decrease of 2.57%.

Table 5-8 Tensile strength in concrete mixes with RCA treated with H₂SO₄.

Mix	f_{ctm} (MPa)	σ	% improvement relative to RC	% improvement relative to RC-RCA
RC	2.88	1.41	—	—
RC-RCA	2.10	0.45	27.03% ▼	—
RCA-0.3 H ₂ SO ₄	2.73	0.14	5.20% ▼	29.92% ▲
RCA-1.0 H ₂ SO ₄	2.22	0.06	22.97% ▼	5.57% ▲
RCA-3.0 H ₂ SO ₄	2.05	0.20	28.90% ▼	2.57% ▼

5.5.3 Tensile strength in concrete incorporating aluminium sulphate (AS)

Table 5-9 presents the results obtained from the concrete mix with the addition of aluminium sulphate. It can be seen that the concrete that had the addition of 1.10% aluminium sulphate showed an increase in its tensile strength by 14.13% compared to the reference concrete RC-RCA, which had a value of 2.4 MPa. As described previously (item 5.3.3), the addition of aluminium sulphate caused reactions with the portlandite of the cement hydration products in RC-RCA, which resulted in an improvement in the ITZ of both RC-RCA and the cementitious matrix, increasing the tensile strength capacity by 14.13% compared to the RC-RCA concrete mix.

Table 5-9 Tensile strength in concrete mixes with RCA treated with the addition of AS.

Mix	f_{ctm} (MPa)	σ	% improvement relative to RC	% improvement relative to RC-RCA
RC	2.88	1.41	—	—
RC-RCA	2.10	0.45	27.03% ▼	—
RCA-AS	2.40	0.14	16.72% ▼	14.13% ▲

According to Song *et al.* (2015), the addition of 1.10% aluminium sulphate in RC-RCA mixes resulted in a 22.3% increase in tensile strength after 28 days.

5.6 Modulus of elasticity

The modulus of elasticity (E_{cm}) is an important measure of the mechanical strength of structural concrete, which reflects its ability to deform elastically. The quality, size and compatibility of the aggregates and the cementitious matrix, as well as the interaction between these components at the ITZ (BUTLER; WEST; TIGHE, 2013; SILVA; DE BRITO; DHIR, 2016). Concrete mixes with RCA tend to have a lower value of modulus of elasticity (E_{cm}) compared to mixes with NA, with an average reduction of 16% in 100% substitutions (LYE; DHIR; GHATAORA, 2016).

5.6.1 Modulus of elasticity in concrete incorporating RCA treated with HCl

Figure 5-21a allows observing the results obtained by the several mixes of concrete relevant to this property. Thus, it can be seen that the increase of HCl acid solution increases the modulus of elasticity (E_{cm}). The lower values of modulus of elasticity E_{cm} of the mixes with RCA can be attributed to higher porosity and lower stiffness of RCA in comparison with NA (ETXEBERRIA; VÁZQUEZ; MARÍ; BARRA,

2007; PEDRO; DE BRITO; EVANGELISTA, 2014; TABSH; ABDELFAH, 2009; THOMAS; THACKAVIL; WILSON, 2018) According to Beshr *et al.* (2003), the stiffness of coarse aggregates greatly influences the concrete's modulus of elasticity. Aïtcin and Mehta (1990) also pointed out that the low strength of the aggregate can result in a concrete with a lower modulus of elasticity. It was observed that there is an improvement of the E_{cm} values when RCA treated with 0.3 M, 1.0 M and 3.0 M of HCL solutions is used, attributing this to the good connections of the interface between the aggregate and the cement paste, reducing the propagation of cracks during loading. These results are similar to those found by several authors (ISMAIL, S.; RAMLI, M., 2013; ISMAIL; RAMLI, 2014; PURUSHOTHAMAN; AMIRTHAVALLI; KARAN, 2014; TAM, V. W. Y.; TAM, C. M.; LE, K. N., 2007).

From the results of the modulus of elasticity of the RCA-HCl concrete mixes, it was possible to normalize them in relation to the RC-RCA reference concrete. Figure 5-21b illustrates this normalization, where it is possible to identify two trends: one linear with an R^2 of 0.73 and the other power with an R^2 of 0.84. This clearly shows that there is an improvement of the modulus of elasticity (E_{cm}) in mixes treated with HCl. Due to the large variation in RCA morphology, the linear trend best represents this behaviour.

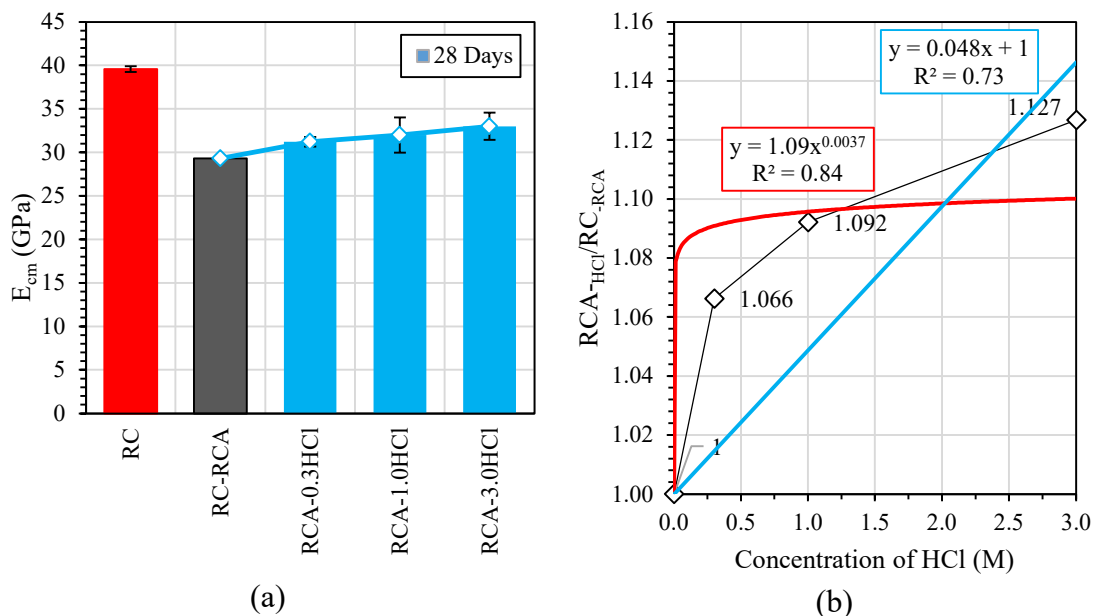


Figure 5-20 Modulus of elasticity of RC, RC-RCA and RCA-HCl concrete mixes tested at 28 days (a); normalisation of modulus of elasticity (E_{cm}) versus acid concentration of HCl (M) (b).

Table 5-10 shows the results of the modulus of elasticity of each concrete mix, along with the respective standard deviation and the percentage variation in relation to

the reference mixes RC and RC-RCA. It is highlighted that the mixes RCA-0.3-HCl, RCA-1.0HCl and RCA-3.0HCl showed improvements of 6.62%, 9.91% and 12.68%, respectively. As described previously in section 5-4-1, this improvement can be explained by the improved surface after acid treatment with HCl, which resulted in the densification of the ITZ, as evidenced by SEM analyses.

Table 5-10 Modulus of elasticity (E_{cm}) at 28 days of concrete mixes with RCA treated with HCl.

Mix	E_{cm} (MPa)	σ	% improvement relative to RC	% improvement relative to RC-RCA
RC	39.58	0.33	—	—
RC-RCA	29.31	0.13	25.97% ▼	—
RCA-0.3 HCl	31.25	0.56	21.07% ▼	6.62% ▲
RCA-1.0 HCl	32.01	2.02	19.15% ▼	9.21% ▲
RCA-3.0 HCl	33.02	1.56	16.58% ▼	12.68% ▲

5.6.2 Modulus of elasticity in concrete incorporating RCA treated with H_2SO_4

The results of the concrete mixes that used RCA treated with an H_2SO_4 acid solution concerning this property are presented in Figure 5-22a,b, where it is observed that there was a decrease in the value of the modulus of elasticity (E_{cm}) with an increase in the acid molarity of H_2SO_4 at 28 days of testing. Figure 21a shows that the mixes with RCA treated with a molarity of 0.3 M- H_2SO_4 had a slight improvement relative to the reference concrete RC-RCA by 2.27%. For the RCA-1.0 H_2SO_4 and RCA-3.0 H_2SO_4 mixes, the modulus of elasticity (E_{cm}) decreased by 10.08% and 12.64%, respectively.

Figure 5-21b illustrates the relationship between the treated molarity of the RCA and the normalization of the modulus of elasticity in relation to the value of the RC-RCA mix. There is a negative linear relationship, with a coefficient of determination (R^2) of 0.72.

This relationship indicates that the second mortar degradation process in the RCA, described in section 5.3.2, increases the distance from the ITZ, resulting in a reduction of this property. Furthermore, the R^2 close to 1 indicates that the relationship is strong and can be relied upon for future predictions. This result is important for understanding the interaction between the RCA and the cementitious matrix, as the ITZ is a critical area in the mechanical behaviour of concrete. The distance from the ITZ has a direct impact on the mechanical properties of concrete, such as the modulus of elasticity, and can be used as an indicator of the quality of the mix.

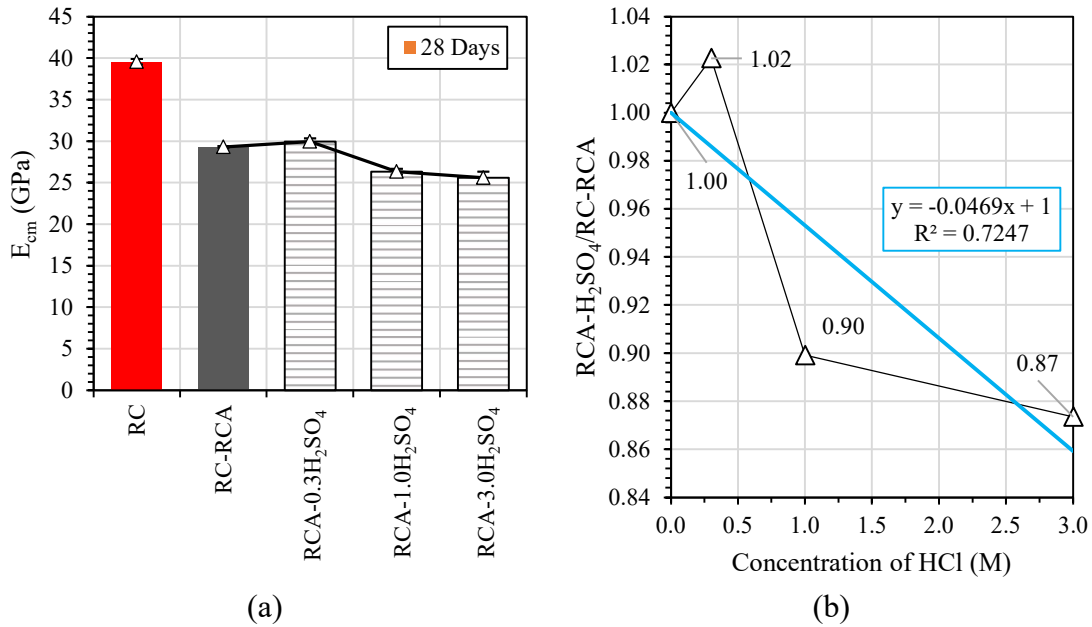


Figure 5-21 Modulus of elasticity of RC, RC-RCA and RCA-H₂SO₄ concrete mixes tested at 28 days (a); normalisation of modulus of elasticity (E_{cm}) versus acid concentration of H₂SO₄ (M) (b).

Table 5-11 presents the reduction in the value of the modulus of elasticity with respect to RC and RC-RCA concrete mixes, as well as their standard deviation. The results show that there was a reduction in the value of the modulus of elasticity in relation to the concrete mixes without the use of RCA. However, authors such as Tam *et al.* (2007), Ismail and Ramli (2014) and Purushothaman *et al.* (2014) found improvements in the modulus of elasticity values for low concentrations of H₂SO₄. These results indicate that low concentrations of H₂SO₄ improve the aggregate surface, resulting in improvements in the performance of the final concrete.

Table 5-11 Modulus of elasticity (E_{cm}) at 28 days of concrete mixes with RCA treated with H₂SO₄.

Mix	E_{cm}	σ	% improvement relative to RC	% improvement relative to RC-RCA
RC	39.58	0.33	—	—
RC-RCA	29.31	0.13	25.97% ▼	—
RCA-0.3 H ₂ SO ₄	29.97	0.38	24.29% ▼	2.27% ▲
RCA-1.0 H ₂ SO ₄	26.35	0.35	33.43% ▼	10.08% ▼
RCA-3.0 H ₂ SO ₄	25.60	0.75	35.33% ▼	12.64% ▼

Microstructural tests, such as scanning electron microscopy (SEM), were employed to understand the relationship between the treatment of RCA and the quality of the final concrete. From the analysis of section 5.3.4, it was possible to conclude that the ITZ was densified when the aggregate was treated with 0.3 M solution. However, for solutions of higher molarities, such as 1.0 M and 3.0 M, it was observed that the second degradation did not allow this densification.

5.6.3 Modulus of elasticity in concrete incorporating aluminium sulphate (AS)

Table 5-12 shows the result of the modulus of elasticity of the concrete mix with the addition of 1.10% of AS. It can be observed that the value of the modulus of elasticity had an increase of 7.10% compared to the reference mix RC-RCA. This increase in the modulus of elasticity occurred due to the formation of ettringite, which reduces the porosity of RCA, improving the (ITZ) solidity of the cement mortar. At the same time, much calcium hydroxide is consumed, which can reduce the preferential orientations of portlandite in the ITZ and accelerate the tricalcium silicate/dicalcium silicate process. These chemical reactions contribute to the improvement of the ITZ, increasing the strength of cement paste and of RCA (CHATTERJI; JEFFERY, 1963; HE; YANG; GUO; XU *et al.*, 2021; KAN; LAN; KONG; YANG, 2013; SONG; QIAO; WEN, 2015). With the addition of AS, the hardness of ITZ increases, as seen in the SEM analysis (section 5.3.5), resulting in an improvement of the modulus of elasticity.

Table 5-12 Modulus of elasticity (E_{cm}) at 28 days of concrete mixes with RCA and incorporation of aluminium sulphate (AS).

Mix	E_{cm} (MPa)		% improvement relative to RC	% improvement relative to RC-RCA
RC	39.58	0.33	—	—
RC-RCA	29.31	0.13	25.97% ▼	—
RCA-AS	31.39	1.89	20.71% ▼	7.10% ▲

5.7 Fracture energy (G_F)

The tables in the literature (ELICES; PLANAS, 1996), provide values of the specific energy of fracture (G_F) for various materials. However, determining the G_F value for concrete is a more intricate process due to its composite nature. The mechanical and fracture properties of concrete are subject to significant variation based on a range of factors such as component proportions, preparation and curing methods, temperature, and other environmental conditions. As a result, there is a lack of consensus regarding a standardized G_F value for concrete.

Distinct zones were observed during a load-displacement test on concrete, with each zone being influenced by various factors. A curve representing the test results was generated and is depicted in Figure 5-22. Initially, the curve displayed elastic behaviour from the start of the loading until it reached point A. Between points A and B, micro-

cracks present at the cement paste-aggregate interface prior to loading began to expand within the paste and around the aggregates, leading to an inelastic phase that persisted until the specimen reached its peak load, which is its ultimate loading capacity. After point B, the specimen was damaged and fractured due to the coalescence of micro-cracks, causing the curve to fall. As the curve continued to fall, the micro-cracks became unstable and led to localized cracking in a narrow area called the fracture process zone (FPZ). As concrete is a quasi-brittle material, except for high strength concrete (HSC) that exhibits brittle behaviour, the micro-cracks changed to macro-cracks as displacement increased in zone BC. The portion of the curve between points C and D can vary in length, from a few millimetres to several centimetres, depending on the ductility of the specimen, which is influenced by crack bridging and branching (HILLERBORG; MODÉER; PETERSSON, 1976; PERDIKARIS; ROMEO, 1995).

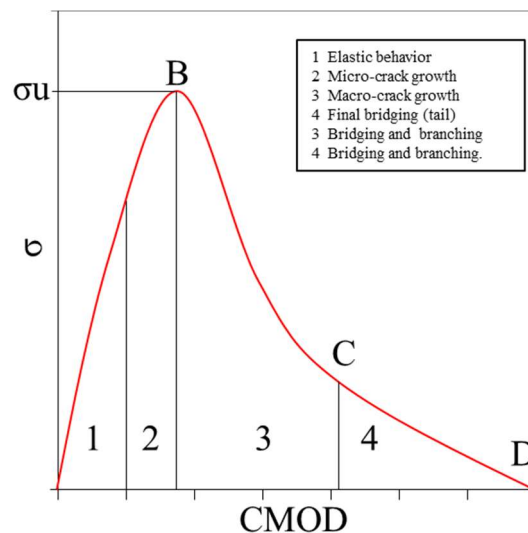


Figure 5-22 Tensile behaviour of concrete.

The fracture energy of concrete is significantly affected by the water/cement ratio, a critical factor in concrete's composition. This ratio has a close correlation with the quality of the ITZ, which is a thin layer, typically measuring 10-50 micrometres, that has lower strength than the surrounding cement paste and aggregates (KHALILPOUR; BANIASAD; DEHESTANI, 2019; MIHASHI; NOMURA; NIISEKI, 1991). A high water-to-cement ratio results in an increased number of micro-cracks in the ITZ area, making it a vital determinant of fracture energy. By reducing the water-to-cement ratio, the porosity between the paste and the ITZ decreases, leading to stronger paste and increased bond strength. This makes it more likely for cracks to pass through the aggregates rather than around them, shifting the fracture mode of concrete. Additionally,

from a fractal theory perspective, concrete with a lower water-to-binder ratio tends to have a smoother fracture surface. When a crack path crosses larger aggregates, it consumes more energy, resulting in a higher fracture energy.

Figure 5-23 illustrates the results of the relationship between splitting force and crack mouth opening displacement (CMOD) for mixes with NA. The analysis showed that the average fracture energy G_F for this type of concrete is 139 N/m. The results indicated a linear increase up to the maximum load, followed by a softening by tensile stress. To evaluate the post-peak behaviour, the analytical model proposed by Wardeh and Ghorbel (2015) was used. In this model, it is assumed that cracking starts in the middle section when the tensile stress reaches its maximum limit, f_{ctm} , in the bottom fibre. As the load is increased, a dummy crack starts to grow, and the material is softened by cohesive forces in the fracture process zone. When the crack opening reaches a critical value, σ_c (Figure 5-22), the section enters the third stage, during which the crack is no longer able to transfer stresses. In the fracture state, the cracking process is described by the smoothing relationship between the splitting force and CMOD.

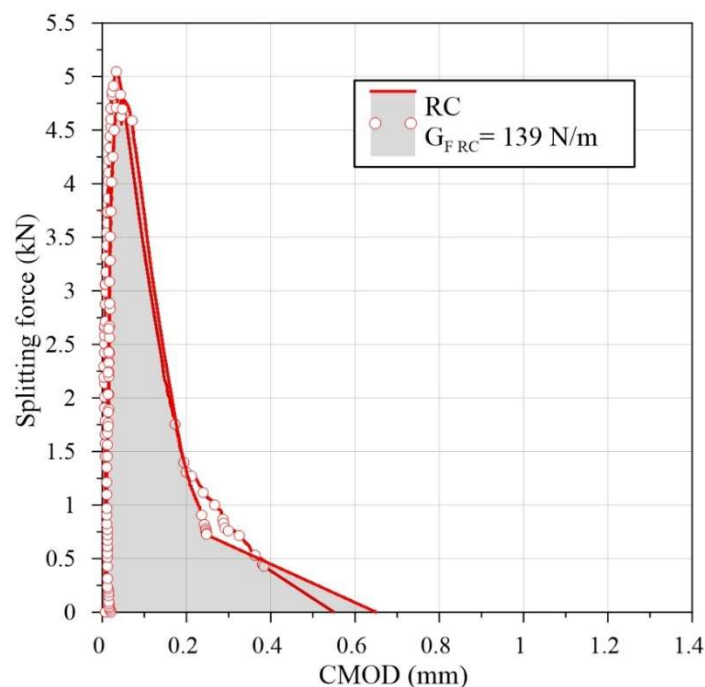


Figure 5-23 Splitting force *versus* CMOD curves for mixes RC.

When replacing the coarse NA with RCA, a decrease of 54.5% in the values of fracture energy (G_F) was observed, a trend reported by several authors, such as Casuccio *et al.* (2008), Garcia-Gonzalez *et al.* (2017), Ishiguro *et al.* (1995), Bordelon *et al.* (2009) and Sato *et al.* (2007). This decrease is attributed to the large amount of broken coarse

aggregates, with less crack branching in the cementitious matrix, present in the RCA mix. Ghorbel and Wardeh (2017) also showed a decrease in G_F of about 35%, 39% and 40%, for respectively 30%, 65% and 100% incorporation of RCA in relation to NAC, but stated that this impact is offset by the increase in the volume of the paste.

Another important factor for the propagation of cracks is the interaction between the aggregate and the cementitious matrix, and as previously explained, the ITZ between the RCA and the cementitious matrix presents a lower densification compared to the NA mixes. Moreover, the micro-cracks already present in RCA will propagate in different scales, leaving this concrete with a lower value of fracture energy (Figure 5-24). These micro-cracks and densification of the ITZ can be observed in section 5.3.2.

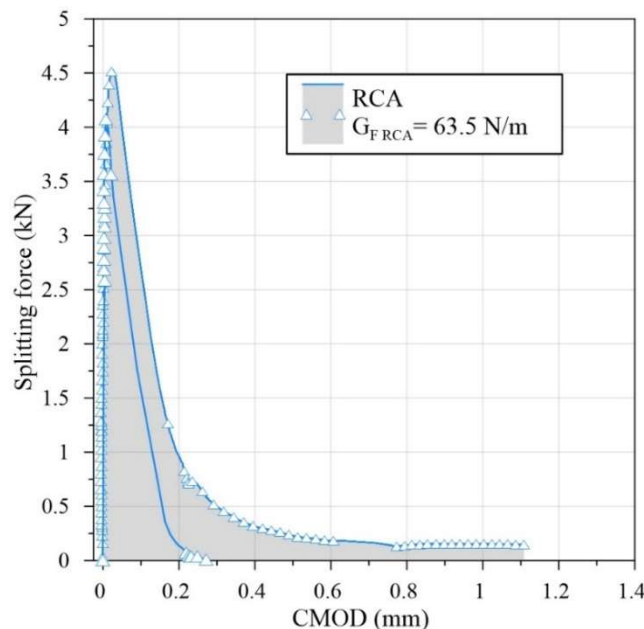


Figure 5-24 Splitting force *versus* CMOD curves for mixes RCA.

The results of the RC and RC-RCA reference mixes, along with their standard deviations and percentage reductions in relation to RC, are presented in Table 5-13.

Table 5-13 Fracture energy (G_F) for RC and RC-RCA reference mixes.

Mix	28 days		
	G_F (N/m)	σ	% improvement relative to RC
RC	139.03	9.45	
RC-RCA	63.27	3.80	54.49% ▼

5.7.1 Fracture energy (G_F) in concrete incorporating RCA treated with HCl

Figure 5-25a,b,c presents the splitting strength *versus* CMOD responses of the

mixes containing RCA treated with HCl at concentrations of 0.3 M, 1.0 M and 3.0 M, respectively. It can be observed that the mixes containing RCA treated with 1.0 M and 3.0 M exhibit smoother softening curves compared to RCA-0.3 HCl concrete. These smoother softening curves and higher peak failures result in an increase in fracture energy (G_F) compared to the RC-RCA concrete. This improvement is associated with the acid removal with HCl of weakly adhered particles and the cleaning of the surface, ensuring a better bond between the RCA and the cementitious matrix (WANG; YU; LI, 2020). Moreover, the reduction of micro-cracks in the zone near the ITZ, as observed in section 5.3.3, also contributes to this improvement.

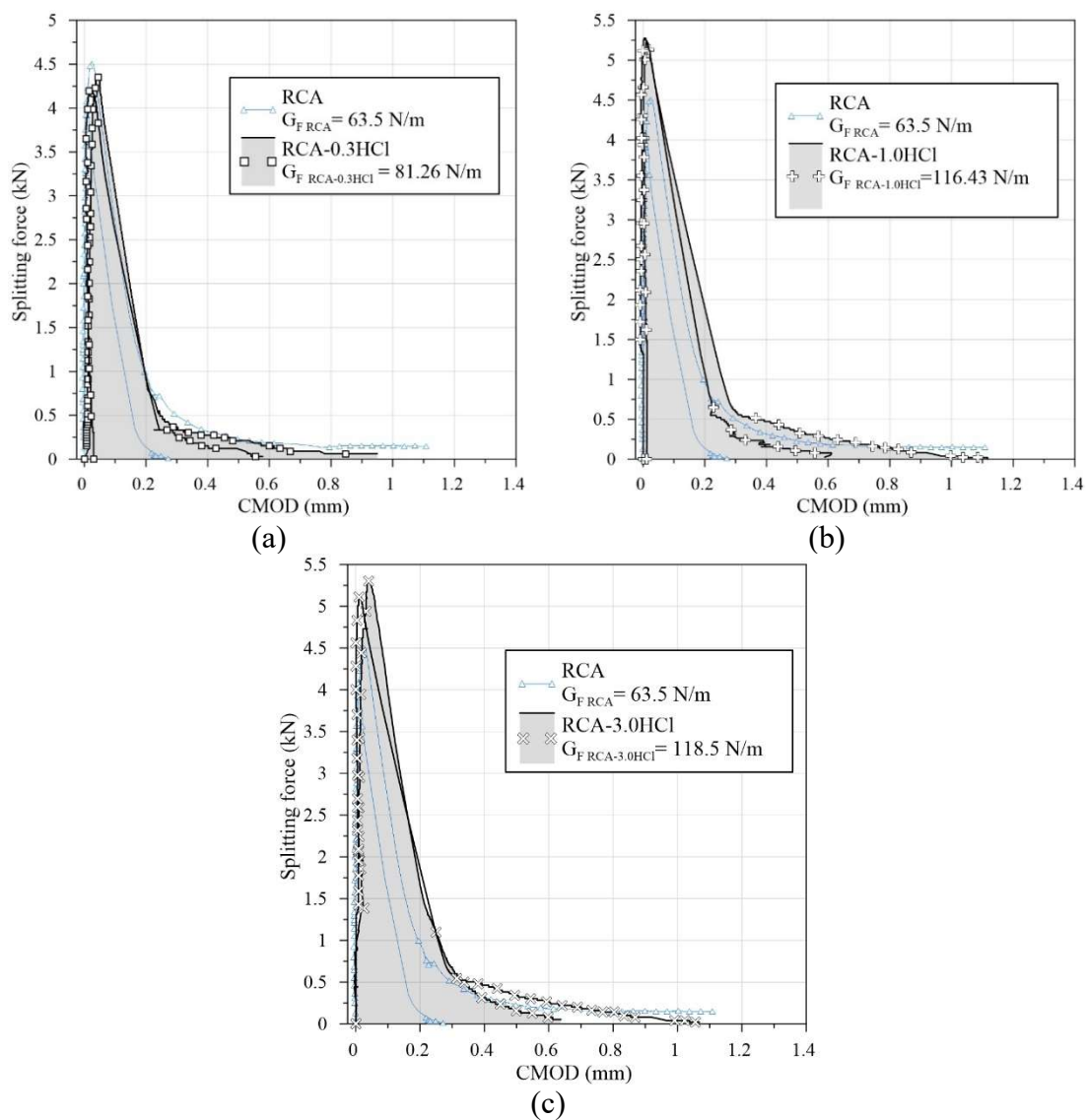


Figure 5-25 Splitting force versus CMOD curves for mixes: RCA-0.3HCl(a), RCA-1.0HCl (b), RCA-3.0HCl (c).

Authors such as Kazemian *et al.* (2019) presented a non-significant variation of 5% with incorporations of 25% and 50% of RCA treated in two stages, first with HCl and then

with calcium metasilicate, indicating that there is an improvement in the absorption of fracture energy with this type of RCA.

Table 5-14 presents the fracture energy values of all concrete mixes containing RCA treated with HCl to remove adhered mortar, as well as their standard deviation and percentage variation from the RC and RC-RCA reference mixes.

Table 5-14 Fracture energy (G_F) for the mixes with HCl treated RCA.

Mix	28 days			
	$G_F(N/m)$	σ	% improvement relative to RC	% improvement relative to RC-RCA
RC	139.03	9.45	—	—
RC-RCA	63.27	3.80	54.49% ▼	—
RCA-0.3 HCl	81.26	8.21	41.55% ▼	28.44% ▲
RCA-1.0 HCl	116.44	12.14	16.25% ▼	84.04% ▲
RCA-3.0 HCl	118.5	4.5	14.77% ▼	87.30% ▲

5.7.2 Fracture energy (G_F) in concrete incorporating RCA treated with H_2SO_4

Regarding the concrete mixes containing RCA treated with acid solutions of H_2SO_4 , an increase in fracture energy was observed for the RCA-0.3 H_2SO_4 concrete mixes, with an improvement of 45.83% relative to the RC-RCA reference concrete. However, the RCA-1.0 H_2SO_4 and RCA-3.0 H_2SO_4 mixes showed a 9.59% and 10.65% reduction in fracture energy, respectively, compared to RC-RCA. Figure 5-26a presents the splitting force *versus* CMOD response for the RCA-0.3 H_2SO_4 mixes, while Figures 5-26b and c present the splitting force *versus* CMOD response for the RCA-1.0 H_2SO_4 and RCA-3.0 H_2SO_4 mixes, respectively.

As with the HCl-treated RCA mixes, H_2SO_4 at molar concentration (M) of 0.3 had an effect of removing weakly adhered particles in RCA, along with adhered mortar, resulting in improved bond between the aggregate and the ITZ. However, for the mixes with higher concentrations of 1.0 M and 3.0 M, the effect of a continuous degradation of RCA was observed due to contamination with sulphate ions that were not removed during the RCA's washing process.

Table 5-15 presents the values obtained from the fracture energy test for each concrete mix containing RCA treated with H_2SO_4 , along with their standard deviation and the percentage variation relative to the reference mixes RC and RC-RCA.

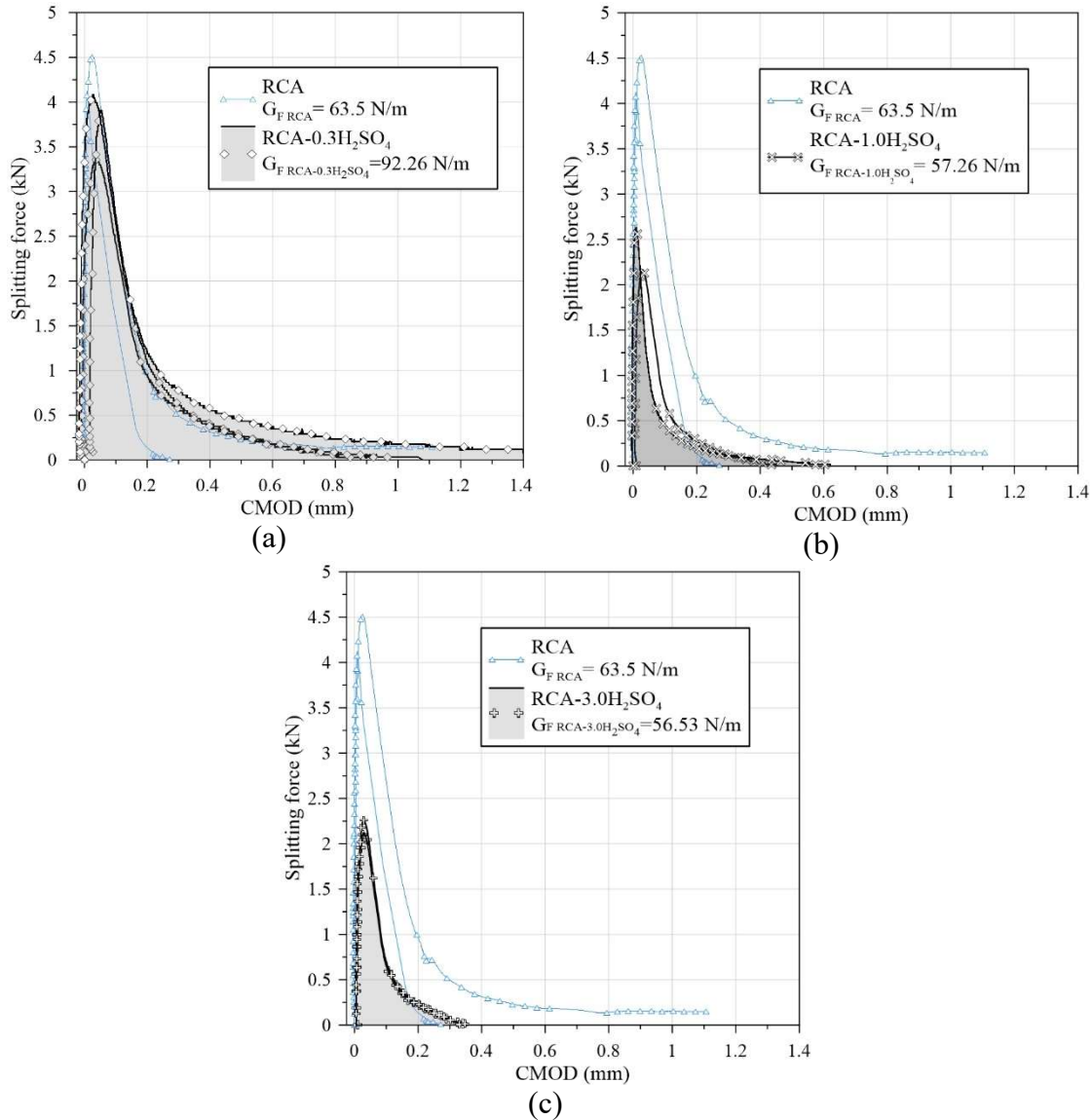


Figure 5-26 Splitting force versus CMOD curves for mixes: RCA-0.3 H₂SO₄ (a), RCA-1.0 H₂SO₄ (b), RCA-3.0 H₂SO₄ (c).

Table 5-15 Fracture energy (G_F) for the mixes with H₂SO₄ treated RCA.

Mix	28 days			
	G_F (N/m)	σ	% improvement relative to RC	% improvement relative to RC-RCA
RC	139.03	9.45	—	—
RC-RCA	63.27	3.80	54.49% ▼	—
RCA-0.3 H ₂ SO ₄	92.26	3.53	33.64% ▼	45.83% ▲
RCA-1.0 H ₂ SO ₄	57.20	4.34	58.86% ▼	9.59% ▼
RCA-3.0 H ₂ SO ₄	56.53	5.89	59.34% ▼	10.65% ▼

5.7.3 Fracture energy (G_F) in concrete incorporating aluminium sulphate (AS)

The results (Figure 5-27) indicated that concrete mixes with addition of 1.10% aluminium sulphate (AS) showed a more brittle response. The softening curve was lower,

which translated into a slight reduction in fracture energy compared to the RC-RCA reference concrete. The production of ettringite, which reduces the porosity of RCA, together with the consumption of calcium hydroxide, which reduces the orientations of portlandite in the ITZ, possibly left this zone more prone to micro-crack formations. This embrittlement has been discussed in previous works (CHATTERJI; JEFFERY, 1963; HAN; WANG; WANG; SHI, 2016; KAN; LAN; KONG; YANG, 2013; LIU; MA; TAN; GU et al., 2020). The mixes with AS had a reduction of 6.48% compared to RC-RCA.

Table 5-16 shows the values of fracture energy (G_F) for the compositions with AS incorporation. It is possible to observe the percentage of reduction in relation to the RC and RC-RCA reference mixes. The table indicates that the mixes with AS addition had an average reduction of 6.48% in fracture energy, compared to the reference mixes.

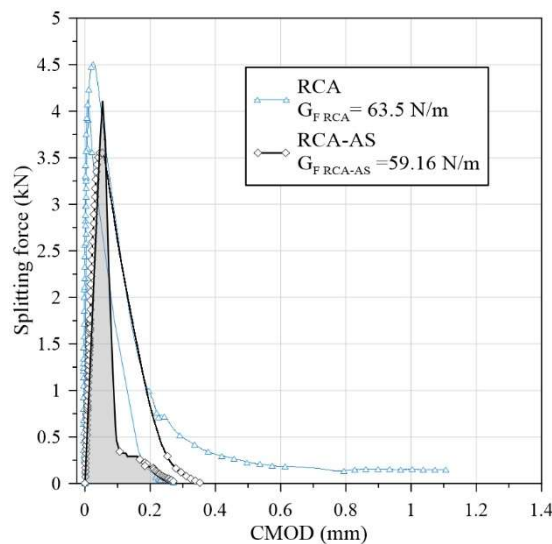


Figure 5-27 Splitting force versus CMOD curves for mixes incorporating AS.

Table 5-16 Fracture energy (G_F) for the mixes incorporating AS.

Mix	28 days			
	G_F (N/m)	σ	% improvement relative to RC	% improvement relative to RC-RCA
RC	139.03	9.45	—	—
RC-RCA	63.27	3.80	54.49% ▼	—
RCA-AS	59.17	3.01	57.44% ▼	6.48% ▼

5.7.4 The effective double K_I fracture criterion

The effective double K_I fracture criterion is derived through the use of the double G_F (Griffith) fracture model (ISHIGURO; STANZL-TSCHEGG; TSCHEGG; TRAVNICEK, 1995; KUMAR; BARAI; KUMAR; BARAI, 2011; PETERSON, 1980), which is a fracture

mechanics-based approach commonly employed to analyse the fracture behaviour of brittle materials like concrete. This model characterizes the fracture process in two stages, namely micro-crack growth and macroscopic crack coalescence. During the first stage of micro-crack growth, micro-cracks are assumed to occur at a constant stress intensity factor, K_I . The second stage, macroscopic crack coalescence, occurs when the stress intensity factor reaches a critical value, K_{Ic} , and involves the merging of micro-cracks into a larger crack (KUMAR; BARAI; KUMAR; BARAI, 2011; SHAH; SWARTZ; OUYANG, 1995).

The effective double K_I fracture criterion is obtained by equating the total energy release rate to the sum of the energies released by the tensile and shear modes of fracture. This criterion is expressed as:

$$K_I = (G_F E_{cm})^{\frac{1}{2}} \quad \text{Equation 5-5}$$

where G is the total energy release rate, K_I is the stress intensity factor for the tensile mode of fracture, and E_{cm} represents the effective modulus of elasticity of concrete. By utilizing this criterion, engineers can design concrete structures that are more resilient to cracking and failure, and they can also evaluate the safety and durability of existing concrete structures.

In Table 5-17, it is possible to observe the average values of the stress intensity factor (K_I) for all mixes, along with the variation in relation to the RC and RC-RCA reference mixes. It is concluded that the treatment with HCl is more effective in cracking resistance than the treatment with H_2SO_4 , due to its effectiveness in higher concentrations. Finally, the incorporation of AS did not show significant improvements in comparison with the RC-RCA reference concrete.

Table 5-17 Stress intensity factor (K_I) results.

Mix	K_I (Mpa.m ^{1/2})	% improvement relative to RC	% improvement relative to RC-RCA
RC	2.35	—	—
RC-RCA	1.36	41.91% ▼	—
RCA-0.3 HCl	1.59	32.06% ▼	16.95% ▲
RCA-1.0 HCl	1.93	17.69% ▼	41.69% ▲
RCA-3.0 HCl	1.98	15.67% ▼	45.17% ▲
RCA-0.3 H ₂ SO ₄	1.64	29.94% ▼	20.60% ▲
RCA-1.0 H ₂ SO ₄	1.23	47.63% ▼	9.86% ▼
RCA-3.0 H ₂ SO ₄	1.20	48.71% ▼	11.72% ▼
RCA-AS	1.36	41.90% ▼	0.01% ▲

5.8 Combining mechanical properties and comparing standards

In this item, related properties are presented, with the objective of obtaining correlations that can be used to determine one property as a function of another. Generally, the main property considered is the compressive strength (f_{cm}). In Figure 5-28a, the correlation between the compressive strength of concrete mixes containing HCl and the tensile strength of these same mixes is shown. In Figure 5-28b, the correlations between the compressive strength in concrete with RCA treated with H_2SO_4 and their tensile strength are shown. These correlations generally follow the equation $f_{ctm} = a.f_{cm}^b$, as described in ACI318-08 (2007), NBR 6118 (2014) and Eurocode 2 (2007). From the correlations proposed by these standards, a correlation with a power function was established, resulting in R^2 of 0.94 and 0.62 for the concrete mixes with RCA-HCl and RC- H_2SO_4 , respectively. It is observed that the power factor of the compressive strength (b) of the equation $f_{ctm} = a.f_{cm}^b$ differs significantly from the value proposed by the standards NBR 6118 (2014) e Eurocode 2 (EN, 2007), which is 2/3. Therefore, the fixed value of 2/3 for b was adopted, resulting in Equations 5-6 for the mixes with RCA treated with HCl and 5-7 for the mixes with RCA treated with H_2SO_4 .

$$f_{ctm} = 1.22 f_{cm}^{\frac{2}{3}} \quad \text{Equation 5-6}$$

$$f_{ctm} = 1.11 f_{cm}^{\frac{2}{3}} \quad \text{Equation 5-7}$$

Figure 5-28c also shows the results of the relationship between compressive strength and tensile strength, together with the predictions of the aforementioned standards. Confidence intervals were determined, and all mixes were found to be within this range.

Similarly, there is a relationship between the modulus of elasticity and compressive strength, and these two properties have been correlated through empirically derived expressions. In Figure 5-28a and b, the normalized results of the relationship between these two properties are observed, with coefficients of determination of 0.96 for both concrete mixes (RCA-HCl and RCA- H_2SO_4). This linear relationship indicates that the properties of the constituent materials, especially the aggregates, have improved, particularly in the case of concrete with RCA treated with HCl, as it possesses a stronger internal structure (ITZ).

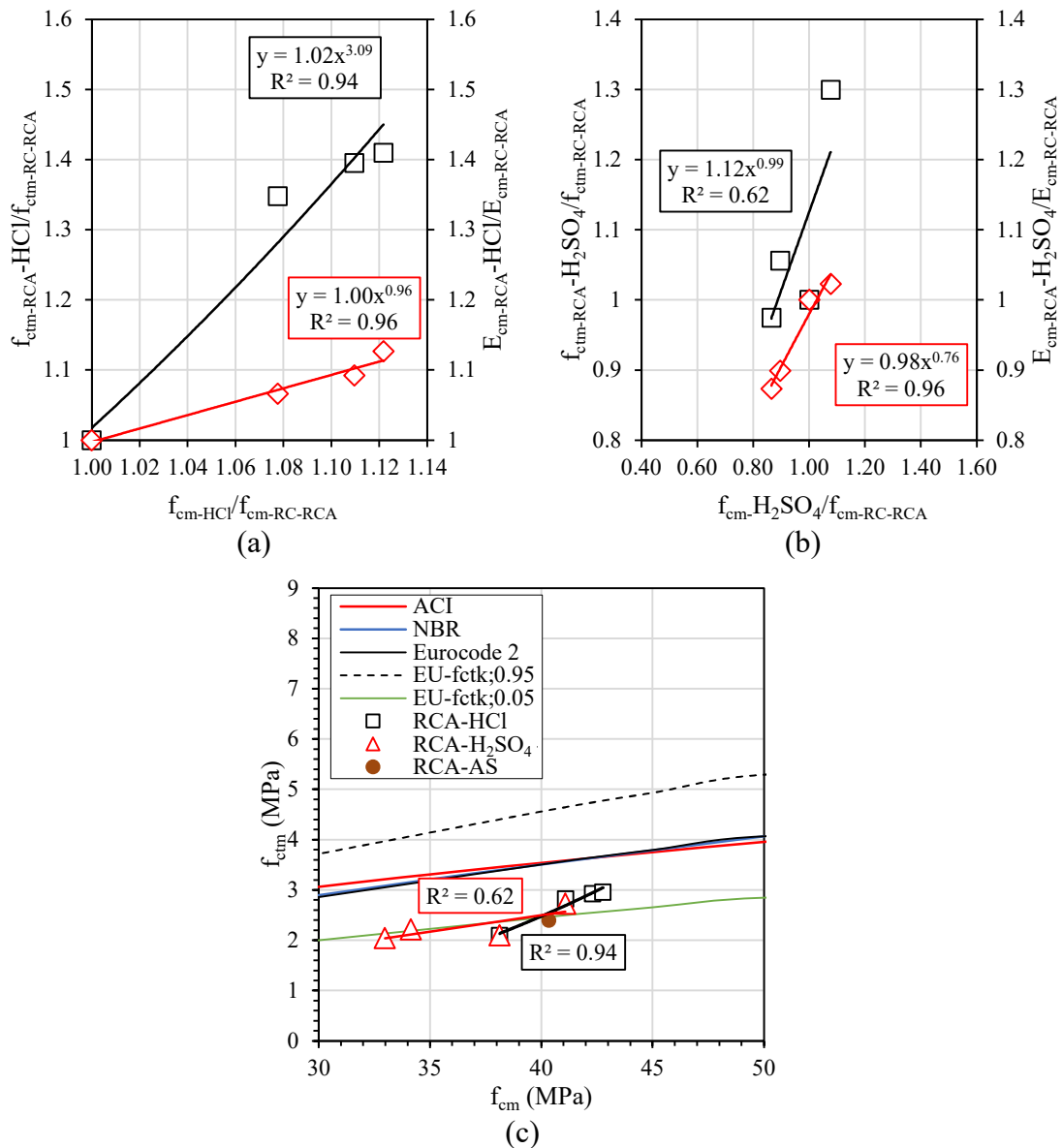


Figure 5-28 Normalized relations between compressive strength (f_{cm}), tensile strength (f_{ctm}) and modulus of elasticity (E_{cm}) of concrete mixes with RCA treated with HCl (a); H₂SO₄ (b); and comparison of concrete mixes with RCA treated with HCl, H₂SO₄ and AS with ACI, NBR and Eurocode 2 (ABNT, 2014; ACI, 2008; EN, 2007)(c).

In Figure 5-28b, the relationship between normalized compressive strength and fracture energy is shown for each concrete mix with RCA treated with HCl (Figure 5-29a) and concrete with RCA treated with H₂SO₄ (Figure 5-29b). From Figures 5-28a and b, it can be concluded that, as compressive strength increases, the fracture energy proportionally increases, indicating a greater capacity to resist fracture. From Figure 5-29a and b, it can also be concluded that as the stress intensity factor (K_I) increases, the energy required to propagate the crack also increases. This indicates that the mixes with RCA treated with HCl and H₂SO₄ require higher fracture energy for crack propagation.

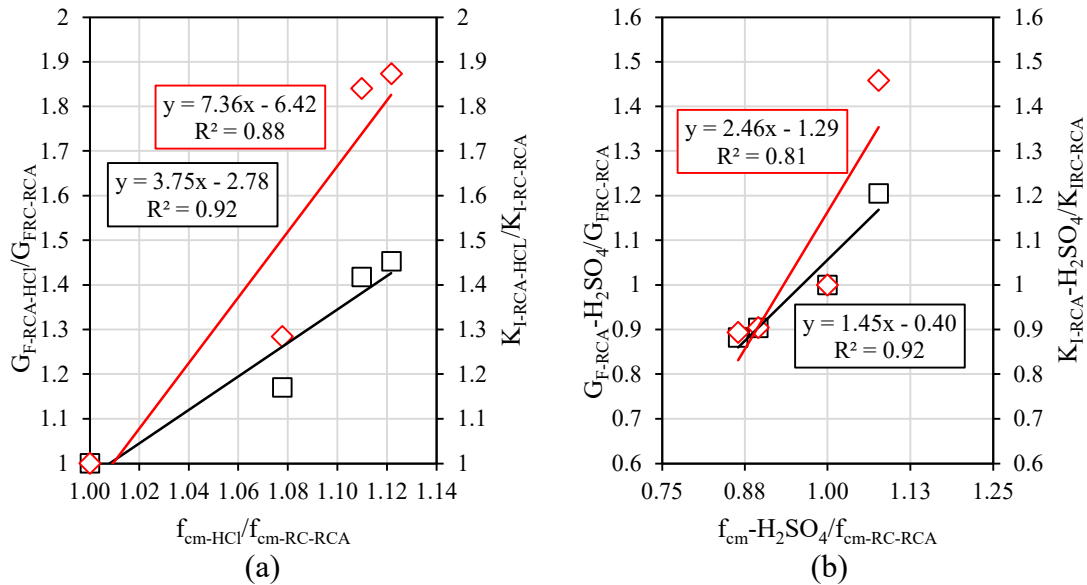


Figure 5-29 Normalised relationships between compressive strength (f_{cm}), fracture energy (f_{cm}) and intensity factor (K_I) of concrete mixes with RCA treated with HCl (a); H₂SO₄ (b).

5.9 Water absorption by immersion

One of the factors that affects the durability of concrete is its permeability to fluids. The water permeability of concrete is generally evaluated by two tests: water absorption by immersion and capillarity. The immersion water absorption test evaluates the water permeability of concrete at atmospheric pressure, measuring the open porosity of the concrete structure. This property can be influenced essentially by three factors: the addition of more mixing water than is necessary for the hydration of the cement, the air which arises when mixing the components of concrete and the existing pores in the aggregates (TEGGUER, 2012). The results of concrete mixing are presented below.

5.9.1 Water absorption by immersion in concrete incorporating RCA treated with HCl

The water absorption test by immersion was performed according to the recommendations of NP EN 1097-6 (2013). This test, besides indicating the voids content of concrete, is also useful to evaluate the open porosity, which is accessible to water. The results of water absorption by immersion obtained for the different types of concrete produced with RCA treated with HCl, as well as their variation in relation to RC and RC-RCA, can be observed in Figure 5-30a and b. In Figure 5-30a, the water absorption values (%) are presented as a function of the molarity of the RCA treatment. A reduction in the water absorption value was observed in relation to the concrete mixes with untreated

RCA. In Figure 5-30b, a linear trend in the reduction of water absorption can be observed with a correlation $R^2 = 0.77$. This reduction in water absorption was expected as the recycled concrete (RCA) aggregates had an improvement after pre-soaking in HCl. As shown in Section 5.3.3, the ITZ was reduced and the amount of adhered mortar in the RCA was also reduced, resulting in a reduction in porosity and hence a reduction in water absorption. Purushothaman *et al.* (2015) obtained reductions in water absorption by weight of 12.02% compared to concrete with untreated RCA, attributing this reduction to the fact that there was less amount of adhered mortar in the RCA.

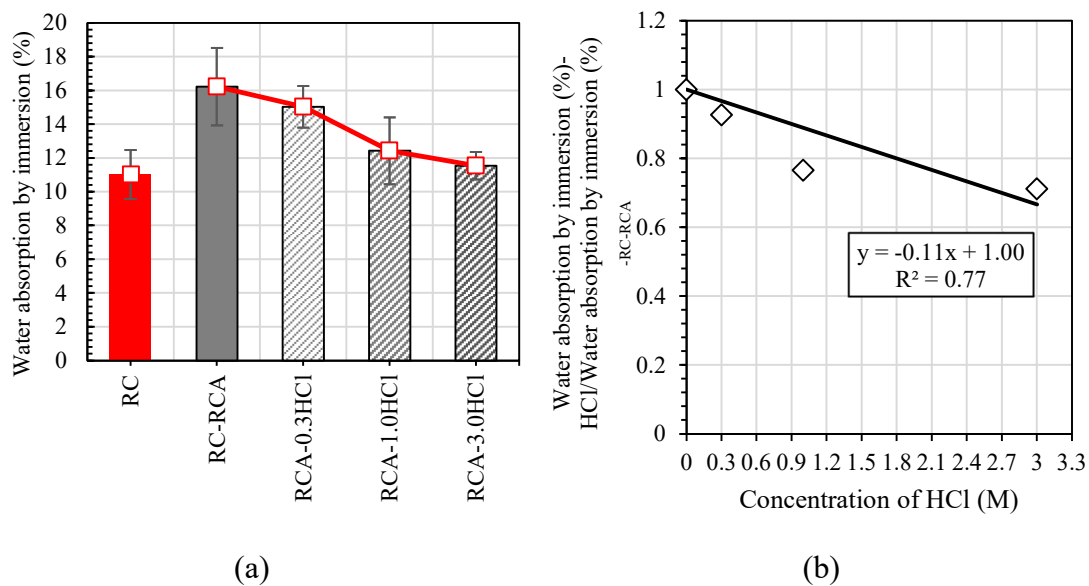


Figure 5-30 Water absorption by immersion (%) versus mixes of concrete with RCA treated with HCl (a); normalization of water absorption (%) versus HCl concentration (M) (b).

In Table 5-18, the values of water absorption by immersion are presented, as well as the percentage of improvement compared to RC and RC-RCA concrete mixes, along with the respective standard deviations.

Table 5-18 Water absorption at 28 days in concrete mixes with RCA treated with HCl.

Mix	28 days			
	Water absorption by immersion (%)	σ	% improvement relative to the water absorption by immersion of RC	immersion of RC-RCA
RC	11.03	1.45	—	—
RC-RCA	16.23	2.29	47.17%▲	—
RCA-0.3 HCl	15.04	1.23	36.34%▲	7.35%▼
RCA-1.0 HCl	12.43	1.98	12.72%▲	23.41%▼
RCA-3.0 HCl	11.55	0.81	4.69%▲	28.86%▼

From Table 5-18, a reduction of 7.35%, 23.41% and 28.86% compared to the RC-RCA reference concrete can be observed for the compositions with RCA treated with 0.3 M, 1.0 M and 3.0 M, respectively. This reduction in water absorption is closely related to

the oven dry density of RCA, as shown in Figure 5-31, where it is possible to observe the linear relationship existing between these two properties, with an R^2 of 0.87.

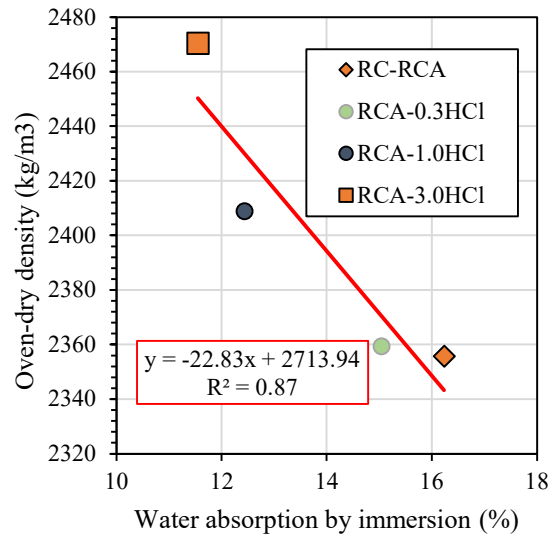


Figure 5-31 Water absorption versus oven-dry density (kg/m^3)

5.9.2 Water absorption by immersion in concrete incorporating RCA treated with H_2SO_4

Figure 5-32a shows the water absorption for mixes containing RCA treated with H_2SO_4 . It is observed that there is an improvement relative to the reference concrete RC-RCA for mixes with RCA treated at a molarity (M) of 0.3 M, with an increase of 2.84%. However, mixes treated at molarities of 1.0 M and 3.0 M showed higher water absorption than the RC-RCA reference concrete, with values of 5.72% and 8.74%, respectively. As mentioned in section 5.3.4, the presence of micro-cracks in the ITZ, caused by the second degradation, increases the permeability of concrete (OLLIVIER; MASO; BOURDETTE, 1995). Moreover, the size of the aggregates also influences the water absorption, with larger aggregates increasing permeability due to the larger area in the ITZ (VALENTA, 1961). Purushothaman *et al.* (2015) found that water absorption was reduced by 28.10% relative to the reference concrete when RCA was treated with a 0.1 M solution, demonstrating the same trend of improvement when the RCA was treated with low-concentration solutions.

It is possible to correlate the increase in water absorption as a function of the acid molarity of H_2SO_4 , evidencing a linear correlation with a coefficient of determination of $R^2 = 0.76$ with increasing molarity (Figure 5-32b). The values of water absorption by immersion, their respective standard deviations and the percentages of reduction in

relation to the RC and RC-RCA reference mixes are presented in Table 5-19.

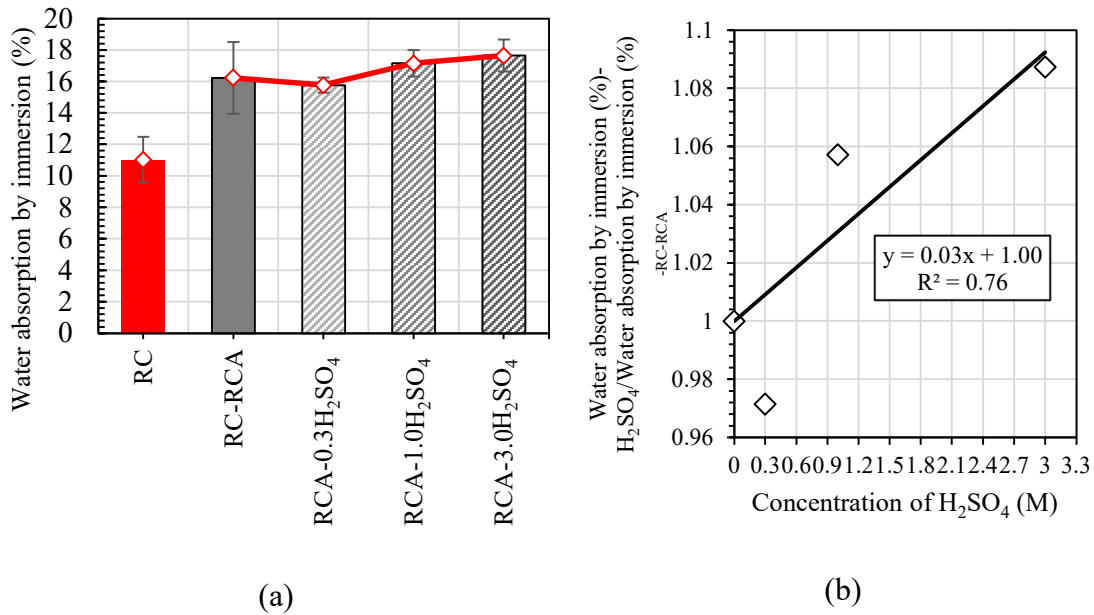


Figure 5-32 Water absorption by immersion (%) versus concrete mixes with RCA treated with H₂SO₄ (a); normalization of water absorption (%) versus H₂SO₄ concentration (M) (b).

Table 5-19 Water absorption at 28 days in concrete mixes with RCA treated with H₂SO₄.

Mix	28 days			
	Water absorption by immersion (%)	σ	% improvement relative to f_{cm} of	
			RC	RC-RCA
RC	11.03	1.45	—	—
RC-RCA	16.23	2.29	47.17% ▲	—
RCA-0.3H ₂ SO ₄	15.77	0.47	42.98% ▲	2.84% ▼
RCA-1.0H ₂ SO ₄	17.16	0.85	55.59% ▲	5.72% ▲
RCA-3.0H ₂ SO ₄	17.65	1.02	60.02% ▲	8.74% ▲

As in the HCl-treated concrete mixes, a correlation was obtained between the oven-dry density and the water absorption in the mixes containing RCA. As expected, the oven-dry density of RCA showed lower values as the water absorption increased. This correlation was evaluated with a coefficient of determination of $R^2 = 0.74$, as shown in Figure 5-33.

5.9.3 Water absorption by immersion in concrete incorporating aluminium sulphate (AS)

It was observed that the addition of aluminium sulphate in mixes containing RCA resulted in a 19.38% improvement in water absorption compared to the RC-RCA reference mixes. This improvement is attributed to the fact that aluminium sulphate accelerates and enhances the formation of ettringite, which fills pores and compensates

for micro-cracks caused by volume shrinkage during cement hydration. As a result, the waterproofing of concrete is improved (HAN; WANG; WANG; SHI, 2016; HE; WANG; WANG, 2019; LIU; MA; TAN; GU et al., 2020). All 28-day water absorption values are shown in Table 5-20.

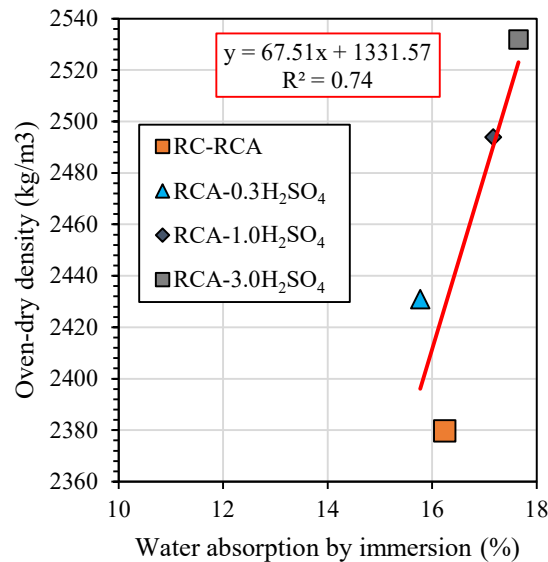


Figure 5-33 Water absorption versus oven-dry density (kg/m³).

In section 5.3.5 of the research, scanning electron microscopy (SEM) analysis revealed that aluminium sulphate densified the ITZ between RCA and cementitious matrix. In addition, the formation of tricalcium silicate/dicalcium silicate was observed (SONG; QIAO; WEN, 2015).

Table 5-20 Water absorption at 28 days in concrete mixes with RCA treated with AS

Mix	28 days			
	Water absorption by immersion (%)	σ	% improvement relative to f_{cm} of	
			RC	RC-RCA
RC	11.03	1.45	—	—
RC-RCA	16.23	2.29	47.17%▲	—
RCA-AS	13.09	0.52	18.64%▲	19.38%▼

5.10 Water absorption by capillarity

The absorption by capillarity is a phenomenon that occurs when a fluid penetrates into concrete due to a pressure difference, driven by capillary forces present in the pores of the material. The capillarity absorption test intends to measure the capillary absorption of concrete, resulting from the pressure differential between the free surface of the liquid in contact with concrete and the free surface of the liquid in the capillaries of the material itself. This test is important to evaluate concrete permeability, which can affect its strength

and durability. During the test, it is essential to consider the distribution and connectivity of the pores in concrete, in order to obtain accurate results about the permeability of the material (KURDA; DE BRITO; SILVESTRE, 2019; NEVILLE; BROOKS, 1987).

The pores present in concrete can be classified as continuous and non-continuous. Continuous pores are those that extend through the material, while non-continuous pores are interconnected only at a microscopic level. The presence of continuous pores in concrete can increase its permeability, allowing water and other fluids to more easily penetrate the material, while non-continuous pores can have a minor effect on concrete permeability. The results of water absorption by capillarity of all mixes under analysis are presented below.

5.10.1 Water absorption by capillarity in concrete incorporating RCA treated with HCl

The results indicate that water absorption is higher in the untreated RCA due to the porosity and amount of mortar present in RCA. However, in mixes containing recycled aggregate treated with HCl, water absorption tends to decrease as the acid molarity increases, as can be observed in Figure 5-34a. As presented in Table 5-21, the reductions are 2.68%, 7.02% and 9.36% for molarities of 0.3 M, 1.0 M and 3.0 M, respectively. This occurs because the pre-treatment with HCl promotes a densification in the microstructure of RCA, reducing the amount of mortar and, consequently, of pores, besides cleaning the aggregate surface, allowing the ITZ densification phenomenon and eliminating micro-cracks. This fact was also observed by Xuan *et al.* (2017), who found a densification of the microstructure after pre-treatment of RCA with pre-carbonation.

Another important factor influencing water absorption is the water/cement ratio (w/c), which is higher in mixes with RCA compared to the reference concrete with NA (RC), but lower in mixes with treated RCA compared to the reference concrete mix (RC-RCA), which results in a reduction of pores in the cementitious matrix.

Based on the reduction in water absorption as the molarity of the treatment in the RCA is increased, it is possible to establish a correlation between these two parameters. As presented in Figure 5-34b, there is a coefficient of determination of $R^2 = 0.82$ with a negative linear regression, indicating that this process has a linear trend.

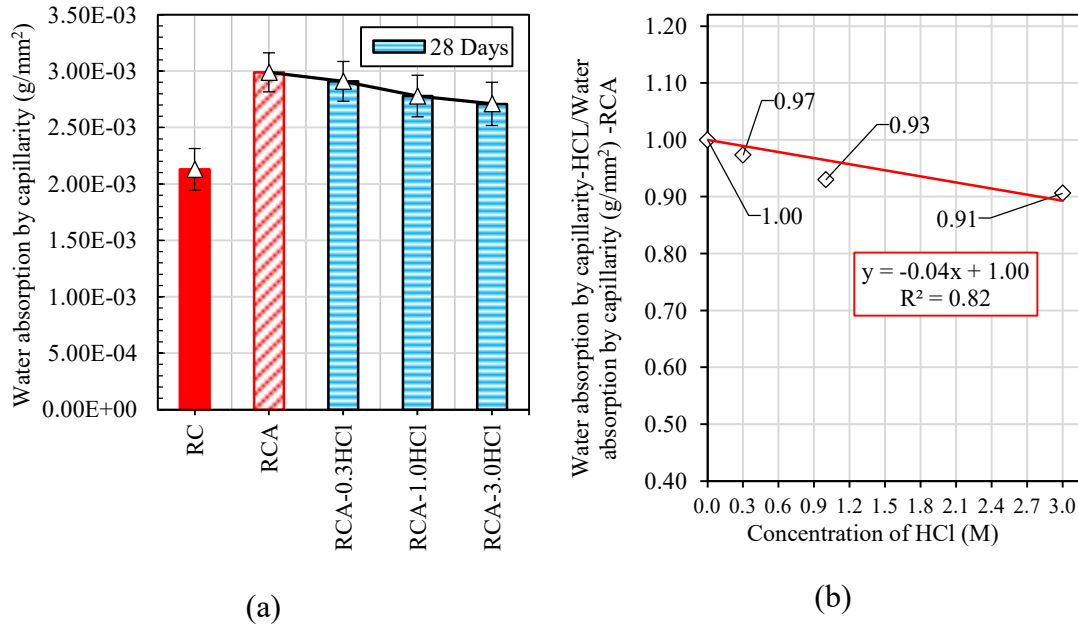


Figure 5-34 Water absorption by capillarity of concrete mixes with RCA treated with RCA (a); correlation between HCl concentration (M) versus water absorption by capillarity (g/mm²).

Table 5-21 presents the results of water absorption by capillarity of the mixes with HCl treated RCA as well as their standard deviations and percentages of reduction with respect to RC and RC-RCA.

Table 5-21 Results of water absorption by capillarity for the mixes with RCA treated with HCl

Mix	28 days			
	Water absorption by capillarity (g/mm ²)	σ	% improvement relative to RC	% improvement relative to RC-RCA
RC	2.13E-03	1.85E-04	—	—
RCA	2.99E-03	1.74E-04	40.38%▲	—
RCA-0.3 HCl	2.91E-03	1.76E-04	36.62%▲	2.68%▼
RCA-1.0 HCl	2.78E-03	1.84E-04	30.52%▲	7.02%▼
RCA-3.0 HCl	2.71E-03	1.91E-04	27.23%▲	9.36%▼

The evolution of water absorption by capillarity over time can be observed in Figure 5-35. It is noteworthy that the water absorption occurs more intensely in the first hours after concrete contact with the water surface for all mixes evaluated. This behaviour is attributed to the initial pressure difference existing (SIDDIQUE; CACHIM, 2018).

5.10.2 Water absorption by capillarity in concrete incorporating RCA treated with H₂SO₄

The results of the experiments performed on concrete mixes containing RCA treated with H₂SO₄ are presented in Figure 5-36a. It can be seen that the RC-0.3 H₂SO₄ mix presented a 3.51% reduction in water absorption compared to the RC-RCA reference concrete.

However, the mixes containing RCA treated with H₂SO₄ at high molarities (1.0 M, 3.0 M) showed a less favourable behaviour than the RC-RCA reference concrete. As mentioned earlier, there was a second degradation that reduced the densification of the ITZ and increased micro-cracks, facilitating the formation of pores conducive to greater water absorption.

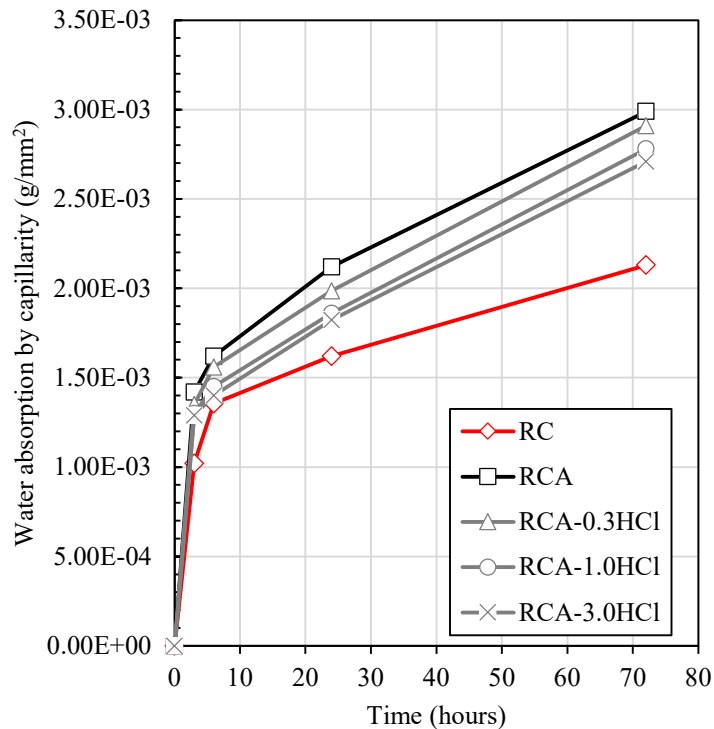


Figure 5-35 Evolution of water absorption by capillarity over time in concrete mixes with RCA treated with HCl.

As the acid concentration (M) increased, a relationship with water absorption could be established. Figure 5-36b shows a coefficient of determination $R^2 = 0.61$, which is expected since the second degradation depends on the amount of sulphate ions present in the RCA that remain after washing the treated RCA. This phenomenon was observed in the scanning electron microscopy (SEM) analysis described in section 5.3.4, where a greater amount of pores was found and the ITZ was compromised, increasing the conditions for water absorption.

In Table 5-22, the results of water absorption by capillarity are presented, as well as its evolution over time (Figure 5-37). Similarly, to the mixes with HCl, a higher rate of water absorption was observed at early ages. This phenomenon was already explained.

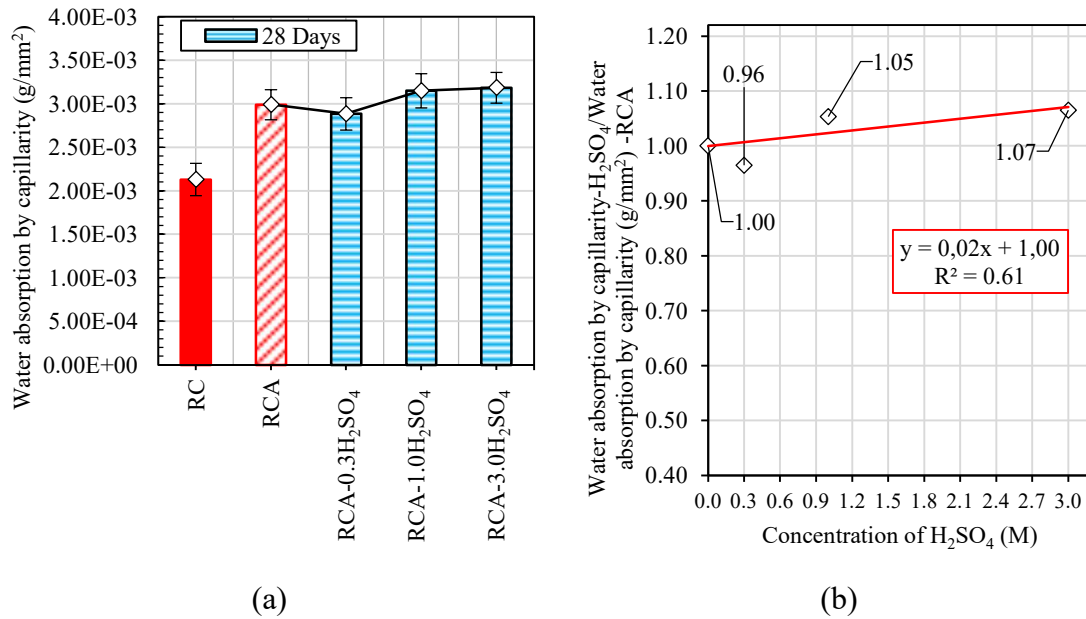


Figure 5-36 Water absorption by capillarity of concrete mixes with RCA treated with RCA (a); correlation between H₂SO₄ concentration (M) versus water absorption by capillarity (g/mm²).

Table 5-22 Results of water absorption by capillarity for the mixes with RCA treated with H₂SO₄.

Mix	28 days			
	Water absorption by capillarity (g/mm ²)	σ	% improvement relative to RC	% improvement relative to RC-RCA
RC	2.13E-03	1.85E-04	—	—
RC-RCA	2.99E-03	1.74E-04	40.38%▲	—
RCA-0.3 H ₂ SO ₄	2.89E-03	1.86E-04	35.45%▲	3.51%▼
RCA-1.0 H ₂ SO ₄	3.15E-03	1.96E-04	47.89%▲	5.35%▲
RCA-3.0 H ₂ SO ₄	3.19E-03	1.76E-04	49.53%▲	6.52%▲

5.10.3 Water absorption by capillarity in concrete incorporating AS

When aluminium sulphate is added to the cement matrix of the concrete, the resulting chemical reactions help to improve the microstructure of the material, reducing micro-cracks. The results of water absorption by capillarity are presented in Table 5-23, in which it is possible to observe a reduction of 17.73% in water absorption by capillarity in relation to the RC-RCA reference concrete. It is important to note that the mixes with addition of aluminium sulphate showed an initial high absorption; however, over time, this absorption was reduced due to the accelerating effect caused by aluminium sulphate, which increases the production of the C₃S compound.

The evolution of water absorption by capillarity over time can be seen in Figure 5.38.

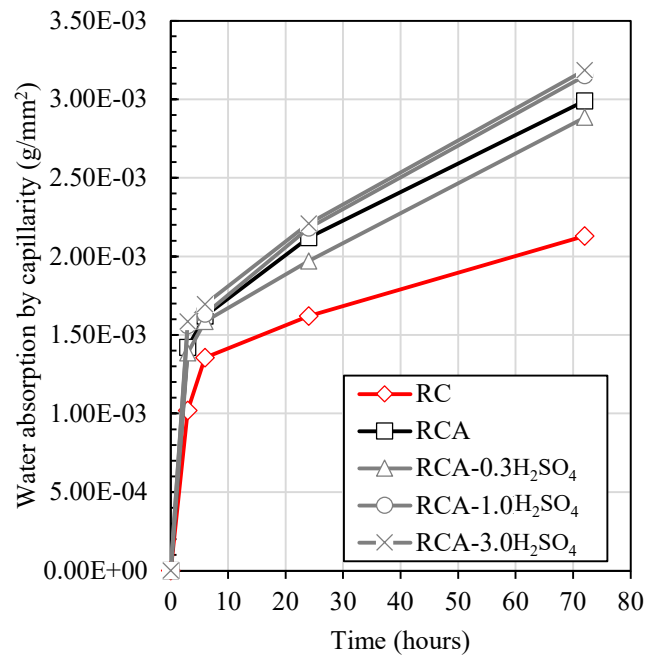


Figure 5-37 Evolution of water absorption by capillarity over time in concrete mixes with RCA treated with H₂SO₄.

Table 5-23 Water absorption by capillarity for the mixes with RCA incorporating AS

Mix	28 days			
	Water absorption by capillarity (g/mm ²)	σ	% improvement relative to RC	% improvement relative to RC-RCA
RC	2.13E-03	1.85E-04	—	—
RCA	2.99E-03	1.74E-04	40.38%▲	—
RCA-AS	2.46E-03	1.86E-04	15.49%▲	17.73%▼

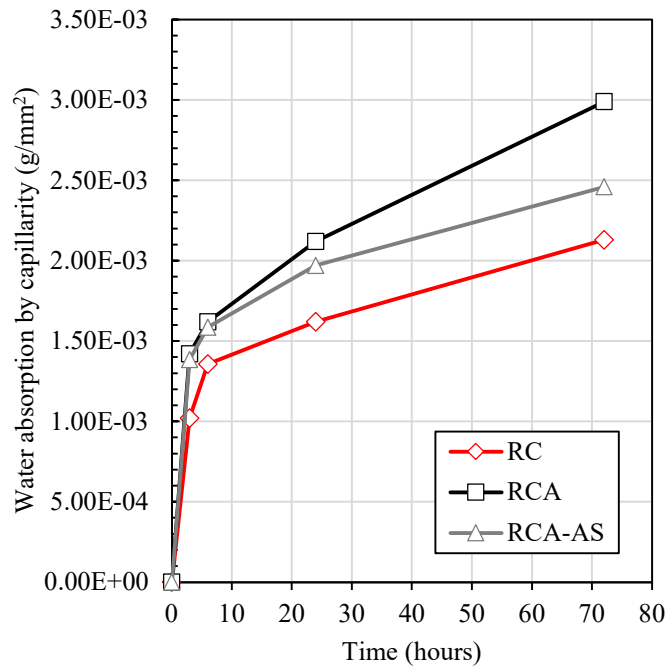


Figure 5-38 Evolution of water absorption by capillarity over time in concrete mixes with RCA incorporating AS.

5.11 Carbonation depth

Carbonation is one of the most prevalent durability problems of concrete and is referred to as the chemical reaction of hydrated and unhydrated cement products with carbon dioxide. This reaction can decrease the alkalinity of concrete, which can further cause corrosion of steel bars. Several methods have been suggested to predict the carbonation depth in natural aggregate concrete (NAC) based on previous research (HILLS; GORDON; FLORIN; FENNELL, 2015; KARI; PUTTONEN; SKANTZ, 2014; SILVA; DE BRITO; DHIR, 2014). One of the main differences between RAC and NAC is the addition of recycled aggregates (RA) during concrete mixing. However, a thorough review of existing research reveals significant inconsistencies in conclusions, as well as limited analysis and comparisons of available data (THOMAS; SETIÉN; POLANCO; ALAEJOS et al., 2013). While some studies suggest that the addition of RCA to concrete has a negative impact on carbonation resistance (MUDULI; MUKHARJEE, 2020; OTSUKI; MIYAZATO; YODSUDJAI, 2003), others claim that the use of high quality RCA does not affect the carbonation resistance of concrete (MATIAS; DE BRITO; ROSA; PEDRO, 2014). The contradictory findings can be attributed to different exposure conditions of the concrete specimens, the different ingredients of the mix and respective dosage, the composition and inherent variability of the RCA and various specific RAC production processes (DE BRITO; SAIKIA, 2012). The results of carbonation in the concrete mixes studied in this research will be presented below.

5.11.1 Carbonation depth in concrete incorporating RCA treated with HCl

In the present thesis, the resistance to carbonation was evaluated by means of accelerated tests, in which concrete specimens subjected to high concentrations of CO₂ (5%) were used. The results obtained were presented in Table 5-24, which includes information on the periods of 7, 28 and 91 days, as well as the percentage of variation in relation to RC and RC-RCA reference concrete, and the respective standard deviation. As expected, the concrete mixes treated with HCl presented a reduction in CO₂ penetration when compared to RC-RCA. This behaviour was predictable in view of the results obtained in the water absorption test.

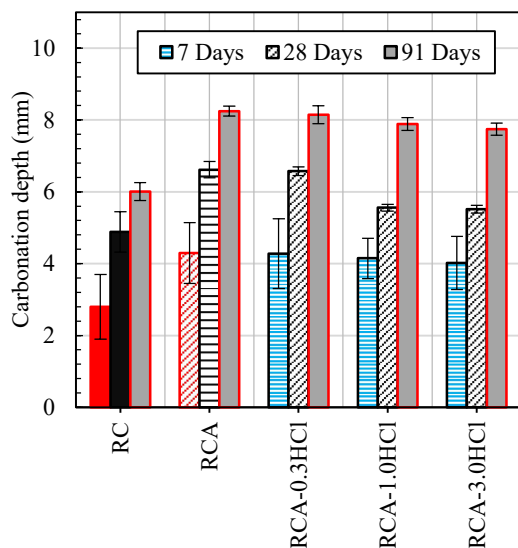
Kim *et al.* (2018) obtained similar results in concrete mixes with HCl-treated RCA, in which concrete with RCA treated with HCl in molarities of 0.1 M showed

improvements in carbonation resistance compared to the reference concrete. This improvement phenomenon is associated with the same mechanisms described in the water absorption test.

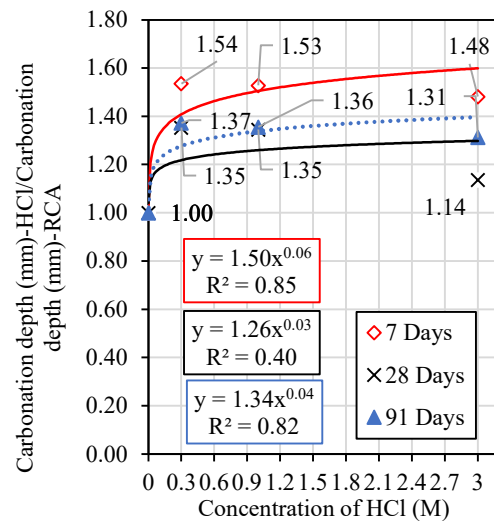
Figure 5-39a illustrates the carbonation depth for the mixes containing RCA treated with HCl at the 7-, 28- and 91-day periods. It is clearly observed that there is an improvement in the carbonation resistance as the acid concentration increases. This evolution can be correlated (Figure 5-39b), presenting determination coefficients of $R^2 = 0.85$, $R^2 = 0.40$ and $R^2 = 0.82$ for the periods of 7, 28 and 91 days, respectively.

Table 5-24 Carbonation depth (mm) for mixes with RCA treated with HCl.

Time	Mix	Carbonation depth (mm)	σ	% improvement relative to RC	% improvement relative to RC-RCA
7 days	RC	2.80	0.90	—	—
	RCA	4.30	0.85	53.57%▲	—
	RCA-0.3HCl	4.28	0.97	52.86%▲	0.47%▼
	RCA-1.0HCl	4.15	0.56	48.21%▲	3.49%▼
	RCA-3.0HCl	4.02	0.74	43.57%▲	6.51%▼
28 days	RC	4.89	0.56	—	—
	RCA	6.62	0.23	35.38%▲	—
	RCA-0.3HCl	6.58	0.12	34.56%▲	0.60%▼
	RCA-1.0HCl	5.56	0.09	13.70%▲	16.01%▼
	RCA-3.0HCl	5.52	0.11	12.88%▲	16.62%▼
91 days	RC	6.01	0.25	—	—
	RCA	8.25	0.14	37.27%▲	—
	RCA-0.3HCl	8.15	0.25	35.61%▲	1.21%▼
	RCA-1.0HCl	7.89	0.18	31.28%▲	4.36%▼
	RCA-3.0HCl	7.75	0.17	28.95%▲	6.06%▼



(a)



(b)

Figure 5-39 Depth of carbonation (mm) of concrete mixes with RCA treated with HCl (a); HCl concentration *versus* carbonation depth normalisation (b).

Finally, the analysis of the evolution of carbonation depth over time in the studied compositions with HCl was carried out, as shown in Figure 5-40. It can be observed that there was a greater penetration of CO₂ at early ages.

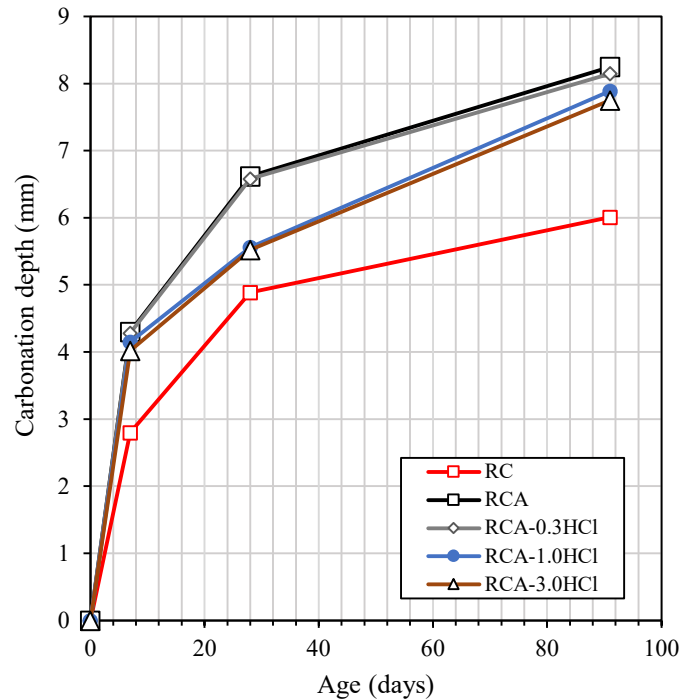


Figure 5-40 Evolution of carbonation depth with time in RCA treated with HCl.

5.11.2 Carbonation depth in concrete incorporating RCA treated with H₂SO₄

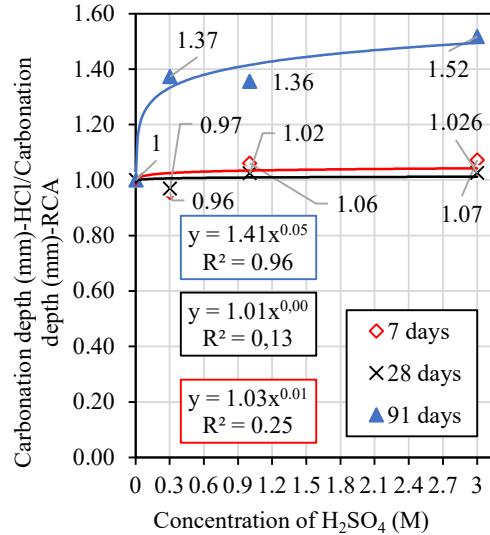
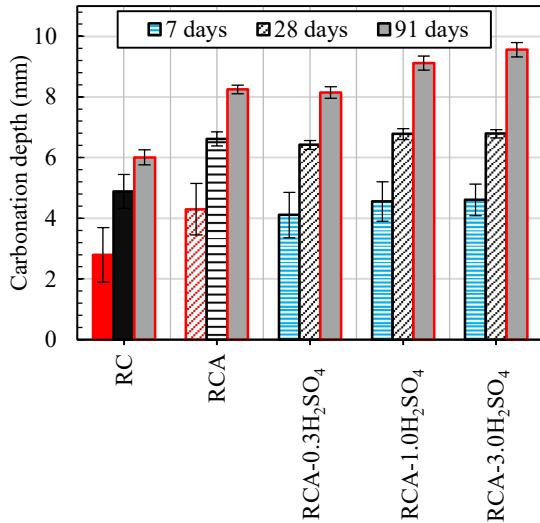
In Table 5-25, the results of carbonation depth in concrete mixes containing recycled aggregates (RCA) treated with H₂SO₄, tested on days 7, 28 and 91, along with the variations from the reference, RC and RC-RCA, mixes are presented. Based on these results, it can be concluded that there is an improvement in carbonation depth for the RCA-0.3H₂SO₄ mixes, with improvement values of 4.42%, 3.02% and 1.21% on days 7, 28 and 91 of accelerated carbonation, respectively. This improvement can be attributed, as discussed earlier, to the reduction of mortar content in RCA and porosity, as found in the SEM analysis in section 5.3.4. Regarding the mixes RCA-1.0H₂SO₄ and RCA-3.0H₂SO₄, an increase in the carbonation front was observed at all ages (7, 28 and 91 days) due to the degradation caused by the presence of sulphate ions (SO₄⁻).

To facilitate understanding, Figure 5-41a presents the evolution of the carbonation depth as a function of the concrete mixes containing RCA treated with H₂SO₄, displaying

the values for each mix at different test ages. From figure 5-41b, it is possible to observe a trend in the results of carbonation depth at each age, related to the acid molarity of H₂SO₄. This trend is more evident for the age of 91 days, with a coefficient of determination (R²) of 0.96, while at the other ages it is not possible to observe a clear trend.

Table 5-25 Carbonation depth (mm) for mixes with RCA treated with H₂SO₄.

Time	Mix	Carbonation depth (mm)	σ	% improvement relative to RC	% improvement relative to RC-RCA
7 days	RC	2.8	0.9	—	—
	RCA	4.3	0.85	53.57%▲	—
	RCA-0.3H ₂ SO ₄	4.11	0.75	46.79%▲	4.42%▼
	RCA-1.0H ₂ SO ₄	4.56	0.65	62.86%▲	6.05%▲
	RCA-3.0H ₂ SO ₄	4.61	0.52	64.64%▲	7.21%▲
28 days	RC	4.89	0.56	—	—
	RCA	6.62	0.23	35.38%▲	—
	RCA-0.3H ₂ SO ₄	6.42	0.15	31.29%▲	3.02%▼
	RCA-1.0H ₂ SO ₄	6.78	0.18	38.65%▲	2.42%▲
	RCA-3.0H ₂ SO ₄	6.79	0.14	38.85%▲	2.57%▲
91 days	RC	6.01	0.25	—	—
	RCA	8.25	0.14	37.27%▲	—
	RCA-0.3H ₂ SO ₄	8.15	0.19	35.61%▲	1.21%▼
	RCA-1.0H ₂ SO ₄	9.12	0.23	51.75%▲	10.55%▲
	RCA-3.0H ₂ SO ₄	9.56	0.24	59.07%▲	15.88%▲



(a)

(b)

Figure 5-41 Depth of carbonation (mm) of concrete mixes with RCA treated with H₂SO₄ (a); H₂SO₄ concentration versus carbonation depth normalisation (b).

The evolution of carbonation penetration over time reveals that the phenomenon of CO₂ penetration in concrete mixes with recycled aggregates treated with H₂SO₄ is equally intense in the early stages of the process (7 days).

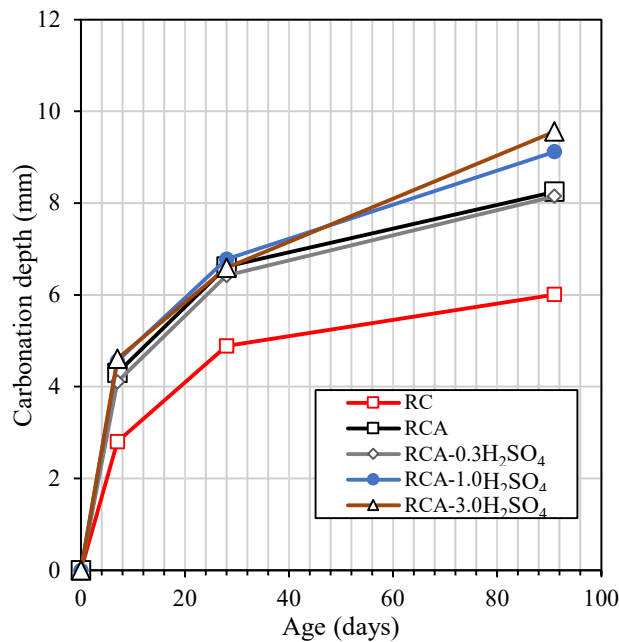


Figure 5-42 Evolution of carbonation depth with time in RCA treated with H₂SO₄.

5.11.3 Carbonation depth in concrete incorporating AS

As explained in the various properties investigated in this thesis, the addition of AS increases the compactness of the ITZ and reduces microcracks, resulting in a decrease in CO₂ penetration. Table 5-26 presents the results of the carbonation depth of mixes containing AS at a proportion of 1.10% by weight of cement. The carbonation depth is reduced at all ages, with values of 3.49%, 1.06% and 1.70% for days 7, 28 and 91, respectively.

Table 5-26 Carbonation depth (mm) for mixes with RCA and addition of AS.

Time	Mix	Carbonation depth (mm)	σ	% improvement relative to RC	% improvement relative to RC-RCA
7 days	RC	2.8	0.9	—	—
	RCA	4.3	0.85	53.57% ▲	—
	RCA-AS	4.15	0.75	48.21% ▲	3.49% ▼
28 days	RC	4.89	0.56	—	—
	RCA	6.62	0.23	35.38% ▲	—
	RCA-AS	6.55	0.56	33.95% ▲	1.06% ▼
91 days	RC	6.01	0.25	—	—
	RCA	8.25	0.14	37.27% ▲	—
	RCA-AS	8.11	0.21	34.94% ▲	1.70% ▼

These results are graphically illustrated in Figure 5-43a, where it is possible to observe the carbonation depth in relation to the RC and RC-RCA reference mixes. Figure 5-43b demonstrates the evolution of CO₂ penetration over time, showing that, similarly to the previously described treatments with RCA, when adding AS, this trend is maintained, with a more pronounced initial carbonation depth.

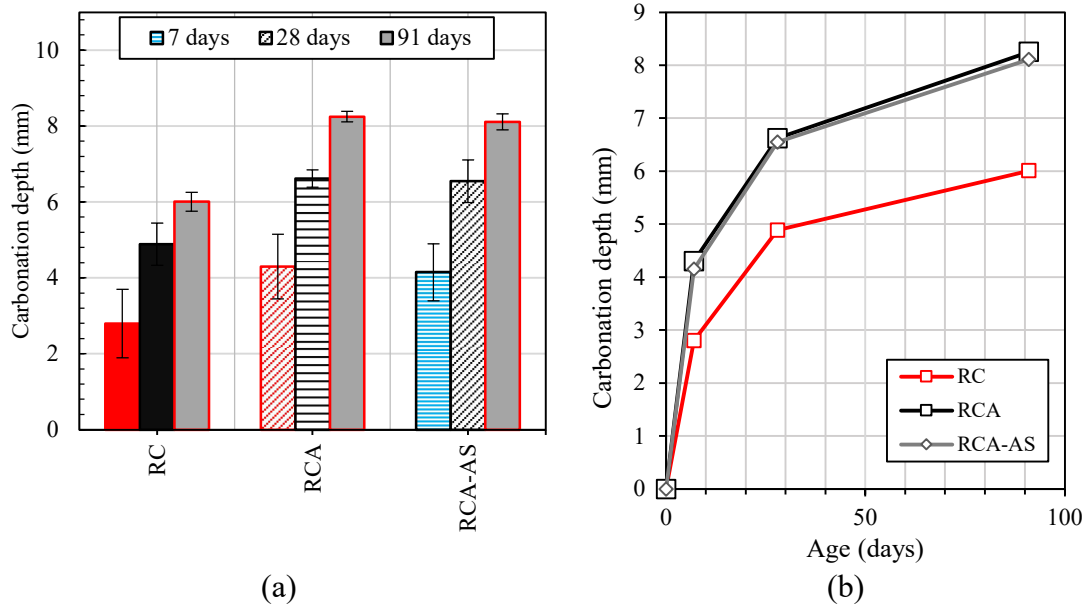


Figure 5-43 Depth of carbonation (mm) of concrete mixes with RCA and addition of AS (a); evolution of carbonation depth with time in RCA and addition of AS (b).

5.12 Resistance to the penetration of chloride ions

One of the most relevant factors in the degradation of concrete in terms of durability is reinforcement corrosion. It is one of the most significant pathological manifestations and of difficult intervention that occurs in reinforced concrete structures. The aggressiveness of this process is related to the cement content, the type of aggregate and the permeability of concrete (MEDINA; FRÍAS; DE ROJAS; THOMAS *et al.*, 2012; SILVA; BRITO; NEVES; DHIR, 2015; YODSUDJAI; NITICHOTE, 2022).

Normally, the resistance to chloride ion penetration is higher in concrete mixes containing RCA relative to those using natural aggregates. This resistance increases as the replacement content of RCA increases. This phenomenon is attributed to the permeability existing in RCA, as well as the bond between the aggregate and the cementitious matrix (ITZ), together with the micro-cracks present in RCA. Next, the results of the chloride ion penetration resistance tests on mixes containing RCA treated with HCl are presented.

5.12.1 Resistance to the penetration of chloride ions in concrete incorporating RCA treated with HCl

The results of the chloride penetration test are presented in Figure 5-44a, where an increase in chloride ion values is observed. This occurs because the hydrochloric acid (HCl) is composed of chloride ions (Cl⁻) and hydrogen ions (H⁺), and during the acid

removal process, HCl reacts with concrete, dissolving the cement and releasing chloride ions. The chloride ions released during the acid removal may remain and be adsorbed or incorporated into the recycled aggregate matrix. Therefore, in these aggregates, gradual leaching of the remaining chloride ions may occur (YING; HAN; SHEN; LI, 2020; YUAN; MAO; LI, 2023). This was proven by measuring the pH of RCA before and after treatment, with an initial pH of 9.2 and pH of 8.5 after treatment.

Due to this increase due to the chloride ion content, it is possible to establish a correlation between the acid molarity with which the RCA was treated and the chloride penetration resistance. Figure 5-44b presents this correlation, observing a good relationship between these two parameters, with a coefficient of determination of $R^2 = 0.88$. Table 5-27 presents the chloride ion penetration resistance results for the mixes with HCl-treated RCA, as well as their respective standard deviations and variations with respect to the RC and RC-RCA reference mixes.

Table 5-27 Resistance to penetration of chloride ions in concrete mixes with RCA treated with HCl.

Mix	Chloride diffusion coefficient ($\times 10^{-12} \text{m}^2/\text{s}$)	σ	% improvement relative to RC	% improvement relative to RC-RCA
RC	11.89	0.23	—	—
RC-RCA	14.56	0.12	22.46%▲	—
RCA-0.3HCl	14.62	0.25	22.96%▲	0.41%▲
RCA-1.0HCl	14.89	0.14	25.23%▲	2.27%▲
RCA-3.0HCl	15.06	0.11	26.66%▲	3.43%▲

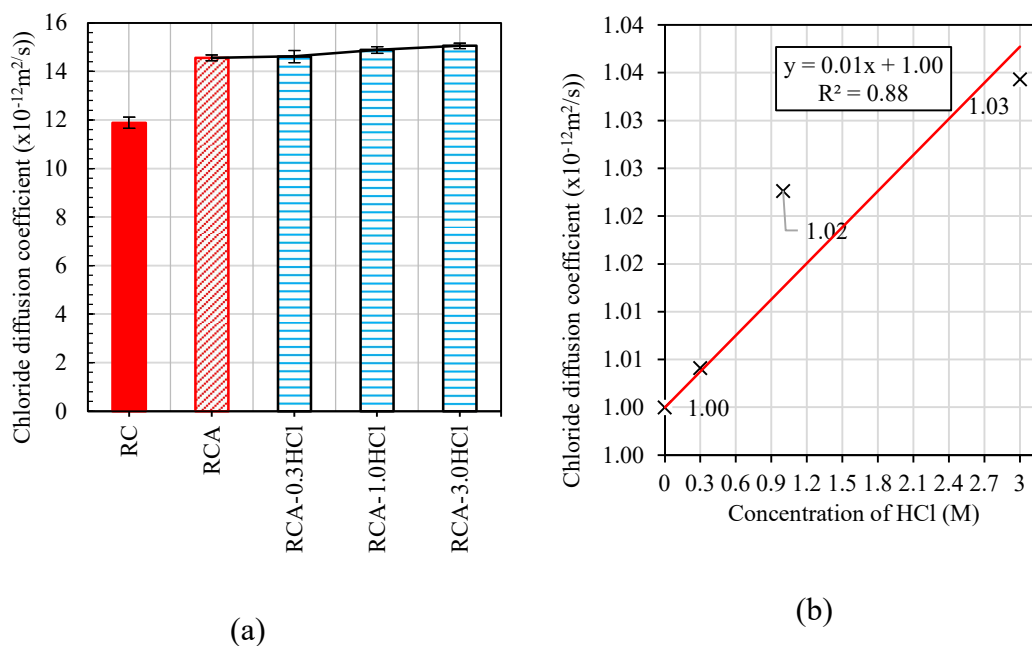


Figure 5-44 Resistance to penetration of chloride ions in concrete mixes with RCA treated with HCl (a); relationship between HCl concentration and resistance to penetration of chloride ions at 28 days (b).

Results presented by Kim *et al.* (2018) showed that the permeability to chloride ions of untreated RCA mixes is 27% higher than that of mixes with NA only. Regarding the permeability to chloride ions of the mixes containing RCA treated with HCl and Na₂SO₄, the penetration was 11% and 14% higher, while those with NA showed an improvement. This improvement can be attributed to the washing process of RCA, where, in this study, the treated aggregates went through an exclusive washing stage.

5.12.2 Resistance to the penetration of chloride ions in concrete incorporating RCA treated with H₂SO₄

The results concerning the resistance to chloride ion penetration in concrete mixes containing RCA treated with H₂SO₄ are presented in Figure 5-45. A reduction in chloride ion penetration resistance is observed in mixes with RCA treated with concentrations of 1.0 M and 3.0 M of sulphuric acid. This reduction can be explained by the degradation suffered by RCA after treatment, resulting in the formation of micro-cracks. Furthermore, in the mix with RCA treated with a concentration of 3.0 M, a second degradation mechanism due to the removal of sulphate ions occurs. However, in the mix with RCA treated with 0.3 M, a slight improvement in the resistance to chloride ion penetration is observed, since the H₂SO₄ used does not contain chloride ions (Cl⁻) detectable in the test.

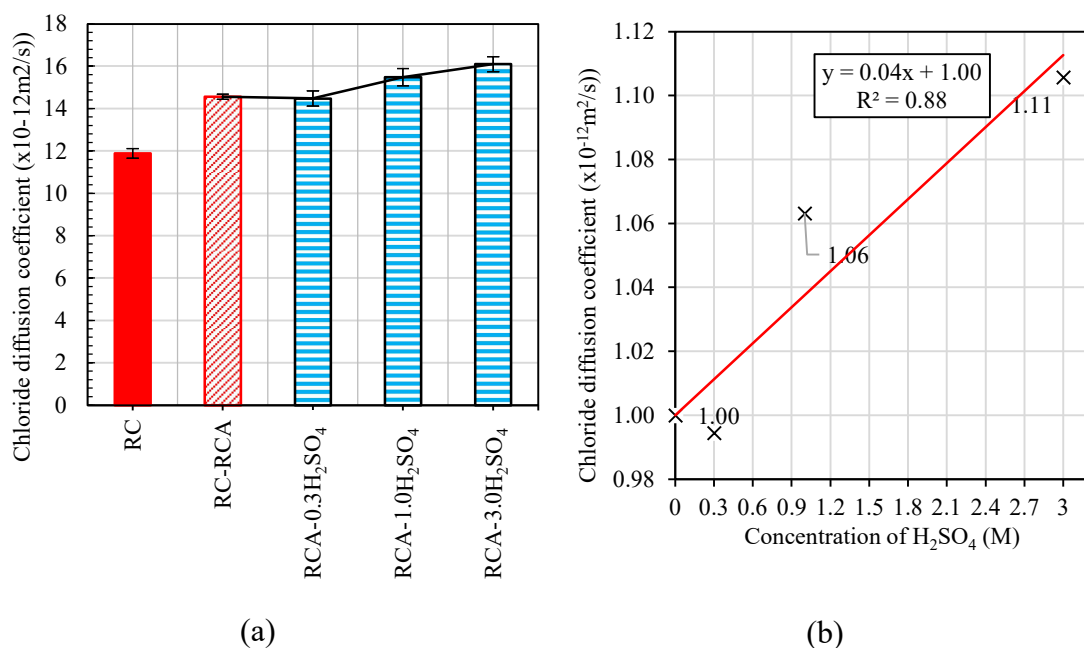


Figure 5-45 Resistance to penetration of chloride ions in concrete mixes with RCA treated with H₂SO₄ (a); relationship between H₂SO₄ concentration and resistance to penetration of chloride ions at 28 days (b).

In Figure 5-45b, the correlation between molarity and chloride ion penetration resistance is presented, revealing a linear relationship with a coefficient of determination of $R^2 = 0.88$, which indicates a strong dependence between molarity and chloride penetration resistance. The results for each concrete mix are presented in Table 5-28.

Table 5-28 Resistance to penetration of chloride ions in concrete mixes with RCA treated with H₂SO₄.

Mix	Chloride diffusion coefficient (x10 ⁻¹² m ² /s)	σ	% improvement relative to RC	% improvement relative to RC-RCA
RC	11.89	0.23	—	—
RC-RCA	14.56	0.12	22.46%▲	—
RCA-0.3H ₂ SO ₄	14.48	0.35	21.78%▲	0.55%▼
RCA-1.0H ₂ SO ₄	15.48	0.41	30.19%▲	6.32%▲
RCA-3.0H ₂ SO ₄	16.10	0.36	35.41%▲	10.58%▲

5.12.3 Resistance to the penetration of chloride ions in concrete incorporating AS

The addition of AS to the concrete compositions containing RCA led to an improvement in the resistance to chloride ion penetration. This improvement was 1.44% relative to concrete mixes without AS. Such improvement was due to the reaction of aluminium sulphate with the hydration products, resulting in the reduction of porosity and the improvement of the ITZ, as observed in the SEM analyses.

The process and chemical reactions that occur in the cementitious matrix when AS is added were described previously. Table 5-29 presents the chloride penetration resistance values for the mixes with added AS, as well as their variation from the reference mixes, with RCA (RC) and without added RCA (RC-RCA).

Table 5-29 Resistance to penetration of chloride ions for mixes with RCA and addition of AS.

Mix	Chloride diffusion coefficient (x10 ⁻¹² m ² /s)	σ	% improvement relative to RC	% improvement relative to RC-RCA
RC	11.89	0.23	—	—
RC-RCA	14.56	0.12	22.46%▲	—
RCA-AS	14.35	0.27	20.69%▲	1.44%▼

5.13 Combination of durability and mechanical properties

In this item, the possible correlations between durability properties and some mechanical properties are presented. In Figure 5-46a, it is possible to observe a linear relationship between water absorption by immersion and compressive strength (f_{cm}). This relationship is confirmed by the coefficient of determination values, which are $R^2 = 0.98$ for the concrete mixes containing RCA treated with HCl (RCA-HCl) and $R^2 = 0.85$ for

the mixes with RCA treated with H₂SO₄. These results indicate a strong association between water absorption and compressive strength.

Furthermore, a correlation was observed between the properties of water absorption by immersion and water absorption by capillarity, as seen in Figure 5-46b. In this case, the coefficients of determination were $R^2 = 0.99$ and $R^2 = 0.97$ for the RCA-HCl and RCA-H₂SO₄ concrete mixes, respectively. These coefficients close to 1 demonstrate a highly significant relationship between the two properties.

These correlations play a crucial role, providing valuable insights into the performance and durability of concrete under different environmental conditions. Moreover, the correlation between water absorption by immersion and water absorption by capillarity plays an important role in evaluating the permeability of concrete and its ability to resist water ingress.

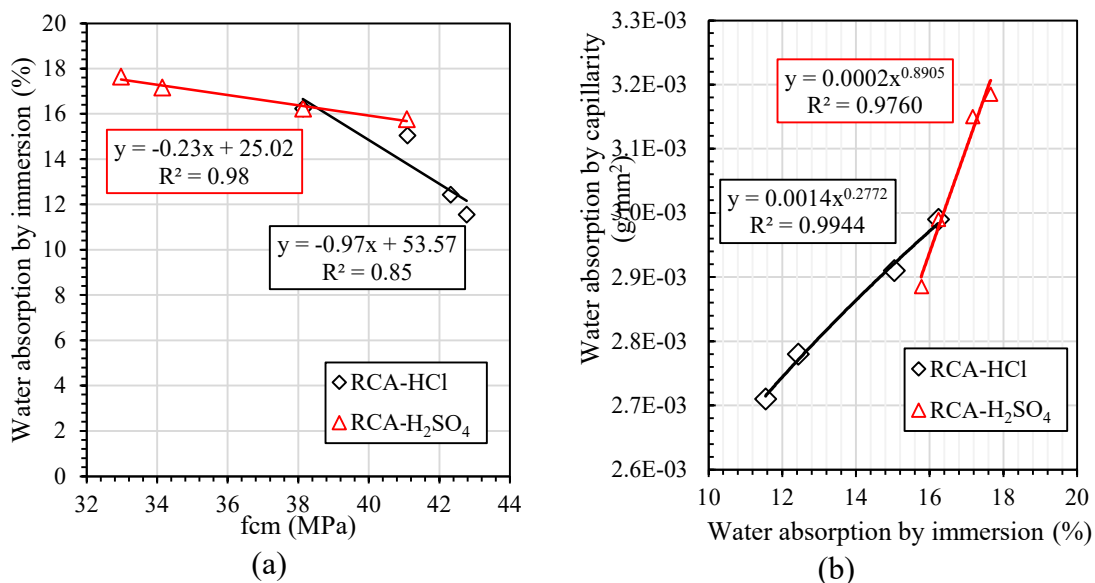


Figure 5-46 Relationship between water absorption by immersion and compressive strength (f_{cm}) (a); relationship between water absorption by capillarity and water absorption by immersion (b)

To evaluate water absorption by capillarity, two models were suggested by Wirquin *et al.* (2000) The first model was proposed by Hall (1989), who suggested that Equation 5-8 is the most adequate to describe water absorption by capillarity.

$$W = A + S \cdot \sqrt{t} - C \cdot t \quad \text{Equation 5-8}$$

The first model, proposed by Hall (1989), describes water absorption (W) as a function of time (t) and the sorptivity of the material (S), as shown in Equation 5-8. The

second model, proposed by Schonlin (1992), establishes the relationship between water absorption over time, as determined by Equation 5-9, where W and t were defined previously and W_1 is the amount of water absorbed after one hour and n is a constant.

$$W = W_1 \cdot n^t \quad \text{Equation 5-9}$$

Hall's model (HALL, 1989) was used to determine the water absorptions over time. This model was fitted to the results of all mixes, as shown in Figure 5-47a, b and c, and presented a good fit to the results obtained from each mix.

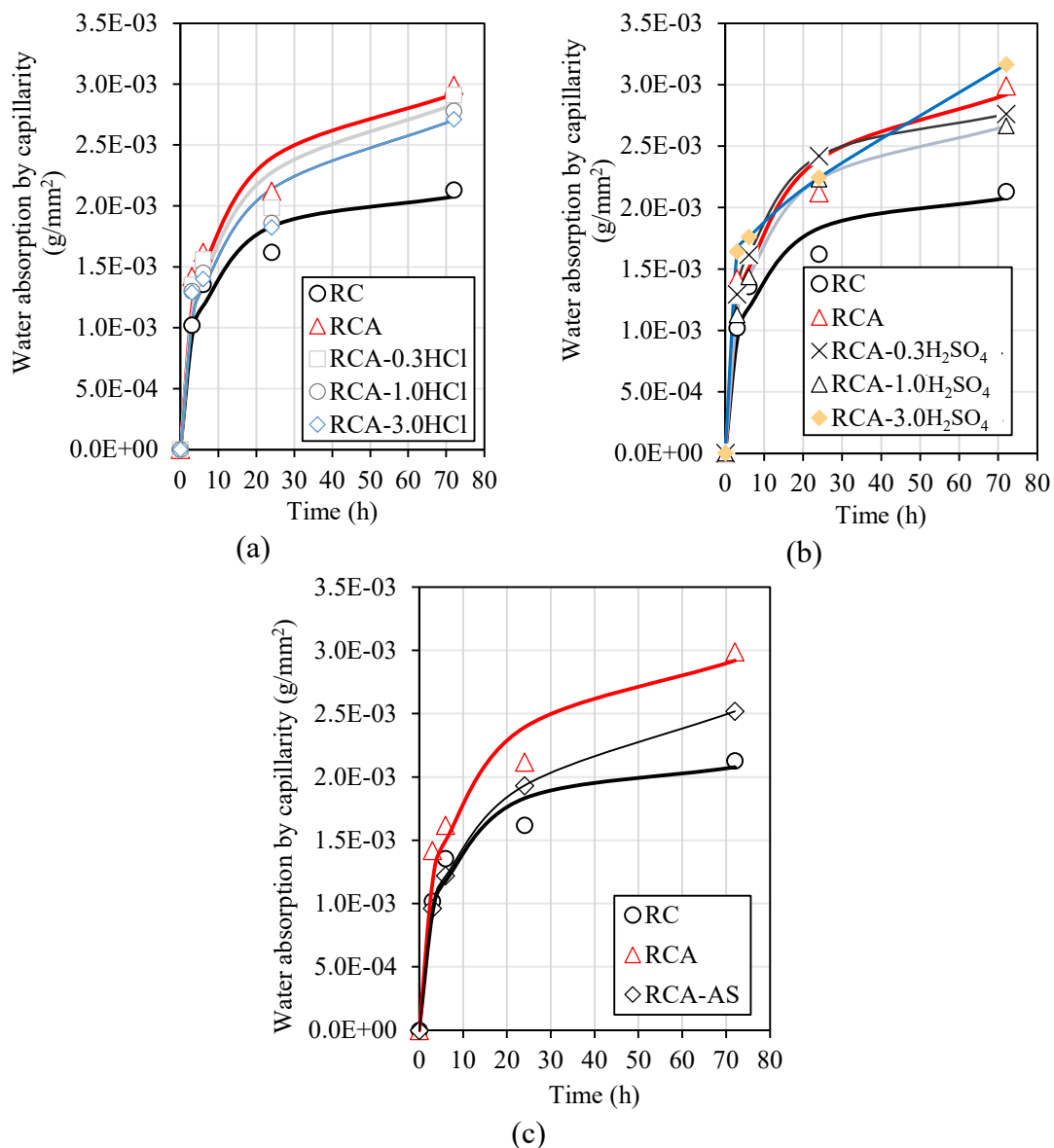


Figure 5-47 Capillary water absorption of the RCA concrete treated with HCl (a); H₂SO₄ (b); and AS (c).

Table 5-30 presents the fit coefficients of Equation 5-8 (A and C), as well as the sorptivity coefficient for all the mixes analysed in this study. From the results in Table 5-30, it can be observed that the sorptivity coefficient of the mixes with RCA treated with

HCl had a reduction between 6.74% and 18.56% in relation to the RC-RCA reference concrete. This reduction occurred with a coefficient of determination (R^2) between 0.98 and 0.99, which confirms an improvement in sorptivity. This indicates that concrete with this type of RCA has a greater ability to absorb and transmit water by capillary suction, resulting in better concrete resistance to exposure to aggressive environments.

Table 5-30 Capillary water absorption, sorptivity, and adjustment parameters of the Hall's capillarity model for each concrete mix.

Mixes	A	C	S	σ	% improvement relative to RC	% improvement relative to RC-RCA
RC	1.42E-04	3.26E-05	5.05E-04	0.984	—	—
RCA	1.77E-04	3.61E-05	6.29E-04	0.985	24.61%▲	—
RCA-0.3HCl	1.74E-04	3.22E-05	5.87E-04	0.982	16.22%▲	6.74%▼
RCA-1.0HCl	1.81E-04	2.84E-05	5.39E-04	0.981	6.78%▲	14.31%▼
RCA-3.0HCl	1.46E-04	-2.33E+00	5.12E-04	0.994	1.48%▲	18.56%▼
RCA-0.3H ₂ SO ₄	3.49E-04	3.86E-05	6.12E-04	0.977	21.13%▲	2.80%▼
RCA-1.0H ₂ SO ₄	2.33E-04	3.39E-05	5.74E-04	0.980	13.68%▲	8.77%▼
RCA-3.0H ₂ SO ₄	1.39E-03	-9.84E-06	1.25E-04	1.000	75.18%▼	80.08%▼
RCA-AS	2.56E-04	2.11E-05	4.46E-04	0.973	11.76%▲	29.19%▼

This improvement was also observed in mixes with RCA treated with H₂SO₄, with a reduction between 2.80% and 8.77% in sorptivity and a coefficient of determination (R^2) between 0.97 and 0.98. However, it should be mentioned that the mix with RCA treated with 3.0 M of H₂SO₄ showed a great improvement over the RC and RCA reference mixes. However, these results were not representative due to the degradation that occurred in the cementitious matrix and that modified these results. Finally, the results obtained for the mixes with AS addition were also analysed. The sorptivity was reduced by 29% in relation to the RC-RCA reference mix (Figure 5-47c).

To validate the results obtained in this analysis, Media *et al.* (2014) in their study on concrete with RCA addition at substitution ratios of 25% and 50%, found similar sorptivity, with an increase in values between 11% and 20% in the mixes with RCA compared to the reference concrete with NA.

Considering the influence of porosity in concrete, both on water absorption and carbonation resistance, it is expected that these two properties are correlated. In Figure 5-48a, this correlation is presented, obtaining linear determination coefficients (R^2) of 0.94 for mixes with RCA treated with HCl and 0.89 for mixes with RCA treated with H₂SO₄. This indicates the existence of a relationship between water absorption by immersion and carbonation resistance of the mixes studied. Parrot (1992) also concluded that this correlation between the two properties exists.

Another important correlation is associated with compressive strength (Figure 5-48b). It is observed that there is correlation with determination coefficients R^2 of 0.85 and 0.98 for the mixes with RCA treated with HCl and H_2SO_4 , respectively. As explained previously, this negative linear correlation occurs due to the increase of porosity in the aggregates, which decreases in mixes with low molarity of the acids in the case of HCl, and in mixes with high molarity (1M and 3M) in the case of H_2SO_4 .

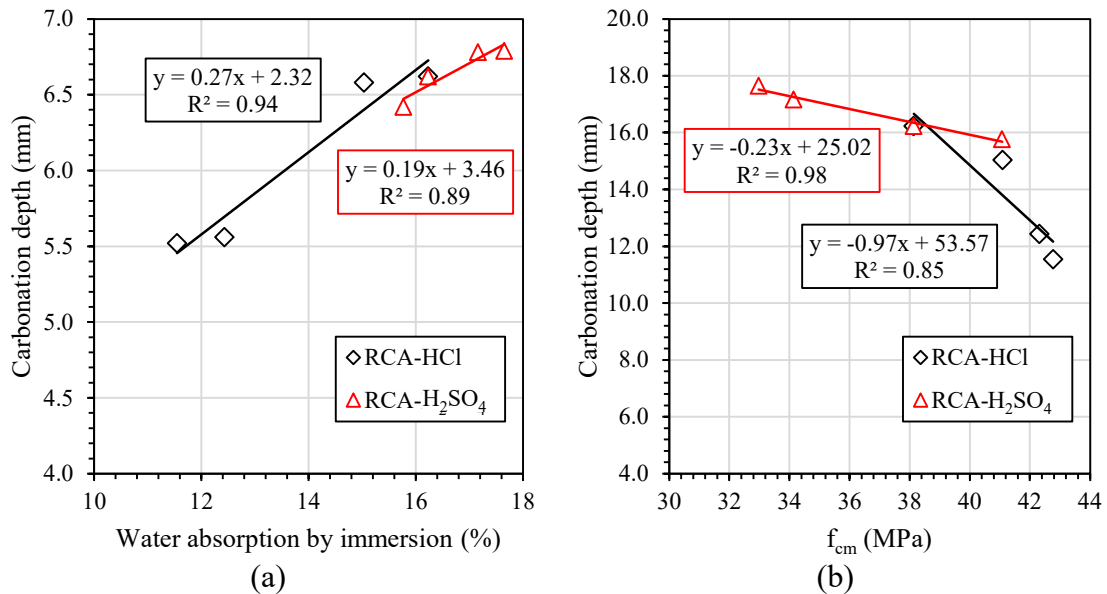


Figure 5-48 Relationship between carbonation resistance and water absorption by immersion (a); relationship between carbonation resistance and compressive strength (f_{cm}) (b).

The mechanism through which chloride ions penetrate is primarily by capillary water absorption. For this reason, a correlation was determined between capillary water absorption and chloride ion penetration resistance. The correlations of the mixes with RCA treated with HCl and H_2SO_4 showed acceptable coefficients of determination with R^2 values of 0.97 and 0.88, respectively (Figure 5-49a). It is important to highlight that as water absorption increases, chloride ion penetration proportionally increases for mixes with RCA- H_2SO_4 . On the other hand, mixes with RCA-HCl, due to residual chloride ion content, exhibit an increased value, which is reflected in the trend (Figure 5.49a).

Silva *et al.* (2015), found a relationship between chloride ion penetration resistance and compressive strength, exhibiting an exponential relationship of the form $d = a \cdot e^{bf_{cm}}$. In this thesis, an exponential regression was performed to determine which model best fits the experimental results. Based on the model proposed by Silva *et al.* (2015), exponential regressions were carried out for concrete mixes with RCA treated with HCl and H_2SO_4 , as shown in Figure 5-49b, with coefficients of determination (R^2) of 0.74 and 0.89 respectively

for each mix, confirming that the model fits the data accurately.

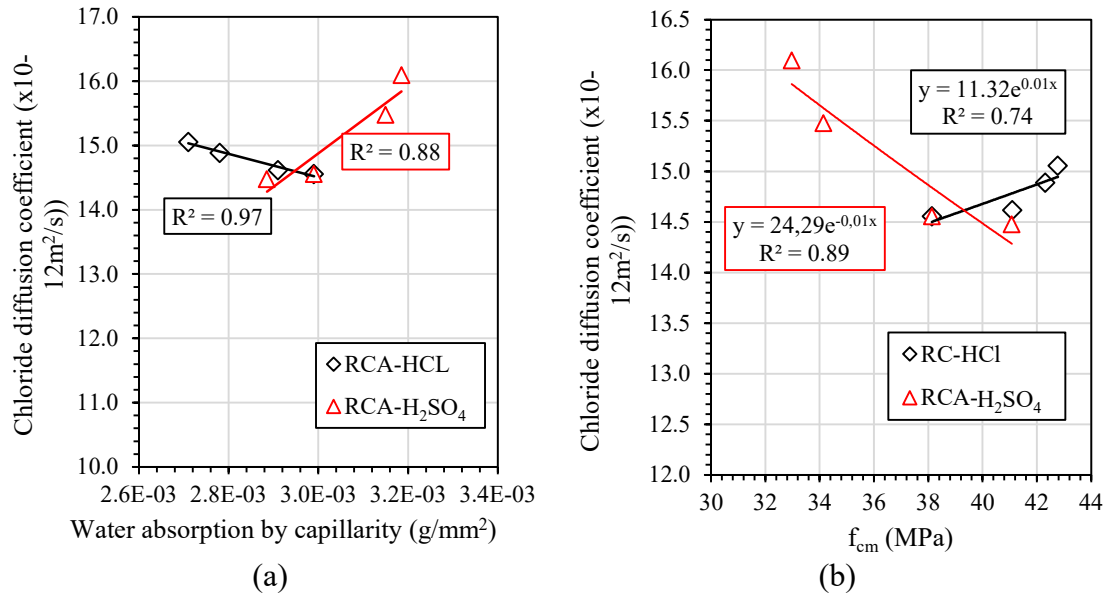


Figure 5-49 Relationship between Chloride diffusion coefficient ($\times 10^{-12} \text{m}^2$) and Water absorption by capillarity (g/mm^2) (a); and f_{cm} (MPa) (b).

5.14 Drying shrinkage of concrete

This item addresses the results and discussion of shrinkage by drying of mixes incorporating RCA treated with HCl, H₂SO₄ and AS acids, evaluated from 1 to 91 days. The shrinkage phenomenon can occur through several mechanisms such as: ambient temperature, atmospheric carbon dioxide (CO₂), w/c ratio and ambient humidity. Shrinkage causes tensile stresses that can originate cracking of structural elements, so it is important to evaluate the influence of mixes incorporating treated RCA and AS.

The mechanism studied to evaluate the dimensional stability of concrete with RCA-treated and aluminium sulphate addition (AS) was shrinkage by drying, caused by self-drying and drying. Self-drying occurs due to the consumption of evaporable water by the chemical reactions of hydration while drying is by evaporation of water from the pores, due to the existing difference between the internal relative humidity and the humidity of the external environment. The study of drying shrinkage mechanisms depends on the state of water-solid surface bond within the material. The exit of free water from the capillary pores does not cause dimensional change, since only the water bound to the solid can cause a deformation of this solid (HUA; EHRLACHER; ACKER, 1997). The results of the drying shrinkage of all mixes are presented below.

5.14.1 Drying shrinkage in concrete incorporating RCA treated with HCl

In Figure 5-50, the extent of shrinkage of RC, RC-RCA and RCA-HCl concrete mixes for molarities 0.3 M, 1.0 M and 3.0 M over the first 91 days of age can be observed. It is highlighted that in all concrete mixes, the strain increases over time in a logarithmic manner with coefficients of determination R^2 close to 1: 0.92, 0.89, 0.92, 0.93 and 0.94 for the RC, RC-RCA, RCA-0.3HCl, RCA-1.0HCl and RCA-3.0HCl mixes, respectively. This behaviour was expected, as the strain values tend to stabilise over time, with a greater shrinkage at early ages. One of the reasons for the increased shrinkage at early ages (7 days) may be caused by the relatively easier loss of moisture in the RCA aggregates as it is likely that this is free water and not required to hydrate the cement in the cementitious paste. It is important to point out that the mixes had compensating water and it is possible that the water is lost relatively quickly (SZELAĞ, 2018).

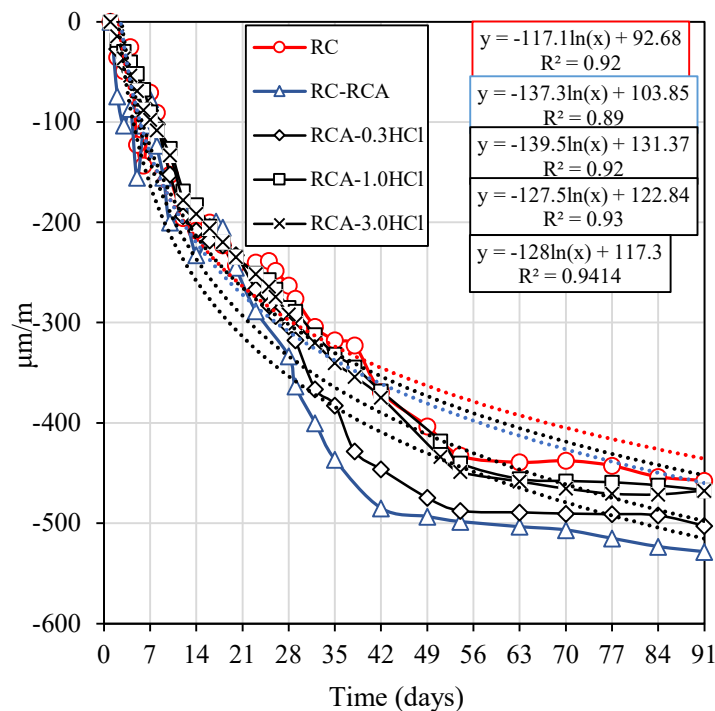


Figure 5-50 Drying shrinkage of HCl-treated RCA concrete mixes *versus* drying time.

Ismail and Ramli (2014) observed that the shrinkage of mixes with treated and untreated recycled concrete aggregates (RCA), measured over a total period of 180 days, fell below a micro strain of 500. Based on the results at early ages (up to 28 days), the drying shrinkage behaviour of all mixes containing untreated RCA was observed to be extremely pronounced. However, after 28 days, the drying shrinkage measured after 180 days for the untreated RCA concrete was 26% higher than that of the control concrete.

From Table 5-31, it is possible to see that the shrinkage values for mixes RCA-0.3HCl, RCA-1.0HCl and RCA-3.0HCl at 7 days had a slight improvement caused by the morphological improvement of the aggregate, by reducing and eliminating weakly adhered mortar particles in RCA.

Table 5-31 Drying shrinkage of concrete mixes with RCA treated with HCl.

Acid Mix	HCl (µm/m)								
	7 days	ΔRC (%)	ΔRC-RCA (%)	28 days	ΔRC (%)	ΔRC-RCA (%)	91 days	ΔRC (%)	ΔRC-RCA (%)
RC	-70.42	—	—	-262.92	—	—	-457.50	—	—
RC-RCA	-77.08	9.47%▲	—	-363.33	38.19%▲	—	-528.33	15.48%▲	—
RCA-0.3HCl	-88.33	25.44%▲	14.59%▲	-303.33	15.37%▲	16.51%▼	-502.50	9.84%▲	4.89%▼
RCA-1.0HCl	-90.00	27.81%▲	16.76%▲	-285.00	8.40%▲	21.56%▼	-467.08	2.09%▲	11.59%▼
RCA-3.0HCl	-97.50	38.46%▲	26.49%▲	-291.67	10.94%▲	19.72%▼	-467.50	2.19%▲	11.51%▼

The evolution of shrinkage over time has been the object of several investigations, intending to predict this behaviour. Eurocode 2 (EN, 2007) proposes the use of Equation 5-10 to perform a non-linear regression of the values obtained during the test in a given time (t), in order to determine the corresponding extension (ϵ_{cs}). This equation considers separately the extension due to drying (ϵ_{cd}) and to autogenous shrinkage (ϵ_{ca}). Equations 5-11 to 5-15 presented below are used to calculate these shrinkage fractions.

$$\epsilon_{cs} = \epsilon_{cd} + \epsilon_{ca} \quad \text{Equation 5-10}$$

$$\epsilon_{cd}(t) = \beta_s(t, t_s) \cdot k_h \cdot \epsilon_{cd0} \quad \text{Equation 5-11}$$

$$\beta_s(t, t_s) = \frac{(t - t_s)}{(t - t_s) + 0.04 \cdot \sqrt{h_0^3}} \quad \text{Equation 5-12}$$

$$\epsilon_{cd0} = \epsilon_s \cdot (f_{cm}) \cdot \left[-1.55 \cdot \left(1 - \left(\frac{HR}{100} \right)^3 \right) \right] \quad \text{Equation 5-13}$$

$$\epsilon_s(f_{cn}) = 0.85 \cdot \left[(220 + 110 \cdot \alpha_{ds1}) \cdot e^{\left(-\alpha_{ds2} \frac{f_{cm}}{10} \right)} \right] \cdot 10^{-6} \quad \text{Equation 5-14}$$

$$\epsilon_{ca};(t) = (1 - e^{-0.2 \cdot t^{0.5}}) \cdot [2.5 \cdot (f_{ck} - 10) \cdot 10^{-6}] \quad \text{Equation 5-15}$$

Where;

- t - time in days;
- t_s - time in 0 days;
- $\beta_s(t, t_s)$ - curve depending on the equivalent thickness (h_0);
- k_h - empirical term depending on the equivalent thickness (equal to 1);

- ε_{cd0} - corresponds to the extension by reference drying shrinkage;
- h_0 - equivalent thickness, which is equal to the double of the cross-section area of the specimen divided by its perimeter (equal to 50%);
- HR - relative ambient humidity (equal to 50%);
- α_{ds1} - value depending on the type of cement (equal to 6 for cement type R);
- α_{ds} - value depending on the type of cement (equal to 0.11 for R type cement);
- f_{cm} - average compressive strength at 28 days (MPa);
- f_{ck} - characteristic compressive strength at 28 days (MPa).

ACI 209.2 R (2008) proposes a model based on Equation 5-16 to determine shrinkage over time. This model was initially established by Branson and Christiason (1971) and describes shrinkage in terms of hyperbolic experimental curves, which are asymptotic in relation to the maximum shrinkage value of concrete. The term ε_{shu} is used to denote the maximum predictable extent, whose value is determined by seven factors that influence concrete shrinkage. These factors are successively multiplied to obtain the value of the factor γ_{sh} , as presented in Equation 5-17.

$$\varepsilon_{sh} \left(\frac{(t - t_c)^\alpha}{f + (t - t_c)^\alpha} \right) \varepsilon_{shu} \quad \text{Equation 5-16}$$

$$\varepsilon_{shu} = 780 \cdot 10^{-6} \cdot \gamma_{sh} \quad \text{Equation 5-17}$$

Where;

- t - time in days;
- t_c - curing time;
- α - value considered to be unitary;
- f - term depending on the specimen geometry (considered, equal 26);
- ε_{shu} - shrinkage maximum predictable;

- γ_{sh} - multiplying factor for determining the maximum extent that takes into account the curing time, relative humidity, geometry of the specimens, slump of concrete, concrete composition and mixing air content (in this case, equal to 1.2%).

In Figure 5-51a, it is possible to observe the comparison of the results obtained in this investigation in relation to the estimate of RCA-1.0HCl calculated by the previously mentioned expressions. It can be seen that Eurocode 2 (2007) shows a good prediction capacity, since the calculated coefficients of determination were $R^2=0.96, 0.95, 0.98, 0.99$ and 0.99 for the RC, RC-RCA, RCA-0.3HCl, RCA-1.0HCl and RCA-3.0HCl concrete mixes, respectively. This indicates that the predictions made by Eurocode 2 (2007) can be used in this type of concrete.

Another prediction analysis was performed using the model proposed by ACI 209.2R (2008) that was mentioned previously. From this analysis, it can be concluded that the aforementioned prediction model is not suitable for concrete containing RCA treated with HCl. This is evidenced by the observation of a divergence in the mixes in relation to the model proposed by ACI 209.2R (ACI, 2008) as shown in Figure 5-51b.

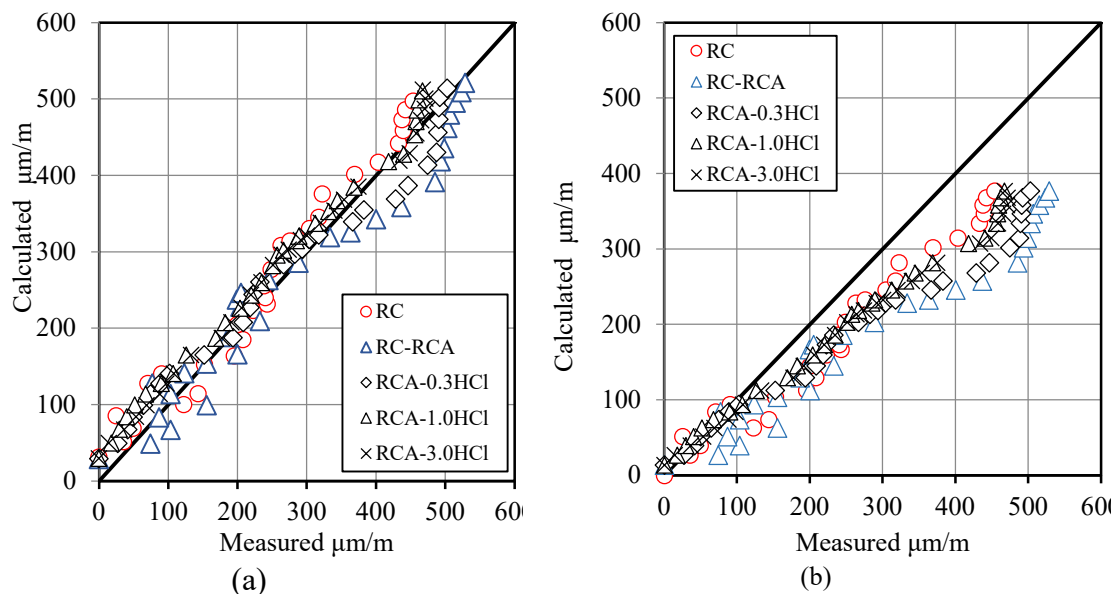


Figure 5-51 Shrinkage calculated according to the EC2 prediction model (a); ACI 209.2 R prediction model (b).

5.14.2 Drying shrinkage in concrete incorporating RCA treated with H_2SO_4

The volume variation in concrete mixes with RCA treated with sulphuric acid

(H₂SO₄) over a period of 91 days can be observed in Figure 5-52. Similarly, the mixes exhibited higher shrinkage over time compared to RC. Regarding the RC-RCA mix, an improvement was observed in the RCA-0.3H₂SO₄ mix. However, this was not the case for the RCA-1.0H₂SO₄ and RCA-3.0H₂SO₄ mixes, as the shrinkage values at 91 days were 538.75, 524.58, and 528.33 μm/m, respectively. This can be attributed to increased porosity, which leads to higher water absorption and subsequently increased volumetric shrinkage.

It is noteworthy that all concrete mixes with RCA treated with H₂SO₄ experienced an increase in deformation over time, following a logarithmic trend. The determination coefficient (R²) was 0.94, 0.93, and 0.98 for mixes treated with 0.3 M, 1.0 M, and 3.0 M of sulphuric acid, respectively. Table 5-32 presents all the results of RCA treated with H₂SO₄ mixes for 7, 28, and 91 days, as well as the respective reductions compared to the reference mixes RC and RC-H₂SO₄.

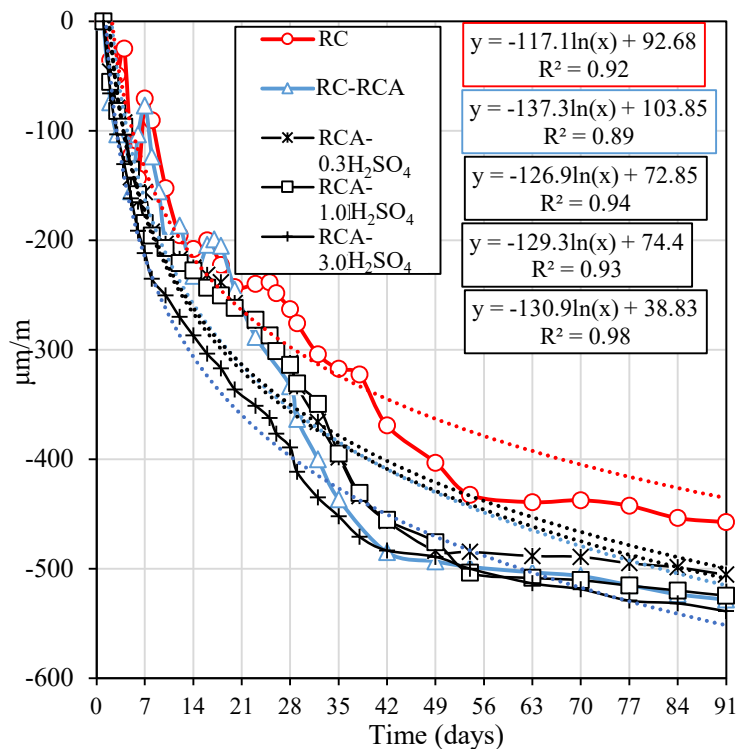


Figure 5-52 Drying shrinkage of H₂SO₄-treated RCA concrete mixes *versus* drying time.

Table 5-32 Drying shrinkage of concrete mixes with RCA treated with H₂SO₄.

Acid	H ₂ SO ₄								
	7 days	ΔRC-RCA		28 days	ΔRC-RCA		91 days	ΔRC-RCA	
Mix	(μm/m)	ΔRC (%)	(%)	(μm/m)	ΔRC (%)	(%)	(μm/m)	ΔRC (%)	(%)
RC	-70.42	-	-	-262.92	-	-	-457.50	-	-
RC-RCA	-77.08	9.47% ▲	-	-363.33	38.19% ▲	-	-528.33	15.48% ▲	-
RCA-0.3H ₂ SO ₄	-155.83	121.30% ▲	102.16% ▲	-312.08	18.70% ▲	14.11% ▼	-505.42	10.47% ▲	4.34% ▼
RCA-1.0H ₂ SO ₄	-184.17	161.54% ▲	238.92% ▲	-313.75	19.33% ▲	13.65% ▼	-524.58	14.66% ▲	0.71% ▼
RCA-3.0H ₂ SO ₄	-211.67	200.59% ▲	274.59% ▲	-389.17	48.02% ▲	7.11% ▲	-538.75	17.76% ▲	1.97% ▲

The results of the shrinkage of these mixes were compared according to Eurocode 2 (2007) and ACI 209.2R (2008) guidelines. The prediction model for shrinkage in Eurocode 2 (2007) was appropriately adjusted for this type of concrete with RCA treated with H₂SO₄. This is evident from the R² values obtained from the experimental data and the predicted values provided by Eurocode 2 (2007), with determination coefficients (R²) of 0.96, 0.97 for the mixes with 0.3 M, 1.0 M, and 3.0 M, as shown in Figure 5-53a.

Similarly, the results were compared with the ACI 209.2R (2008) guideline, as presented in Figure 5-53b. It can be observed that the predictions made by ACI 209.2R (2008) do not reflect the results obtained in the mixes with RCA treated with H₂SO₄.

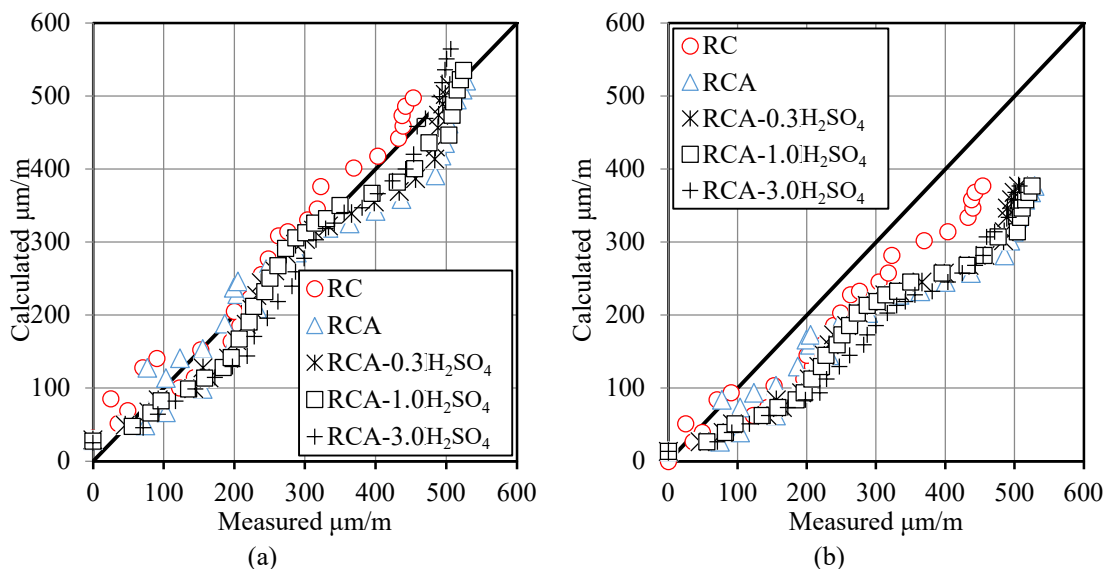


Figure 5-53 Shrinkage calculated according to the EC2 prediction model (a); ACI 209.2 R prediction model (b).

5.14.3 Drying shrinkage in concrete in concrete incorporating AS

The results of the concrete mixes with AS addition are presented in Figure 5-54, illustrating the drying shrinkage evolution over 91 days. It can be observed that there was a reduction in shrinkage of 24.84% and 12.72% at 28 and 91 days, respectively. Song *et al.* (2015) found reductions in shrinkage in concrete using aluminium sulphate of 43.1% and 37.3% at 7 and 28 days, respectively, compared to the reference concrete with RCA.

This reduction occurs due to the reaction of aluminium sulphate with the water present in concrete and with the calcium compounds, resulting in the formation of aluminium hydrates, calcium silicate hydrate (C-S-H) and ettringite, as described previously in item

5.4.3. These hydrates have the capacity to absorb water, thus reducing the amount available for evaporation during the drying of the concrete. The values of shrinkage for the ages of 7, 28, and 91 days of the mixes with the addition of AS, as well as the variation compared to the reference mixes RC and RC-RCA, are presented in Table 5-33.

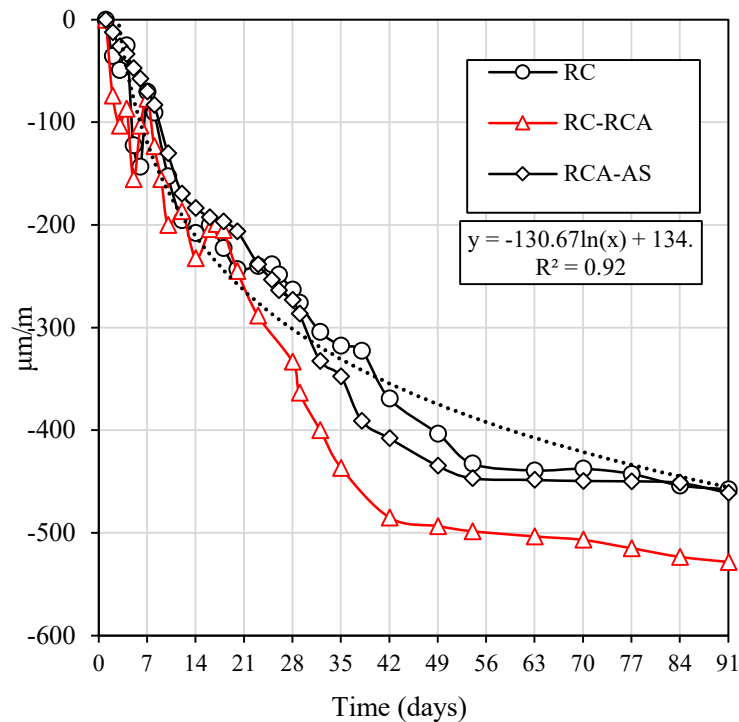


Figure 5-54 Drying shrinkage of concrete mixes with RCA and addition of AS versus drying time

Table 5-33 Drying shrinkage of concrete mixes with RCA and addition of AS.

Mix	AS								
	7 days (µm/m)	ΔRC (%)	ΔRC-RCA (%)	28 days (µm/m)	ΔRC (%)	ΔRC-RCA (%)	91 days (µm/m)	ΔRC (%)	ΔRC-RCA (%)
RC	-70.42	-	-	-262.92	-	-	-457.50	-	-
RC-RCA	-77.08	9.47%▲	-	-363.33	38.19%▲	-	-528.33	15.48%▲	-
RCA-AS	-70.05	0.51%▼	9.12%▼	-273.07	3.86%▲	24.84%▼	-461.13	0.79%▲	12.72%▼

Similar to the other mixes evaluated in this study, the results were compared with the Eurocode 2 (2007) and ACI 209.2R (2008) guidelines. It can be observed that the results compared with Eurocode 2(2007) demonstrate a good fit of the proposed model to the obtained results for these mixes (Figure 5-55a) with $R^2 = 0.95$. In contrast, the prediction model of ACI 209.2R (2008) did not match the results obtained in this study, as shown in Figure 5-55b.

As is widely known, the modulus of elasticity of concrete is directly associated with its shrinkage. In Figure 5-52, a linear trend can be observed with coefficient of determination (R^2) values of 0.84, and 0.15 for all the analysed mixes. This observation

indicates that, as the modulus of elasticity decreases, the drying shrinkage increases, confirming the influence of aggregates and microstructure on these properties.

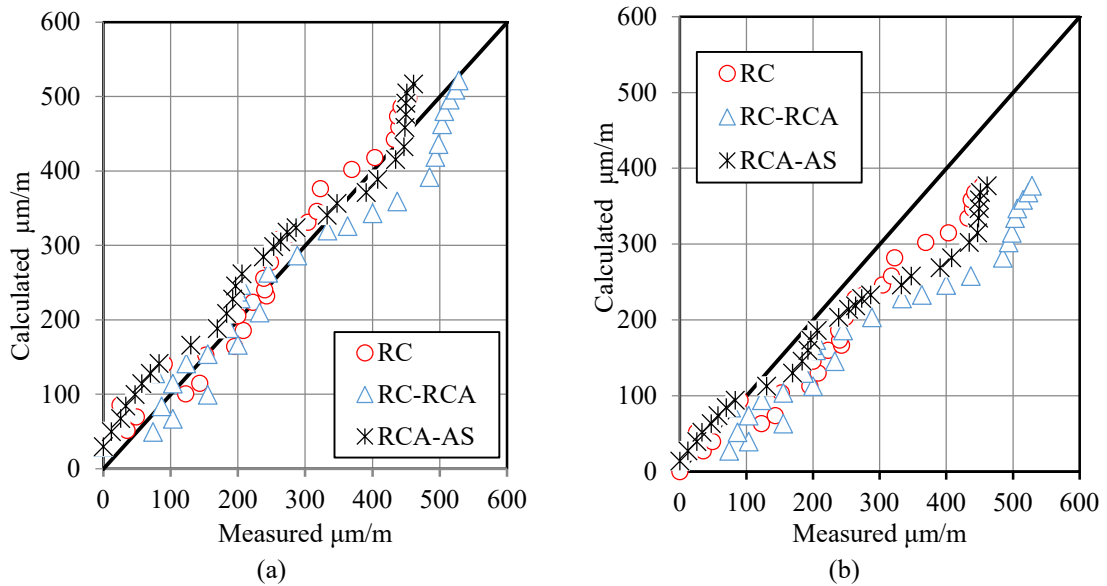


Figure 5-55 Shrinkage calculated according to the EC2 prediction model (a); ACI 209.2 R prediction model (b).

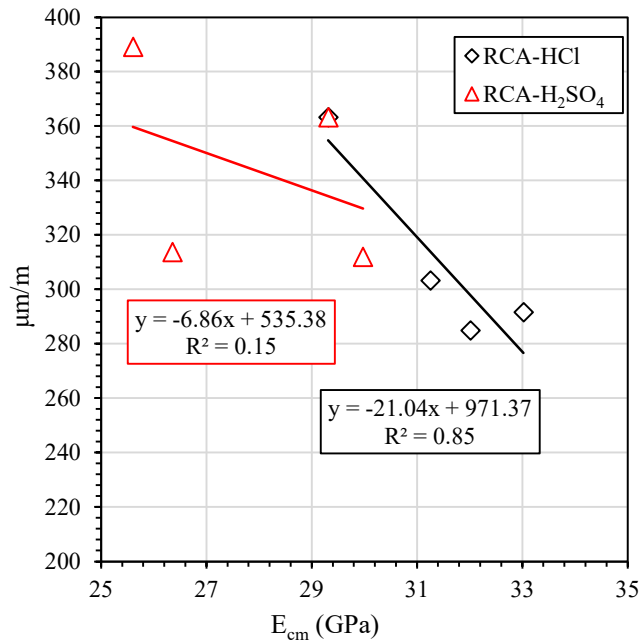


Figure 5-56 Relationship between shrinkage ($\mu\text{m/m}$) and modulus of elasticity (E_{cm})

5.15 Summary of Chapter 5

In the current chapter, the characterization and analysis of the properties of concrete in both fresh and hardened states were carried out in terms of mechanics and durability.

Regarding the tests conducted on concrete with HCl-treated RCA in the fresh state (slump test), improvements were observed compared to the reference concrete RC-HCl due to the change in RCA geometry. As for concrete with H₂SO₄, improvements were also observed except for the 3.0 M molarity. In terms of bulk density, all mixes showed improvements compared to the reference concrete RC-RCA.

Regarding the microstructure, the HCl treatments showed an improvement in the ITZ for all molarities, as well as a similar improvement in mixes with the addition of aluminium sulphate. However, for H₂SO₄, this improvement was only observed at a concentration of 0.3 M, as higher molarities resulted in a microstructure with a thicker ITZ, microcracks, and increased porosity due to the sulphate ions.

Regarding the mechanical tests, it was observed that mixes with HCl-treated RCA exhibited better performance for all molarities, with improvements of up to 40% in compressive strength, up to 40.08% in tensile strength, up to 12.08% in modulus of elasticity, and 87.07% in fracture energy. Similarly, mixes with H₂SO₄-treated RCA followed the same improvement trend, but this improvement was only present at a molarity of 0.3 M. Mixes with addition of sulphate showed significant improvement in all these properties.

Finally, concerning the durability properties, the mixes followed the same trend as for the mechanical properties, except for chloride ion penetration resistance, where the mixes with HCl-treated RCA experienced a reduction in this property due to the presence of chloride ions.

6 SUMMARY AND FINAL CONCLUSIONS

The present thesis aimed to perform a thorough analysis of mixes with recycled concrete aggregate (RCA) that was treated with acid solutions of HCl and H₂SO₄. The main objective was to remove the adhered mortar in the RCA and improve the microstructure through the addition of aluminium sulphate (AS). The experimental campaign was divided into two phases: the characterization of the aggregates and the characterization of the concrete containing RCA treated with the acid solutions. The outcomes were analysed in detail to validate the effectiveness of acid removal on RCA and its influence on mechanical and durability properties. Additionally, the thesis provides an explicit criterion for the application of this type of removal, presenting advantages and disadvantages that may occur. The methodology described in the thesis contributed to determining the appropriate parameters for the use of this type of removal, including the acid immersion time, acid concentration, and type of acid most used in mining, which often becomes useless waste.

In this chapter, a synthesis of the contribution of this thesis is made, and the conclusions resulting from the results presented are presented. Although each chapter of the thesis contains its own conclusions, the aim here is to gather the general conclusions to answer the question posed in section 1.3.

6.1 Summary of phase 1- optimal determination of acid molarity for removal of mortar adhered to RCA

When the RCA was submitted to treatment with HCl (chloric acid), a maximum removal of up to 14% of the mass was observed after one day of immersion. Similar values of removal of mortar present in the RCA were obtained after treatments carried out for 1, 3 and 6 days. Furthermore, it was found that increasing the acid concentration to values below 1.0 M of HCl did not result in great improvements in the performance of the acid removal. However, concentrations of 1.0 M and 3.0 M presented a greater impact on the mortar removal. In view of this, it is concluded that pre-soaking time is not a significant parameter for the removal of mortar in RCA.

With regard to RCA submerged in H_2SO_4 , it was found that low molarities are a suitable option to remove the mortar adhered to the RCA. This is because at molarities of 1M and 3M, the sulphate ion content contributes to a continuous degradation of the RCA, leaving it more brittle. As a result, it was concluded that it is necessary to improve the washing of the RCA, which entails greater water consumption and does not guarantee the total removal of sulphate ions. The obtained results contributed to reach the objectives proposed in the determination of the appropriate technique of removal. Besides, the methodology employed in this phase allowed decoupling the individual effects in the physical properties of the RCA, confirming that:

- Physical properties, such as water absorption and bulk density, showed significant improvements with the use of HCl;
- The morphology of the RCA after treatment with HCl and H_2SO_4 presented a smoother and rounder surface.

6.2 Summary of phase 2 - Evaluation of the mechanical, fracture and durability performance of mixes concrete incorporating RCA treated with acid solutions and with addition of aluminium sulphate

In this phase, the mechanical performance of mixes containing RCA treated with HCl and H_2SO_4 was evaluated, as well as concrete mixes with addition of aluminium sulphate (AS). The results indicated that the treatment with HCl solution improved the mechanical properties due to the removal of the mortar and the improvement of the surface, which increased the interaction between the aggregate and the cementitious matrix. This effect was evidenced in microstructural tests, in which the transition zone of influence (ITZ) interface was quantitatively evaluated using the Ca/Si atomic mass ratio technique obtained by EDS analysis. With regard to the concrete mixes treated with H_2SO_4 , it was concluded that the lower concentrations had a positive influence on the mechanical characteristics of the mixes. This occurred because high concentrations of H_2SO_4 for mortar removal resulted in the degradation of the adhered mortar when it comes into contact with the water in the mix, which is known as second degradation. As a result, the mechanical properties with this type of RCA were negatively affected.

Another technique used in this thesis was the addition of aluminium sulphate in a

proportion of 1.10% of the cement weight. The results indicated that this approach was effective in improving the mechanical properties. However, this improvement was not significant compared to the reference concrete. Specifically, when analysing the fracture energy results, a negative trend was observed compared to the reference concrete.

With regard to durability, the results followed the same trend, with the mixes containing RCA treated with HCl presenting improvements in relation to the reference concrete. Similarly, the mixes treated with H₂SO₄ showed improvements only at the lowest concentrations.

6.3 Final conclusions and future perspective.

In this thesis, the question that initiated this research has been addressed, presenting the most suitable procedures for acid removal, encompassing various types of acids, and their influence on different properties, especially in mixes containing aluminium sulphate (AS). The main conclusion of this study is that acid removal has shown remarkable efficacy at low acid concentrations and immersion times should not exceed one day to minimize potential environmental impacts. However, to fully comprehend the impact of these treatments on Compressive Strength of Mortar (CSM) and ensure a high level of confidence, both for potential industrial implementation and specific construction applications, it is essential to continue addressing some knowledge gaps related to the use of these mixes.

To deepen the study of acid treatments in mixes with recycled aggregates, it is important to consider some future aspects, such as:

- To observe the changes in the performance of these mixes when submitted to different curing conditions;
- To perform an economic analysis of the life cycle of these mixes with recycled aggregates;
- To evaluate the environmental impact of the acid removal processes in terms of the life cycle of the production of the RCA treated with acids;
- To carry out acid removal in recycled aggregates from recycling plants.

With regard to the use of aluminium sulphate, some possibilities for future study include:

- Addition of aluminium sulphates from waste from treatment plants that use a high concentration of aluminium sulphate as a flocculant;
- Evaluate the interaction of aluminium sulphate in different types of cement to determine the chemical influence of this compound in different cement compositions;
- To thermally modify the structure of aluminium sulphate present in waste from treatment plants, using the temperatures normally employed in industry.

7 REFERENCES

ABBAS, A.; FATHIFAZL, G.; FOURNIER, B.; ISGOR, O.B. ISGOR, R. ZAVIDIL, A.G. RAZAQPUR; and S. FOO. **Quantification of the residual mortar content in recycled concrete aggregates by image analysis**. *Materials Characterization*, 60, n. 7, p. 716-728, 2009.

ABBAS, A.; FATHIFAZL, G.; ISGOR, O. B.; RAZAQPUR, A. RAZAPQUR; B. FOUNIER and S. FOO. **Proposed method for determining the residual mortar content of recycled concrete aggregates**. *Journal of ASTM International*, 5, n. 1, p. 1-12, 2007.

ABNT. **Associação Brasileira de Normas Técnicas (ABNT)., NBR-15116 “Recycled aggregate of solid residue of building constructions-Requirements and Methodologies”**. Rio de Janeiro-RJ 2004.

ABNT. **Associação Brasileira de Normas Técnicas (ABNT)., NBR 6118: Projeto de estruturas de concreto — Procedimento**. Rio de Janeiro-RJ: 238 p. 2014.

ACI. **Guide for modeling and calculating shrinkage and creep in hardened concrete. ACI report. 209** 2008.

ACI. **ACI PRC-555-01: Removal and reuse of hardened concrete**. Farmington Hills 2022.

ACI **CODE 318-08: Building code requirements for structural concrete and commentary**. Farmington Hills, MI 48331: 473 p. 2007.

ADAM, I.; SAKATA, K.; AYANO, T. **Influence of coarse aggregate on the shrinkage of normal and high-strength concretes**. Okayama University Faculty of Environmental Science and Engineering Research Report, 6, n. 1, p. 41-45, 2001.

AİTCIN, P.-C.; MEHTA, P. K. **Effect of coarse aggregate characteristics on mechanical properties of high-strength concrete**. *Materials Journal*, 87, n. 2, p. 103-107, 1990.

AKBARNEZHAD, A.; ONG, K.; ZHANG, M.; TAM, C. **Acid treatment technique for determining the mortar content of recycled concrete aggregates**. *Journal of Testing and Evaluation*, 41, n. 3, p. 441-450, 2013.

AKBARNEZHAD, A.; ONG, K.; ZHANG, M.; TAM and T. FOO. **Microwave-assisted beneficiation of recycled concrete aggregates**. *Construction and Building Materials*, 25, n. 8, p. 3469-3479, 2011.

AKTAR, M. A.; ALAM, M. M.; AL-AMIN, A. Q. **Global economic crisis, energy use, CO2 emissions, and policy roadmap amid COVID-19**. *Sustainable Production and Consumption*, 26, p. 770-781, 2021.

AL-BAYATI, H. K. A.; DAS, P. K.; TIGHE, S. L.; BAAJ, H. **Evaluation of various treatment methods for enhancing the physical and morphological properties of coarse recycled concrete aggregate.** Construction and Building Materials, 112, p. 284-298, 2016.

ALEXANDER, M.; FOURIE, C. **Performance of sewer pipe concrete mixtures with portland and calcium aluminate cements subject to mineral and biogenic acid attack.** Materials and Structures, 44, n. 1, p. 313-330, 2011.

ALLAHVERDI, A.; SKVARA, F. **Acidic corrosion of hydrated cement based materials. Part 1.: Mechanism of the phenomenon.** Ceramics (Praha), 44, n. 3, p. 114-120, 2000.

ALLAHVERDI, A.; ŠKVÁRA, F. **Acidic corrosion of hydrated cement based materials.** Ceramics– Silikáty, 44, n. 4, p. 152-160, 2000.

AMORIM, P.; DE BRITO, J.; EVANGELISTA, L. **Concrete made with coarse concrete aggregate: influence of curing on durability.** ACI Materials Journal, 109, n. 2, p. 195-204, 2012.

ANGULO, S. C. **Caracterização de agregados de resíduos de construção e demolição reciclados e a influência de suas características no comportamento de concretos.** Universidade de São Paulo, 2005.

ANGULO, S. C.; OLIVEIRA, L. S.; MACHADO, L. **Pesquisa setorial ABRECON 2020: a reciclagem de resíduos de construção e demolição no Brasil.** 2022.

ANGULO, S. C.; CARRIJO, P. M.; FIGUEIREDO, A. D. D.; CHAVES and V. M. JOHN. **On the classification of mixed construction and demolition waste aggregate by porosity and its impact on the mechanical performance of concrete.** Materials and Structures, 43, n. 4, p. 519-528, 2010.

BALAYSSAC, J.-P. **Relations entre performances mécaniques, microstructure et durabilité des bétons.** 1992. -, Toulouse.

BARBUDO, A.; AGRELA, F.; AYUSO, J.; JIMÉNEZ, and C.S. POON. **Statistical analysis of recycled aggregates derived from different sources for sub-base applications.** Construction and Building Materials, 28, n. 1, p. 129-138, 2012.

BARBUDO, A.; DE BRITO, J.; EVANGELISTA, L.; BRAVO, and F. AGRELA. **Influence of water-reducing admixtures on the mechanical performance of recycled concrete.** Journal of Cleaner Production, 59, p. 93-98, 2013.

BARGER, G.S.; BAYLES, J.; BLAIR, B.; BROWN, D.; CHEN, H.; CONWAY, T.; HAWKINS, P. **Ettringite Formation and the Performance of Concrete.** Portland Cement Association R&D, New York, pp. 1–16, 2001.

BEDDOE, R. E.; DORNER, H. W. **Modelling acid attack on concrete: Part I. The essential mechanisms.** Cement and Concrete Research, 35, n. 12, p. 2333-2339, 2005.

BELIN, P.; HABERT, G.; THIERY, M.; ROUSSEL, N. **Cement paste content and water absorption of recycled concrete coarse aggregates**. *Materials and Structures*, 47, n. 9, p. 1451-1465, 2014.

BESHR, H.; ALMUSALLAM, A.; MASLEHUDDIN, M. **Effect of coarse aggregate quality on the mechanical properties of high strength concrete**. *Construction and Building Materials*, 17, n. 2, p. 97-103, 2003.

BORDELON, A.; CERVANTES, V.; ROESLER, J. R. **Fracture properties of concrete containing recycled concrete aggregates**. *Magazine of Concrete Research*, 61, n. 9, p. 665-670, 2009.

BRANSON, D. E.; CHRISTIASON, M. **Time dependent concrete properties related to design-strength and elastic properties, creep, and shrinkage**. *Special Publication*, 27, p. 257-278, 1971.

BRAZ, I.G.; SHINZATO, M.C.; MONTANHEIRO, T.J.; DE ALMEIDA, T.M. and DE SOUZA CARVALHO, F.M. **Effect of the addition of aluminum recycling waste on the pozzolanic activity of sugarcane bagasse ash and zeolite**. *Waste Biomass Valor* 10, 3493–3513 (2019).

BRITISH STANDARD, E. 206, *Concrete specifications, performance, production and conformity*. BSI, London, 2016.

BROWN, J. D. **Advanced statistics for the behavioral sciences**. Springer, 2018. 331993547X.

BROWN, P.; TAYLOR, H. **The role of ettringite in external sulfate attack. Special Issue Sulfate attack mechanisms**. *Materials Science of Concrete*, p. 73-98, 1999.

BROWN, T.; LEMAY, H.; BURSTEN, B. B. *JR Química: A ciência central.* : São Paulo: Pearson Education 2007.

BROWN, T. L.; LEMAY JR, H. E.; BURSTEN, B. E.; BURDGE, J. R. **Química: la ciencia central**. Pearson educación, 2004. 9702604680.

BRYKOV, A.; ANISIMOVA, A. **Efficacy of aluminum hydroxides as inhibitors of alkali-silica reactions**. *Mater. Sci. Appl.* 4, 1–6, 2013.

BUTLER, L.; WEST, J.; TIGHE, S. **The effect of recycled concrete aggregate properties on the bond strength between RCA concrete and steel reinforcement**. *Cement and Concrete Research*, 41, n. 10, p. 1037-1049, 2011.

BUTLER, L.; WEST, J. S.; TIGHE, S. L. **Effect of recycled concrete coarse aggregate from multiple sources on the hardened properties of concrete with equivalent compressive strength**. *Construction and Building Materials*, 47, p. 1292-1301, 2013.

ÇAKIR, Ö. **Experimental analysis of properties of recycled coarse aggregate (RCA) concrete with mineral additives**. *Construction and Building Materials*, 68, p. 17-25,

2014.

CASUCCIO, M.; TORRIJOS, M.; GIACCIO, G.; ZERBINO, R. **Failure mechanism of recycled aggregate concrete.** Construction and Building Materials, 22, n. 7, p. 1500-1506, 2008.

CHATTERJI, S.; JEFFERY, J. **Studies of early stages of paste hydration of different types of portland cements.** Journal of the American Ceramic Society, 46, n. 6, p. 268-273, 1963.

CHEN, C.; SUN, Z. **Influence of aluminum sulfate on hydration and properties of cement pastes.** Journal of Advanced Concrete Technology, 16, n. 10, p. 522-530, 2018.

CHU, D. C.; KLEIB, J.; AMAR, M.; BENZERZOUR, M. and N-E. ABRIAK. **Determination of the degree of hydration of Portland cement using three different approaches: scanning electron microscopy (SEM-BSE) and Thermogravimetric analysis (TGA).** Case Studies in Construction Materials, 15, p. e00754, 2021.

CLIFTON, J. R.; POMMERSHEIM, J. **Sulfate attack of cementitious materials: volumetric relations and expansions.** NIST IR, 5390, 1994.

CODY, A.; LEE, H.; CODY, R.; SPRY, P. **The effects of chemical environment on the nucleation, growth, and stability of ettringite $[\text{Ca}_3\text{Al}(\text{OH})_6]_2(\text{SO}_4)_3 \cdot 26\text{H}_2\text{O}$.** Cement and Concrete Research, 34, n. 5, p. 869-881, 2004.

COMMITTEE, A. **ACI 211.1-91 Standard practice for selecting proportions for normal, heavyweight, and mass concrete, no. 9.** Unites States, p. 120-121, 2002.

COUTINHO, A. D. S.; GONÇALVES, A. **Fabrico e propriedades do betão.** Lisboa: Laboratório Nacional de Engenharia Civil, p. 401, 1997.

CUI, H.; SHI, X.; MEMON, S. A.; XING, F. and TANG, W. **Experimental study on the influence of water absorption of recycled coarse aggregates on properties of the resulting concretes.** Journal of Materials in Civil Engineering, 27, n. 4, p. 04014138, 2014.

DE BRITO, J.; AGRELA, F.; SILVA, R. V. **Legal regulations of recycled aggregate concrete in buildings and roads.** In: *New Trends in Eco-efficient and Recycled Concrete*: Elsevier, 2019. p. 509-526.

DE BRITO, J.; SAIKIA, N. **Recycled aggregate in concrete: use of industrial, construction and demolition waste.** Springer Science & Business Media, 2012. 1447145402.

DE BRITO, J.; SILVA, R. **Current status on the use of recycled aggregates in concrete: Where do we go from here?.** RILEM Technical Letters, 1, p. 1-5, 2016.

DE JUAN, M. S.; GUTIÉRREZ, P. A. **Study on the influence of attached mortar content on the properties of recycled concrete aggregate.** Construction and Building Materials, 23, n. 2, p. 872-877, 2009.

- DERMATAS, D. **Ettringite-induced swelling in soils: State-of-the-art.** 1995.
- DIN 4226-100, Aggregates for concrete and mortar - Part 100: Recycled aggregates.** DiN; Berlin: 29 p. 2002.
- DYER, T. **Concrete durability.** CRC Press, 2014. 0203862112.
- ELICES, M; PLANAS, J. **Fracture mechanics parameters of concrete: an overview.** Advanced Cement Based Materials. 1996 Oct 1;4(3-4):116-27.
- EN. Eurocode 2: **Design of concrete structures—Part 1-1: General rules and rules for buildings.** London: British Standard Institution, 2004.
- EN. Eurocode 2: **Design of concrete structures-Part 2: Concrete bridges, Design and detailing rules+ National Annex.** Bratislava, SUTN, 2007.
- ETXEBERRIA, M.; VÁZQUEZ, E.; MARÍ, A.; BARRA, M. **Influence of amount of recycled coarse aggregates and production process on properties of recycled aggregate concrete.** Cement and Concrete Research, 37, n. 5, p. 735-742, 2007.
- EU, C. D. **98/83/EC of 3 November 1998 on the quality of water intended for human consumption.** Official Journal of the European Communities, 1998.
- EVANGELISTA, L.; DE BRITO, J. **Concrete with fine recycled aggregates: a review.** European Journal of Environmental and Civil Engineering, 18, n. 2, p. 129-172, 2014.
- FATHIFAZL, G.; ABBAS, A.; RAZAQPUR, A. G.; ISGOR, O. B. and S. FOO. **New mixture proportioning method for concrete made with coarse recycled concrete aggregate.** Journal of Materials in Civil Engineering, 21, n. 10, p. 601-611, 2009.
- FAURY, J. **Le béton.** 3^{ème} édition ed. Paris: 1985.
- FERREIRA, L.; DE BRITO, J.; BARRA, M. **Influence of the pre-saturation of recycled coarse concrete aggregates on concrete properties.** Magazine of Concrete Research, 63, n. 8, p. 617-627, 2011.
- FORERO, J. A.; BRITO, J. D.; EVANGELISTA, L.; PEREIRA, C. **Improvement of the quality of recycled concrete aggregate subjected to chemical treatments: A review.** Materials, 15, n. 8, p. 2740, 2022.
- GARCÍA-GONZÁLEZ, J.; BARROQUEIRO, T.; EVANGELISTA, L.; DE BRITO, J. DE BELIE.; J. MORÁN-DEL POZO. and JUAN-VALDÉS. **Fracture energy of coarse recycled aggregate concrete using the wedge splitting test method: influence of water-reducing admixtures.** Materials and Structures, 50, n. 2, p. 120, 2017.
- GESOGLU, M.; GÜNEYISI, E.; ÖZ, H. Ö.; TAHA, I. and YASEMIN, M. T. **Failure characteristics of self-compacting concretes made with recycled aggregates.** Construction and Building Materials, 98, p. 334-344, 2015.

GHORBEL, E.; WARDEH, G. **Influence of recycled coarse aggregates incorporation on the fracture properties of concrete.** Construction and Building Materials, 154, p. 51-60, 2017.

GHORBEL, E.; WARDEH, G.; FARES, H. **Mechanical and fracture properties of recycled aggregate concrete in design codes and empirical models.** Structural Concrete, 20, n. 6, p. 2156-2170, 2019.

HALL, C. **Water sorptivity of mortars and concretes: a review.** Magazine of Concrete Research, 41, n. 147, p. 51-61, 1989.

HAN, J.; WANG, K.; WANG, Y.; SHI, J. **Study of aluminum sulfate and anhydrite on cement hydration process.** Materials and Structures, 49, n. 4, p. 1105-1114, 2016.

HANSEN, T. C. **Recycled aggregates and recycled aggregate concrete second state-of-the-art report developments 1945–1985.** Materials and Structures, 19, p. 201-246, 1986.

HANSEN, T. C.; NARUD, H. **Strength of recycled concrete made from crushed concrete coarse aggregate.** Concrete International, 5, n. 1, p. 79-83, 1983.

HE, H.; WANG, Y.; WANG, J. **Effects of aggregate micro fines (AMF), aluminum sulfate and polypropylene fiber (PPF) on properties of machine-made sand concrete.** Applied Sciences, 9, n. 11, p. 2250, 2019.

HE, T.; YANG, R.; GUO, X.; XU, R. and FAN, X. **Effects of liquid accelerators on carbonation properties of C3A and C3S hydration products.** Advances in Cement Research, 33, n. 8, p. 367-376, 2021.

HELENE, P. D. L. **Contribuição ao estudo da corrosão em armaduras de concreto armado.** São Paulo, 231, p. 14, 1993.

HEWLETT, P.; LISKA, M. **Lea's chemistry of cement and concrete.** Butterworth-Heinemann, 2019. 0081007957.

HILLERBORG, A.; MODÉER, M.; PETERSSON, P.-E. **Analysis of crack formation and crack growth in concrete by means of fracture mechanics and finite elements.** Cement and Concrete Research, 6, n. 6, p. 773-781, 1976.

HILLS, T. P.; GORDON, F.; FLORIN, N. H.; FENNELL, P. S. **Statistical analysis of the carbonation rate of concrete.** Cement and Concrete Research, 72, p. 98-107, 2015.

HUA, C.; EHRLACHER, A.; ACKER, P. **Analyses and models of the autogenous shrinkage of hardening cement paste II. Modelling at scale of hydrating grains.** Cement and Concrete Research, 27, n. 2, p. 245-258, 1997.

IEA. **Buildings.** Paris. 2022a.

IEA. **Global Energy Review: CO₂ Emissions in 2021-Global emissions rebound sharply to highest ever level: International Energy Agency Paris, France 2022b.**

ISHIGURO, S.; STANZL-TSCHEGG, S.; TSCHEGG, E.; TRAVNICEK, R. **Mode I fracture behaviour of recycled concrete**. Fracture Mechanics of Concrete Structures, ProceediRgs FRAMCOS-2, p. 145-154, 1995.

ISMAIL, S.; RAMLI, M., 2013, **Effect surface treatment of recycled concrete aggregate on properties of fresh and hardened concrete**. IEEE. 651-656.

ISMAIL, S.; RAMLI, M. **Engineering properties of treated recycled concrete aggregate (RCA) for structural applications**. Construction and Building Materials, 44, p. 464-476, Jul 2013.

ISMAIL, S.; RAMLI, M. **Mechanical strength and drying shrinkage properties of concrete containing treated coarse recycled concrete aggregates**. Construction and Building Materials, 68, p. 726-739, 2014.

Instituto Brasileiro de Geografia e Estatística | Secretaria Especial de Articulação Social. **Indicadores Brasileiros para os objetivos de desenvolvimento sustentável**. Disponível em: <https://odsbrasil.gov.br/>. Acesso em: 10 Agosto de 2023.

JIS. **JIS A 5021, JIS A5021. Recycled aggregate for concrete-Class H (Amendment 1)**. 2006.

JOHN, V. M. **Reciclagem de resíduos na construção civil: contribuição à metodologia de pesquisa e desenvolvimento**. 2000. -, Universidade de São Paulo.

KAN, C. Y.; LAN, M. Z.; KONG, L. M.; YANG, J. B., 2013, **Effect of aluminium sulfate on cement properties**. Trans Tech Publ. 285-291.

KAPOOR, K.; BOHROO, A. U. R. **Study on the influence of attached mortar content on the properties of recycled concrete aggregate**. Sustainable Engineering: Proceedings of EGRWSE 2018, p. 337-347, 2019.

KARI, O.-P.; PUTTONEN, J.; SKANTZ, E. **Reactive transport modelling of long-term carbonation**. Cement and Concrete Composites, 52, p. 42-53, 2014.

KAZEMIAN, F.; ROOHOLAMINI, H.; HASSANI, A. **Mechanical and fracture properties of concrete containing treated and untreated recycled concrete aggregates**. Construction and Building Materials, 209, p. 690-700, 2019.

KHALILPOUR, S.; BANIASAD, E.; DEHESTANI, M. **A review on concrete fracture energy and effective parameters**. Cement and Concrete Research, 120, p. 294-321, 2019.

KHEDER, G.; AL-WINDAWI, S. **Variation in mechanical properties of natural and recycled aggregate concrete as related to the strength of their binding mortar**. Materials and Structures, 38, n. 7, p. 701-709, 2005.

KIM, H.-S.; KIM, B.; KIM, K.-S.; KIM, J.-M. **Quality improvement of recycled aggregates using the acid treatment method and the strength characteristics of the**

resulting mortar. Journal of Material Cycles and Waste Management, 19, n. 2, p. 968-976, 2017.

KIM, Y.; HANIF, A.; KAZMI, S. M.; MUNIR, M. J. and PARK, C. **Properties enhancement of recycled aggregate concrete through pretreatment of coarse aggregates—Comparative assessment of assorted techniques.** Journal of Cleaner Production, 191, p. 339-349, 2018.

KOU, S.-C.; POON, C.-S. **Properties of concrete prepared with PVA-impregnated recycled concrete aggregates.** Cement and Concrete Composites, 32, n. 8, p. 649-654, 2010.

KUMAR, S.; BARAI, S. V.; KUMAR, S.; BARAI, S. V. **Introduction to Fracture Mechanics of Concrete.** Concrete Fracture Models and Applications, p. 1-8, 2011.

KUNTHER, W.; FERREIRO, S.; SKIBSTED, J. **Influence of the Ca/Si ratio on the compressive strength of cementitious calcium–silicate–hydrate binders.** Journal of Materials Chemistry A, 5, n. 33, p. 17401-17412, 2017.

KURDA, R.; DE BRITO, J.; SILVESTRE, J. D. **Water absorption and electrical resistivity of concrete with recycled concrete aggregates and fly ash.** Cement and Concrete Composites, 95, p. 169-182, 2019.

KURDOWSKI, W. **Cement and concrete chemistry.** Springer Science & Business, 2014. 9400779453.

KWAN, W. H.; RAMLI, M.; KAM, K. J.; SULIEMAN, M. Z. **Influence of the amount of recycled coarse aggregate in concrete design and durability properties.** Construction and Building Materials, 26, n. 1, p. 565-573, 2012.

LEE, C.-H.; DU, J.-C.; SHEN, D.-H. **Evaluation of pre-coated recycled concrete aggregate for hot mix asphalt.** Construction and Building Materials, 28, n. 1, p. 66-71, 2012.

LEITE, M. B. **Avaliação de propriedades mecânicas de concretos produzidos com agregados reciclados de resíduos de construção e demolição.** Tese doutorado, Universidade Federal do Rio Grande do Sul, Escola de Engenharia, Porto Alegre-Brasil, 290pp, 2001.

LI, Z. **Advanced concrete technology.** John Wiley & Sons, 2022. 1119806259.

LIU, X.; MA, B.; TAN, H.; GU, B.; ZHANG, T.; CHEN, P.; LI, H and MEI, J. **Effect of aluminum sulfate on the hydration of Portland cement, tricalcium silicate and tricalcium aluminate.** Construction and Building Materials, 232, p. 117179, 2020.

LNEC. **E 391 Betões: determinação da resistência à carbonatação.** Lisboa 1993.

LNEC. **E 463 Betões: Determinação do coeficiente de difusão dos cloretos por ensaio de migração em regime estacionário.** Lisboa 2004.

LNEC. E 471-2009. Guia para a utilização de agregados reciclados grossos em betões de ligantes hidráulicos. Lisboa 2009.

LNEC E 398 Betões: determinação da retracção e da expansão. Lisboa: 2 p. 1993.

LYE, C.-Q.; DHIR, R. K.; GHATAORA, G. S. **Elastic modulus of concrete made with recycled aggregates.** Proceedings of the Institution of Civil Engineers-Structures and Buildings, 169, n. 5, p. 314-339, 2016.

MAKUL, N. **A review on methods to improve the quality of recycled concrete aggregates.** Journal of Sustainable Cement-Based Materials, p. 1-27, 2020.

MAKUL, N. **A review on methods to improve the quality of recycled concrete aggregates.** Journal of Sustainable Cement-Based Materials, 10, n. 2, p. 65-91, 2021.

MATIAS, D.; DE BRITO, J.; ROSA, A.; PEDRO, D. **Durability of concrete with recycled coarse aggregates: influence of superplasticizers.** Journal of Materials in Civil Engineering, 26, n. 7, p. 06014011, 2014.

MEDINA, C.; FRÍAS, M.; DE ROJAS, M. S.; THOMAS, C. and POLACO, J-A. **Gas permeability in concrete containing recycled ceramic sanitary ware aggregate.** Construction and Building Materials, 37, p. 597-605, 2012.

MEDINA, C.; ZHU, W.; HOWIND, T.; DE ROJAS, M. I. S. and FRIAS, M. **Influence of mixed recycled aggregate on the physical–mechanical properties of recycled concrete.** Journal of Cleaner Production, 68, p. 216-225, 2014.

MEHTA, P. K. **Mechanism of sulfate attack on portland cement concrete—Another look.** Cement and Concrete Research, 13, n. 3, p. 401-406, 1983.

MEHTA, P. K.; MONTEIRO, P. J. **Concrete microstructure, properties and materials.** McGraw-Hill education, 2017.

MEYER, R.; KRUEGER, D. **Minitab guide to statistics.** Prentice Hall PTR, 2001. 0130141569.

MIHASHI, H.; NOMURA, N.; NIISEKI, S. **Influence of aggregate size on fracture process zone of concrete detected with three dimensional acoustic emission technique.** Cement and Concrete Research, 21, n. 5, p. 737-744, 1991.

MIN, H.; SONG, Z. **Investigation on the sulfuric acid corrosion mechanism for concrete in soaking environment.** Advances in Materials Science and Engineering, 2018.

MINDESS, S.; YOUNG, F.; DARWIN, D. **Concrete 2nd Edition.** Technical Documents, 2003.

MOVASSAGHI, R. **Durability of reinforced concrete incorporating recycled concrete as aggregate (RCA).** Master`s Thesis, University of Waterloo, 2006.

MUDULI, R.; MUKHARJEE, B. B. **Performance assessment of concrete incorporating recycled coarse aggregates and metakaolin: A systematic approach.** Construction and Building Materials, 233, p. 117223, 2020.

NEVILLE, A. M. **Properties of concrete.** Longman London, 1995.

NEVILLE, A. M.; BROOKS, J. J. **Concrete technology.** Longman Scientific & Technical England, 1987.

NP EN 12390-1. EN 12390-1 Ensaios ao betão endurecido. Parte 1: Forma, dimensão e outros requisitos para o ensaio de provetes e para moldes. IPQ, Caparica Portugal 2012.

NP EN 197-1. Cimento - Parte 1: Composição, especificação e critérios de conformidade para cimentos correntes. IPQ, Caparica Portugal 2001.

NP EN. 206-1: 2007–Betão. Parte I: Especificação, desempenho, produção e conformidade. IPQ, Caparica Portugal 2007.

NP EN 933-1, Ensaios das propriedades geométricas dos agregados Parte 1: Análise granulométrica Método da peneiração. IPQ, Caparica Portugal 2014.

NP EN 1097-6, Test for mechanical and physical properties of aggregates-Part 6: Determination of particle density and water absorption. IPQ, Caparica Portugal 2013.

NP EN 1097-6, Tests for mechanical and physical properties of aggregates - Part 6: Determination of particle density and water absorption. IPQ, Caparica Portugal 2013.

NP EN 12350-6. Ensaios do betão fresco. Parte 6. IPQ, Caparica Portugal: 13 p. 2002.

NP EN 12390-3, Ensaios do betão endurecido. Parte 3: Resistência à compressão dos provetes de ensaio. IPQ, Caparica Portugal : 23 p. 2021.

NP EN-126020. Aggregates for concrete. IPQ, Caparica Portugal: 61 P. 2010.

NTC. Norme Tecniche per le Costruzioni, Decreto del Ministero delle infrastrutture, Supplemento Ordinario n.30 alla Gazzetta Ufficiale. Italian Ministry of Infrastructure and Transport, NTC 2008 - Italian Building Code. 2008.

OGAWA, H.; NAWA, T. **Improving the quality of recycled fine aggregate by selective removal of brittle defects.** Journal of Advanced Concrete Technology, 10, n. 12, p. 395-410, 2012.

OLLIVIER, J.; MASO, J.; BOURDETTE, B. **Interfacial transition zone in concrete.** Advanced Cement Based Materials, 2, n. 1, p. 30-38, 1995.

OTSUKI, N.; MIYAZATO, S.-I.; YODSUDJAI, W. **Influence of recycled aggregate on interfacial transition zone, strength, chloride penetration and carbonation of concrete.** Journal of Materials in Civil Engineering, 15, n. 5, p. 443-451, 2003.

PANDURANGAN, K.; DAYANITHY, A.; PRAKASH, S. O. **Influence of treatment methods on the bond strength of recycled aggregate concrete.** Construction and Building Materials, 120, p. 212-221, 2016.

Panorama – Abrelpe. Disponível em: <<https://abrelpe.org.br/panorama/>>

PARROTT, L. **Water absorption in cover concrete.** Materials and Structures, 25, p. 284-292, 1992.

PAVLIK, V. **Corrosion of hardened cement paste by acetic and nitric acids Part III: Influence of water/cement ratio.** Cement and Concrete Research, 26, n. 3, p. 475-490, 1996.

PAVLIK, V.; UNČÍK, S. **The rate of corrosion of hardened cement pastes and mortars with additive of silica fume in acids.** Cement and Concrete Research, 27, n. 11, p. 1731-1745, 1997.

PEDRO, D.; DE BRITO, J.; EVANGELISTA, L. **Influence of the use of recycled concrete aggregates from different sources on structural concrete.** Construction and Building Materials, 71, p. 141-151, 2014.

PELISSER, F.; GLEIZE, P. J. P.; MIKOWSKI, A. **Effect of the Ca/Si molar ratio on the micro/nanomechanical properties of synthetic CSH measured by nanoindentation.** The Journal of Physical Chemistry C, 116, n. 32, p. 17219-17227, 2012.

PERDIKARIS, P. C.; ROMEO, A. **Size effect on fracture energy of concrete and stability issues in three-point bending fracture toughness testing.** Materials Journal, 92, n. 5, p. 483-496, 1995.

Pesquisa Setorial - Abrecon. Disponível em: <<https://abrecon.org.br/pesquisa/>>. Acesso em: 12 jul. 2023.

PETERSON, P. **Fracture energy of concrete: Method of determination.** Cement and Concrete Research, 10, n. 1, p. 79-89, 1980.

PINTO, T. D. P. **Metodologia para a gestão diferenciada de resíduos sólidos da construção urbana.** 1999. Tese (Doutorado)-Universidade de São Paulo, São Paulo, 1999.

POON, C. S.; SHUI, Z.; LAM, L. **Effect of microstructure of ITZ on compressive strength of concrete prepared with recycled aggregates.** Construction and Building Materials, 18, n. 6, p. 461-468, 2004.

PURUSHOTHAMAN, R.; AMIRTHAVALLI, R. R.; KARAN, L. **Influence of treatment methods on the strength and performance characteristics of recycled aggregate concrete.** Journal of Materials in Civil Engineering, 27, n. 5, p. 04014168, 2014.

PURUSHOTHAMAN, R.; AMIRTHAVALLI, R. R.; KARAN, L. **Influence of**

treatment methods on the strength and performance characteristics of recycled aggregate concrete. Journal of Materials in Civil Engineering, 27, n. 5, p. 04014168, 2015.

RADEVIĆ, A.; DESPOTOVIĆ, I.; ZAKIĆ, D.; OREŠKOVIĆ, M. and JEVIT'Ć, D. **Influence of acid treatment and carbonation on the properties of recycled concrete aggregate.** Chemical Industry and Chemical Engineering Quarterly/CICEQ, 24, n. 1, p. 23-30, 2018.

RAMASWAMY, K.; SANTHANAM, M. **Influence of mineralogical nature of aggregates on acid resistance of mortar.** In: Sixth International Conference on Durability of Concrete Structures, Leeds, United Kingdom, 2019.

RILEM, T. 121-DRG. **Specifications for concrete with recycled aggregates.** Materials and Structures, 27, n. 9, p. 557-559, 1994.

RODRÍGUEZ, G.; ALEGRE, F. J.; MARTÍNEZ, G. **The contribution of environmental management systems to the management of construction and demolition waste: The case of the Autonomous Community of Madrid (Spain).** Resources, Conservation and Recycling, 50, n. 3, p. 334-349, 2007.

RYU, H.-S.; KIM, D.-M.; SHIN, S.-H.; LIM, S.-M. and -J. PARK. W. **Evaluation on the surface modification of recycled fine aggregates in aqueous H₂SiF₆ solution.** International Journal of Concrete Structures and Materials, 12, p. 1-11, 2018.

SALESA, Á.; PÉREZ-BENEDICTO, J. A.; COLORADO-ARANGUREN, D.; LÓPEZ-JULIÁN, P. L. ESTEBAN, L. M.; SANZ-BALDÚZ, L. J.; SÁEZ-HOSTALED, J.L.; RAMIS, J. and OLIVARES, D. **Physico-mechanical properties of multi-recycled concrete from precast concrete industry.** Journal of Cleaner Production, 141, p. 248-255, 2017.

SÁNCHEZ DE JUAN, M. **Estudio sobre la utilización de árido reciclado para la fabricación de hormigón estructural.** Teses Doctoral - Universidad Politécnica de Madrid. Departamento de Ingeniería Civil: Construcción-Caminos, Madrid, 2017, 381p.

SARAVANAKUMAR, P.; ABHIRAM, K.; MANOJ, B. **Properties of treated recycled aggregates and its influence on concrete strength characteristics.** Construction and Building Materials, 111, p. 611-617, 2016.

SARKAR, S.; MAHADEVAN, S.; MEEUSSEN, J.; VAN DER SLOOT, H. and KOSSON, D. **Numerical simulation of cementitious materials degradation under external sulfate attack.** Cement and Concrete Composites, 32, n. 3, p. 241-252, 2010.

SATO, R.; MARUYAMA, I.; SOGABE, T.; SOGO, M. **Flexural behavior of reinforced recycled concrete beams.** Journal of Advanced Concrete Technology, 5, n. 1, p. 43-61, 2007.

SCRIVENER, K.; YOUNG, J. F. **Mechanisms of chemical degradation of cement-based systems.** CRC Press, 1997. 0429178409.

SCRIVENER, K.; YOUNG, J. F. **Mechanisms of chemical degradation of cement-based systems**. CRC Press, 2014. 1482294958.

SHABAN, W. M.; YANG, J.; SU, H.; MO, K. H., and XIE, J. **Quality Improvement Techniques for Recycled Concrete Aggregate: A review**. Journal of Advanced Concrete Technology, 17, n. 4, p. 151-167, 2019.

SHAH, S. P.; SWARTZ, S. E.; OUYANG, C. **Fracture mechanics of concrete: applications of fracture mechanics to concrete, rock and other quasi-brittle materials**. John Wiley & Sons, 1995. 0471303119.

SHI, C.; LI, Y.; ZHANG, J.; LI, W.; CHONG, L. and XIE, Z. **Performance enhancement of recycled concrete aggregate—a review**. Journal of Cleaner Production, 112, p. 466-472, 2016.

SHI, C.; STEGEMANN, J. **Acid corrosion resistance of different cementing materials**. Cement and Concrete Research, 30, n. 5, p. 803-808, 2000.

SHIMA, H.; TATEYASHIKI, H.; MATSUHASHI, R.; YOSHIDA, Y. **An advanced concrete recycling technology and its applicability assessment through input-output analysis**. Journal of Advanced Concrete Technology, 3, n. 1, p. 53-67, 2005.

SIDDIQUE, R.; CACHIM, P. **Waste and supplementary cementitious materials in concrete: characterisation, properties and applications**. Woodhead Publishing, 2018. 0081021577.

SIDOROVA, A.; VAZQUEZ-RAMONICH, E.; BARRA-BIZINOTTO, M.; ROA-ROVIRA, J. J. and JIMENEZ-PIQUE, E. **Study of the recycled aggregates nature's influence on the aggregate–cement paste interface and ITZ**. Construction and Building Materials, 68, p. 677-684, 2014.

SILVA, R.; DE BRITO, J.; DHIR, R. **The influence of the use of recycled aggregates on the compressive strength of concrete: A review**. European Journal of Environmental and Civil Engineering, 19, n. 7, p. 825-849, 2015.

SILVA, R.; DE BRITO, J.; DHIR, R. **Fresh-state performance of recycled aggregate concrete: A review**. Construction and Building Materials, 178, p. 19-31, 2018.

SILVA, R.; NEVES, R.; DE BRITO, J.; DHIR, R. **Carbonation behaviour of recycled aggregate concrete**. Cement and Concrete Composites, 62, p. 22-32, 2015.

SILVA, R. V.; BRITO, J. D.; NEVES, R.; DHIR, R. **Prediction of chloride ion penetration of recycled aggregate concrete**. Materials Research, 18, p. 427-440, 2015.

SILVA, R. V.; DE BRITO, J.; DHIR, R. **Properties and composition of recycled aggregates from construction and demolition waste suitable for concrete production**. Construction and Building Materials, 65, p. 201-217, 2014.

SILVA, R. V.; DE BRITO, J.; DHIR, R. K. **Establishing a relationship between modulus of elasticity and compressive strength of recycled aggregate concrete**.

Journal of Cleaner Production, 112, p. 2171-2186, 2016.

SIMEONOV, P.; AHMAD, S. **Effect of transition zone on the elastic behavior of cement-based composites.** Cement and Concrete Research, 25, n. 1, p. 165-176, 1995.

SONG, X.; QIAO, P.; WEN, H. **Recycled aggregate concrete enhanced with polymer aluminium sulfate.** Magazine of Concrete Research, 67, n. 10, p. 496-502, 2015.

SRI RAVINDRARAJAH, R.; TAM, C. **Properties of concrete made with crushed concrete as coarse aggregate.** Magazine of Concrete Research, 37, n. 130, p. 29-38, 1985.

SUI, Y.; MUELLER, A. **Development of thermo-mechanical treatment for recycling of used concrete.** Materials and Structures, 45, n. 10, p. 1487-1495, 2012.

SZELĄG, M. **Influence of specimen's shape and size on the thermal cracks' geometry of cement paste.** Construction and Building Materials, 189, p. 1155-1172, 2018.

TABSH, S. W.; ABDEL FATAH, A. S. **Influence of recycled concrete aggregates on strength properties of concrete.** Construction and Building Materials, 23, n. 2, p. 1163-1167, 2009.

TAM, V. W.; SOOMRO, M.; EVANGELISTA, A. C. J. **A review of recycled aggregate in concrete applications (2000–2017).** Construction and Building Materials, 172, p. 272-292, 2018.

TAM, V. W.; TAM, C. M. **Parameters for assessing recycled aggregate and their correlation.** Waste Management & Research, 27, n. 1, p. 52-58, 2009.

TAM, V. W.; TAM, C. M.; LE, K. N. **Removal of cement mortar remains from recycled aggregate using pre-soaking approaches.** Resources, Conservation and Recycling, 50, n. 1, p. 82-101, 2007.

TAM, V. W. Y.; TAM, C. M.; LE, K. N. **Removal of cement mortar remains from recycled aggregate using pre-soaking approaches.** Resources Conservation and Recycling, 50, n. 1, p. 82-101, Mar 2007.

TANG, A. J.; DE JESUS, R.; CUNANAN, A. **Microstructure and mechanical properties of concrete with treated recycled concrete aggregates.** International Journal, 16, n. 57, p. 21-27, 2019.

TAYLOR, H.; NEWBURY, D. **An electron microprobe study of a mature cement paste.** Cement and Concrete Research, 14, n. 4, p. 565-573, 1984.

TEGGUER, A. D. **Determining the water absorption of recycled aggregates utilizing hydrostatic weighing approach.** Construction and Building Materials, 27, n. 1, p. 112-116, 2012.

THOMAS, C.; SETIÉN, J.; POLANCO, J.; ALAEJOS, P. and DE JUAN, M. S.

Durability of recycled aggregate concrete. Construction and Building Materials, 40, p. 1054-1065, 2013.

THOMAS, J.; THAICKAVIL, N. N.; WILSON, P. **Strength and durability of concrete containing recycled concrete aggregates.** Journal of Building Engineering, 19, p. 349-365, 2018.

THOMPSON, M. R. **The split-tensile strength of lime-stabilized soils.** Highway Research Record, 1966.

VALENTA, O. **The significance of the aggregate-cement bond for the durability of concrete.** Durabilite des Betons, pp.53-87, 1961.

VERIAN, K. P.; ASHRAF, W.; CAO, Y. **Properties of recycled concrete aggregate and their influence in new concrete production.** Resources, Conservation and Recycling, 133, p. 30-49, 2018.

WALPOLE, R. E.; MYERS, R. H.; MYERS, S. L.; YE, K. **Probability and statistics for engineers and scientists.** Boston: Prentice Hall, 1993.

WANG, L.; WANG, J.; QIAN, X.; CHEN, P.; XU, Y. and GUO, J. **An environmentally friendly method to improve the quality of recycled concrete aggregates.** Construction and Building Materials, 144, p. 432-441, 2017.

WANG, R.; YU, N.; LI, Y. **Methods for improving the microstructure of recycled concrete aggregate: A review.** Construction and Building Materials, 242, p. 118164, 2020.

WANG, Y.; HE, X.; SU, Y.; MA, B. and JIANG, B. **Effect of aluminium phases on thaumasite formation in cement slurries containing limestone powder.** Magazine of Concrete Research, 70, n. 12, p. 610-616, 2018.

WARDEH, G.; GHORBEL, E. **Prediction of fracture parameters and strain-softening behavior of concrete: effect of frost action.** Materials and Structures, 48, p. 123-138, 2015.

WB(W) (ED.). **Specifications Facilitating the Use of Recycled Aggregates.** Disponível em: <https://www.devb.gov.hk/filemanager/technicalcirculars/en/upload/138/1/wb1202.pdf>. Acesso em: 12 jul. 2023.

WIRQUIN, E.; HADJIEVA-ZAHARIEVA, R.; BUYLE-BODIN, F. **Use of water absorption by concrete as a criterion of the durability of concrete-application to recycled aggregated concrete.** Materials and Structures, 33, p. 403-408, 2000.

XIAO, J.; LI, W.; SUN, Z.; LANGE, D. A. and SHAH, S. P. **Properties of interfacial transition zones in recycled aggregate concrete tested by nanoindentation.** Cement and Concrete Composites, 37, p. 276-292, 2013.

XUAN, D.; ZHAN, B.; POON, C. S. **Durability of recycled aggregate concrete**

prepared with carbonated recycled concrete aggregates. Cement and Concrete Composites, 84, p. 214-221, 2017.

YING, J.; HAN, Z.; SHEN, L.; LI, W. **Influence of parent concrete properties on compressive strength and chloride diffusion coefficient of concrete with strengthened recycled aggregates.** Materials, 13, n. 20, p. 4631, 2020.

YODSUDJAI, W.; NITICHOTE, K. **Chloride penetration behavior of concrete made from various types of recycled concrete aggregate.** Sustainability, 14, n. 5, p. 2768, 2022.

YONEZAWA, T.; KAMIYAMA, Y.; YANAGIBASHI, K.; KOJIMA, K. ARAKAWA and YAMADA, M. **A study on a technology for producing high quality recycled coarse aggregate.** Zairyo, 50, n. 8, p. 835-842, 2001.

YU, Y.; YAZAN, D. M.; BHOCHHIBHOYA, S.; VOLKER, L. **Towards Circular Economy through Industrial Symbiosis in the Dutch construction industry: A case of recycled concrete aggregates.** Journal of cleaner production, 293, p. 126083, 2021.

YUAN, W.-B.; MAO, L.; LI, L.-Y. **A two-step approach for calculating chloride diffusion coefficient in concrete with both natural and recycled concrete aggregates.** Science of the Total Environment, 856, p. 159197, 2023.

ZHAO, H.; WU, Z.; LIU, A.; ZHANG, L. **Numerical insights into the effect of ITZ and aggregate strength on concrete properties.** Theoretical and Applied Fracture Mechanics, 120, p. 103415, 2022.

ZHOU, F.; LYDON, F.; BARR, B. **Effect of coarse aggregate on elastic modulus and compressive strength of high performance concrete.** Cement and Concrete Research, 25, n. 1, p. 177-186, 1995.

ZIMBELMANN, R. **A contribution to the problem of cement-aggregate bond.** Cement and Concrete Research, 15, n. 5, p. 801-808, 1985.